Finanziato dall'Unione europea NextGenerationEU
Ministero dell'Università e della Ricerca
Italiadomani PIANO NAZIONALE DI RIPRESA E RESILIENZA
UNIVERSITÀ DI SIENA 1240

Percorso dottorale sviluppato con il sostegno finanziario di NextGenerationEU:
Missione 4, Componente 2, Investimento 1.5, CUP B63C22000680007

Borsa MUR ex DM 35x/2022

Dipartimento di Biotecnologie Mediche

Dottorato in Biotecnologie Mediche

38° Ciclo

Coordinatore Prof. Francesco Iannelli

The impact of Digital Technologies in Orthodontics: 3D Imaging, Additive manufacturing, *In Vitro* testing and Clinical Outcomes of Materials and Therapeutic Devices

Settore scientifico disciplinare: MED/28

Candidato
Dott. Carlo Bosoni
Department of Medical Biotechnologies
University of Siena

CARLO
BOSONI
02.02.2026
07:45:09
GMT+01:00

Firma digitale del/della candidato/a

Supervisore
Dott. Cecilia Goracci
Department of Medical Biotechnologies
University of Siena

Anno accademico di conseguimento del titolo di Dottore di ricerca
2024/25

Università degli Studi di Siena
Dottorato in Biotecnologie Mediche
38° Ciclo

Data dell'esame finale
23 febbraio 2026

Commissione giudicatrice
- Prof. Reiner Siebert
- Prof.ssa Claudia Sala
- Prof. Lorenzo Franchi
- Prof.ssa Flavia Artese
- Prof. Francesco Iannelli
- Prof. Francesco Santoro

Supplenti
- Prof. German Ott
- Prof.ssa Arianna Di Napoli
- Prof.ssa Teresa Marafioti
- Prof. Stefano Lazzi

The Impact of Digital Technologies in Orthodontics: 3D Imaging, Additive Manufacturing, *In Vitro* Testing and Clinical Outcomes of Materials and Therapeutic Devices.

The Impact of Digital Technologies in Orthodontics: 3D Imaging, Additive Manufacturing, *In Vitro* Testing and Clinical Outcomes of Materials and Therapeutic Devices.

This thesis is based on the following papers:

Bosoni C, Nieri M, Franceschi D, Souki BQ, Franchi L, Giuntini V. Comparison between digital and conventional impression techniques in children on preference, time and comfort: A crossover randomized controlled trial. Orthod Craniofac Res. 2023 Nov;26(4):585-590. doi: 10.1111/ocr.12648. Epub 2023 Mar 20. PMID: 36891891.

Rosa B, Bosoni C, Miguel JA, Carvalho F, Artese F. Reliability and reproducibility of a best fit superimposition method of digital dental models from adult patients. – *under revision for publication on American Journal and Dentofacial Orthopedics*

Bosoni C, Vichi A, Franchi L, Al-Johani H, Goracci C. Influence of Printing Orientation on Flexural Strength and Flexural Modulus of 3D Printed Resins for Occlusal Splints before and after Water Aging. – *submitted for publication on Materials*

Goracci C, Bosoni C, Marti P, Scotti N, Franchi L, Vichi A. Influence of Printing Orientation on Surface Roughness and Gloss of 3D Printed Resins for Orthodontic Devices. Materials (Basel). 2025 Jan 23;18(3):523. doi: 10.3390/ma18030523. PMID: 39942190; PMCID: PMC11818063.

Machado Maia G, Machado Maia R, Siqueira Calaes de Oliveira A, Bosoni C, Franchi L, Souki BQ. Dental Arch Expansion with In-House Clear Aligners: An Exploratory Prospective Clinical Study on Torque, Vertical Control, and Attachment Configuration. – *under revision for publication on Orthodontic and Craniofacial Research*

Bosoni C, Franchi L, Marti P, Vichi A, Goracci C. Comparison between Customized and Standard Facemasks for Early Treatment of Class III Malocclusion: a Crossover Randomized Controlled Trial – *to be submitted for publication on American Journal and Dentofacial Orthopedics*

Artese F, Bosoni C. A diagnostic and treatment planning checklist for vertical problems in orthodontic patients. J World Fed Orthod. 2025 Oct 31:S2212-4438(25)00796-9. doi: 10.1016/j.ejwf.2025.09.002. Epub ahead of print. PMID: 41176444.

Souki BQ, Azevedo GM, Maia RA, Tavares LDF, Bosoni C. Guia prático de fabricação de alinhadores in-house – Parte 1: Introdução ao sistema. Orthod. Sci. Pract. 2023; 16(61):91-108.
DOI: 10.24077/2023;1661-98246715

Souki BQ, Azevedo GM, Maia RM, Tavares LDF, Bosoni C. Guia prático da fabricação de alinhadores in-house – Parte 2: Planejamento e Estagiamento. Orthod. Sci. Pract. 2023; 16(62):119-130.
DOI: 10.24077/2023;1662-91458a01

Souki BQ, Maia RM, Azevedo GM, Tavares LDF, Bosoni C. Guia prático de fabricação de alinhadores in house- Parte 3: impressão de modelos, pós-processamento, termoplastificação, acabamento e gestão clínica. Orthod. Sci. Pract. 2023; 16(63):115-133.
DOI: 10.24077/2023;1663-063013258

Chapter 1: Introduction

The mid-twentieth century witnessed the onset of what is now referred to as the digital revolution. The invention of the transistor, followed by the development of semiconductors and integrated circuits, significantly transformed the way information is processed. As a result of these technological advancements, information transitioned from analogue to digital formats. This revolution affected every aspect of society, rapidly altering routine activities. One clear example is photography. Previously, the process of capturing an image relied on cameras and photographic film, with the final product requiring chemical development. Today, photographs are produced instantly using digital cameras, eliminating the need for image development and considerably accelerating the process. Dentistry, including orthodontics, has also been profoundly influenced by the digital revolution. Over the past decade, substantial changes have occurred, both in the collection of patient information and in the utilization of clinical resources. Digital orthodontics essentially encompasses the capture of facial and oral images, the treatment planning, and the design and production of appliances, mechanisms which will be described and examined throughout this thesis in a compilation of 10 manuscripts.

1.1 Digital Technologies in Orthodontics

Digital technologies in Orthodontics has significantly enhanced the efficiency of diagnosis and treatment planning [1]. Data acquisition through digital 3D imaging, 3D models and CAD CAM integration have deeply changed orthodontic practice [2]. In particular, all these aspects changed the perspective from a 2D image representation to 3D integrated reconstruction of hard and soft tissues. Additive manufacturing was also a major advancement in the production of new types of orthodontic appliances, ranging from intraoral appliances such as aligners and retainers and extraoral devices like customized facemasks.

1.2 Digital 3D Imaging

Technological innovations that have influenced image acquisition in orthodontics include digital photography and videography, digital radiology including cone-beam computed tomography (CBCT), intraoral scanning and digital models. [3].

1.2.1 Digital Radiology, Photography and Videography

With technological improvements there is a general move towards keeping digital records, and many professions now use digital images exclusively [4]. Traditionally, dental models, facial and intra-oral photographs and a set of two-dimensional radiographs are used for orthodontic diagnosis and treatment planning [5]. Intraoral and panoramic radiographs are used to assess the condition and developmental status of the teeth and hard tissue supporting structures, and to identify any dental anomalies or pathology. Lateral cephalometric radiographs are employed to analyze dentoskeletal relationships, while CBCT can serve as an additional imaging modality to provide supplementary diagnostic information [6]. Digital imaging has several potential advantages over traditional radiology. These include instant image acquisition, no need of physical space for storage, immediate transmission, image post-processing is possible, reduced exposure to radiation for patients, and digital data evaluation, such as cephalometric analysis [7].

Very similar advantages are possible with digital photography, which offers instant image review, eliminates film-processing costs, and facilitates seamless data transmission for remote consultation. With digital cameras videography also became an straightforward tool allowing esthetic analysis of dynamic functions such as spontaneous smiling and speech [8].

1.2.2 Cone beam computed tomography (CBCT)

British engineer Godfrey Hounsfield began developing a prototype for the CT scanner in 1967 while working at the EMI company, which was also owned by Abbey Road Studios. The substantial profits generated by The Beatles during that period provided financial support for Hounsfield’s project. However, the commercial development of CBCT did not begin until 1996, when Italian developers Attilio Tacconi and Piero Mozzo introduced the first dental CBCT model, the Newtom 9000 [9]. Since then, numerous other models have become commercially available, and tomograms, thanks to their three-dimensional imaging capabilities, have become indispensable diagnostic tools in orthodontics. CBCT uses a cone-shaped X-ray beam that passes through the patient and is captured on a two-dimensional, flat-panel detector. These two-dimensional projections are then converted into three-dimensional (3D) images using computer-based software programs [5]. The benefits of CBCT imaging include the generation of images free from magnification artifacts, the capacity for post-acquisition correction of head positioning errors, and the superior visualization of structures which are challenging to evaluate with conventional two-dimensional (2D) imaging.

Nevertheless, due to increased radiation compared to conventional radiography, CBCT imaging is indicated in specific orthodontic situations, such as impacted or supernumerary teeth. CBCT scanning is justified if the exact position of the tooth, its relationship with intimate anatomical structures, and possible resorption of neighbouring teeth cannot reliably be assessed from 2D radiographs or if CBCT imaging will otherwise influence treatment planning [9]. In traumatic or congenital loss of permanent teeth autotransplantation can be a treatment option and the dimensions of both the tooth transplant and the recipient site bone volume can be measured reliably from CBCT images. CBCT image reconstruction has also significantly enhanced treatment planning for the management of craniofacial anomalies. Craniofacial syndromes, skeletal asymmetries requiring surgical intervention, and orthognathic surgery are other possible indications for CBCT imaging. CBCT can also help for planning for Temporary Anchorage Devices (TADs) placement. Finally, the volumetric nature of the scan allows for quantitative airway analysis. As children and young patients are at greater risk of adverse effects of ionizing radiation, as ALARA recommends, special care must be taken when imaging these patient groups.

1.2.3 3D Photography

Recent advancements in 3D photography enable the acquisition of volumetric images of the patient's face. This is achieved either through the synchronized triggering of professional cameras, assisted by specific softwares, or by reconstruction obtained from facial scanners. The integration of this volumetric facial data currently allows for the generation of algorithms capable of simulating the facial outcomes resulting from the movement of the teeth and underlying skeletal structures following orthognathic surgery. These simulated images provide an excellent tool for treatment planning and communication, helping patients to better understand the available treatment options. This approach could also serve as a non-invasive and radiation-free method for quantifying soft tissue changes during growth or for evaluating post-treatment soft tissue outcomes. [10].

1.2.4 Intraoral Scanning

The first in office digital impression system capable of full arch scanning (Cadent iTero) was made available in the dental market in 2008 [11]. Intraoral scanning incorporates a variety of technologies, ranging from light emitters to red or blue lasers, combined with 3D matching software to create a virtual model of the dentition and adjacent gingiva. The digital scanning system can fundamentally be segmented into three components: image acquisition, data processing, and on-screen reproduction of the scan. The primary factor influencing the performance of scanners is the underlying imaging technology. There are three basic mechanisms for image acquisition, namely, the triangulation technique, the confocal laser scanning and the active wavefront sampling. The highestperforming technique is confocal laser scanning, wherein the emitting laser is projected onto the target through a filter featuring a minute pinhole aperture. The confocal plane is characterized by the capture of only the light reflected from the in-focus object, while out-of-focus data are not registered. Consequently, the entire 3D structure is reconstructed by recovering 2D images across multiple confocal planes. Digital impressions have brought innovation to impression taking and have sidelined the conventional methods (alginate and PVS). Intraoral scanners can offer significant advantages, such as reduced patient discomfort, time efficiency, simplification of clinical procedures, and the benefit of capturing and storing highly accurate information [12]. Intraoral scanning effectively avoids the demanding process of pouring and trimming traditional plaster models, eliminating a significant component of laboratory workload and the necessity for physical model storage. [13].

1.3 3D Models

The first orthodontic digitation system was developed by Cadent in 1999 [14]. Since then, plaster models have been rapidly replaced by digital models with high precision, reliability and reproducibility. Literature confirms the accuracy and reliability of digital orthodontic study models acquired through methods such as intraoral scanning, CBCT, and the scanning of plaster models or impressions, with the resulting data stored in .STL format, which stands for standard tessellation language. The majority of studies conclude that measurements taken on these digital models exhibit no clinically significant differences compared to conventional plaster models, establishing their clinical acceptability for orthodontic diagnosis [15]. Digital models have several advantages such as accuracy and speed in obtaining data for diagnosis, no physical space needed for storage, less chances of permanent damage, possibility of information transfer through a digital environment, easier orthodontic analysis, and creation of virtual setups, simulating different treatment modalities using the same digital model [15]. Virtual setups are less time-consuming than the manual plaster-cutting and waxing process, allowing for easier movement quantification, visualization through model superimposition, and simulation videos, which enhances patient communication. Virtual setups also enables the direct manufacture of devices like indirect bonding trays and clear aligners, directly aiding in treatment execution. However, obstacles to full adoption remain, including the high initial cost of software and the requirement for adequate training of orthodontists in these new technologies [16].

1.3.1 Clinical application

Diagnostic model analysis in orthodontics entails a comprehensive assessment of dental alignment and occlusion. This process extends to examining inter-maxillary and dento-maxillary relationships.

Reliable measurements are consistently obtained for key diagnostic parameters, including crowding and spacing, arch length, intercanine/intermolar distances, mesiodistal tooth size, overjet, and overbite allowing for automated space analysis and Bolton discrepancy calculation.

1.3.2 Clinical outcome evaluation

Clinical orthodontics has traditionally focused on achieving controlled tooth movement in all three spatial planes according to a specific treatment plan. Technological advances now offer practitioners increasingly precise tools to assess treatment efficacy. One such instrument is the superimposition of STL files, which presents a relatively straightforward method of analysis [18]. The reference area selected for aligning serial 3D dental models significantly influences the validity of the comparison. Specifically, registration on the medial part of the third rugae and a small adjacent dorsal zone yields accurate and reproducible results [19].

1.4 3D Printing

In 1986, Charles Hull introduced the first 3D printing technology based on stereolithography (SLA) [17]. Since then, it has been used in many different fields for nearly 30 years. The integration of 3D printing into dentistry has led to a revolution in the precision and personalization of dental care. Additive manufacturing has made substantial inroads into various fields of healthcare, with dentistry being one of the most rapidly advancing sectors. The technology enables the creation of highly detailed and accurate 3D objects directly from digital designs, significantly enhancing dental procedures. In orthodontics, 3D printing has revolutionized the production of custom orthodontic models and appliances, such as aligners, retainers, and brackets [18].

1.4.1 3D Printing technology

Three primary categories of 3D printing technologies are employed in dentistry: Powder Bed Fusion (PBF), Light Curing, and Fused Deposition Modeling (FDM). PBF technologies, including SLM and SLS, use heat or electron beams to fuse powdered materials (such as Ti and Co-Cr) for the manufacture of metal frameworks. Light Curing methods (SLA, DLP, PJ) utilize photosensitive liquid resins cured by light, enabling the creation of 3D models. FDM is a cost-effective method that involves melting and extruding thermoplastic filaments (like PLA) [17]. Both DLP and SLA produce 3D-printed results that are compatible with orthodontic clinical needs [19]. 3D printers build models layer-by-layer from liquid resin, using either an ultraviolet laser (SLA) or visible light projector (DLP) for photopolymerization. The DLP process may result in a faster model print time because a whole layer of resin is cured simultaneously, whereas SLA involves the laser moving sequentially across the print layer. SLA/DLP printers form the model on a metal build platform such that models are suspended upside down and 'pulled' out of the resin. The platform is raised incrementally as each target area of resin is cured [20].

1.4.2 Study Models

The integration of 3D printing in orthodontics has enabled the production of high-resolution digital study models. Digital models are accurate and can be used to replace plaster models [21]. These models offer significant operational and clinical advantages: they facilitate digital storage, thereby eliminating the necessity for physical archival space and mitigating the risk of degradation. The use of digital models enhances the precision of progress evaluation and tracking over time. Furthermore, digital models streamline multidisciplinary care through easy sharing and enable the direct computer-aided fabrication of various orthodontic devices, ultimately improving workflow efficiency [22].

1.4.2.1 Resins

Resin constitutes the most widely used material for 3D printing, regardless of the technology employed. Initially utilized to print stereolithographic study models with standard formulations, it is currently possible to directly print appliances or accessories using biocompatible resins. Two major categories are alcohol-washable and water-washable resins, each with specific implications for storage and cleaning procedures. In recent years, to address environmental concerns, new plant-based resin formulations have been proposed.

1.4.2.2 Polymers

Companies have proposed advances in aligner material in the past few years, especially involving shape memory polymers, with the potential to bring new insights into the clinical applications of orthodontic clear aligner therapy [23]. This new concept allows for the direct printing of aligners without the need for a physical support, such as resin models, as is required for thermoformed aligners. At the same time, it eliminates the need for plastics and their trimming, allowing a faster production process. On the other hand, new workflows mean new equipment; therefore, the need to update the manufacturing could represent a significant cost for the orthodontist, especially at a time when new materials are launched without sufficient scientific support.

1.4.3 3D Printing Mechanical Properties

The mechanical behavior of 3D printing resins is related to printing parameters that enforce anisotropy within the printed part. Layer thickness, governing photopolymerization kinetics and energy delivery, directly influences the degree of inter-layer coalescence; while thinner layers enhance surface resolution, they risk creating weak inter-layer zones that reduce bulk mechanical strength. Consequently, the printing orientation determines the component's principal axis of mechanical resistance, with maximal load-bearing capacity often observed when forces are applied perpendicular to the build layers. Surface integrity, characterized by roughness and gloss, is clinically critical, as high roughness acts as a microscopic stress concentrator, predisposing the appliance to premature fatigue failure while simultaneously hindering biological integration and promoting biofilm adhesion.

1.4.4 Orthodontic Devices

1.4.4.1 Intraoral devices

3D printing is most commonly used in orthodontics to produce working models for thermoformed or 3D printed aligners, 3D metal printed fixed appliances, including custom brackets and bands, indirect bonding trays, removable appliances, occlusal splints, insertion guides for TAD placement and retainers.

1.4.4.2 Clear Aligners

Clear aligners were introduced in the United States, where they were born at the end of the 1990s by the company Align Technology [24]. Since their introduction, clear aligner therapy has become an increasingly common addition to the orthodontic armamentarium. The technology has clearly been employed, in modified forms, at least as far back as the Tooth Positioner by Dr Harold Kesling in 1946 and subsequently improved and developed by Nahoum, Ponitz, McNamara, Sheridan and Truax, before being combined recently with advances in transparent thermoplastic materials and computer technology [25]. Clear aligner treatment can be outsourced when the treating clinician sends digital models to a laboratory which allows the appliances to be manufactured via the use of 3D scanning technology. The final digital model produced by the laboratory or by a computer algorithm can be, in turn, manipulated via manual adjustment by the clinician to the final occlusal result. From each digital model, 3D-printed aligners or models are generated in a sequence, each one representing a different stage of the treatment.

Parameters that influence the biomechanical characteristics of aligners include the properties of the material, the thickness of the material, and the fitting accuracy of the aligner to the teeth and any attachments. Various thermoplastic materials, or combinations of materials, are being used for fabrication due to their characteristics. These include polyvinyl chloride, polyurethane, polyethylene terephthalate, and polyethylene terephthalate glycol [26].

An alternative to thermoformed aligners is represented by 3D printed aligners. Use of a clear aligner that is 3D printed for direct usage can eliminate the cumulative errors introduced from analog impression taking and the subsequent thermoplastic workflow. In addition to greater accuracy, direct printing produces shorter supply chains, significantly shorter lead times, and lower costs. It is also a more sustainable process that generates significantly less waste than subtractive and thermoforming processes [26].

1.4.4.3 3D metal printing

3D metal printing has been recently proposed by Graf as an alternative of analogic procedures without the need of physical support to print custom bands, fixed appliances such as expanders, transpalatal bars, lingual arches and palatal bone anchored appliances [27].

3D printing of metallic appliances offers several advantages over the conventional analog process in terms of patient comfort, clinical efficiency, accuracy, and flexibility in design. The greatest advantage is the customization, improved communication with the laboratory technician, reduced laboratory waste, enhanced accuracy, better standardization, improved patient comfort, and reduced orthodontic appointments by eliminating the need for separators. As with most new technology, the greatest disadvantage is the equipment expense. Another disadvantage is the limited availability of alloys for printing, which are very rigid and unbendable, intolerant for minor inaccuracies, and more difficult to debond compared to traditional appliances [28].

1.4.4.4 Indirect Bonding Trays

Indirect bonding has been suggested as a valid method for bonding orthodontic brackets and has several advantages, including saving chair time and reducing patient discomfort [29]. To reach these goals, Silverman and Cohen introduced the first indirect bonding method in 1972 [30]. With the advancement of technology, computers entered the practice of orthodontics, thereby enhancing the indirect bonding technique. Several companies offer 3D CAD-CAM-generated methods for the fabrication of indirect bonding trays. Nevertheless, despite the technological precision offered by digital tools, the accuracy of bracket placement ultimately depends on the clinician's judgment in selecting ideal bracket positions and ultimately no significant clinical differences compared to direct bonding in terms of treatment outcomes have been recorded [31].

1.4.4.5 Removable Appliances

With the same principles mentioned above, removable appliances can be manufactured indirectly on resin 3D models or directly 3D printed using biocompatible resins. The first direct 3D printed removable appliance was introduced by Graf in 2022, who presented a fully digital Twin Block appliance [32].

1.4.4.6 Occlusal splints

The traditional milling process to produce occlusal splints includes interocclusal wax occlusal registration for the upper and lower dentition of the working models and alginate impressions. With CAD and 3D printing, several splints can be manufactured with biocompatible resins simultaneously, which greatly improves the manufacturing efficiency and saves time and cost. However, the antistress and antiaging abilities of 3D printing materials are not as good as those of traditional or milling resin materials, which will adversely affect their long-term use. Differences in technologies and materials will affect the performance of the occlusal splints [17].

1.4.4.7 Surgical Guides for TADs placement

One of the main outcomes of technological advance was the digitalization of guided procedures for the insertion of palatal TADs. By matching CBCT DICOM files and intraoral scanning stl files, pre-operative planning and the use of surgical guides allow for precise and controlled placement while minimizing risks associated with this procedure [33]. Another advantage of pre-operative planning with a CBCT is the possibility of planning a bicortical position, which guarantees greater stability, better mechanical results, lower stress and strain values, decreased deformation and fracture.

By using 3D printing to create surgical guides, orthodontists can ensure a higher degree of precision and reduce the risk of complications. Despite digital planning, minor linear (1-2 mm) and angular (2°-10°) deviations in TADs placement during the insertion could be expected. For this reason, factors like imaging quality, clinician expertise, and guide stability affect their effectiveness [34].

Similarly, corticotomies or piezocision-assisted orthodontics, which are minimally invasive surgical techniques to accelerate tooth movement, also benefit from 3D-printed surgical guides.

1.4.4.8 Retainers

Orthodontic retainers could be either fixed or removable. Fixed retainers are placed lingually after finishing the orthodontic treatment and usually extend from canine to canine. These retainers can be 3D metal printed, and, by using this method, there is an improved placement accuracy compared to traditional ones [14]. Removable retainers could be thermoformed or 3D resin printed retainers with very similar behaviour in terms of fit [35]. Nevertheless, rigorous control of the manufacturing process is essential to limit biological risks in the long term.

1.4.5 Extraoral devices

1.4.5.1 Facemask

Conventional facemasks are currently limited to standardized shapes, sizes, and colors, which compromises both precise anatomical fit and aesthetic appearance. Customization achieved through CAD/CAM techniques offers a viable solution to these limitations [36,37].

A customized design allows for the creation of forehead and chin pads with optimal anatomical adaptation, ensuring a larger and more uniform contact area. This improved fit is essential for accurate force transmission, which may minimize undesirable pressure points, and ultimately enhancing patient comfort and compliance. The central vertical bar can also be designed to precisely reproduce the patient's soft tissue profile, eliminating the need for manual bending required for standardized appliances [38]. Furthermore, digital technologies allow for the objective monitoring of treatment efficacy both in intra and extraoral devices. Specifically, the integration of a TheraMon sensor enables clinicians to test and record patient cooperation during treatment.

References

1. Gracea RS, Winderickx N, Vanheers M, Hendrickx J, Preda F, Shujaat S, et al. Artificial intelligence for orthodontic diagnosis and treatment planning: A scoping review. J Dent. 2025;152:105442. https://doi.org/10.1016/j.jdent.2024.105442
2. Pandey R, Kamble R, Kanani H. Revolutionizing Smiles: Advancing Orthodontics Through Digital Innovation. Cureus. 2024;16:e64086. https://doi.org/10.7759/cureus.64086
3. Graber LW, Vanarsdall RL, Vig KWL, Huang GJ, editors. Orthodontics: current principles and techniques. Sixth edition. St. Louis, Missouri: Elsevier; 2017.
4. Sandler PJ, Murray AM, Bearn D. Digital Records in Orthodontics. Dent Update. 2002;29:18–24. https://doi.org/10.12968/denu.2002.29.1.18
5. Rischen RJ, Breuning KH, Bronkhorst EM, Kuijpers-Jagtman AM. Records Needed for Orthodontic Diagnosis and Treatment Planning: A Systematic Review. Glogauer M, editor. PLoS ONE. 2013;8:e74186. https://doi.org/10.1371/journal.pone.0074186
6. Tanna NK, AlMuzaini AAAY, Mupparapu M. Imaging in Orthodontics. Dental Clinics of North America. 2021;65:623–41. https://doi.org/10.1016/j.cden.2021.02.008
7. Forsyth DB, Shaw WC, Richmond S. Digital imaging of cephalometric radiography, Part 1: Advantages and limitations of digital imaging. Angle Orthod. 1996;66:37–42. https://doi.org/10.1043/0003-3219(1996)066<0037:DIOCRP>2.3.CO;2
8. Van Der Geld P, Oosterveld P, Schols J, Kuijpers-Jagtman AM. Smile line assessment comparing quantitative measurement and visual estimation. American Journal of Orthodontics and Dentofacial Orthopedics. 2011;139:174–80. https://doi.org/10.1016/j.ajodo.2009.09.021
9. Kaasalainen T, Ekholm M, Siiskonen T, Kortesniemi M. Dental cone beam CT: An updated review. Physica Medica. 2021;88:193–217. https://doi.org/10.1016/j.ejmp.2021.07.007
10. Trotman C-A. Faces in 4 dimensions: Why do we care, and why the fourth dimension? Am J Orthod Dentofacial Orthop. 2011;140:895–9. https://doi.org/10.1016/j.ajodo.2011.07.014
11. Christopoulou I, Kaklamanos EG, Makrygiannakis MA, Bitsanis I, Perlea P, Tsolakis AI. Intraoral Scanners in Orthodontics: A Critical Review. IJERPH. 2022;19:1407. https://doi.org/10.3390/ijerph19031407
12. Mangano F, Gandolfi A, Luongo G, Logozzo S. Intraoral scanners in dentistry: a review of the current literature. BMC Oral Health. 2017;17:149. https://doi.org/10.1186/s12903-017-0442-x
13. Warnecki M, Nahajowski M, Papadopoulos MA, Kawala B, Lis J, Sarul M. Assessment of the reliability of measurements taken on digital orthodontic models obtained from scans of plaster

models in laboratory scanners. A systematic review and meta-analysis. Eur J Orthod. 2022;44:522–9. https://doi.org/10.1093/ejo/cjac005

14. Francisco I, Ribeiro MP, Marques F, Travassos R, Nunes C, Pereira F, et al. Application of Three-Dimensional Digital Technology in Orthodontics: The State of the Art. Biomimetics (Basel). 2022;7:23. https://doi.org/10.3390/biomimetics7010023
15. Camardella LT, Breuning H, De Vasconcellos Vilella O. Accuracy and reproducibility of measurements on plaster models and digital models created using an intraoral scanner. J Orofac Orthop. 2017;78:211–20. https://doi.org/10.1007/s00056-016-0070-0
16. Camardella LT, Rothier EKC, Vilella OV, Ongkosuwito EM, Breuning KH. Virtual setup: application in orthodontic practice. J Orofac Orthop. 2016;77:409–19. https://doi.org/10.1007/s00056-016-0048-y
17. Tian Y, Chen C, Xu X, Wang J, Hou X, Li K, et al. A Review of 3D Printing in Dentistry: Technologies, Affecting Factors, and Applications. Relucenti M, editor. Scanning. 2021;2021:1–19. https://doi.org/10.1155/2021/9950131
18. Almarshadi R, Hamdi S, Hadi F, Alshehri A, Alsahafi R, Aljohani N, et al. Redefining Digital Dentistry: Multidisciplinary Applications of 3D Printing for Personalized Dental Care. Cureus. 2025;17:e86791. https://doi.org/10.7759/cureus.86791
19. ElShebiny T, Menezes LM de, Matthaios S, Tsolakis IA, Palomo JM. Effect of printing technology and orientation on the accuracy of three-dimensional printed retainers. Angle Orthod. 2024;94:657–63. https://doi.org/10.2319/120823-812.1
20. Cousley RR. Introducing 3D printing in your orthodontic practice. J Orthod. 2020;47:265–72. https://doi.org/10.1177/1465312520936704
21. Camardella LT, Vilella OV, Van Hezel MM, Breuning KH. Accuracy of stereolithographically printed digital models compared to plaster models. J Orofac Orthop. 2017;78:394–402. https://doi.org/10.1007/s00056-017-0093-1
22. Gökmen Ş, Görgülü S, Topsakal KG, Duran GS. Accuracy of 3D Printer Technologies Using Digital Dental Models. Turk J Orthod. 2024;37:257–64. https://doi.org/10.4274/TurkJOrthod.2024.2023.8
23. Torkomian T, De La Iglesia F, Puigdollers A. 3D-printed clear aligners: An emerging alternative to the conventional thermoformed aligners? – A systematic review. Journal of Dentistry. 2025;155:105616. https://doi.org/10.1016/j.jdent.2025.105616

24. Putrino A, Barbato E, Galluccio G. Clear Aligners: Between Evolution and Efficiency—A Scoping Review. IJERPH. 2021;18:2870. https://doi.org/10.3390/ijerph18062870
25. Weir T. Clear aligners in orthodontic treatment. Australian Dental Journal. 2017;62:58–62. https://doi.org/10.1111/adj.12480
26. Tartaglia GM, Mapelli A, Maspero C, Santaniello T, Serafin M, Farronato M, et al. Direct 3D Printing of Clear Orthodontic Aligners: Current State and Future Possibilities. Materials. 2021;14:1799. https://doi.org/10.3390/ma14071799
27. Graf S, Tarraf NE, Kravitz ND. Three-dimensional metal printed orthodontic laboratory appliances. Seminars in Orthodontics. 2021;27:189–93. https://doi.org/10.1053/j.sodo.2021.09.005
28. Graf S, Tarraf NE. Advantages and disadvantages of the three-dimensional metal printed orthodontic appliances. Journal of the World Federation of Orthodontists. 2022;11:197–201. https://doi.org/10.1016/j.ejwf.2022.10.003
29. Czolgosz I, Cattaneo PM, Cornelis MA. Computer-aided indirect bonding versus traditional direct bonding of orthodontic brackets: bonding time, immediate bonding failures, and cost-minimization. A randomized controlled trial. European Journal of Orthodontics. 2021;43:144–51. https://doi.org/10.1093/ejo/cjaa045
30. Silverman E, Cohen M, Gianelly AA, Dietz VS. A universal direct bonding system for both metal and plastic brackets. American Journal of Orthodontics. 1972;62:236–44. https://doi.org/10.1016/S0002-9416(72)90264-3
31. Alhafi ZM, Hajeer MY, Alam MK, Jaber S, Jaber ST. Effectiveness and efficiency of indirect bonding techniques: An umbrella review with meta-analysis of the pooled findings. International Orthodontics. 2025;23:101036. https://doi.org/10.1016/j.ortho.2025.101036
32. Graf S, Tarraf NE, Vasudavan S. Direct printed removable appliances: A new approach for the Twin-block appliance. American Journal of Orthodontics and Dentofacial Orthopedics. 2022;162:103–7. https://doi.org/10.1016/j.ajodo.2021.08.019
33. Pozzan L, Migliorati M, Dinelli L, Riatti R, Torelli L, Di Lenarda R, et al. Accuracy of the digital workflow for guided insertion of orthodontic palatal TADs: a step-by-step 3D analysis. Prog Orthod. 2022;23:27. https://doi.org/10.1186/s40510-022-00423-6
34. Dipalma G, Inchingolo AM, Trilli I, Di Noia A, De Vecchio G, Palermo A, et al. Accuracy of the surgical template used in the placement of implants and orthodontic miniscrews. BMC Oral Health. 2025;25:999. https://doi.org/10.1186/s12903-025-06328-0

35. Cole D, Bencharit S, Carrico CK, Arias A, Tüfekçi E. Evaluation of fit for 3D-printed retainers compared with thermoform retainers. American Journal of Orthodontics and Dentofacial Orthopedics. 2019;155:592–9. https://doi.org/10.1016/j.ajodo.2018.09.011
36. Franchi L, Vichi A, Marti P, Lampus F, Guercio S, Recupero A, et al. 3D Printed Customized Facemask for Maxillary Protraction in the Early Treatment of a Class III Malocclusion: Proof-of-Concept Clinical Case. Materials (Basel). 2022;15:3747. https://doi.org/10.3390/ma15113747
37. Caroccia F, Juloski J, Juloski J, Marti P, Lampus F, Vichi A, et al. 3D printed customized facemask for early treatment of Class III malocclusion: a two-center case series feasibility study. Minerva Dent Oral Sci. 2025;74:42–8. https://doi.org/10.23736/S2724-6329.24.05013-7
38. Abdulkareem GB, Cobourne MT, Abid M. The effectiveness of novel 3D printed customized facemask appliance for treatment of class III malocclusion: a randomized clinical trial. European Journal of Orthodontics. 2025;47:cjaf075. https://doi.org/10.1093/ejo/cjaf075

Chapter 2: 3D Imaging

2.1 Comparison between digital and conventional impression techniques in children on preference, time and comfort: A crossover randomized controlled trial

Abstract

To compare the conventional alginate impression and the digital impression taken with an intraoral scanner of both dental arches in children, using a randomized crossover design. This is a monocentric, controlled, superiority, randomized, crossover, open study. Twenty-four orthodontic patients between 6 and 11 years of age underwent intraoral scanning (TRIOS 3; 3Shape) and alginate impression of both dental arches with an interval of 1 week between the two procedures. Participants were recruited from September 2021 to March 2022 and the study was completed in April 2022. Impression time for the two procedures was compared. Patients were asked which one of the two impression procedures they preferred. A questionnaire including Visual Analogue Scale (VAS) for comfort, pain, gag reflex and difficulty in breathing, was administered to the patients. Eighteen out of 24 patients preferred digital impression (75%, 95% confidence interval [CI]: 55% to 88%; $P = .014$). Scanning time was significantly shorter than alginate impression time (difference −118 seconds; 95% CI: −138 to −99; $P < .001$). Comfort was significantly higher for digital impression (difference 1.7; 95% CI: 0.5 to 2.8; $P = .007$). There was no difference in pain (difference −0.2; 95% CI: −1.5 to 1.0; $P = .686$) while gag reflex and breathing difficulties were smaller for digital impression (gag reflex difference −2.5; 95% CI: −4.0 to −0.9; $P = .004$ and breathing difficulties difference −1.5; 95% CI: −2.5 to −0.5; $P = -.004$). Digital impression is preferred by children aged 6–11 years and it is significantly faster in acquisition time than conventional alginate impression.

Introduction

The impression is a necessary step for the orthodontic diagnosis.1 Plaster models of dental arches have been used traditionally to obtain 3D diagnostic records. Digital impression has been introduced recently by means of intraoral optical scanners that produce a three-dimensional image of the teeth.2–4 This overcomes the problem of pouring and trimming plaster casts, thus eliminating a major component of laboratory work and the need to store the models. Conventional cast analysis allows the clinician to evaluate the location and severity of dental crowding and to evaluate tooth-size relationships within the dental arches.5 This analysis now can be done more easily by means of software for virtual dental models.6–8 Semiautomated software can be used to measure the arch length and Bolton discrepancies, and multiple virtual treatment setups can be performed with minimal effort.

Since digital models can be a reliable alternative to stone casts in analysing mixed6 and permanent dentitions,7 few studies have compared the conventional alginate impression with the digital impression with intraoral scanners in growing patients.9–12 These studies have shown that digital impression could have some advantages in terms of greater satisfaction and less discomfort for the paediatric patient with respect to conventional alginate impression. Only one study was randomized and analysed patients between 10 and 17 years.9 To our knowledge, no previous RCT compared preference, time and comfort between conventional alginate impression and digital impression in orthodontic patients between 6 and 11 years.

The objective of the present study was to compare the conventional alginate impression with the digital impression of both dental arches in orthodontic patients between 6 and 11 years of age with a randomized crossover design. In particular, the preference, comfort, impression time, pain, gag reflex and breathing difficulty were analysed.

Materials and Methods

The experimental design followed the Consolidated Standards of Reporting Trials (CONSORT) statement and extension checklist for reporting within-person randomized trials.13,14

Ethics statement

The principles outlined in the Declaration of Helsinki on clinical research involving human subjects were adhered to. The study was approved by the Paediatric Ethics Committee of the Region of Tuscany, Italy (approval number 07/2020).

Protocol registration

The study was registered on ClinicalTrials.gov with registration number NCT04220957 in January 2020 (https://clinicaltrials.gov/ct2/ show/NCT04220957).

Trial design

This is a monocentric, controlled, superiority, randomized, crossover, open study. Two impression procedures of both dental arches (conventional alginate and digital with intraoral scanner) were compared in two sessions with an interval of 1 week between the two procedures.

Participants

The subjects were enrolled in the study at the Orthodontic Clinic of the Careggi University Hospital, in Florence, Italy by an operator (LF). To be included in the study, patients had to be aged between 6 and 11 years and not in treatment with fixed orthodontic appliances. Patients were included if they were not in treatment or if they were in treatment with removable appliances.

Exclusion criteria were:

1. Non-compliant patients;
2. Patients with syndromes or systemic diseases;
3. Patients suffering from cleft lip and palate.

Patients' parents signed an informed consent before starting the trial.

Interventions

A single experienced operator (VG) performed both impression procedures of the dental arches. Conventional impressions of both arches were taken with alginate (Orthoprint, Zhermack Sp) with steel impression trays according to the manufacturer's instructions. Red wax (Tenatex, Kemdent) was used for bite registration. The procedure consisted of the following steps: test of the tray, preparation of the alginate for the lower impression, impression of the lower arch, preparation of the alginate for the upper impression, impression of the upper arch and bite registration with red wax. The alginate was hand-mixed with tap drinking water. The digital impressions were made with the TRIOS 3 intraoral optical scanner (3Shape) following the procedure reported by the manufacturer. In the lower arch, the occlusal, lingual and vestibular surfaces were scanned in sequence. In the upper arch, the occlusal, buccal and lingual surfaces were scanned in sequence. Finally, bite registration was taken. The two impression procedures of both dental arches (conventional alginate and intraoral scanning) were carried out in two sessions with an interval of 1 week between the two procedures.
Another operator (CB) hand-mixed the alginate and registered impression time for both procedures.

Outcomes

The primary outcome of the study was the patient's preference for one of the two procedures. Secondary outcomes were duration of the procedure, comfort, pain, gag reflex and difficulty in breathing.

Patients were asked which one of the two impression procedures they preferred. In addition, a questionnaire including VAS for comfort, pain, gag reflex and difficulty in breathing was provided to the patients. The VAS consisted of a scale with a score from 0 to 10 (Figure 1).

Figure 1. Visual Analogue Scale with Wong–Baker scale to evaluate patient comfort, pain, gag reflex, and breathing difficulty in the two impression methods.

In the case of comfort, 0 corresponded to very uncomfortable while 10 to maximum comfort. To facilitate interpretation, the Wong-Baker Scale was also used.15 In case of pain, 0 corresponded to no pain while 10 to very painful. For gag reflex, 0 corresponded to no gag reflex while 10 to vomiting. For breathing difficulty, 0 corresponded to no respiratory difficulty while 10 to maximum respiratory difficulty. Similar VAS scores have been used already in a previous study.10 Finally, the duration of the impression procedure was recorded with a digital chronometer.

Sample size

Considering a null hypothesis for a proportion of 50% in the preference between the two treatments and an alternative hypothesis of 80%, with alpha set at 0.05, a power of 80% and a dropout rate of 10%, 24 patients were required.

Randomization

The order of the two procedures was block randomized so that 12 patients received as first impression procedure the conventional alginate and 12 patients received as first impression procedure the intraoral scanning. The randomization list was computer-generated by the statistician (MN) and hidden inside numbered, opaque and sealed envelopes that were opened at the time of impression taking. The second impression procedure was performed after 1 week. Patients were enrolled by one operator LF and they were assigned to the impression procedure by another operator VG.

Blinding

Both the operator who took the impressions and the patients could not be blinded as for the impression procedure.

Statistical methods

Descriptive statistics were performed for all variables (frequency and percentage for qualitative variables and mean and standard deviation for quantitative variables). For the primary endpoint variable (impression procedure preference) the test was performed for one proportion and the 95% confidence interval [CI] was calculated using the Clopper-Pearson method.

As for the secondary endpoint variables, duration of the procedure, comfort, pain, gag reflex, breathing difficulty, the two procedures were compared with the *t*-test for paired data. McNemar test was used to evaluate complications.

For quantitative variables, the W Shapiro–Wilk test was performed to test for normality of the data. In case of statistical significance of the test, a non-parametric sensitivity analysis was performed using the Wilcoxon test. Statistical analysis was carried out according to the intention-to-treat method. All statistical tests were performed with JMP 13.0 (SAS Institute Inc.) using a level of statistical significance of .05.

Results

Twenty-four participants were randomized to the two impression procedures (Figure 2).

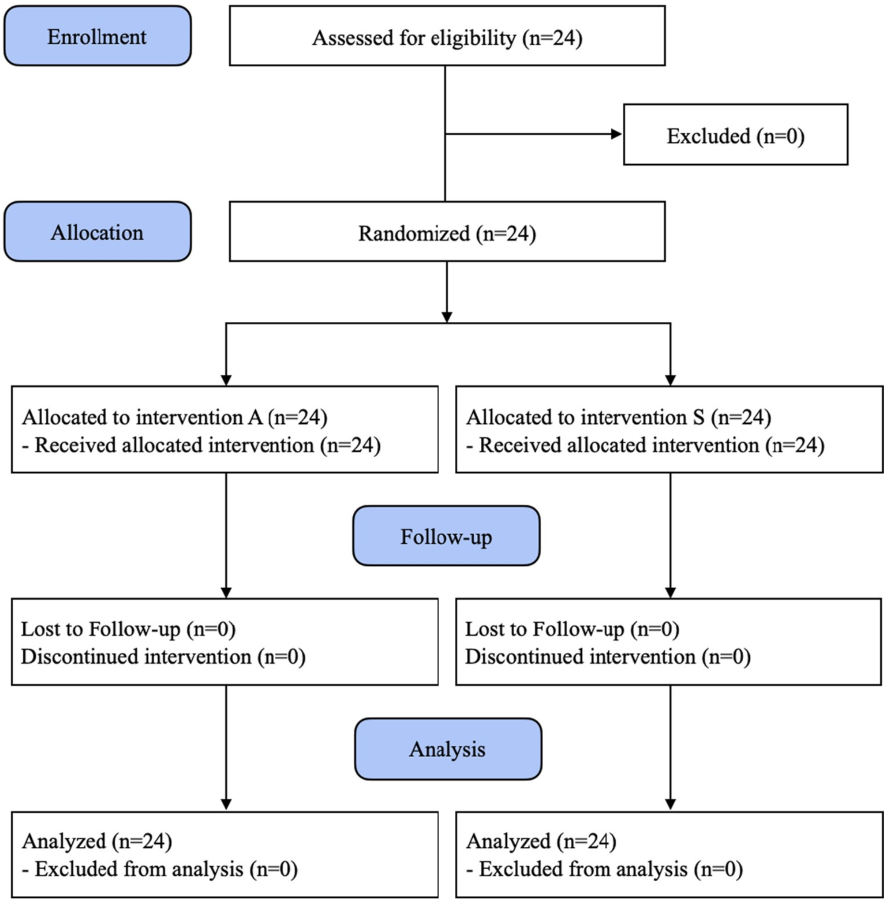

Figure 2. Consort 2010 flow diagram. A, Alginate Group; S, Scanner Group.

Participants were recruited from September 2021 to March 2022 and the study was completed in April 2022.

There were no dropouts and there were no deviations from the planned protocol.

The mean age of the participants was 8.8 years (SD 1.0) (min 6.7 years; max 10.7 years). There were 13 females and 11 males.

Twelve participants were allocated to alginate impression as first impression procedure (Alginate Group) and 12 participants were allocated to digital impression with the intraoral scanner as first impression procedure (Scanner Group).

Six patients preferred alginate impression (25%, 95% CI: 12% to 45%) while 18 patients preferred digital impression (75%, 95% CI: 55% to 88%). This difference in preference was statistically significant (P = .014).

The differences between the two impression procedures as for scanning time, comfort, pain, gag reflex and breathing difficulty are reported in Table I.

Table I. Impression time (duration), comfort, pain, gag reflex, and breathing difficulty for the two impression procedures.

	Alginate group (N = 24)	**Scanner group (N = 24)**			
Variable	**Mean (SD)**	**Mean (SD)**	**Difference**	**95% CI**	***P*-value**
Duration (seconds)	301 (31)	183 (38)	−118	−138; −99	<.001
Comfort	6.6 (2.7)	8.3 (1.8)	1.7	0.5; 2.8	.007
Pain	1.7 (2.5)	1.5 (2.5)	−0.2	−1.5; 1.0	.686
Gag reflex	2.5 (3.7)	0.1 (0.4)	−2.5	−4.0; −0.9	.004
Breathing difficulty	2.4 (2.3)	0.9 (1.8)	−1.5	−2.5; −0.5	.004

Impression time was significantly shorter for the Scanner Group (difference −118; 95% CI: −138 to −99; $P < .001$). Difference in comfort was statistically significant favouring the Scanner Group (difference 1.7; 95% CI: 0.5 to 2.8; $P = .007$). Differences in gag reflex and breathing difficulties also were significant favouring the Scanner Group (difference for gag reflex −2.5; 95% CI: −4.0 to −0.9; $P = .004$, difference for breathing difficulties −1.5; 95% CI: −2.5 to −0.5; $P = .004$). On the contrary, no differences in pain were found between the two groups (difference −0.2; 95% CI: −1.5 to 1.0; $P = .686$). There were two vomiting-related complications in the Alginate group (8%) and none in the Scanner group ($P = .157$). The W Shapiro–Wilk test for normality was significant for pain and for gag reflex. The *P* values of the Wilcoxon tests ($P = .424$ for pain and $P = .003$ for gag reflex), however, were similar to those of the *t*-test for paired data.

Discussion

The aim of this study was to compare the conventional alginate impression with the digital impression of both dental arches in orthodontic patients between 6 and 11 years, an age interval that has not been analysed in the literature yet. As reported in a recent systematic review,4 intraoral scanners appear to be a promising new resource in the hands of orthodontists, as they have advantages in terms of experience and individual preferences.4 In the present study, 18 out of 24 children with an age between 6 and 11 years, preferred the digital impression versus conventional impression with alginate. This outcome may be related to the lower invasiveness of the digital impression compared to the conventional impression confirmed by the more favourable results in comfort, gag reflex and breathing difficulties. In addition to the reduced invasiveness, there was also a significant reduction in impression time. No difference between the two impression procedures was recorded for pain.

Several studies have been conducted on the preference between intraoral scanning and conventional impression in growing subjects (younger than 18 years).9–12 The results of the present study are in agreement with Mangano et al,11 Yilmaz and Aydin10 and Burhardt et al9 that reported a greater preference for intraoral scanning (100%, 75% and 51%).

As for the duration of the impression procedure, in our study scanning time was significantly shorter with respect to alginate impression time. Scanning of both arches and bite registration took about 3 minutes on average while impressions of both arches with alginate and bite registration with wax required about 5 minutes on average. A difference of about 2 minutes between the two impression procedures could have a clinically relevant impact, especially in children. On the contrary, similar studies in the literature9–11 did not show a shorter time for digital impression when compared to conventional impression. In particular, Yilmaz and Aydin10 did not find a significant difference in total impression time between the two procedures, while Burhardt et al9 Mangano et al11 reported a significantly shorter time for conventional impression with alginate. This outcome can be explained by the fact that both studies used a relatively older technology for digital impression. In addition, patients included in the present study were between 6 and 11 years old, at a stage of dentition prior to the eruption of the second molars. The absence of the permanent second molars, in an area difficult to reach by the scanner tip, could have contributed to speeding up the scanning procedure.10

In the present study, a statistically significant difference between the two impression procedures favouring the Scanner Group in terms of comfort, gag reflex and breathing difficulty, was recorded. Two studies found similar outcomes for these variables.11,12 Another study10 found significant differences in comfort and gag reflex (favouring intraoral scanning) though nonsignificant differences were reported in breathing difficulty between the two procedures.

In the present study, no statistically significant difference was found between the two procedures for pain. A similar outcome was also reported by Yilmaz and Aydin.10

A limitation of our study was that previous experience with any kind of impression techniques was not considered. Another limitation of the present study was that no intra-rater agreement of the VAS was performed. A possible additional limitation could be related to the fact that the intraoral scanner used in this study is not the latest version available from the manufacturer. All patients in our sample received intraoral scanning for the first time while they had varying experience with the alginate impression. The results of the present study can be generalized to patients younger than 12 years.

Conclusions

In children between 6 and 11 years

1. 75% of patients preferred digital impression.
2. Impression with intraoral scanner was significantly shorter than alginate impression.
3. Digital impression performed significantly better than alginate impression in terms of comfort, gag reflex and breathing difficulty.
4. No pain differences were found between the two impression procedures.
5. No statistically significant differences for “vomiting-related” complications between the two impression procedures were found.

References

39. Saccomanno S, Saran S, Vanella V, Mastrapasqua RF, Raffaelli L, Levrini L. The potential of digital impression in orthodontics. *Dent J*. 2022;10(8):147.
40. Sjögren AP, Lindgren JE, Huggare JA. Orthodontic study cast analysis— reproducibility of recordings and agreement between conventional and 3D virtual measurements. *J Digit Imaging*. 2010;23(4):482-492.
41. Goracci C, Franchi L, Vichi A, Ferrari M. Accuracy, reliability, and efficiency of intraoral scanners for full-arch impressions: a systematic review of the clinical evidence. *Eur J Orthod*. 2016;38(4):422-428.
42. Christopoulou I, Kaklamanos EG, Makrygiannakis MA, Bitsanis I, Tsolakis AI. Patient-reported experiences and preferences with intraoral scanners: a systematic review. *Eur J Orthod*. 2022;44(1):56-65.
43. Han UK, Vig KW, Weintraub JA, Vig PS, Kowalski CJ. Consistency of orthodontic treatment decisions relative to diagnostic records. *Am J Orthod Dentofacial Orthop*. 1991;100(3):212-219.
44. Schieffer L, Latzko L, Ulmer H, et al. Comparison between stone and digital cast measurements in mixed dentition: validity, reliability, reproducibility, and objectivity. *J Orofac Orthop*. 2022;83(Suppl 1):75-84.
45. Kong L, Li Y, Liu Z. Digital versus conventional full-arch impressions in linear and 3D accuracy: a systematic review and meta-analysis of in vivo studies. *Clin Oral Investig*. 2022;26(9):5625-5642.
46. Adel SM, Vaid NR, El-Harouni N, Kassem H, Zaher AR. Digital model superimpositions: are different software algorithms equally accurate in quantifying linear tooth movements? *BMC Oral Health*. 2022;22(1):103.
47. Burhardt L, Livas C, Kerdijk W, van der Meer WJ, Ren Y. Treatment comfort, time perception, and preference for conventional and digital impression techniques: a comparative study in young patients. *Am J Orthod Dentofacial Orthop*. 2016;150(2):261-267.
48. Yilmaz H, Aydin MN. Digital versus conventional impression method in children: comfort, preference and time. *Int J Paediatr Dent*. 2019;29(6):728-735.
49. Mangano A, Beretta M, Luongo G, Mangano C, Mangano F. Conventional vs digital impressions: acceptability, treatment comfort and stress among young orthodontic patients. *Open Dent J*. 2018;12:118-124.

50. Glisic O, Hoejbjerre L, Sonnesen L. A comparison of patient experience, chair- side time, accuracy of dental arch measurements and costs of acquisition of dental models. *Angle Orthod*. 2019;89(6):868-875.
51. Moher D, Hopewell S, Schulz KF, et al. CONSORT 2010 explanation and elaboration: updated guidelines for reporting parallel group randomised trials. *Int J Surg*. 2012;10(1):28-55.
52. Pandis N, Chung B, Scherer RW, Elbourne D, Altman DG. CONSORT 2010 statement: extension checklist for reporting within person randomised trials. *BMJ*. 2017;357:j2835.
53. Wong DL, Baker CM. Pain in children: comparison of assessment scales. *Okla Nurse*. 1988;33(1):8.

Chapter 3: 3D models superimpositions

3.1 Reliability and reproducibility of a best fit superimposition method of digital dental models from adult patients.

Abstract

Cone Beam Computed Tomography (CBCT) is considered the gold standard for three-dimensional (3D) superimposition in assessing tooth movement during orthodontic treatment. However, given current guidelines emphasizing the reduction of radiation exposure, this study aimed to evaluate the reliability and reproducibility of a novel digital model superimposition method that does not require CBCT. This retrospective study included 10 adult patients who underwent comprehensive orthodontic treatment without extractions. All patients had full-head CBCT scans and corresponding upper and lower digital dental models. Two evaluators assessed tooth movement using a new superimposition technique based on .stl files, using as superimposition references the palatal rugae for the maxillary arch and the occlusion for the mandibular arch. The accuracy of this method was compared to the gold standard, which involved superimposing .stl files with CBCT data. The mean variation in reference landmark positions across the three spatial planes was similar between methods for both arches. Inter-evaluator differences (Δ) ranged from -0.07 to 0.06 mm, which is not clinically significant. Student's t-tests showed no statistically significant differences between evaluators for any axis in either method ($p>0.05$). Intraclass correlation coefficients (ICCs) demonstrated high agreement between the two methods, ranging from 0.88 to 0.98. The 3D digital model superimposition technique using the palatal rugae for the upper arch and the occlusion for the lower arch as reference areas is a reliable and reproducible alternative to CBCT-based methods for evaluating orthodontic tooth movement in non-growing patients treated without extractions.

Introduction

In orthodontics, superimposition techniques have been commonly used by both researchers and clinicians to measure growth modifications, tooth movements and to assess treatment outcomes. Traditionally, these assessments have relied on the superimposition of serial cephalometric radiographs registered on stable skeletal structures such as the cranial base, maxilla, or mandible.[27] However, this two-dimensional (2D) method has significant limitations, including image distortion and the inability to accurately capture three-dimensional (3D) changes in all planes of space.[1–3] Cone

Beam Computed Tomography (CBCT) has addressed many of these limitations and is now regarded as the gold standard for 3D assessment of complex dentofacial structures.[4] CBCT allows for the acquisition of high-resolution skeletal imaging and the 3D reconstruction of maxillary and mandibular bones, enabling volumetric visualization of oral and maxillofacial anatomy with a high degree of accuracy and detail.[4–6]

Serial CBCT voxel-based superimposition on the cranial base has been proposed as a reliable reference for evaluating facial growth and orthodontic treatment outcomes.[7] However, this approach requires full-skull imaging and, in accordance with the ALARA principle "As Low As Reasonably Achievable", efforts must be made to minimize radiation exposure. Consequently, current guidelines recommend against the routine use of CBCT in conventional orthodontic practice.[8] Given these radiation concerns, the development of reliable, radiation-free method for evaluating treatment outcomes is imperative for routine clinical use.

Intraoral scanning offers a non-invasive means of obtaining full-arch digital dental models, facilitating accurate diagnosis, treatment planning, and progress monitoring.[2, 3, 9] Superimposition of 3D digital models, using either landmark-based or surface-based registration techniques, enables precise analysis of tooth movement and arch dimensional changes in all three spatial planes, without the need for radiation.[3, 10, 11] Compared to 2D cephalometric superimposition, this digital method provides several advantages, such as the elimination of tracing errors, accurate size representation, absence of image distortion, and radiation-free assessment.[11] Consequently, numerous studies have explored various methods for applying 3D model superimposition in orthodontics.[1–3, 6, 10, 12–21]

Successful superimposition of digital models before and after treatment requires the identification of stable reference regions.[3, 17] For maxillary models, the medial 2/3 of the third ruga and the posterior area along the midpalatal suture have been proposed as stable reference structures since the least changes during treatment and the minimal deformation of the palatal mucosa during impression due to unmovable soft tissues of this area.[1, 2, 6, 10, 18, 19] However, a recent systematic review highlighted the scarcity of evidence supporting reference areas for mandibular digital model superimposition.[11]

An et al.,[3] evaluated the use of alveolar bone surfaces as reference regions for 3D mandibular model superimposition and reported unsatisfactory results in patients without mandibular tori, especially when the lingual alveolar surfaces of the anterior teeth were included, with discrepancies ranging from 1.5 to 10 mm when compared with cephalometric measurements. Park et al.,[6] proposed a method combining 3D CBCT images and digital models, suggesting that the best fit method on the basal bone surface of the mandible, which is unaltered by orthodontic treatment, offers a reliable, reproducible, and straightforward reference for mandibular arch superimposition, despite requiring the use of radiation to be performed.

To date, one study has attempted to validate a mandibular model superimposition technique without CBCT. Souza et al.,[20] presented a step-by-step protocol for 3D model superimposition of both arches using a single reference point defined within the Universal Coordinate System (UCS): the palatal rugae region for the maxilla and the lingual mucogingival junction for the mandible. However, since the study did not compare the method against a gold standard such as CBCT based superimpositions, its accuracy was not assessed.

Given the growing demand for radiation-free assessment methods and the lack of validated stable structures for digital model superimposition, the aim of the present study was to evaluate the reliability and reproducibility of a digital model superimposition technique, using the palatal rugae for the upper arch and the occlusion as the transfer reference for the lower arch, in comparison to CBCT-based superimposition.

Materials and Methods

This retrospective study included a sample of 10 patients (2 males, 8 females) with a mean age of 26 years at the beginning (ranging from 20 to 29 years) and 28 years (ranging from 22 to 32 years) at the end of treatment were selected. All patients underwent comprehensive non-extraction orthodontic treatment between 2016 to 2021. Inclusion criteria were complete permanent dentition, skeletal maturation cervical stage (CS) CS6 evaluated by cervical stage valuation (CSV) method [22] at pre- (T0) and post-treatment (T1) phases with records including full skull CBCTs, and upper and lower dental casts.

Each dental cast was scanned separately and in occlusion with the intraoral scanner iTero Element 2®, (Align Technologies, San Jose, California) and exported in a Standard Tessellation Language format (.stl). The digital casts were analyzed using a specific software (Geomagic Qualify 2013.0.1:64 Bit Edition program, Raindrop Geomagic, Inc, Cary, NC).

The superimposition method consisted of four main steps as follows (Figure 1):

1. CBCT orientation, superimposition, and segmentation
2. Superimposition of digital models onto CBCT
3. Superimposition of digital models on palatal rugae and occlusion
4. Landmark placement and accuracy assessment

		T0: pre-treatment	T1: post-treatment
Dolphin	Step 1: CBCT orientation, superimpositi-on and segmentation	Acquisition of CBCT (T0: pre-treatment)	Acquisition of CBCT (T1: post-treatment)
		CBCT T0 orientation	CBCT T1 superimposed on T0 and exported as T1's orientation
		Reconstruction of 3D maxillary and mandibular bones	Reconstruction of 3D maxillary and mandibular bones
		.stl files exportation as reference model T0 **(RMT0)**	.stl files exportation as reference model T1 **(RMT1)**
Geomagic	Step 2: Superimpositi on of digital model onto CBCT	Impression taking (T0: pre-treatment)	Impression taking (T1: post-treatment)
		Digital scanning of T0 upper and lower models **(MUT0 and MLT0)**	Digital scanning of T1 upper and lower models **(MTUT1 and MTLT1)**
		Digital models in occlusion .stl files exportation **(MOT0)**	Digital models in occlusion .stl files exportation **(MTOT1)**
		Integration with step 1	Integration with step 1
		MOT0 digital models on **RMT0** superimposition	**MTOT1** digital models on **RMT1** superimposition
		MOT0 digital models and **MUT0** digital model superimposition **MOT0** digital models and **MLT0** digital model superimposition	**MTOT1** digital models and **MTUT1** digital model superimposition **MTOT1** digital models and **MTLT1** digital model superimposition
	Step 3: Superimpositi on of digital model on palatal rugae and occlusion		T0 upper **(MUT0)** and T1 upper **(MAUT1)** digital models on palatal rugae superimposition
			MAUT1 and T1 model in occlusion **MAOT1** superimposition
			MAOT1 and T1 lower **(MALT1)** digital model superimposition
	Step 4: Landmark placement and accuracy assessment	Landmarks positioning (molars, canines and central incisors): **MUT0**, **MLT0**, **MTUT1**, **MTLT1**, **MAUT1** and **MALT1**	

Figure 1. Flowchart illustrating the four main steps of the superimposition method. Step 1 was performed using Dolphin Imaging, while steps 2 to 4 were completed in Geomagic Qualify software.

The digital datasets and abbreviations used in the study can be seen in the schematic illustration of Figure 2.

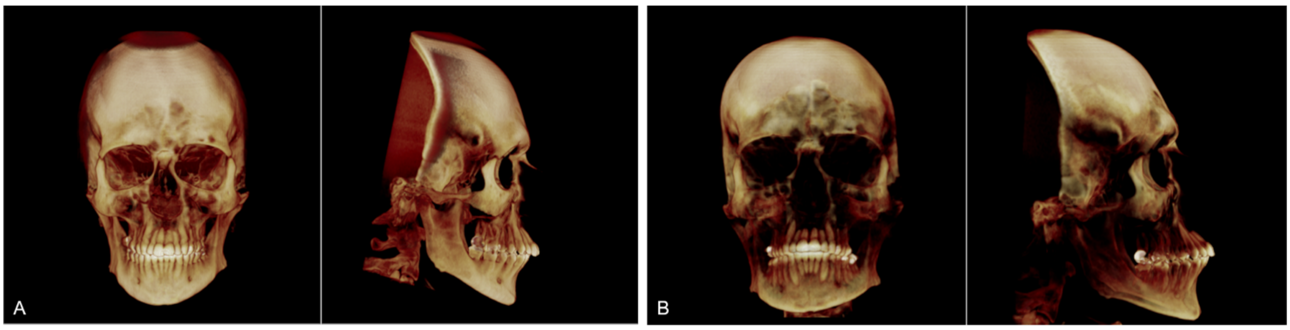

Figure 2. Schematic illustration of the digital datasets and abbreviations used in the study at pre- (initial: T0) and post-treatment (final: T1) for Tomography (Tomo) and Anatomy (Aanat) Groups.

Step 1. CBCT orientation, superimposition, and segmentation

Full head 3D CBCT image data was acquired with KODAK K9500® cone beam scanner (Carestream Health, Rochester, USA). The patient underwent CBCT scanning in facial mode (FOV 20 x 18 cm) with 0.2 mm isotropic voxel, exposure time of 10.8 seconds, 90 kVp and 10 mA. The reconstructed digital data was downloaded as digital imaging and communications in medicine (DICOM) files. Both initial and final (T0 and T1) DICOM data were uploaded to the Dolphin Imaging program (Dolphin

International, Chatsworth, California) and CBCT T0 was oriented according to the Frankfurt plane (Figure 3A). Since the patients examined in our sample were non-growing individuals, each CBCT T1 was superimposed on the CBCT T0 using the Dolphin Imaging voxel-based image registration on the cranial base (Figure 3B and 3C).

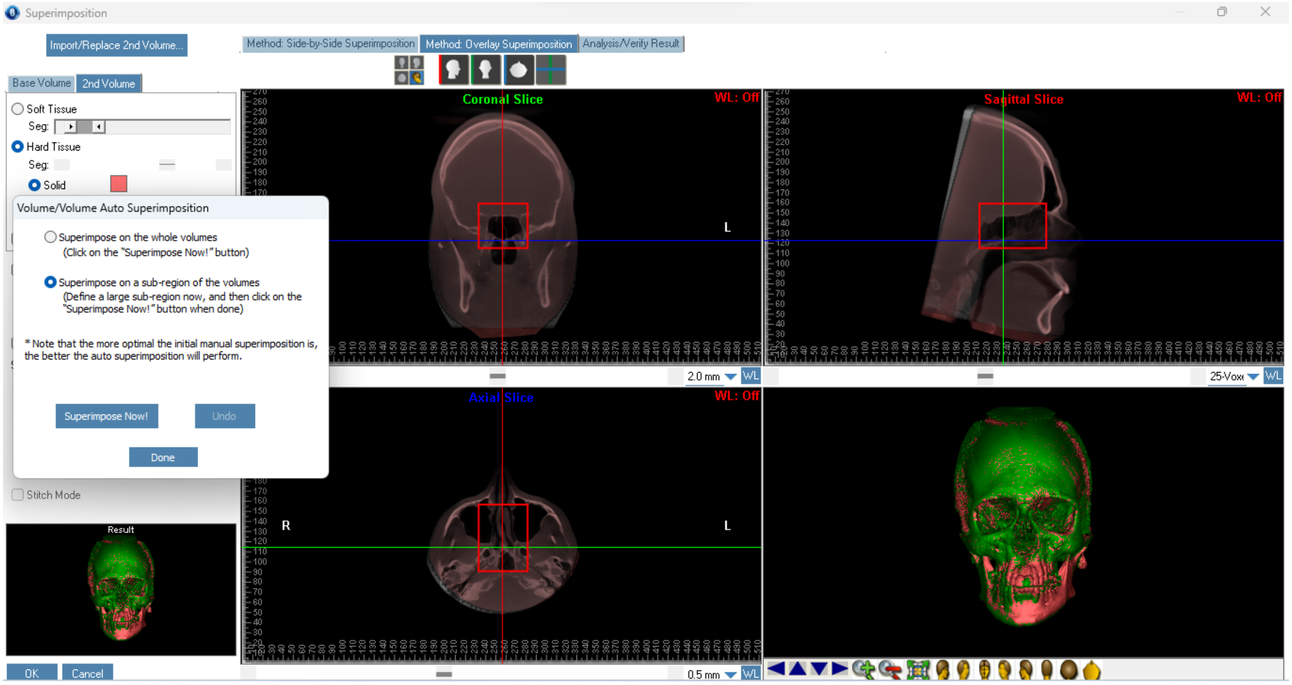

Figure 3. (A) Initial CBCT (**CBCT T0**) orientation based on the Frankfurt plane. (B) Final CBCT (**CBCT T1**) scan (yellow) superimposed onto the initial CBCT (**CBCT T0**) (blue) using voxel-based image registration on the cranial base (region outlined in red). (C) And final CBCT (**CBCT T1**) orientation after cranial base registration on the initial scan.

Then, upper and lower jaws of the CBCTs were segmented and exported as single .stl files named **RefT0** (reference model at T0) and **RefT1** (reference model at T1) (Figure 4).

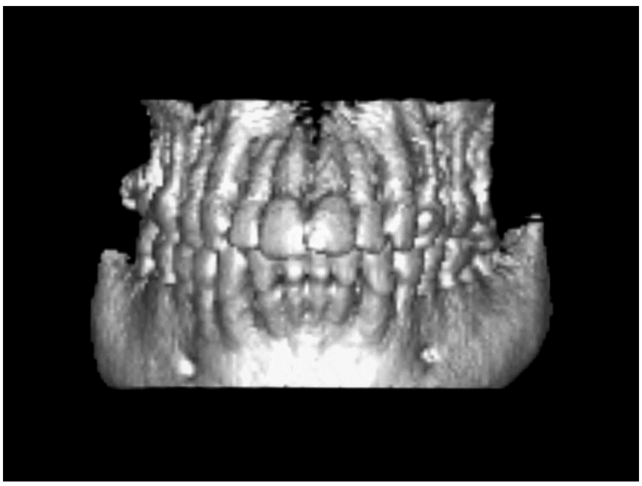

Figure 4. Segmentation of the upper and lower jaws in Dolphin Imaging Program of the initial and final CBCTs (**CBCT T0** and **CBCT T1**), exported as .stl files representing the reference models (**RefT0** and **RefT1** respectively).

Step 2. Superimposition of digital models onto CBCT

T0 and T1 digital models in occlusion, named respectively **ModelsT0** and **ModelsTomoT1**, were superimposed on their respective reference models (**RefT0** and **RefT1**) through the best fit alignment. To provide the best and larger common area to superimpose the buccal, lingual and occlusal surfaces of dental crowns of **ModelsT0** with **RefT0** and **ModelsTomoT1** with **RefT1** were selected (Figure 5).

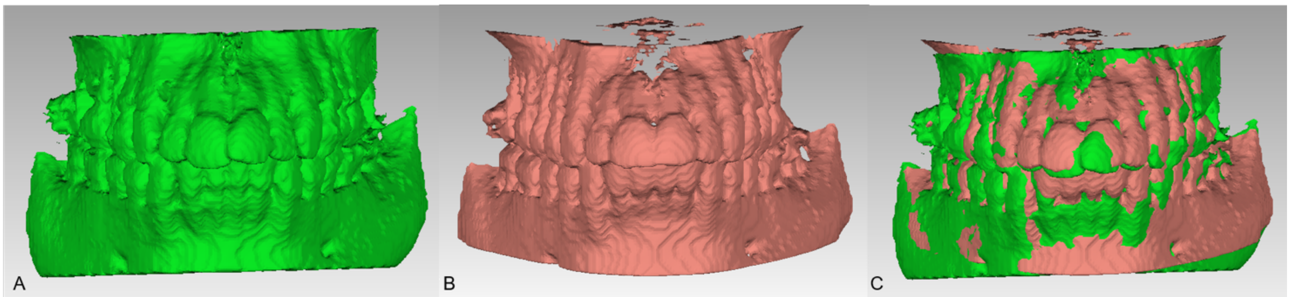

Figure 5. Dental crowns selected on digital model in occlusion (A) and CBCT (B) at T0. Final superimposition using best-fit alignment, registering the model to the CBCT (C). The same process was done to the digital models and CBCT at T1 of the Tomography Group.

Subsequently, single upper (**UModelT0** and **UTomoT1**) and lower (**LModelT0** and **LTomoT1**) digital models were individually superimposed on T0 and T1 digital models in occlusion (**ModelsT0** and **ModelsTomoT1**), which was previously superimposed to **RefT0** and **RefT1** (Figure 6).

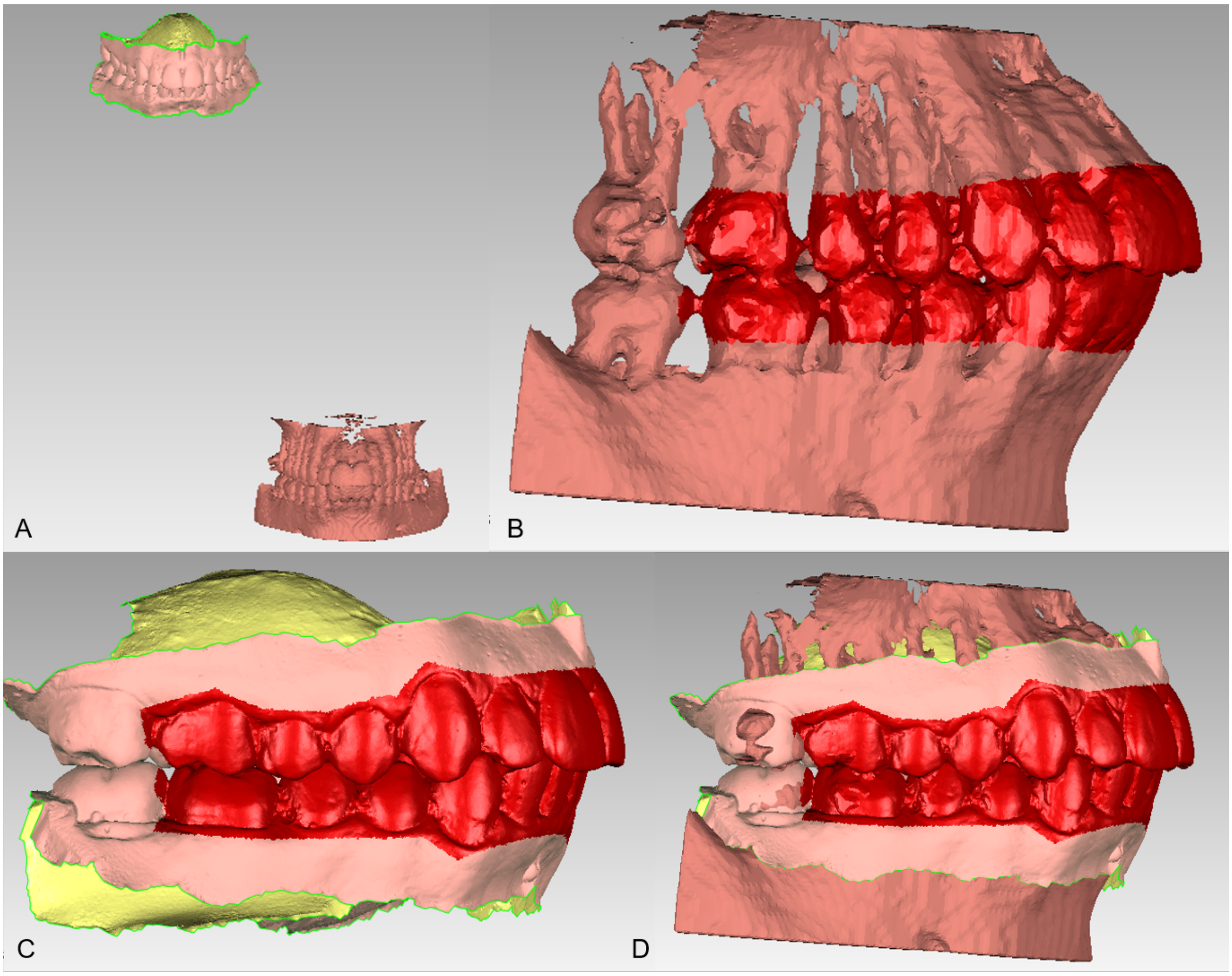

Figure 6. Single upper (**UModelT0** and **UTomoT1**) and lower (**LModelT0** and **LTomoT1**) digital models were individually superimposed on T0 and T1 digital models in occlusion (**ModelsT0** and **ModelsT1**), which was previously superimposed onto **RefT0** and **RefT1**. Initial superimposition is illustrated in blue and final superimposition in yellow.

Since the CBCTs orientation were the reference for superimposition, this group of superimpositions was called tomography (Tomo or t).

Step 3. Superimposition of digital models on palatal rugae and occlusion

A narrow area below the 2/3 of the third palatal rugae and along the mid palatal suture was selected to superimpose T1 (**UAnatT1**) and T0 (**UModelT0**) upper digital models using the best fit alignment.[6, 17, 18] Then, T1 digital model in occlusion (**ModelsAnatT1**) was superimposed to **UAnatT1**. Finally, T1 lower digital model (**LAnatT1**) was superimposed using the occlusion as reference (**ModelsAnatT1**). Since the superimposition reference areas were all anatomic structures, this group of superimpositions was called anatomy (Anat or a) (Figure 7).

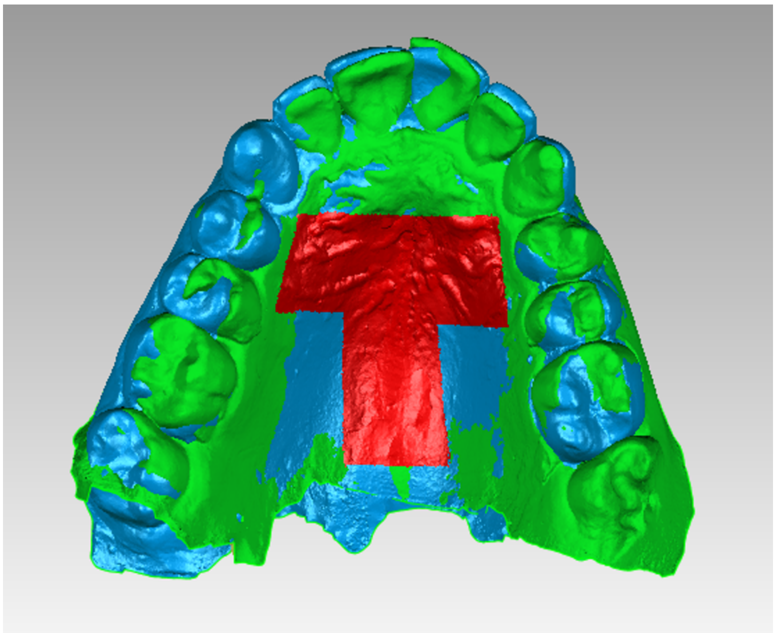

Figure 7. (A) Superimposition of final upper digital model on the initial upper (**UAnatT1** on **UModelT0**). (B) Then, T1 digital model in occlusion (**ModelsAnatT1**) was superimposed to **UAnatT1**. (C) Finally, T1 lower digital model (**LAnatT1**) was superimposed using the occlusion as reference (**ModelsAnatT1**). This was the superimposition of the anatomy group.

Step 4. Landmark placement and accuracy assessment

Landmarks were defined in the central fossa of the first molars, on the cusp tip of the canines and on the middle of the incisal edge of the central incisors. These landmarks were located on 6 models: **UModelT0**, **LModelT0**, **UTomoT1**, **LTomoT1**, **UAnatT1** and **LAnatT1** (Figure 8).

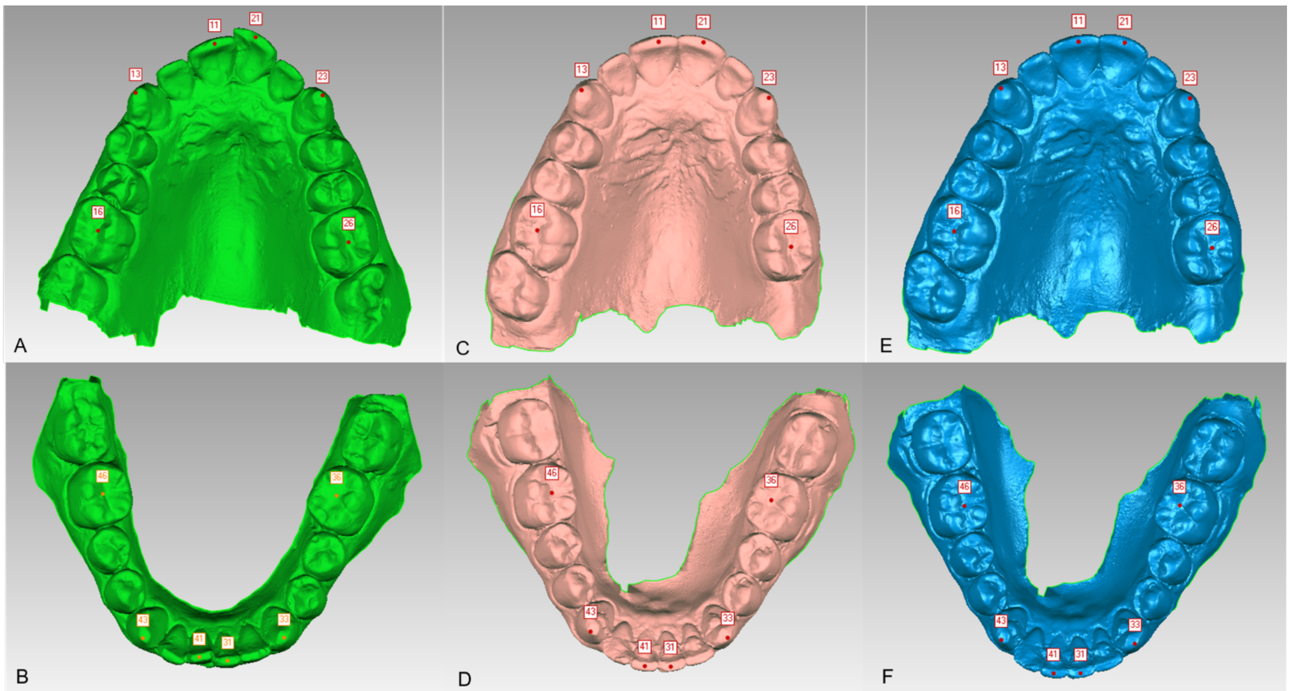

Figure 8. Marking of reference points on central incisors, canines, and first molars of the initial digital models (blue); final digital models superimposed using CBCT reference (yellow); and final digital models superimposed using rugae and occlusion reference (purple).

To establish an adequate reference system, a Cartesian coordinate system based on CBCT T0 orientation was determined for each patient. The axial plane corresponds to the x and y axis, the sagittal plane corresponds to the y and z axis, and the coronal plane to the x and z axis (Figure 9).

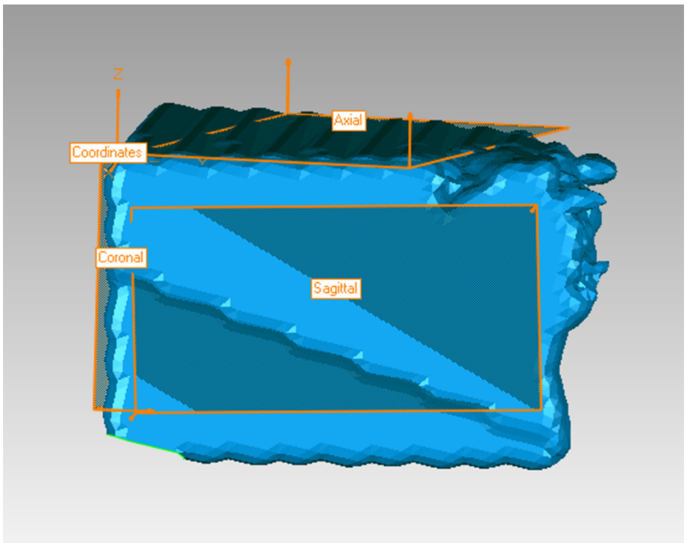

Figure 9. Illustration of the Cartesian Coordinate System based on the orientation of the CBCT T0. The axial plane corresponds to the x and y axes, the sagittal plane to the y and z axes, and the coronal plane to the x and z axes.

To evaluate the method accuracy, mean differences among **UTomoT1** and **UAnatT1** landmarks, and mean differences among **LTomoT1** and **LAnatT1** were examined (Figure 10).

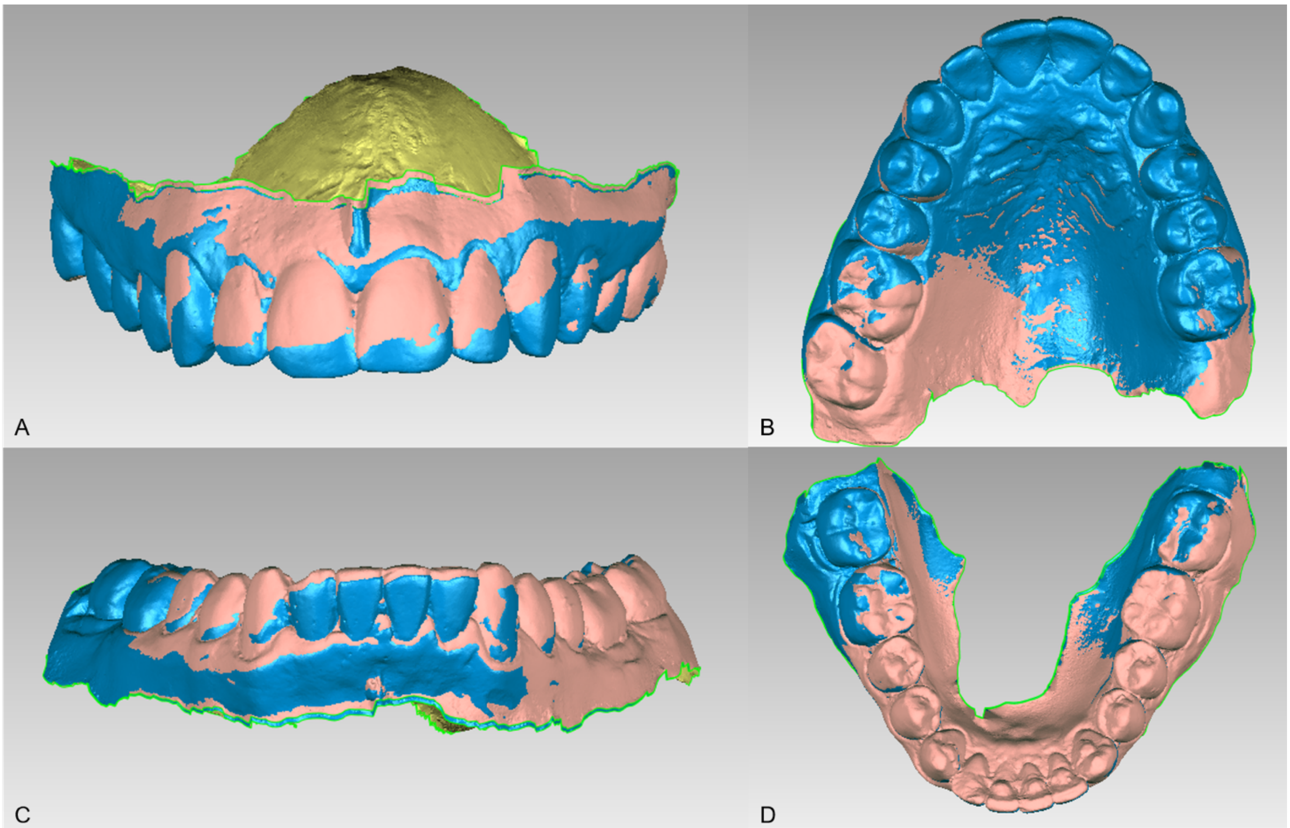

Figure 10. Comparison of superimposition methods for the upper and lower arches. Final digital models superimposed using CBCT reference are shown in A; those using rugae and occlusion are shown in B, and differences among Tomo and Anat groups are shown in C with models illustrated in yellow and purple respectively.

For each landmark, x, y, and z axis positions were recorded. Deviations in the z axis represents vertical movements (extrusion or intrusion); in the y axis anteroposterior movements for the incisors (retrusion or protrusion) and lateral movements for the molars (mesialization or distalization); and in the x axis lateral movements for the incisors (mesiodistal movements) or buccolingual movements for the molars. To determine the greatest divergences between the methods, mean differences for each landmark on each axis were compared.

Results

The mean and standard deviation of the tooth displacement measurements along each axis (x, y, and z) between T0 and T1, for each method (t and a) and each evaluator (1 and 2) are shown in Table I. The mean values for each method were similar for all types of movement in both arches. The inter-evaluator differences (Δ) ranged from-0.07 to 0.06, which is not considered clinically relevant.

Table 2 presents the intraclass correlation coefficients (ICCs) calculated to evaluate the reliability of each method. Coefficients were high ranging from 0.87 to 0.98. Student's t-test revealed no statistically significant differences between evaluators for each axis in each method (p>0.05). These results demonstrate that both methods were reliable, as each evaluator had high ICC values when superimposing models using either CBCT or anatomical structures as references.

Agreement between both methods was also high as shown in Table III. ICC values were ≥0.90 for all measurements, except for the z axis, which indicate vertical movements, where the ICC for evaluator 1 was 0.88.

The reproducibility of the methods assessed by ICCs is shown in Table IV. Both evaluators demonstrated high reproducibility, with ICCs ranging from 0.81 to 0.99 for evaluator 1 and from 0.95 to 0.99 for evaluator 2.

Figure 11 shows the Bland-Altman plot, where the Y axis represents the differences between the methods (Δ) and the X axis represents the tomography gold standard. The Bland-Altman 95% limits of agreement for the Δx, which describes lateral movements for the incisors (mesiodistal movements) or buccolingual movements for the molars, ranged from −2.18 mm to 1.89 mm for evaluator 1 and from −1.72 mm to 1.80 mm for evaluator 2, with the mean of 0.70 and 0.13 mm respectively (Figures A and D).

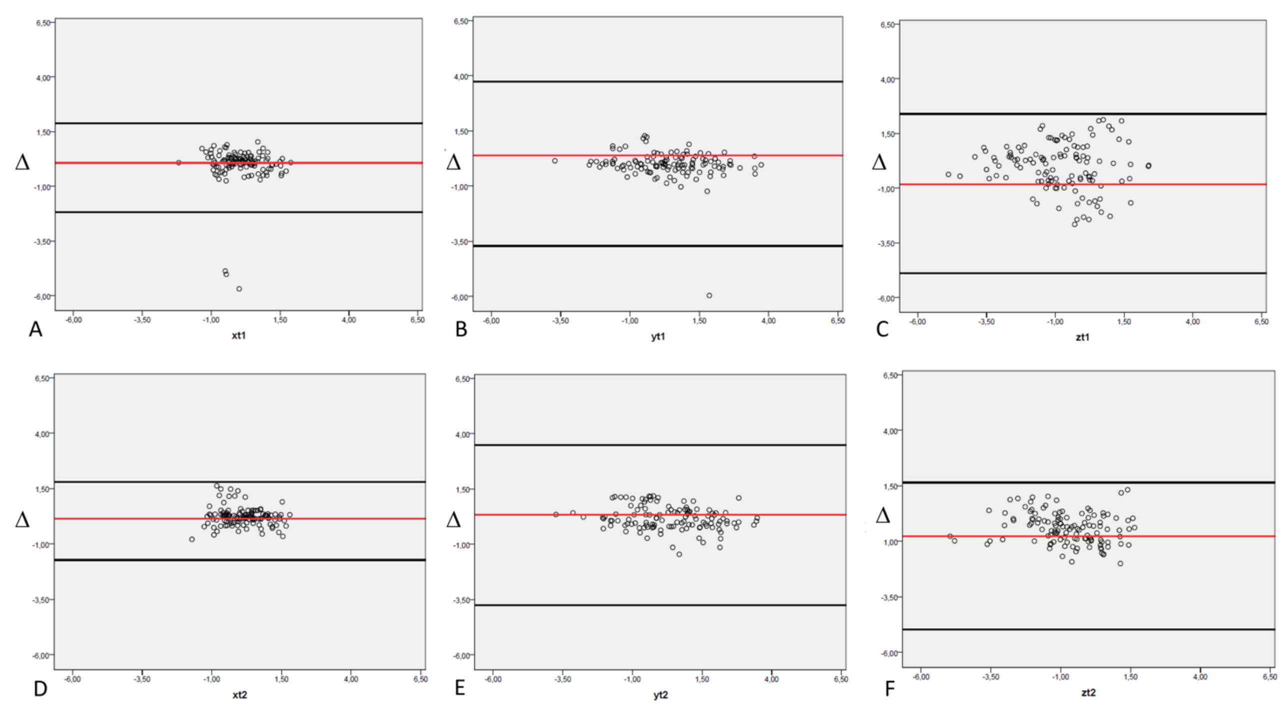

Figure 11. Bland-Altman plots showing agreement between superimposition methods. The Y-axis represents the difference between methods (Δ), and the X-axis represents the CBCT gold standard measurements.

The Δy, which shows anteroposterior movements for the incisors (retrusion or protrusion) and lateral movements for the molars (mesialization or distalization), ranged from −3.71 mm to 3.73 mm for evaluator 1 and from −3.75 mm to 3.48 mm for evaluator 2, with the mean of 0.38 and 0.33 mm respectively (Figures B and E). And Δz, that represents vertical movements (extrusion or intrusion), showed the greatest variation, ranging from −4.89 mm to 2.39 mm for evaluator 1 and from −4.96 mm to 1.65 mm for evaluator 2, with the mean of-0.83 and-0.76 mm respectively (Figures C and F). Overall, the distribution of results was similar across evaluators with the highest variability observed along the z axis as illustrated in Figure 11, C and F.

The Kaplan–Meier survival curves (Figure 12) illustrate the cumulative probability of maintaining lower measurement errors for each movement axis across the two evaluators.

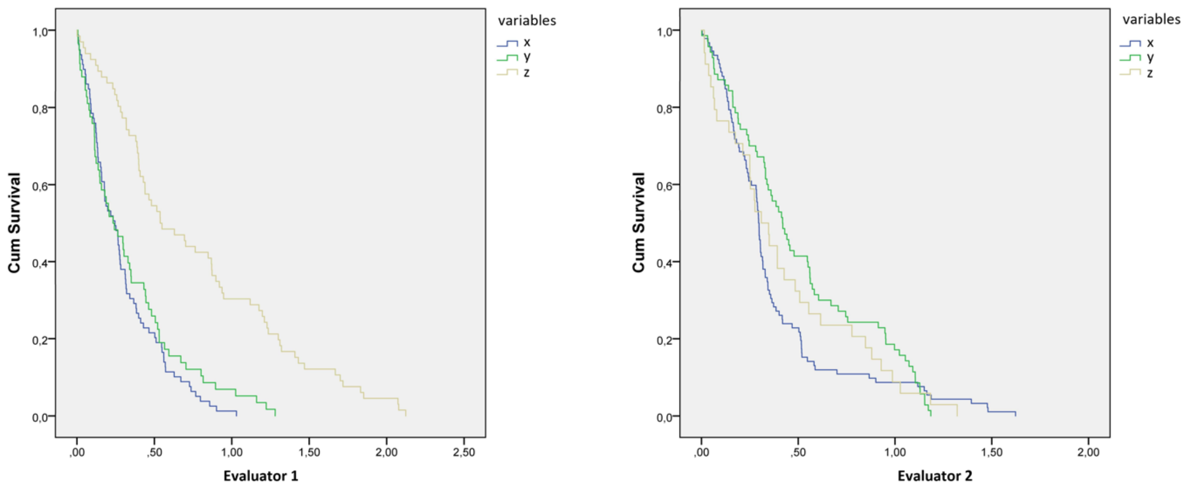

Figure 12. Kaplan–Meier survival curves for tooth movements along the x, y, and z axes assessed by two evaluators. Z axis showed the highest survival, x axis the lowest, and y axis intermediate values. Evaluator 1 demonstrated clearer separation among axes, while evaluator 2 presented a more uniform result.

For both evaluators, vertical movements (z axis) showed the highest survival, indicating greater consistency in detecting extrusion and intrusion. X axis presented the lowest survival probabilities, reflecting reduced reliability, while y axis demonstrated intermediate results. Notably, evaluator 1 showed clearer separation among the three axes, suggesting greater sensitivity to directional differences, whereas evaluator 2 exhibited more overlapping curves, indicating more uniform performance across axes.

Discussion

The present study proposed and validated a new method for superimposing digital models of orthodontic patients without relying on CBCT imaging and therefore without radiation exposure. Previous research has consistently demonstrated the reliability of the palatal rugae for evaluating tooth movement for the maxillary arch before and after orthodontic treatment.[1-3, 10, 13, 15, 17, 21, 23, 24]

In particular, the second and third palatal rugae are considered stable reference structures, whereas the first ruga is more susceptible to displacement,[25] especially during incisor retraction, with or without extractions.[1, 2, 13] Several studies have identified the medial rugae points and the area approximately 5 mm posterior to the third palatal rugae as highly stable and reliable landmarks, often regarded as the gold standard for maxillary model superimposition.[1, 2, 13] Accordingly, in the present study, upper arch superimpositions were based on these regions to maximize stability and consistency.

In contrast, mandibular model superimposition remains less studied, largely due to the scarcity of stable anatomical landmarks in the lower arch.[26] No consensus has yet been reached regarding the optimal technique for serial 3D mandibular superimpositions, and conventional registration references each present inherent limitations. For this reason, the present study used the occlusal plane as the reference area for lower arch superimposition, with results compared against CBCT-based measurements. While the occlusal plane is sensitive to changes in its orientation, potentially introducing variability in z-axis measurements, as shown in the Bland-Altman plots (Figure 11C and F), it demonstrated greater consistency in this study than previously proposed anatomical references.[3, 20] These findings are in accordance with Bailey,[27] where second and third palatal rugae were considered stable in the sagittal and in the transversal plane, with less precision in the vertical plane.

The difficulty in defining reliable mandibular references is supported by previous findings: An et al.[3] reported that alveolar surfaces were unreliable in patients without mandibular tori due to extensive remodeling during orthodontic treatment, particularly in growing individuals, while Souza et al.[20] noted reduced reliability when restorative or periodontal procedures occurred during treatment. Alternative approaches have been proposed, such as using the bilateral mandibular tori[3] or surface-based methods,[6] both of which have shown mean discrepancies of less than 1 mm, consistent with the present study's results. Similarly, Oueiss et al.[12] found no statistically significant differences between 2D cephalometric and 3D model superimposition measurements.

Patient selection was a deliberate methodological choice. The majority of previous research on 3D model superimposition has focused on adult patients, as growth-related changes complicate longitudinal comparisons.[13, 24] In the present study, only non-growing patients were included to validate the method without the confounding influence of growth, in line with evidence on anatomical stability[28] and with ethical considerations to minimize radiation exposure in younger patients. Sample size in the literature varies widely, with substantial methodological heterogeneity and limited standardization.[3, 6, 11, 12, 20] Studies have ranged from single-case reports to larger cohorts. In the present study, 10 patients were included, consistent with prior validation research demonstrating that this sample size is sufficient for drawing reliable conclusions.

Traditionally, orthodontic tooth movement has been assessed by superimposing pre- and post-treatment cephalometric radiographs on stable skeletal landmarks. [3, 13-15, 29] However, this 2D method is limited by magnification errors, image distortion, and superimposition of bilateral structures, all of which complicate landmark identification and introduce tracing errors.[3, 13, 16] Moreover, cephalometric radiographs lack the comprehensive, high-resolution detail of CBCT or 3D intraoral models. Notably, Liu et al.[30] demonstrated that lateral cephalogram superimpositions and palatal rugae-based 3D model superimpositions are equally reliable, supporting the use of radiation-free digital methods when appropriate. For these reasons, CBCT superimposition was adopted as the gold standard for comparison in the present study.

Clinically, discrepancies greater than 2 mm or 2 degrees on lateral cephalograms are generally considered significant. In this context, discrepancies of less than 1 mm between the present method and CBCT-based superimposition can be considered more than acceptable for assessing tooth movement, particularly given that the method is radiation-free. The 3D model superimposition approach evaluated here- using palatal rugae for the maxillary arch and the occlusal plane for the mandibular arch- demonstrated excellent reliability (Table 3) and reproducibility (Table 4). It offers an accurate, efficient, and non-invasive option for assessing orthodontic treatment outcomes in adult non-extraction cases.

In the present study, the superimpositions to assess tooth movement were performed on digital models obtained by scanning plaster casts with an intraoral scanner, rather than on direct intraoral scans. This additional digitization step may introduce minor artefacts, which, as demonstrated by Henninger et al.,[31] can lead to distortions in superimposition outcomes. In addition, although the measurements were performed using high-reliability software,[32, 33] they relied on manually traced points placed by two operators on the upper and lower molars, canines, and incisors at both pre- and post-treatment stages. This procedure may increase the potential for intra- and inter-examiner variability. A possible refinement would be to apply centroid calculations after highlighting a surface with precise coordinates, which was a method previously used successfully by Heni et al.,[34] thereby minimizing distortions attributable to measurement errors.

Future research should investigate the method's applicability in growing patients and in more complex treatment scenarios, such as extractions or orthognathic surgery. Establishing universally accepted, reliable anatomical landmarks, particularly for the lower arch, will be key to integrating 3D model superimposition into routine orthodontic practice as a practical, accurate, and radiation-free alternative to CBCT.

Conclusion

Three-dimensional digital model superimposition, using the palatal rugae as a reference for the maxillary arch and the occlusion for the mandibular arch is a reliable and reproducible method for assessing orthodontic tooth movements in non-growing patients treated without extractions.

References

1. Jang I, Tanaka M, Koga Y, Iijima S, Yozgatian JH, Cha BK, et al. A novel method for the assessment of three-dimensional tooth movement during orthodontic treatment. Angle Orthodontist. 2009;79(3):447–53.
2. Chen G, Chen S, Zhang XY, Jiang RP, Liu Y, Shi FH, et al. Stable region for maxillary dental cast superimposition in adults, studied with the aid of stable miniscrews. Orthod Craniofac Res. 2011;14(2):70–9.
3. 3. An K, Jang I, Choi DS, Jost-Brinkmann PG, Cha BK. Identification of a stable reference area for superimposing mandibular digital models. Journal of Orofacial Orthopedics. 2015;76(6):508–19.
4. Cevidanes LHS, Bailey LJ, Tucker GR, Styner MA, Mol A, Phillips CL, et al. Superimposition of 3D cone-beam CT models of orthognathic surgery patients. Dentomaxillofacial Radiology. 2005;34(6):369–75.
5. Nada RM, Maal TJJ, Breuning KH, Bergé SJ, Mostafa YA, Kuijpers-Jagtman AM. Accuracy and reproducibility of Voxel based superimposition of Cone Beam Computed Tomography Models on the anterior cranial base and the zygomatic arches. PLoS One. 2011;6(2).
6. Park TJ, Lee SH, Lee KS. A method for mandibular dental arch superimposition using 3D cone beam CT and orthodontic 3D digital model. Korean J Orthod. 2012;42(4):169–81.
7. Yatabe M, Prieto JC, Styner M, Zhu H, Ruellas AC, Paniagua B, et al. 3D superimposition of craniofacial imaging—The utility of multicentre collaborations. Orthod Craniofac Res. 2019;22(S1):213–20.
8. Sedentexct. Radiation Protection 172: Cone Beam CT for Dental and Maxillofacial Radiology-Evidence-based Guidelines. Office for Official Publications of the European Communities. 2012;156.
9. Francisco I, Ribeiro MP, Marques F, Travassos R, Nunes C, Pereira F, et al. Application of Three-Dimensional Digital Technology in Orthodontics: The State of the Art. Biomimetics. 2022;7(1):1–14.
10. Cho MY, Choi JH, Lee SP, Baek SH. Three-dimensional analysis of the tooth movement and arch dimension changes in Class i malocclusions treated with first premolar extractions: A guideline for virtual treatment planning. American Journal of Orthodontics and Dentofacial Orthopedics. 2010;138(6):747–57.

11. Stucki S, Gkantidis N. Assessment of techniques used for superimposition of maxillary and mandibular 3D surface models to evaluate tooth movement: A systematic review. Eur J Orthod. 2020;42(5):559–70.
12. Oueiss A, Camia J, Masucci C, Charavet C, Joseph C. Exploring the mylohyoid area as a reference for three-dimensional digital mandibular superimposition. J Stomatol Oral Maxillofac Surg. 2022;123(6):672–6.
13. Anacleto MA, Souki BQ. Superimposition of 3d maxillary digital models using open-source software. Dental Press J Orthod. 2019;24(2):81–91.
14. Cha BK, Lee JY, Jost-Brinkmann PG, Yoshida N. Analysis of tooth movement in extraction cases using three-dimensional reverse engineering technology. Eur J Orthod. 2007;29(4):325–31.
15. Choi J Il, Cha BK, Jost-Brinkmann PG, Choi DS, Jang IS. Validity of palatal superimposition of 3-dimensional digital models in cases treated with rapid maxillary expansion and maxillary protraction headgear. Korean J Orthod. 2012;42(5):235–41.
16. Ashmore JL, Kurland BF, King GJ, Wheeler TT, Ghafari J, Ramsay DS. A 3-dimensional analysis of molar movement during headgear treatment. American Journal of Orthodontics and Dentofacial Orthopedics. 2002;121(1):18–29.
17. Camardella LT, Vilella O V., Breuning KH, de Assis Ribeiro Carvalho F, Kuijpers-Jagtman AM, Ongkosuwito EM. The influence of the model superimposition method on the assessment of accuracy and predictability of setup models. Journal of Orofacial Orthopedics. 2021;175–86.
18. Talaat S, Kaboudan A, Bourauel C, Ragy N, Kula K, Ghoneima A. Validity and reliability of three-dimensional palatal superimposition of digital dental models. Eur J Orthod. 2017;39(4):365–70.
19. Pan Y, Wang X, Dai F, Chen G, Xu T. Accuracy and reliability of maxillary digital model (MDM) superimposition in evaluating teeth movement in adults compared with CBCT maxillary superimposition. Sci Rep. 2020;10(1):1–8.
20. de Souza RXS, de Souza GAS, Colares JP, Ianni TM de S, de Magalhães CS, Guerrero-Vargas JA, et al. A new way of analyzing tooth movement using universal coordinate system geometry single point superposition in a 3D model. Vol. 28, Dental Press Journal of Orthodontics. 2023. 1–53 p.
21. Hoggan BR, Sadowsky C. The use of palatal rugae for the assessment of anteroposterior tooth movements. American Journal of Orthodontics and Dentofacial Orthopedics. 2001;119(5):482–8.

22. Baccetti T, Franchi L, McNamara JA. The Cervical Vertebral Maturation (CVM) method for the assessment of optimal treatment timing in dentofacial orthopedics. Semin Orthod. 2005;11(3):119–29.
23. Peavy DC, Kendrick GS. The effects of tooth movement on the palatine rugae. J Prosthet Dent. 1967;18(6):536–42.
24. Almeida MA, Phillips C, Kula K, Tulloch C. Stability of the palatal rugae as landmarks for analysis of dental casts. Angle Orthod. 1995;65(1):43–8.
25. Pazera C, Gkantidis N. Palatal rugae positional changes during orthodontic treatment of growing patients. Orthod Craniofac Res. 2021 Aug;24(3):351-359. doi: 10.1111/ocr.12441. Epub 2020 Dec 1. PMID: 33200559.
26. Adel SM, Vaid NR, El-Harouni N, Kassem H and Zaher AR. TIP, TORQUE & ROTATIONS: How accurately do digital superimposition software packages quantify tooth movement? Progress in Orthodontics (2022) 23:8 https://doi.org/10.1186/s40510-022-00402-x.
27. Bailey LT, Esmailnejad A, Almeida MA. Stability of the palatal rugae as landmarks for analysis of dental casts in extraction and nonextraction cases. Angle Orthod. 1996;66(1):73-8. doi: 10.1043/0003 3219(1996)066<0073:SOTPRA>2.3.CO;2. PMID: 8678349.
28. Oenning AC, Jacobs R, Pauwels R, Stratis A, Hedesiu M, Salmon B, et al. Cone-beam CT in paediatric dentistry: DIMITRA project position statement. Pediatr Radiol. 2018;48(3):308–16.
29. McDonagh S, Moss JP, Goodwin P, Lee RT. A prospective optical surface scanning and cephalometric assessment of the effect of functional appliances on the soft tissues. Eur J Orthod. 2001;23(2):115–26
30. Liu J, Koh KM, Choi SH, Kim JH, Cha JY. Validation of three-dimensional digital model superimpositions based on palatal structures in patients with maximum anterior tooth retraction following premolar extraction. Korean J Orthod. 2022 Jul 25;52(4):258-267. doi: 10.4041/kjod21.126. PMID: 35875849; PMCID: PMC9314216.
31. Henninger E, Vasilakos G, Halazonetis D, Gkantidis N. The effect of regular dental cast artifacts on the 3D superimposition of serial digital maxillary dental models. Sci Rep. 2019 Jul 19;9(1):10501. doi: 10.1038/s41598-019-46887-1. PMID: 31324833; PMCID: PMC6642138.
32. Adel SM, Vaid NR, El-Harouni N, Kassem H, Zaher AR. Digital model superimpositions: are different software algorithms equally accurate in quantifying linear tooth movements? BMC Oral Health. 2022 Mar 31;22(1):103. doi: 10.1186/s12903-022-02129-x. PMID: 35361187; PMCID: PMC8973572.

33. Meade MJ, Weir T, Byrne G. Comparison of digital study model superimposition methods using implant-supported crowns and best-fit algorithms. Am J Orthod Dentofacial Orthop. 2024 Oct;166(4):384-392.e2. doi: 10.1016/j.ajodo.2024.06.009. Epub 2024 Jul 23. PMID: 39046381.
34. Heni C, Henninger E, Pazera P, Vasilakos G, Gkantidis N. 3D palatal superimposition in adolescent orthodontic patients treated without extractions: method validation. Clin Oral Investig. 2025 May 5;29(5):285. doi: 10.1007/s00784-025-06350-0. PMID: 40320466; PMCID: PMC12050233.

Chapter 4: 3D printing

4.1 Influence of printing orientation on flexural strength and flexural modulus of 3D printed resins for occlusal splints before and after water aging.

Abstract

The aim of this study was to assess the effect of printing orientation and water ageing on the flexural strength and flexural modulus of 3D printed resins for occlusal splints. Bar-shaped specimens were designed with dimensions of 64 × 10 × 3.3 mm according to ISO 20795-2: 2013. Specimens were 3D printed with the Form 3B printer (Formlabs), using Dental LT Clear Resin (CL) or Comfort Resin (CO) (Formlabs), and 3 different printing orientations: as per manufacturer's recommendation (40° N=20), parallel (0° N=20), or perpendicular to the build platform (90° N=20). To simulate intraoral ageing, half of the specimens per material and printing orientation (N=10) were stored in distilled water at 37°C for 30 days prior to testing. Specimens were tested in a 3-point bending apparatus using a universal testing machine equipped with a 50 N load cell moving at a crosshead speed of 5 mm/min. Flexural strength (MPa) and flexural modulus (GPa) data were collected and statistically processed with separate analyses for unaged and aged specimens (two-way or one-way ANOVA; Tukey test; $p < 0.05$). In dry conditions, both resin materials exhbited highest flexural strenghth and modulus in the 90° orientation group and lowest in the 40° orientation group. After water aging, all groups showed reduced flexural strength and modulus, with CO displaying up to 52% loss in flexural strength and values falling below ISO thresholds. CO exhibited consistently significantly lower flexural strength and modulus than CL among irrespective of aging.

Introduction

With a groundbreaking impact on dentistry, additive manufacturing, also known as 3D printing, has been effectively utilized for the fabrication of several customized dental devices, including occlusal splints [1,2]. Occlusal splints are intraoral devices commonly used to address temporomandibular joint disorders and parafunctional muscular activities by modifying occlusal contacts and jaw relationship, with the intention to reduce muscle tightness and alleviate clinical symptoms. They also provide protection against tooth wear [3,4]. Traditionally, occlusal splints have been manufactured with conventional methods, such as wax modelling and thermoforming techniques [5]. However, the new technologies of intraoral scanning, 3D modelling, and 3D printing have enabled the production of occlusal splints with enhanced fit and greater control over materials thicknesses, easing the achievement of occlusal contact balance. Reduction of laboratory time and limitation of material waste are also reported benefits of the digital workflow [3,6,7]. The variety of available materials has been considered as another advantage of 3D printing in dentistry, and resins specifically meant for occlusal splints fabrication have been marketed [2].

When assessing the mechanical properties of 3D-printed occlusal splints [7,8], several factors, such as resin composition [9-13], printing technology [13,14], layer thickness [14-16], and post-curing methods [15-17] were found to be relevant. Nevertheless, printing orientation [16,18-25] and storage media [11,13,15,23,26-29] were identified as the most influential variables.

As 3D printing produces the manufacts in a layer-wise manner, printing orientation has been reported to have a significant influence on the flexural strength and modulus of 3D-printed devices [18,30]. When a force is applied, the between-layer interfaces are deemed as points of weakness, owing to the possible presence of voids or to insufficient adhesion between the layers. [31]. Moreover, the layered configuration renders the 3D printed structures inherently anisotropic, i.e. displaying different mechanical behavior depending on the direction of the force applied. Anisotropy in turn generates varying levels of internal stresses within the printed devices, which can impact their resistance to bending [18,30]. It therefore appeared interesting to verify to what extent the printing orientation parameter affects the mechanical properties of resins indicated for 3D printing of occlusal splints [19,30].

Another phenomenon with relevant influence on the mechanical characteristics of dental resins is water sorption, wherein resin materials absorb moisture from the surroundings. Prolonged water sorption incites the hydrolytic degradation of the chemical bonds between the resin matrix and surrounding fillers, and triggers the release of leachable resin elements into the oral environment, both of which accumulatively weaken the integrity of the overall 3D printed polymer structure [32]. Water sorption of 3D-printed resin restorations has been confirmed to adversely impact their dimensional accuracy, mechanical durability, and long-term stability by means of the plasticizing effect of water molecules [30,32-35].

Few studies previously assessed the mechanical properties of 3D printed resins for occlusal splints, after water storage to simulate intraoral ageing [10,13,15]. However, the adopted experimental set-ups differed largely among studies, hindering a meaningful comparison among their findings. Additionally, the current literature has overlooked a 3D printed resin that has gained significant diffusion in the dental community, also due to its use in the fabrication of orthodontic retainers. The referred resin is Dental LT Clear v2 (Formlabs, Sommerville, MA, USA, C). Lately, the same manufacturer has introduced an innovative resin for 3D printing of occlusal splints, Dental LT Comfort (Formlabs), stating that the material provides increased flexibility, greater resistance to fracture and wear, in addition to enhanced transparency. These claims, however, need to be validated independently.

Thereby, the present study was aimed at comparatively assessing the mechanical behavior under flexural loading of Dental LT Clear v2 and Comfort resin specimens, printed at different angulations to the build platform, before and after water storage. Flexural strength and flexural modulus data were acquired using a three-point bending model. The tested null hypothesis was that no difference in flexural strength or modulus existed between the two materials regardless of printing orientation and ageing.

Materials and Methods

Specimen preparation

Table 1 reports the chemical composition of the two tested resins: Dental LT Clear v2 (CL) and Dental LT Comfort (CO).

Table 1. Description of characteristics and compositions of the investigated dental resins.

Material (manufacturer)	Manufacturing method	Abbr.	System (manufacturer)	Composition (wt %)
Dental LT Clear v2 (Formlabs, Somerville, Massachusetts, USA)	Low force SLA printing	CL	Form 3B (Formlabs)	Bisphenol A dimethacrylate (50-70%) Urethane dimethacrylate (25-45%) Methacrylate Monomer(s) (7-10%) Photoinitiator(s) (<2%)
Dental LT Comfort (Formlabs, Somerville, Massachusetts, USA)	Low force SLA printing	CO	Form 3B (Formlabs)	Urethane dimethacrylate (55-75%) PEG dimethacrylate (15-25%) Methacrylate Monomer (10-20%) Initiator (<1%)

Following ISO 20795-2:2013, which applies to orthodontic base polymers and co-polymers used in both active and passive orthodontic appliances, specimens with dimensions of 64 × 10 × 3.3 mm were designed using Tinkercad software (Autodesk, San Rafael, CA, USA, accessed online on March 3rd, 2023). The design file was exported in STL format and imported into PreForm software 3.28.1 (Formlabs, Somerville, MA, USA) for automatic support generation and slicing.

To assess the influence of printing orientation on flexural properties, specimens were designed at three different orientations relative to the build platform: parallel (0°), perpendicular (90°), and manufacturer-recommended angulation (40°) (Fig. 1).

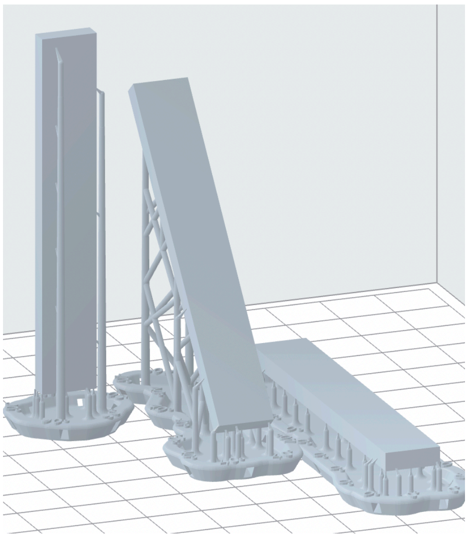

Figure 1. Digital diagram showing the different printing orientations (90°, 40°, 0°) for the resin specimens.

For each material and printing orientation, 20 specimens were fabricated using a Form 3B stereolithography (SLA) printer (Formlabs, Somerville, MA, USA), with a layer thickness of 100 µm. CL specimens were washed in isopropyl alcohol (IPA, ≥99%) using the Form Wash device (Formlabs, Somerville, MA, USA) for 15 minutes. An additional 5-minute wash in fresh IPA followed. After drying at room temperature for at least 30 minutes, specimens were post-cured in the Form Cure curing machine (Formlabs, Somerville, MA, USA) at 60°C for 60 minutes, according to the manufacturer's recommendations. CO specimens were washed with IPA (≥99%) in the Form Wash device (Formlabs, Somerville, MA, USA) for 10 minutes. After drying at room temperature for at least 30 minutes, specimens were post-cured in the Form Cure machine (Formlabs, Somerville, MA, USA) at 60°C for 20 minutes, as per manufacturer's instructions. Subsequently, supports were removed using a cutting disk (Horico Diamond Disc Double Sided Handpiece 355C/220 2.2 mm, HORICO DENTAL Hopf, Ringleb & Co. GmbH & Cie, Berlin, Germany), mounted on a handpiece.

In accordance with ISO 20795-2:2013, the height of the specimens was measured at three points along the long axis using a digital caliper (Beta Utensili S.p.A., Sovico, Italy) with an accuracy of ± 0.01 mm, and it was verified that the deviation between measurements did not exceed ± 0.02 mm.

Artificial ageing protocol

All the specimens were stored in a water bath at 37°C for 5 minutes to simulate the oral environment [36], still in accordance with ISO 20795-1. For each combination of material and printing orientation, half of the specimens, selected at random, were tested immediately after production, at room temperature and under dry conditions. The remaining specimens were stored in distilled water at 37°C for 30 days prior to testing.

Flexural strength test

The three-point bending test apparatus consisted of a central loading plunger (anvil) and two cylindrical supports (rollers), each 3.2 mm in diameter. The distance between the centers of the supports was maintained at 50 ± 0.1 mm, and the loading plunger was positioned within 0.1 mm of the midpoint between the supports (Fig. 2).

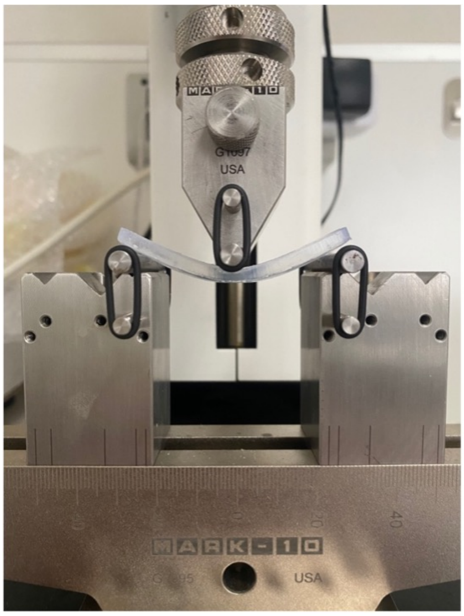

Figure 2. Experimental setup for the three-point bending test. The resin specimen is positioned with its central portion aligned under the crosshead.

Testing was performed using a universal testing machine (ESM 301 Mark-10, Copiague, NY, USA) equipped with a 50 N load cell (M5-50, Mark-10, Copiague, NY, USA), at a crosshead speed of 5 mm/min. The test was terminated when the specimen deflection reached 15 mm, according to the Perea-Lowery protocol [10]. The direction of the applied load in relation to the printed resin layers is illustrated in Figure 3.

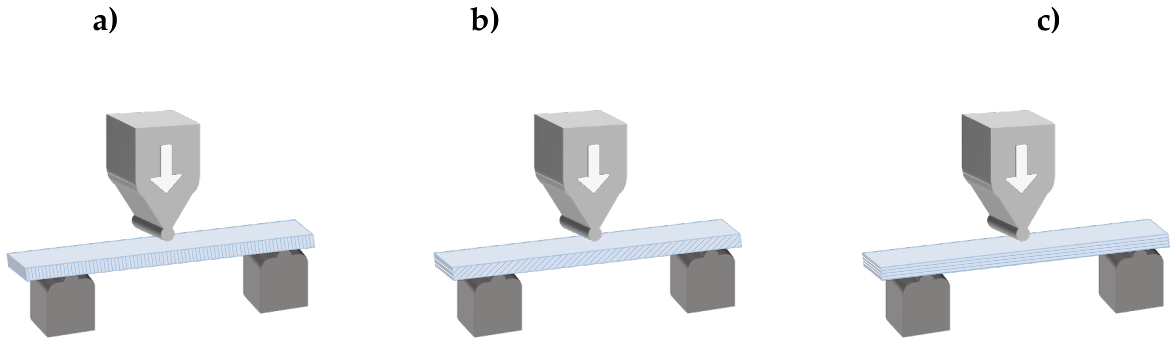

Figure 3. a) Experimental setup for the three-point bending test of a resin specimen printed at 90° (a), 40° (b), and 90° (c) to the build platform.

The fracture load was recorded in Newtons (N), and the flexural strength (σ) was calculated in megapascals (MPa) using the following formula:

$$\sigma = \frac{3Fl}{2wh^2}$$

The flexural modulus (E) was calculated in gigapascals (GPa) using the formula:

$$E = \frac{Fl^3}{4wh^3d}$$

where F is the fracture load in Newton, l is the distance between the supports in millimeters, w is the width in millimeters, h is the height in millimeters and d is the deflection in millimeters at load F.

Statistical analysis

Flexural strength

As the overall distribution of the collected flexural strength data was not normal according to the Shapiro-Wilk test, the use of a three-way Analysis of Variance (ANOVA) with flexural strength as the dependent variable, material type, print angulation, and water storage as factors was precluded. Thereby, two separate statistical analyses were applied to unaged and aged specimens.

Flexural strength of unaged specimens

As the data met the requirements of normality of data distribution (Shapiro-Wilk test) and homogeneity of group variances (Levene test), the two-way ANOVA was applied, with flexural strength as the dependent variable, material type and print angulation as the independent variables. The statistical significance of each factor, as well as of the between-factor interaction was assessed. The Tukey test was applied for post hoc comparisons as needed.

Flexural strength of aged specimens

The finding that the data distribution was not normal according to the Shapiro-Wilk test ruled out the use of a two-way ANOVA with flexural strength as the dependent variable, material type, and print angulation as factors. Therefore, two distinct one-way ANOVAs had to be applied to the data, separately assessing the statistical significance of the influence of material type and of print angulation. The Tukey test was used for post-hoc comparisons as needed.

Flexural modulus

The same statistical analysis as for the flexural strength data of aged specimens had to be applied to the flexural modulus data of aged and unaged specimens separately. In all the tests the level of significance was set at $p < 0.05$. Statistical calculations were handled by the PASW Statistics 18 software (SPSS Inc., Chicago, IL, USA).

Results

Flexural strength of unaged specimens

Table 2 reports the descriptive statistics of flexural strength measurements in MPa of unaged specimens, along with the outcome of the statistical analysis. The two-way ANOVA disclosed that the type of material was an effective factor for flexural strength per se ($p<0.001$). Specifically, regardless of the print angulation, CO exhibited a significantly lower flexural strength than CL. Print angulation was also a significant factor per se ($p<0.001$). Irrespective of the resin type, specimens printed at 40° had the lowest and those printed vertically the highest flexural strength. All the differences among print angulations were statistically significant according to the Tukey test ($p<0.05$).

The between-factor interaction was also statistically significant $p<0.05$). The Tukey test revealed that CL specimens printed at 40° had significantly lower flexural strength than those printed horizontally or vertically, which were similar to each other. Also, CO specimens measured the lowest strength values when printed at 40°, while the highest values were recorded by specimens printed vertically. All the differences among print angulations within the CO group were statistically significant. Additionally, it emerged from the Tukey test that CO yielded significantly lower flexural strength than CL when printing was done horizontally or at 40°, while in vertical prints, the difference between the two resins was not statistically significant.

Table 2. Descriptive statistics of the flexural strength values in MPa of unaged specimens.

Material	Print angulation	N	Mean	Std. Deviation
Dental LT Clear Resin (CL)*	0°aa	10	72.65	1.83
	40°bα	10	68.31	1.46
	90°a	10	72.74	1.02
	Total	30	71.23	2.54
Dental LT Comfort Resin (CO)§	0°bb	10	66.89	2.08
	40°cβ	10	62.71	1.21
	90°a	10	71.47	1.26
	Total	30	67.03	3.94
Total print angulations	0°B	20	69.77	3.51
	40°C	20	65.51	3.15
	90°A	20	72.11	1.29

Different symbols and letters label statistically significant differences. Specifically, capital letters label statistically significant differences among print angulations regardless of material type. Small, bold letters label statistically significant differences among print angulations within CL. Small, underlined letters label statistically significant differences among print angulations within CO. Small italic letters label the statistically significant difference between materials printed at 0° angulation. Greek letters label the statistically significant difference between materials printed at 40° angulation. The difference between materials printed at 90° was not statistically significant.

Flexural strength of aged specimens

Table 3 reports the descriptive statistics of flexural strength measurements in MPa of aged specimens, along with the outcome of the statistical analysis. Water storage reduced the flexural strength in all the experimental groups. For CO the greatest decrease in mean flexural strength occurred for vertically printed specimens (51.18%). The flexural strength values of CO remained significantly lower than those of CL and significantly different among print angulations (p<0.05). Among CL specimens, those printed horizontally manifested the greatest reduction in mean flexural strength with water storage (17.92%), and recorded significantly lower values than vertical prints (p<0.05).

Table 3. Descriptive statistics of the flexural strength values in MPa of aged specimens.

Material	Print angulation	N	Mean	Std. Deviation
Dental LT Clear Resin (CL)*	0°^{B}	10	59.63	2.39
	40°^{AB}	10	61.55	0.79
	90°^{A}	10	62.91	2.19
Dental LT Comfort Resin (CO)§	0°^{C}	10	42.14	2.077
	40°^{E}	10	30.61	1.57
	90°^{D}	10	34.08	0.98

Different superscript letters label statistically significant between-group differences (p<0.05).

Flexural modulus of unaged specimens

Table 4 presents the descriptive statistics of flexural modulus values in GPa of unaged specimens. CO resin exhibited significantly lower flexural modulus than CL resin ($p<0.05$). For either resin flexural modulus increased with increasing print angulation and the differences were statistically significant ($p<0.05$), except for the CL 0°-CL 40° comparison ($p>0.05$). CO specimens printed horizontally, and CL specimens printed vertically had respectively the lowest and the highest flexural modulus.

Table 4. Descriptive statistics of flexural modulus values in GPa of unaged specimens.

Material	Print angulation	N	Mean	Std. Deviation
Dental LT Clear Resin (CL)*	$0°^{B}$	10	0.541	0.017
	$40°^{B}$	10	0.545	0.015
	$90°^{A}$	10	0.582	0.008
Dental LT Comfort Resin (CO)§	$0°^{E}$	10	0.159	0.006
	$40°^{D}$	10	0.224	0.007
	$90°^{C}$	10	0.245	0.005

Different superscript letters label statistically significant between-group differences ($p<0.05$).

Flexural modulus of aged specimens

Table 5 presents the descriptive statistics of flexural modulus values in GPa of aged specimens. Similarly to flexural strength, flexural modulus was decreased by water storage in all the experimental groups, and the greatest reduction in mean flexural modulus was recorded for CO resin in vertically printed specimens (48.16%), while for CL resin in the horizontally printed ones (19.96%). Also, after ageing CO specimens exhibited significantly lower flexural modulus than CL specimens ($p<0.05$). For CL resin flexural modulus increased significantly with increasing print angulations and 90° specimens recorded the highest flexural modulus ($p<0.05$). Conversely, aged CO specimens displayed very low flexural modulus values, which were statistically similar regardless of the print angulation ($p>0.05$).

Table 5. Descriptive statistics of flexural modulus values in GPa of aged specimens.

Material	Print angulation	N	Mean	Std. Deviation
Dental LT Clear Resin (CL)*	0°C	10	0.43	0.018
	40°B	10	0.48	0.006
	90°A	10	0.49	0.016
Dental LT Comfort Resin (CO)§	0°D	10	0.11	0.005
	40°D	10	0.11	0.006
	90°D	10	0.12	0.003

Different superscript letters label statistically significant between-group differences ($p<0.05$).

Discussion

The present study findings revealed significant differences in the flexural strength and flexural modulus of occlusal splint resins printed at different orientations. Moreover, water ageing considerably impacted flexural properties. Thereby, both formulated null hypotheses were rejected herein.

Flexural strength refers to the ability of a material to withstand bending under the application of an external force, quantified as the highest stress the material can endure before failure. Additionally, flexural modulus represents the material's initial resistance to bending under an applied load, wherein a higher modulus indicates a stiffer material [30,37]. Flexural strength and flexural modulus are key mechanical properties used to assess the long-term clinical performance of dental resins undergoing masticatory forces [30]. According to ISO standards for dental resins, the minimum requirement for flexural strength is 65 MPa, while for flexural modulus, the threshold value is 1.5 GPa [38]. Considering the absence of an ISO standard specifically designated for occlusal splint materials, the present study adopted the ISO 20795-1:2013 standards indicated for denture base polymers and copolymers, as had been done in previous studies [8,9,39]. Nevertheless, there are distinct disparities between the chemical compositions of traditionally manufactured acrylic resin splints and additively manufactured occlusal devices, which raises the question of the applicability of such conceived standards, and in turn, challenges the validity of interpreting the previously reported findings and the clinical relevance therein.

It is also noteworthy to highlight the absence of a standardized ageing protocol exclusively indicated for 3D-printed specimens. The employed ageing regimen in the present study involved one month of water storage isothermally at 37°C [7,10,15,40]. This was based on the evidence that occlusal splints do not undergo thermal fluctuations in the oral cavity, considering they are used by patients during the night and not subjected to dietary components of varying temperatures. Nevertheless, the reported ageing protocols in the literature varied widely, ranging from 50 hours at 37°C [9] to 10 or 14 days [41,42], and up to 60-days [21]. Likewise, variations exist in thermocycling ageing regimens, ranging from thermocycling between 5°C and 55°C temperatures for a duration of 1 minute per cycle for 10,000 cycles [43,44], to 30 seconds per cycle for 3,860 cycles [45], and up to 80,000 cycles [19]. The lack of standardization in defining precise storage times that simulate the oral environment may contribute to discrepancies in the measured flexural properties.

In the present study, when tested immediately after fabrication, all unaged resin groups exceeded the ISO recommended minimum requirement flexural strength threshold (> 65 MPa). The findings of the

CL are within the range of the values reported in previous similar studies. While the observed results are consistent with those stated in a study by Prpic et al. (75.25 MPa) [8] and Simeon et al. (78.86-85.81 MPa) [19], they are higher than those reported by Nakornnoi et al. (35.09 MPa) [46], and considerably lower than those reported by Aretxabaleta et al. (147.7 MPa) [47]. Nonetheless, dissimilarities in flexural strength values may be explained by the disparities among specimen dimensions. Prpic et al. [8], as well as Simeon et al. [19] indeed employed similar dimensions as the present study (64.0 × 10.0 × 3.3 mm and 64.0 × 11.0 × 4.0 mm respectively), while Nakornnoi et al. used larger specimens (80 × 10 × 1 mm) [46], and Aretxabaleta et al [47] tested much smaller specimen geometries (25×2x2 mm). Such diversities load-bearing areas, which led to differences in stress distribution and flexural strength. Conversely, to date, no study has investigated the flexural strength of CO, which demonstrated lower flexural strength values compared to CL. Such a difference may be ascribed to variations in the chemical composition of the resins, which play a crucial role in determining their mechanical properties, as the final characteristics of resin-based materials are largely determined by the interactions within the monomer mixture and the characteristics of the resultant polymer network [10,48]. The CL group was primarily composed of bisphenol A dimethacrylate (Bis-GMA) by 50–70 wt%, with lesser quantities of urethane dimethacrylate (UDMA, 25–45 wt%). Differently, the CO group was predominantly composed of UDMA by 55–75 wt%. Although UDMA can form hydrogen bonds by virtue of its urethane groups, these interactions are not as strong as those found in Bis-GMA. Consequently, resins with high amounts of UDMA tend to exhibit higher flexibility, superior degree of monomer conversion, and greater morphological homogeneity. In contrast, the hydroxyl groups in Bis-GMA, combined with its rigid core, result in extensive hydrogen bonding networks, yielding higher viscosity and greater stiffness [49,50]. Moreover, the recorded flexural strength data for both resin materials were considerably lower than those reported by the manufacturer (CL= 84 MPa, CO=: 21 MPa) [51,52], which may be the result of differences in the flexural strength test setup, as the manufacturer employed the 4-point bending test in line with the ASTM D790-15 standards procedure B [53], whereas the present study conducted the 3-point bending test according to the ISO 20795-1:2013 standards [38]. Previous studies have confirmed higher flexural strength values obtained from 3-point bending tests by virtue of the concentrated applied force at one contact point, whereas in the 4-point bending test the applied force is uniformly distributed over a broad surface area, thus fostering uniform stress distribution and lower flexural strength values [54,55].

Despite the introduction of multiple resin formulations into the market indicated for occlusal splint fabrication, there has been limited research assessing their long-term mechanical properties [11,13,15,26,27]. Similarly, the majority of previous comparisons have been drawn between conventional manufacturing methods and 3D printing [5,7-9,41,42,56,57]. However, the increased adoption of 3D printing necessitates a thorough evaluation of the impact of printing parameters. Indeed, the orientation of objects on the build platform influences fabrication accuracy, printing time, and post-processing requirements by altering the number and dimension of overlapping layers [20]. In vertical printing (90°), specimens are built up perpendicular to the printing platform, and each layer comprises a reduced surface area. On the other hand, in horizontal printing (0°), specimens are layered parallel to the printing platform, with each layer displaying a larger surface area. Furthermore, 90° orientation permits the accommodation of a greater number of objects on the build platform, thus reducing resin consumption and the necessity for extensive support structures, which, in turn, streamlines the finishing process. Conversely, 0° orientation results in fewer layers, thereby accelerating the printing process [19]. For these reasons, the present study evaluated specimens printed at 0°, 90°, and at the manufacturer-recommended 40° angulation. While the printing orientation considerably influenced the flexural properties of both resin materials to varying degrees, the specimens printed perpendicular to the printing platform consistently exhibited superior flexural strength and modulus outcomes. This observation has been corroborated in the literature, wherein additively manufactured occlusal splints exhibited the highest flexural strengths when printed vertically [19,21]. Therefore, it can be inferred that when printed resin layers align parallel to the compressive force that mitigates tension-induced fracture, an anisotropic structure is created. Moreover, vertical orientation produces minimal resin build-up due to gravity, thereby yielding greater homogeneity and coherence between printed resin layers [58]. Conversely, the 40° printing orientation obtained the lowest flexural strength results for both resins, which may be attributed to the relative positioning of the printed resin layers in relation to the applied load or to inadequate adhesion between layers. Thus, when force is exerted at an angle that is not perpendicular to the layers (Fig. 3.b), it may lead to increased deflection and reduced resistance to bending among the external resin layers. However, although the observed reduction of approximately 4 MPa at 40° is statistically significant, it is still considered modest in absolute terms and remains within ISO requirements.

In the present study, the flexural modulus parameter of unaged specimens was also significantly influenced by material type and printing orientation, with measured values falling below the ISO

20795-2:2013 requirement (< 1.5 GPa), particularly for the CO resin. The significantly lower flexural modulus of CO is in line with the manufacturer's aim to produce a material with greater flexibility and comfort [52]. Concerning with CL, the flexural modulus values recorded in the present study were lower than those declared by the manufacturer (2.3 GPa) [51], and also inferior to those reported by Simeon et al. (1.94- 2.09 GPa) [19] and Nakornnoi et al. (1.25-1.55 GPa) [46]. This may be justified by the dissimilar flexural test apparatuses (3-point bending vs. 4-point bending) [51], varying specimen dimensions [46], or the parafilm taping of the support pins to prevent specimen sliding and eliminate unwanted friction at the supports [19]. Additionally, specimens printed at 0° demonstrated the lowest flexural modulus among both resins, indicating greater stiffness therein. This may be explained by the unfavorable resin build up when printing parallel to the platform, which caused imbalanced polymerization and adhesion among printed resin layers [58]. While the observed effect of printing angulation on flexural strength and modulus is relatively moderate, it still impacts the overall load-bearing capacity of the printed material. Clinically, these findings indicate perpendicular printing orientation as the most effective for occlusal device applications [41].

After water immersion, aged CL specimens presented increased surface irregularities and roughness, compared to thermoplastic sheet resins tested in the study by Neoh et al. [43]. In contrast, milled occlusal devices offered superior mechanical properties [8], as well as fewer porosities and a higher degree of polymerization [9,59]. Berli et al. reported that 2 out of 3 3D-printed materials absorbed twice as much water as pressed and milled counterparts, indicating higher porosity in the former, a factor that may further compromise their mechanical performance [9]. Exposure to water has multiple effects on the properties of resins, encompassing plasticization and softening of the matrix, along with the elution of unreacted monomers and small oligomers into the oral cavity. Additionally, water sorption results in an overall expansion of the device [33]. In the present investigation, a notable decrease in flexural strength was observed for both CL and CO after one month of water storage. These findings align with those reported by similar studies [9,13,15,26,27], where artificial ageing significantly deteriorated the flexural strength of 3D-printed splint materials. In addition, Xu et al. [17] reported that prolonged washing of occlusal splints adversely affected their flexural strength, with highest strength detected after 5 minutes of washing. Nonetheless, among CL specimens, no differences were observed between printing orientations, and acceptable flexural strength values were maintained after ageing. In contrast, aged CO specimens printed at 40° had their flexural strength reduced by approximately half after water storage, with values falling below the threshold of acceptability set by ISO standards. This occurrence may be ascribed to the hydrophilic nature of urethane linkages in UDMA, which may have further facilitated water penetration in CO [48]. The flexural strength outcomes of CO raise concerns about its long-term clinical performance, when subjected to heavy masticatory forces.

Likewise, water storage also led to a decrease in flexural modulus in both resin groups (< 0.5 GPa), with a similar trend observed among printing orientations, with a pronounced reduction detected in CO compared to CL. Despite the lack of consensus and the complex informed decisions regarding splint material selections [9], in clinical practice the splint materials that display greater flexibility under masticatory forces might lead to premature wear of the occlusal surfaces and are thereby considered less favorable for the treatment of TMJ disorders, where firmer splints are often preferred to ensure timely symptom relief [39].

A limitation of the present study can be considered that the investigated resins herein allow 100 µm printed layer thickness, however, other printable resins offer the possibility of printing layers with minimal thickness, such as 50 µm. Therefore, the effect of layer thickness on flexural properties cannot be concluded based on the present findings. Reducing layer thickness increases the number of layers and interfaces, which could amplify the observed differences among printing orientations. Previous research revealed that decreasing layer thickness can enhance the strength of printed resin prosthesis [15,41,60,61]. Another limitation is that the implemented ageing protocol of 30-day continuous water storage does not fully replicate clinical conditions. Thus, additional studies are needed to evaluate the long-term performance of the available materials under simulated oral conditions such as dynamic loading or, even more relevantly, in the clinical setting. A deeper understanding of the impact of experimental testing variables will aid in optimizing material selection and printing parameters, aiming at enhancing the durability and clinical performance of occlusal splints.

Conclusions

1.Dental LT Comfort resin exhibited significantly lower flexural strength and modulus compared to Dental LT Clear v2 resin.

2. 3D printed occlusal splint resin specimens printed at 90° consistently demonstrated superior flexural strength and modulus.

3. For both resins printing at 40° to the build platform, as recommended by the manufacturer, resulted in significantly lower flexural strength.

4. After water storage, the flexural strength and modulus decreased for both resins, with Dental LT Comfort experiencing up to 52% loss in flexural strength and ex-pressing values that fell below ISO threshold for clinical acceptability.

References

1. Revilla-León, M.; Özcan, M. Additive Manufacturing Technologies Used for Processing Polymers: Current Status and Potential Application in Prosthetic Dentistry. J Prosthodont 2019, 28, 146-158.
2. Tian, Y.; Chen, C.; Xu, X.; Wang, J.; Hou, X.; Li, K.; Lu, X.; Shi, H.; Lee, E.S.; Jiang, H.B. A Review of 3D Printing in Dentistry: Technologies, Affecting Factors, and Applications. Scanning 2021, 2021, 9950131.
3. van Lingen, C.; Tribst, J.P.M. 3D-Printed Occlusal Splints: A Narrative Literature Review. J Adv Oral Res 2025, 16, 25-33.
4. Ma, Y.; Li, W.; Li, L.; Cao, M.; Zhang, C. Clinical evaluation of 3D printed splint in the treatment of temporomandibular disorders. BMC Oral Health 2025, 25, 1263.
5. Benli, M.; Al-Haj Husain, N.; Ozcan, M. Mechanical and chemical characterization of contemporary occlusal splint materials fabricated with different methods: a systematic review. Clin Oral Invest 2023, 27, 7115-7141.
6. Šimunović, L.; Čimić, S.; Meštrović, S. Three-Dimensionally Printed Splints in Dentistry: A Comprehensive Review. Dent J (Basel) 2025, 13.
7. Gibreel, M.; Perea-Lowery, L.; Vallittu, P.K.; Lassila, L. Characterization of occlusal splint materials: CAD-CAM versus conventional resins. J Mech Behav Biomed Mater 2021, 124, 104813.
8. Prpic, V.; Spehar, F.; Stajdohar, D.; Bjelica, R.; Cimic, S.; Par, M. Mechanical Properties of 3D-Printed Occlusal Splint Materials. Dent J (Basel) 2023, 11.
9. Berli, C.; Thieringer, F.M.; Sharma, N.; Müller, J.A.; Dedem, P.; Fischer, J.; Rohr, N. Comparing the mechanical properties of pressed, milled, and 3D-printed resins for occlusal devices. J Prosthet Dent 2020, 124, 780-786.
10. Perea-Lowery, L.; Gibreel, M.; Garoushi, S.; Vallittu, P.; Lassila, L. Evaluation of flexible three-dimensionally printed occlusal splint materials: An in vitro study. Dent Mater 2023, 39, 957-963.
11. Mayta, B.S.; Candido, L.A.; Zancopé, K.; Simamoto Júnior, P.C.; Mendonça, G.; Neves, F.D.D. Effect of preservation on the mechanical properties of 3D printing resins for occlusal splints. Braz Oral Res 2025, 39, e060.
12. Abad-Coronel, C.; Ruano Espinosa, C.; Ordóñez Palacios, S.; Paltán, C.A.; Fajardo, J.I. Comparative Analysis between Conventional Acrylic, CAD/CAM Milled, and 3D CAD/CAM Printed Occlusal Splints. Materials (Basel) 2023, 16.

13. Maleki, T.; Meinen, J.; Coldea, A.; Reymus, M.; Edelhoff, D.; Stawarczyk, B. Mechanical and physical properties of splint materials for oral appliances produced by additive, subtractive and conventional manufacturing. Dent Mater 2024, 40, 1171-1183.
14. Seidler, A.S.; de Melo, L.S.; Limirio, J.; Pesqueira, A.A.; Hilgert, L.A.; de Medeiros, R.A. Comparison of mechanical properties of 3D printer resins for occlusal splints using different models of 3D printers. J Clin Exp Dent 2024, 16, e1067-e1071.
15. Perea-Lowery, L.; Gibreel, M.; Vallittu, P.K.; Lassila, L. Evaluation of the mechanical properties and degree of conversion of 3D printed splint material. J Mech Behav Biomed Mater 2021, 115, 104254.
16. Kaushik, A.; Garg, R.K.; Saini, R.S.; Bennardo, F.; Heboyan, A. Evaluating the effect of printing parameters on the performance of resin occlusal splints for a sustainable dentistry. J Appl Biomater Funct Mater 2025, 23, 22808000251333700.
17. Xu, Y.; Xepapadeas, A.B.; Koos, B.; Geis-Gerstorfer, J.; Li, P.; Spintzyk, S. Effect of post-rinsing time on the mechanical strength and cytotoxicity of a 3D printed orthodontic splint material. Dent Mater 2021, 37, e314-e327.
18. Khalil, A.S.; Zaher, A.R. Effect of printing orientation and resin thickness on flexural strength of direct 3D-printed aligners. BMC Oral Health 2025, 25, 238.
19. Simeon, P.; Unkovskiy, A.; Saadat Sarmadi, B.; Nicic, R.; Koch, P.J.; Beuer, F.; Schmidt, F. Wear resistance and flexural properties of low force SLA- and DLP-printed splint materials in different printing orientations: An in vitro study. J Mech Behav Biomed Mater 2024, 152, 106458.
20. Sfondrini, M.F.; Gariboldi, F.; Cerri, M.; Todaro, C.; Pascadopoli, M.; Casiraghi, G.; Scribante, A. Influence of Printing Orientation on the Flexural Strength of Different Light-Cured Resins Manufactured with Two 3D Printers: In Vitro Study. Materials (Basel) 2025, 18.
21. Wulff, J.; Rauch, A.; Schmidt, M.B.; Rosentritt, M. Biaxial Flexural Strength of Printed Splint Materials. Materials (Basel) 2024, 17.
22. Grymak, A.; Aarts, J.M.; Ma, S.; Waddell, J.N.; Choi, J.J.E. Comparison of hardness and polishability of various occlusal splint materials. J Mech Behav Biomed Mater 2021, 115, 104270.
23. Grymak, A.; Waddell, J.N.; Aarts, J.M.; Ma, S.; Choi, J.J.E. Evaluation of wear behaviour of various occlusal splint materials and manufacturing processes. J Mech Behav Biomed Mater 2022, 126, 105053.

24. Vilela, S.; Franco, A.; Franco, A.; Carvalho, G.; Dias, S.; Junior, S.; Perez, F.; Filho, F.; Martins, C. Analysis of compressive strength of occlusal splints manufactured with three liquid resins at three angles of orientation on 3D printer. Res Soc Dev 2022, 11, e40811326820.
25. Alghauli, M.A.; Alqutaibi, A.Y.; Aljohani, R.; Almuzaini, S.; Saeed, M.H. Influence of different print orientations on properties and behavior of additively manufactured resin dental devices: A systematic review and meta-analysis. J Prosthet Dent 2025, 133, 736.e731-736.e712.
26. Weżgowiec, J.; Małysa, A.; Więckiewicz, M. How does artificial aging affect the mechanical properties of occlusal splint materials processed via various technologies? Dent Med Probl 2025, 62, 527-535.
27. Rosello Jimenez, J.R.; Fuchs, F.; Schmohl, L.; Schulz-Siegmund, M.; Koenig, A. Aging Processes and Their Influence on the Mechanical Properties of Printable Occlusal Splint Materials. Polymers 2023, 15, 4574.
28. Rosentritt, M.; Hickl, V.; Rauch, A.; Schmidt, M. Effects of storage and toothbrush simulation on Martens hardness of CAD/CAM, hand-cast, thermoforming, and 3D-printed splint materials. Clin Oral Investig 2023, 27, 7859-7869.
29. Paradowska-Stolarz, A.; Wezgowiec, J.; Malysa, A.; Wieckiewicz, M. Effects of Polishing and Artificial Aging on Mechanical Properties of Dental LT Clear(®) Resin. J Funct Biomater 2023, 14.
30. Mudhaffer, S.; Haider, J.; Satterthwaite, J.; Silikas, N. Effects of print orientation and artificial aging on the flexural strength and flexural modulus of 3D printed restorative resin materials. J Prosthet Dent 2025, 133, 1345-1357.
31. Shim, J.S.; Kim, J.E.; Jeong, S.H.; Choi, Y.J.; Ryu, J.J. Printing accuracy, mechanical properties, surface characteristics, and microbial adhesion of 3D-printed resins with various printing orientations. J Prosthet Dent 2020, 124, 468-475.
32. Mudhaffer, S.; Silikas, N.; Satterthwaite, J. Effect of print orientation on sorption, solubility, and monomer elution of 3D printed resin restorative materials. J Prosthet Dent 2025, 134, 461.e461-461.e412.
33. Wulff, J.; Merle, C.L.; Hahnel, S.; Rosentritt, M. Wear Behavior and Water Sorption of Additively Manufactured Resin-Based Splint Materials. Materials (Basel) 2024, 17.
34. Greil, V.; Mayinger, F.; Reymus, M.; Stawarczyk, B. Water sorption, water solubility, degree of conversion, elastic indentation modulus, edge chipping resistance and flexural strength of 3D-printed denture base resins. J Mech Behav Biomed Mater 2023, 137, 105565.

35. Özden, Y.E.; Doğu Kaya, B.; Yılmaz Atalı, P.; Ozer, F.; Ozkurt Kayahan, Z. Effect of Print Orientation and Thermal Aging on the Flexural Strength of Zirconia-Reinforced Three-Dimensional-Printed Restorative Resin Materials. Molecules 2025, 30.
36. Hertan, E.; McCray, J.; Bankhead, B.; Kim, K.B. Force profile assessment of direct-printed aligners versus thermoformed aligners and the effects of non-engaged surface patterns. Prog Orthod 2022, 23, 49.
37. Calheiros, F.C.; Pfeifer, C.S.; Brandão, L.L.; Agra, C.M.; Ballester, R.Y. Flexural properties of resin composites: influence of specimen dimensions and storage conditions. Dent Mater J 2013, 32, 228-232.
38. International Organization for Standardization. ISO 20795-1:2013(en) Dentistry — Base polymers — Part 1: Denture base polymers. 2013.
39. Poorna, T.A.; John, B.; E, K.J.; Rao, A. Comparison of the effectiveness of soft and hard splints in the symptomatic management of temporomandibular joint disorders: A randomized control study. Int J Rheum Dis 2022, 25, 1053-1059.
40. Gibreel, M.; Perea-Lowery, L.; Vallittu, P.K.; Garoushi, S.; Lassila, L. Two-body wear and surface hardness of occlusal splint materials. Dent Mater J 2022, 41, 916-922.
41. Väyrynen, V.O.; Tanner, J.; Vallittu, P.K. The anisotropicity of the flexural properties of an occlusal device material processed by stereolithography. J Prosthet Dent 2016, 116, 811-817.
42. Hickl, V.; Strasser, T.; Schmid, A.; Rosentritt, M. Pull-Off Behavior of Hand-Cast, Thermoformed, Milled, and 3D-Printed Splints. Int J Prosthodont 2024, 37, 31-40.
43. Neoh, S.P.; Khantachawana, A.; Chintavalakorn, R.; Santiwong, P.; Srikhirin, T. Comparison of physical, mechanical, and optical properties between thermoplastic materials and 3-dimensional printing resins for orthodontic clear retainers. Am J Orthod Dentofacial Orthop 2025, 167, 95-109.e101.
44. Topsakal, K.G.; Aksoy, M.; Duran, G.S. The effect of aging on the mechanical properties of 3-dimensional printed biocompatible resin materials used in dental applications: An in vitro study. Am J Orthod Dentofacial Orthop 2023, 164, 441-449.
45. Wesemann, C.; Spies, B.C.; Sterzenbach, G.; Beuer, F.; Kohal, R.; Wemken, G.; Krügel, M.; Pieralli, S. Polymers for conventional, subtractive, and additive manufacturing of occlusal devices differ in hardness and flexural properties but not in wear resistance. Dent Mater 2021, 37, 432-442.

46. Nakornnoi, T.; Bunjerdjin, P.; Santiwong, P.; Sipiyaruk, K.; Neoh, S.P.; Chintavalakorn, R. The Influence of Thickness on the Mechanical Behaviors of 3D Printing Resins for Orthodontic Retainers. Int J Biomater 2024, 2024, 7398478.
47. Aretxabaleta, M.; Xepapadeas, A.B.; Poets, C.F.; Koos, B.; Spintzyk, S. Comparison of additive and subtractive CAD/CAM materials for their potential use as Tübingen Palatal Plate: An in-vitro study on flexural strength. Additive Manufacturing 2021, 37, 101693.
48. Szczesio-Wlodarczyk, A.; Domarecka, M.; Kopacz, K.; Sokolowski, J.; Bociong, K. An Evaluation of the Properties of Urethane Dimethacrylate-Based Dental Resins. Materials (Basel) 2021, 14.
49. Sideridou, I.; Tserki, V.; Papanastasiou, G. Effect of chemical structure on degree of conversion in light-cured dimethacrylate-based dental resins. Biomaterials 2002, 23, 1819-1829.
50. Martim, G.C.; Pfeifer, C.S.; Girotto, E.M. Novel urethane-based polymer for dental applications with decreased monomer leaching. Mater Sci Eng C Mater Biol Appl 2017, 72, 192-201.
51. Formlabs Dental LT Clear Resin Technical Datasheet. Accessed 03/09/2025. https://formlabs-media.formlabs.com/datasheets/2001429-TDS-ENUS-0.pdf.
52. Formlabs Dental LT Comfort Resin Technical Datasheet. Accessed 03/09/2025. . https://media.formlabs.com/m/29ef8c96e5ff1a8d/original/-ENUS-Dental-LT-Comfort-TDS.pdf.
53. American Society for Testing and Materials. ASTM D790:2015. Standard Test Method for Flexural Properties of Unreinforced and Reinforced Plastics and Electrical Insulating Materials. 2015.
54. Alhotan, A.; Al-Johani, H.; Altarazi, A.; Alshamrani, A.; Fouda, A.M. Effect of uniaxial bending methods on the flexural strength and Weibull analysis of heat-polymerized, CAD/CAM milled, and 3D-printed denture base resins. Dent Mater 2025, 41, e1-e7.
55. Chitchumnong, P.; Brooks, S.C.; Stafford, G.D. Comparison of three- and four-point flexural strength testing of denture-base polymers. Dent Mater 1989, 5, 2-5.
56. Barbur, I.; Opris, H.; Crisan, B.; Cuc, S.; Colosi, H.A.; Baciut, M.; Opris, D.; Prodan, D.; Moldovan, M.; Crisan, L.; et al. Statistical Comparison of the Mechanical Properties of 3D-Printed Resin through Triple-Jetting Technology and Conventional PMMA in Orthodontic Occlusal Splint Manufacturing. Biomedicines 2023, 11.
57. Jindal, P.; Worcester, F.; Siena, F.L.; Forbes, C.; Juneja, M.; Breedon, P. Mechanical behaviour of 3D printed vs thermoformed clear dental aligner materials under non-linear compressive loading using FEM. J Mech Behav Biomed Mater 2020, 112, 104045.

58. Goracci, C.; Bosoni, C.; Marti, P.; Scotti, N.; Franchi, L.; Vichi, A. Influence of Printing Orientation on Surface Roughness and Gloss of 3D Printed Resins for Orthodontic Devices. Materials (Basel) 2025, 18.
59. de Paula Lopez, V.; Dias Corpa Tardelli, J.; Botelho, A.L.; Marcondes Agnelli, J.A.; Cândido Dos Reis, A. Mechanical performance of 3-dimensionally printed resins compared with conventional and milled resins for the manufacture of occlusal devices: A systematic review. J Prosthet Dent 2024, 132, 1262-1269.
60. AlRumaih, H.S.; Gad, M.M. The Effect of 3D Printing Layer Thickness and Post-Polymerization Time on the Flexural Strength and Hardness of Denture Base Resins. Prosthesis 2024, 6, 970-978.
61. Gad, M.M.; Abdullah Alzaki, F.; Ahmed Abuwarwar, F.; Alhammad, A.; Al Hussain, M.; Khan, S.Q.; Nassar, E.A.; Ayad, N.M. Impact of printing layer thickness on the flexural strength of nanocomposite 3D printed resins: An in vitro comparative study. Saudi Dent J 2024, 36, 1307-1312.

4.2 Influence of Printing Orientation on Surface Roughness and Gloss of 3D Printed Resins for Orthodontic Devices.

Abstract

The study aims to assess the effect of printing orientation on surface roughness and gloss of resins for 3D printing of aligners. Squared specimens (14 × 14 × 4 mm) were printed using Dental LT Clear (Formlabs, Somerville, MA, USA; LT) or Tera Harz TC-85 DAC (Graphy, Seoul, Republic of Korea; TC) with different orientations: 0◦ (horizontal), 90◦ (vertical), and as per the manufacturer's recommendation (40◦ for LT, 60◦ for TC). A profilometer was used to measure roughness (Ra) in µm, while gloss was recorded in gloss units (GU) with a glossmeter. The collected data were statistically analyzed. Material type did not significantly influence roughness, while print orientation was an influential factor, with the orientation recommended by the manufacturer yielding the roughest specimens. Vertical printing resulted in significantly higher roughness than horizontal. Material type was a significant factor for gloss, with TC exhibiting significantly higher gloss than LT. Print direction significantly influenced gloss, with vertical printing resulting in the highest gloss. The finding of higher roughness for vertical prints can be explained by the presence of a greater number of layers. The superior gloss exhibited by TC regardless of print angulation could be related to the effective cleaning of uncured resin by centrifugation and to the high degree of monomer conversion in nitrogen atmosphere.

Introduction

A great interest is currently surrounding the use of resins for the direct three-dimensional (3D) printing of orthodontic aligners. It has been reported that, in comparison with the thermoforming procedure, direct printing simplifies the workflow, reduces the amount of plastic waste, and produces aligners with improved adaptation whose thickness can be better controlled [1–4].

Direct-printed aligners have been tested for fit accuracy, mechanical properties, citotoxicity, and estrogenicity [2,3]. Yet the evidence so far collected on their surface characteristics is limited [5–7]. Nevertheless, such properties are clinically relevant for their bearing on plaque retention, staining and translucency loss of the aligner, tongue comfort, aligner wear, and consequent monomer leaching [2–5]. Additionally, the choice of materials available for the 3D printing of aligners is still reduced. The resin that has been most tested as an aligner material [4], the Dental LT Clear (Formlabs, Somerville, MA, USA), is actually meant for occlusal splint fabrication [5]. Of the few materials currently marketed for the direct printing of aligners [4,5], Tera Harz TC-85 DAC resin (Graphy, Seoul, Republic of Korea) has been recently tested for surface roughness in comparison with Invisalign aligners [6,7]. Koletsi et al. assessed the surface roughness of 'as-received' aligners and after 1 week of intraoral use [7]. It was reported that, for direct-printed aligners, roughness parameters increased significantly with function [7]. The observation that the aligners tested in the mentioned study had been cured according to an earlier protocol in the presence of oxygen prompted Eslami et al. to evaluate the properties of 3D printed aligners cured in a nitrogen chamber [6].

In addition to curing conditions, the orientation of printing layers has also been indicated as a possibly influential factor for the surface characteristics of additively manufactured aligners [2,3]. Yet no study has systematically addressed this issue. Generally speaking, no assessment of the surface gloss has, so far, been provided in the literature for direct-printed aligners.

Therefore, the present study is directed toward assessing the effect of build orientation on surface roughness and gloss of resins for printing orthodontic devices such as aligners and occlusal splints. The null hypothesis that no change in these properties occurs when the material is layered at different angulations relative to the print platform was placed under test.

Materials and Methods

Square specimens of 14 × 14 mm and 4 mm in thickness were designed using the Tinkercad software (Autodesk, San Rafael, CA, USA; www.tinkercad.com accessed on 19 May 2024) (Figure 1) to be printed either with Dental LT Clear V2 resin (LT) or with Tera Harz TC-85 DAC (TC).

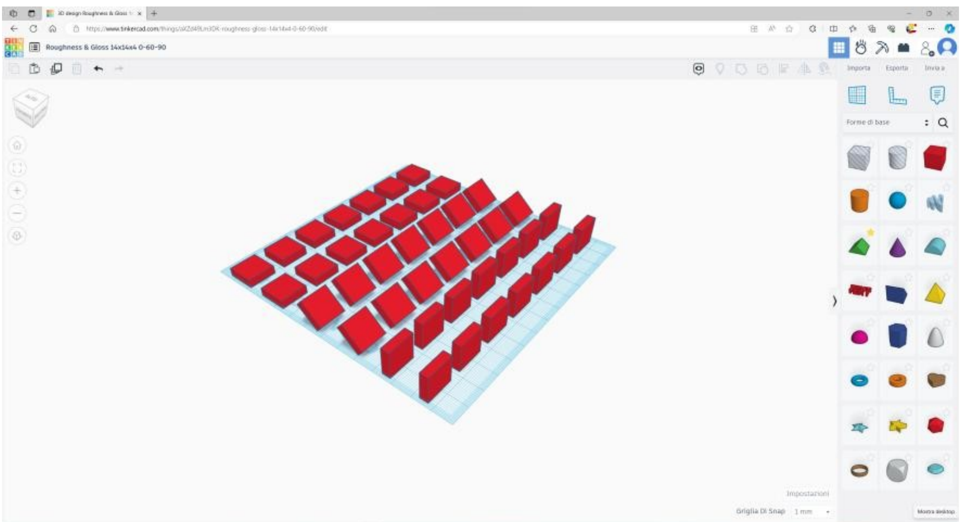

(a)

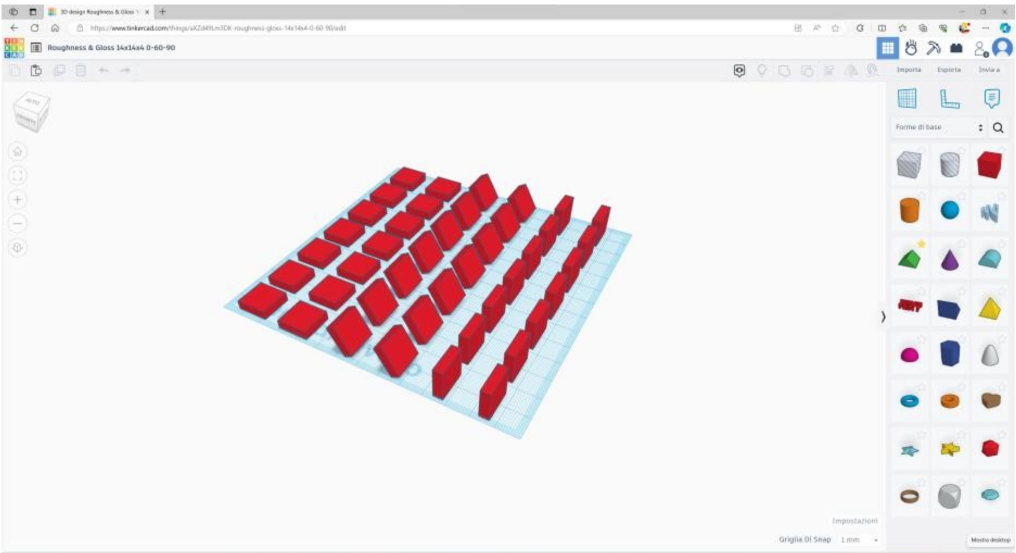

(b)

Figure 1. Design of specimens with the Tinkercad software. (**a**) Specimens to be printed with Dental LT Clear V2 resin, with angulations of 0◦, 40◦, and 90◦ to the building platform. (**b**) Specimens to be printed with Tera Harz TC-85 DAC resin, with angulations of 0◦, 60◦, and 90◦ to the building platform.

Table 1 reports the chemical composition of the tested resins [8,9].

Table 1. Chemical composition of the tested materials.

Name	Manufacturer	Chemical Composition
Tera Harz TC-85 DAC	Graphy, Seoul, Republic of Korea	GR30860 and GR3060 oligomers, bis(2,4,6-trimethylbenzoyl)-phenylphosphine oxide (Irgacure 819, BASF SE, Ludwigshafen, Germany)
Dental LT Clear	Formlabs, Somerville, MA, USA	Bisphenol A dimethacrylate (50–70 wt%, 2 hydroxyethyl methacrylate, 7–10 wt%, urethane dimethacrylate 25–45 wt%) [9]

The specimens were designed with three different orientations relative to the printing platform: 0◦ (horizontal, H), 90◦ (vertical, V), and with the orientation recommended by the resin's manufacturer (M), i.e., 40◦ for LT [10] and 60◦ for TC [11]. The experimental groups were, therefore, defined as follows: (TC-H) TC specimens printed horizontally; (TC-V) TC specimens printed vertically; (TC-M) TC specimens printed at the angulation recommended by the manufacturer; (LT-H) LT specimens printed horizontally; (LT-V) LT specimens printed vertically; (LT-M) LT specimens printed at the angulation recommended by the manufacturer. The projects were then exported in the .stl file format. Based on sample size calculations performed in previous studies with similar objectives [12,13], 10 specimens per experimental group were printed.

LT Specimens Printing and Post-Processing

For the manufacturing of LT specimens, the .stl file was imported into the PreForm software (Formlabs, Somerville, MA, USA; https://formlabs.com/it/software/preform/ accessed on 19 May 2024) for automatic support calculations and slicing. The printing layer thickness was set to 100 µm. Specimens were 3D printed with the Formlabs 3B 3D printer (Formlabs, Somerville, MA, USA). After printing, specimens were removed from the platform and, while still retaining raft and supports, they were subjected to washing to remove the uncured resin. Such a procedure was performed for 15 min by means of the FormWash automated washing machine (Formlabs, Somerville, MA, USA), using 99% isopropyl alcohol (IPA). After washing, the specimens were immersed for 5 min in fresh 99% IPA. Then, post-curing was performed for 20 min at 60°, using the proprietary device FormCure (Formlabs, Somerville, MA, USA). Subsequently, the supports were removed.

TC Specimens Printing and Post-Processing

To design the supports for the TC specimens, the .stl file was imported into the Uniz software, version 2.6.1.11 (Uniz, San Diego, CA, USA). Printing was performed with the Sonic XL 4K 2022 printer (Phrozen, Hsinchu, Taiwan) in layers of 100 µm in thickness. Thereafter, specimens were separated from the building plate and placed twice for 5 min in a centrifuge spinning at 1000× *g* revolutions per minute. Specimens were then dried with compressed air and the supports were removed. Post-polymerization was performed for

14 min in the absence of oxygen within a curing unit equipped with a nitrogen generator (Graphy Cure THC 2, Graphy Inc., Seoul, Republic of Korea). Following post-curing, the supports were removed, and specimens were washed in an ultrasonic cleaning machine filled with distilled water at 80° for 2 min. Subsequently, specimens were placed in boiling water at 100° for 1 min and, finally, dried with a drying machine for 5 min [14].

Surface Roughness Assessment

A profilometer (Mitutoyo SJ-201P, Mitutoyo, Kanagawa, Japan) set with a cutoff value of 0.8 mm, a stylus speed of 0.5 mm/s, and a tracking length of 5.0 mm was used to assess surface roughness (Ra).

The measurement set up was standardized by means of a custom mold for both the handpiece of the instrument and the specimen [15]. Mean Ra (μm) was recorded.

Surface Gloss Assessment

Gloss was recorded using a small-area glossmeter (JNDXA6-SA; VTSYIQI Lab Measuring Instruments, Hafei, China) with a 2 mm × 2 mm square measuring area at a 60° angle [16]. A proprietary grey mold was utilized to eliminate the influence of room light and maintain the exact position of the specimen relative to the glossmeter reading area.

All surface roughness and gloss recordings were taken by the same operator who was experienced with the measuring devices and techniques (AV).

Statistical Analysis

Having checked that the collected data met the requirements of normality of data distribution (Shapiro–Wilk test) and homogeneity of group variances (Levene's test), two separate two-way analyses of variance (ANOVAs) were applied to the surface roughness and gloss datasets. In each analysis, the optical property was considered as the dependent variable, while type of material and print direction were the factors. The Tukey's test was used for post-hoc comparisons as needed. In all the tests, the level of significance was set to $p < 0.05$. The statistical calculations were handled by the PASW Statistics 18 software (SPSS Inc., Chicago, IL, USA).

Results

Surface Roughness

Table 2 reports the descriptive statistics of the roughness measurements. The two-way ANOVAs revealed that the material type did not significantly influence roughness ($p = 0.08$). Conversely, print direction was an influential factor ($p < 0.001$), and the post-hoc test disclosed that the print orientation recommended by the respective manufacturer yielded the roughest specimens ($p < 0.05$). Printing in the vertical direction resulted in higher roughness than in the horizontal direction, and also this difference was found to be statistically significant ($p < 0.05$). The material–print-direction interaction was not statistically significant ($p = 0.12$).

Table 2. Descriptive statistics of surface roughness measurements (Ra, μm). Different superscript letters highlight statistically significant differences in roughness among print directions regardless of the material type, according to the post-hoc test ($p < 0.05$).

Material	Printing Orientation	N	Mean ± Standard Deviation
LT Clear V2	Horizontal	10	1.36 ± 0.14
	Manufacturer's instructions	10	4.86 ± 0.21
	Vertical	10	1.73 ± 0.10
	Total	30	2.65 ± 1.60
TC-85 DAC	Horizontal	10	1.39 ± 0.13
	Manufacturer's instructions	10	4.79 ± 0.26
	Vertical	10	1.49 ± 0.32
	Total	30	2.55 ± 1.62
Print direction	Horizontal [a]	20	1.38 ± 0.13
	Manufacturer's instructions [c]	20	4.82 ± 0.23
	Vertical [b]	20	1.61 ± 0.26

Surface Gloss

Table 3 reports the descriptive statistics of the gloss measurements. The two-way ANOVAs revealed that material type was a significant factor for surface gloss per se ($p < 0.001$), and, regardless of the print direction, TC exhibited significantly higher gloss than LT ($p < 0.05$). Also, print direction was found to be a significant factor per se ($p < 0.001$). According to the post-hoc test, regardless of the material, vertical printing resulted in significantly higher specimens' gloss than printing in the other two directions ($p < 0.05$). The between-factor interaction was not statistically significant ($p = 0.06$).

Table 3. Descriptive statistics of surface gloss measurements (GU). Different superscript capital letters mark the significant difference between the materials regardless of the print direction. Different superscript lowercase letters label statistically significant differences in gloss among print directions regardless of the material type, according to the post-hoc test ($p < 0.05$).

Material	Printing Orientation	N	Mean ± Standard Deviation
LT Clear V2 [B]	Horizontal	10	1.95 ± 0.15
	Manufacturer's instructions	10	2.05 ± 0.15
	Vertical	10	5.50 ± 1.22
	Total	30	3.16 ± 1.81
TC-85 DAC [A]	Horizontal	10	4.05 ± 0.43
	Manufacturer's instructions	10	2.80 ± 0.48
	Vertical	10	7.00 ± 1.63
	Total	30	4.61 ± 2.04
Print direction	Horizontal [b]	20	3.00 ± 1.12
	Manufacturer's instructions [b]	20	2.42 ± 0.51
	Vertical [a]	20	6.25 ± 1.61

Discussion

The performed roughness and gloss measurements were meant to investigate surface characteristics of 3D printed resins for aligners and occlusal splints that affect their esthetic properties and biofilm resistance.

Roughness can be quantified by different linear (Ra, Rq, Rz) or three-dimensional (Sa, Sq, Sz) variables. The Ra parameter determined in the present study is the arithmetic average of the absolute values of the profile heights over the evaluation length [17]. Ra was selected because it provides an assessment of the average surface roughness [18].

Gloss quantifies the specular reflection from a surface [19].

It is computed by relating the amount of light reaching a surface at a 60° angle to the amount of light bouncing from the surface at an equal and opposite angle. Gloss is influenced by the optical characteristics of the material, particularly the refractive index, as well as by the surface morphology of the object. A coarser surface appears less glossy and, by reflecting a relatively greater amount of light back to the observer's eye, it makes the orthodontic device visible in the mouth [2].

The data collected in the present investigation led to rejection of the formulated null hypothesis.

Concerning the surface roughness, print direction was found to be a significant factor regardless of the material. The smoothest surface was obtained when the resin was layered horizontally. This finding had been predicted in previous literature [2,3,20], and was attributed to the increased number of layers in vertical prints which create multiple surface steps.

Print angulation was not found to significantly influence the accuracy of the aligners printed with LT [21], as well as the mechanical properties of the aligners printed with TC [22]. Controversial information is present in the literature regarding the amount of time and material needed for vertical versus horizontal prints of aligners, although these issues have not been systematically addressed yet. The manufacturers of the tested resins recommend printing the appliances obliquely, at an angle of 40◦ (LT) or 60◦ (TC) to the build platform. According to the manufacturer of TC, when printing at a 60◦ angle, resin tends to overflow in the incisors. Resin excess in this area is more easily removed with centrifugation than the diffuse build ups that develop in horizontally printed manufacts.

Interestingly, both materials exhibited the greatest roughness when printed obliquely. This finding can be ascribed to the printing geometry. In a horizontally printed object, the tracking length of the profilometer remains within the same printed layer (Figure 2a), while, in a vertically printed specimen, the stylus moves along a series of layers (Figure 2b) whose number depends on the printing resolution. Still, in a vertical print, the layers are levelled (Figure 2b). Conversely, in oblique printing, layers are not at the same level, yielding a staired surface that the profilometer detector steps through (Figure 2c,d).

The printing material did not emerge as an influential factor for roughness per se. The two tested resins differed not only in chemical composition, but also in the post-printing protocol. For TC, the procedure involved centrifugation, rather than immersion, in an organic solvent and curing in a nitrogen chamber that replaced oxygen. It has been stated that a deeper curing of the polymer, as obtained in nitrogen-saturated conditions, results in lower surface roughness of the printed manufact [23]. However, in the present study, no significant difference in Ra emerged between TC specimens post-cured in a nitrogen generator and LT specimens post-polymerized in an oxygen atmosphere. As for LT, it should be reiterated that, although it has been tested in previous research as an aligner material, it is actually marketed for printing occlusal splints. The manufacturer also recommends polishing the outer surface of the splint 'with traditional polishing tools and materials commonly used for dental acrylics' [10]. This treatment was omitted in the present study protocol as it is not indicated for aligners.

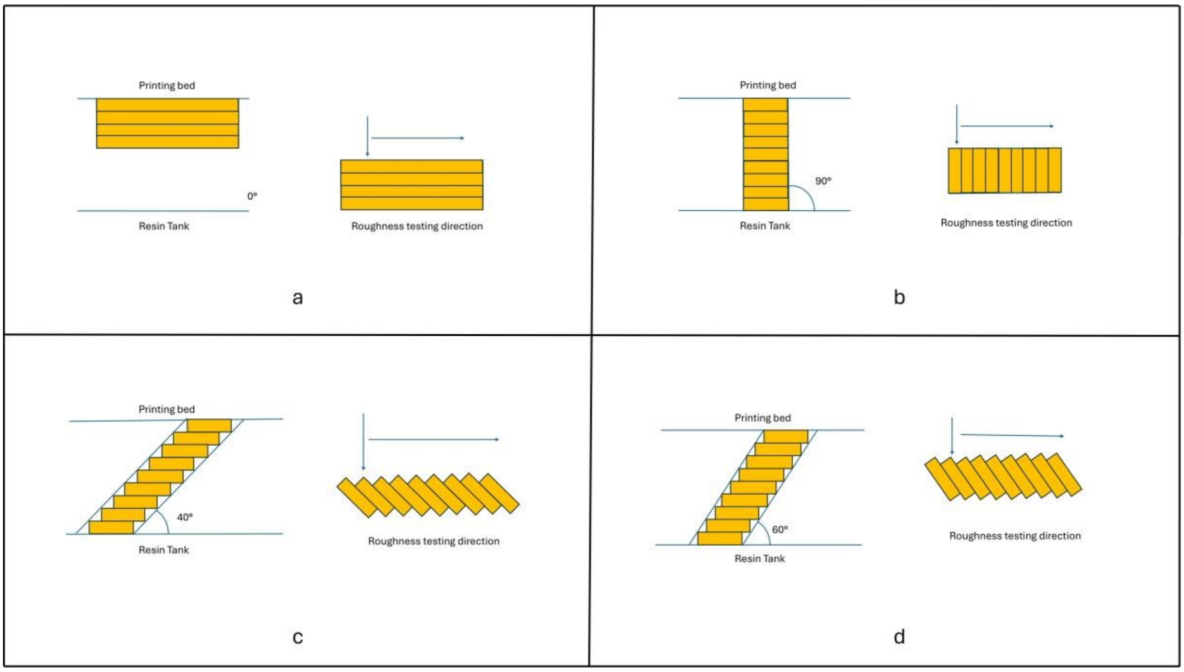

Figure 2. Diagrams illustrating the different tracks followed by the profilometer stylus when measuring surface roughness on specimens printed with different angulations to the printing bed: (**a**) 0°, horizontal; (**b**) 90°, vertical, (**c**) 40°, oblique according to Dental LT Clear V2 resin's manufacturer, and (**d**) 60°, oblique according to TC-85 DAC resin's manufacturer (Graphy, Seoul, Republic of Korea).

A direct comparison of the roughness measurements reported in the present study with data available in the literature is not feasible, as the two previous studies where TC has been tested recorded different surface parameters than Ra [6,7]. Regarding LT, no prior assessment of roughness has been provided.

In any case, the Ra values measured for 3D printed resins in the present study were significantly lower than those reported for thermoformed PET-G by Staderini et al. [17]. This finding is consistent with the results of the investigation by Eslami et al. [6], who compared TC aligners cured in a nitrogen chamber with Invisalign retainers.

Gloss resulted to be significantly influenced by both material type and print direction.

With either resin, vertical printing yielded the highest gloss, and the difference was statistically significant. A possible explanation for this finding is that the vertical print orientation minimized the gravity-driven collection of resin, which may render the aligner surface foggy.

When considering the resin irrespective of the build orientation, specimens printed with TC were significantly glossier. Centrifugal cleaning may have positively contributed to the glossier aspect of TC specimens. Mechanical cleaning by centrifugation has been reported to be more effective at removing uncured resin than chemical cleaning by immersion in IPA [24], with an additional benefit to esthetics. In contrast, the presence of residual uncured monomer would cause the resin to appear foggy [2,20].

The superiority of TC in gloss terms may also be ascribed to the advanced curing of the resin obtained in the nitrogen-containing chamber [14,23]. Vichi et al. assessed gloss and roughness of a 3D printed resin for permanent prosthetic restorations and reported that the specimens post-cured in a nitrogen chamber were significantly glossier than those finished and polished with different systems [13]. Another study indicated that post-curing in a nitrogen-saturated atmosphere significantly increased the resistance to discoloration to wine and curry of a resin marketed by Graphy for the 3D printing of permanent prosthodontic crowns [25].

A direct comparison of the collected gloss measurements with existing evidence is not feasible, as this relevant optical characteristic has been overlooked by previous research that has focused on other properties, such as transparency, translucency, and color stability [26,27].

As a possible limitation of the study, it can be mentioned that unused specimens were tested. It may, indeed, be meaningful to assess surface roughness and gloss of specimens that have been aged in the laboratory to simulate the effects of clinical service. Also, aligners retrieved after use could be subjected to surface roughness and gloss measurements; that, however, would require different equipment from that used in the present investigation, as readings should be performed on curved surfaces.

With regard to the stability of the optical properties, some concern has been raised that 3D printed resins may be relatively more prone to discoloration with time due to their greater susceptibility to absorbing water and pigmented solutions [28]. Nevertheless, although this issue is understandably relevant for 3D printed restorative materials, it can be downsized for aligners that are meant to be replaced after 7–10 days of clinical service, according to the current clinical protocols.

Based on this same observation, the concern regarding the increase in surface roughness and porosity reported by Eslami et al. [6] for aligners 3D printed with TC after 1 week of use can also be reconsidered.

Conclusions

Although LT is marketed as a material for occlusal splints, it has been utilized to 3D print aligners. The type of resin was not an influential factor for surface roughness per se. The finding of a higher roughness for vertically printed specimens in comparison with horizontally printed ones is in line with previous research and can be explained by the presence of a greater number of layers in vertical specimens. Horizontal printing produced the smoothest specimens. However, this print direction requires a larger surface on the building platform and may favor the development of resin build-ups in some areas of the aligner due to gravity. The Ra values measured for 3D printed resins in the present study were remarkably lower than those reported in the literature for thermoformed PET-G. The superior gloss exhibited by TC regardless of the print angulation could be related to the effective cleaning of the uncured resin by centrifugation, as well as to a high degree of conversion of the monomers achieved by curing in a nitrogen atmosphere. No previous data are available for gloss for comparative purposes, as the present study is the first one to assess this property for aligner materials.

References

1. Bichu, Y.M.; Alwafi, A.; Liu, X.; Andrews, J.; Ludwig, B.; Bichu, A.Y.; Zou, B. Advances in orthodontic clear aligner materials. *Bioact. Mater.* 2023, *22*, 384–403.
2. Panayi, N.; Cha, J.-Y.; Kim, K.B. 3D Printed Aligners: Material Science, Workflow and Clinical Applications. *Sem. Orthod.* 2023, *29*, 25–33.
3. Panayi, N.C. Directly Printed Aligner: Aligning with the Future. *Turk. J. Orthod.* 2023, *21*, 62–69.
4. Goracci, C.; Juloski, J.; D'Amico, C.; Balestra, D.; Volpe, A.; Juloski, J.; Vichi, A. Clinically Relevant Properties of 3D Printable Materials for Intraoral Use in Orthodontics: A Critical Review of the Literature. *Materials* 2023, *16*, 2166.
5. Eliades, T.; Panayi, N.; Papageorgiou, S.N. From biomimetics to smart materials and 3D technology: Applications in orthodontic bonding, debonding, and appliance design or fabrication. *Jpn. Dent. Sci. Rev.* 2023, *59*, 403–411.
6. Eslami, S.; Kopp, S.; Goteni, M.; Dahmer, I.; Sayahpour, B. Alterations in the surface roughness and porosity parameters of directly printed and Invisalign aligners after 1 week of intraoral usage: An in vivo prospective investigation. *Am. J. Orthod. Dentofacial Orthop.* 2024, *165*, 73–79.
7. Koletsi, D.; Panayi, N.; Laspos, C.; Athanasiou, A.E.; Zinelis, S.; Eliades, T. In vivo aging-induced surface roughness alterations of Invisalign® and 3D-printed aligners. *J. Orthod.* 2023, *50*, 352–360.
8. Lee, S.Y.; Kim, H.; Kim, H.J.; Chung, C.J.; Choi, Y.J.; Kim, S.J.; Cha, J.Y. Thermo-mechanical properties of 3D printed photocurable shape memory resin for clear aligners. *Sci. Rep.* 2022, *12*, 6246.
9. Formlabs. Available online: https://formlabs-media.formlabs.com/datasheets/2001421-SDS-ENEU-0.pdf (accessed on 15 September 2024).
10. Formlabs. Available online: https://support.formlabs.com/s/article/Printing-Splints-with-Dental-LT-Clear-Resin?language= en_US#resources (accessed on 15 September 2024).
11. Migliorati, M.; Drago, S.; Lagazzo, A.; Campobasso, A.; Battista, G.; Kerberger, R.; Drescher, D.; Becker, K. Effect of Curing Time and Nitrogen Generator Usage on Direct 3D-Printed Aligners Thicknesses—An In Vitro Micro-CT Study. *Appl. Sci.* 2023, *13*, 11952.
12. Erturk-Avunduk, A.T.; Atılan-Yavuz, S.; Filiz, H.; Cengiz-Yanardag, E. A comparative study of polishing systems on optical properties and surface roughness of additively manufactured and conventional resin based composites. *Sci. Rep.* 2024, *27*, 25658. [
13. Vichi, A.; Balestra, D.; Louca, C. Effect of Different Finishing Systems on Surface Roughness and Gloss of a 3D-Printed Material for Permanent Dental Use. *Appl. Sci.* 2024, *14*, 7289.

14. Campobasso, A.; Ariano, A.; Battista, G.; Posa, F.; Migliorati, M.; Drago, S.; Lo Muzio, E.; Mori, G. Comparison of the cytotoxicity of 3D-printed aligners using different post-curing procedures: An in vitro study. *Aust. Orthod. J.* 2023, *39*, 49–56.
15. Han, D.S.; Kim, R.; Hyun, H.K.; Yoon, H.I.; Jeong, H.R.; Jeon, S.H.; Park, C. The Impact of Oxygen Concentration on the postcuring of 3D-Printed Dental Resin. *Int. J. Prosthodont.* 2024, *37*, 151–158.
16. *EN 623-624*; The European Standard. Advanced Technical Ceramics. Monolithic Ceramics. General and Textures Properties. Part 4: Determination of Surface Roughness. European Committee for Standardization: Brussels, Belgium, 2004.
17. Staderini, E.; Chiusolo, G.; Guglielmi, F.; Papi, M.; Perini, G.; Tepedino, M.; Gallenzi, P. Effects of Thermoforming on the Mechanical, Optical, Chemical, and Morphological Properties of PET-G: In Vitro Study. *Polymers* 2024, *16*, 203.
18. Lambart, A.L.; Xepapadeas, A.B.; Koos, B.; Li, P.; Spintzyk, S. Rinsing postprocessing procedure of a 3D-printed orthodontic appliance material: Impact of alternative post-rinsing solutions on the roughness, flexural strength and cytotoxicity. *Dent. Mater.* 2022, *38*, 1344–1353.
19. Vichi, A.; Louca, C.; Corciolani, G.; Ferrari, M. Color related to ceramic and zirconia restorations: A review. *Dent. Mater.* 2011, *27*, 97–108.
20. Narongdej, P.; Hassanpour, M.; Alterman, N.; Rawlins-Buchanan, F.; Barjasteh, E. Advancements in Clear Aligner Fabrication: A Comprehensive Review of Direct-3D Printing Technologies. *Polymers* 2024, *16*, 371.
21. McCarty, M.C.; Chen, S.J.; English, J.D.; Kasper, F. Effect of print orientation and duration of ultraviolet curing on the dimensional accuracy of a 3-dimensionally printed orthodontic clear aligner design. *Am. J. Orthod. Dentofac. Orthop.* 2020, *158*, 889–897.
22. Camenisch, L.; Polychronis, G.; Panayi, N.; Makou, O.; Papageorgiou, S.N.; Zinelis, S.; Eliades, T. Effect of printing orientation on mechanical properties of 3D-printed orthodontic aligners. *J. Orofac. Orthop.* 2024. *Online ahead of print*.
23. Lim, B.; Kim, D.; Song, J.S.; Kim, S.; Kim, H.; Shin, Y. Influence of Post-Curing in Nitrogen-Saturated Condition on the Degree of Conversion and Color Stability of 3D-Printed Resin Crowns. *Dent. J.* 2024, *12*, 68.

4.3 Dental Arch Expansion with In-House Clear Aligners: An Exploratory Prospective Clinical Study on Torque, Vertical Control, and Attachment Configuration.

Abstract

To evaluate short-term expansion efficacy, torque expression, and vertical control with in-house aligners (IHA), and secondarily to compare attachment design/position using a contralateral within-subject approach. In a prospective exploratory trial (n = 21; 12–30 y), six aligners were used over 6 weeks. Inclusion criteria: Class I dentoskeletal pattern and mild crowding. Digital models were planned in ArchForm; aligners were fabricated using 0.75 mm PETG sheets. Different attachments were bonded to canines and first molars. Programmed (AF), baseline (T0), and final (T1) models were oriented and registered in 3D Slicer; movements were referenced to global XYZ axes with Q3DC (torque = roll; rotation = yaw; buccolingual = ΔX; vertical = ΔZ). Paired t-tests compared planned vs. achieved movements and right vs. left attachment configurations. Equivalence (TOST, α = 0.05) was tested on planned−achieved differences using movement-scaled margins anchored to measurement error. ICC and Dahlberg's error assessed reliability. Reliability was excellent (ICC 0.998–1.000); error small (0.19 mm; 0.8°). Expansion effectiveness was highest in premolars (first/second: 59%/46%), moderate in canines (42% overall; maxillary 51%, mandibular 33%), and lowest in first molars (31%; maxillary 29%, mandibular 33%). Vertical control was maintained (several rows met TOST equivalence). Canine torque showed small, systematic buccal crown torque and did not meet equivalence under pre-specified margins. First-molar torque changes were <1° with no significant differences between beveled and horizontal-rectangular attachments. A slice attachment with an incisal base improved canine torque control versus a gingival base ($p<0.001$). Short-term IHA expansion was more effective in premolars than in canines or molars and maintained vertical control. Under movement-scaled margins, canine torque did not reach equivalence, underscoring the relevance of attachment positioning; an incisal-base slice improved torque control. Effect-size and variance estimate from this exploratory design can guide future adequately powered multicenter trials.

Introduction

The ability of the thermoplastic aligners to exert force on interproximal and axial surfaces during orthodontic treatment plays a fundamental role in biomechanical control of dental movements with clear aligners.1,2 Thus, in the initial stages of treatment, orthodontic expansion can be a valuable clinical strategy, particularly in cases where arch width deficiencies are present.3–5 However, aligner-induced expansion influences not only the transverse tooth positioning but also displacements across all three spatial planes.4–6 This complexity necessitates meticulous planning to predict and manage potential unwanted effects, such as excessive buccal torque and loss of vertical control.

Recent systematic reviews synthesize the evidence on aligner-mediated transverse changes. De Castro Aragón et al.7 reported dentoalveolar expansion in adults and children but decreasing predictability toward posterior segments and unclear skeletal effects. D'Antò et al.8 likewise found that transverse changes are only partially predictable (e.g., ≈64–70% accuracy in the lower arch) with lower predictability for molar inclinations. Levrini et al.,9 in mixed dentition, observed significant maxillary dentoalveolar expansion with limitations in bodily movement and substantial heterogeneity. Collectively, these data support low-to-moderate certainty and ongoing concerns about the predictability of transverse outcomes. Recognizing these limitations underscores the need to control biomechanics during expansion, particularly via attachment design and placement.

Multiple factors may affect the torque control and predictability of tooth movements during clear aligner expansion, including the material composition of the aligners, the rate of movement, and the type and positioning of attachments.10–15 During arch expansion with clear aligners, attachments improve control by increasing aligner- tooth coupling and guiding force application.12,15 Their shape and position can significantly influence the effectiveness of expansion, as different designs, such as slice, rectangular, or beveled attachments, can improve torque control and minimize unwanted tipping.15 Strategically positioned attachments can help guide buccal displacement, thereby contributing to a more controlled expansion process and reducing unwanted rotations, as reported in the literature.4

While commercial aligner systems, such as Invisalign, benefit from continuous investment in material optimization and advanced algorithms, improved by clinical performance feedback throughout refinement stages, in-house aligner (IHA) systems rely heavily on clinician experience and lack standardization in biomechanical optimization, making prospective validation critical.16 Although IHA can offer cost and customization advantages, these benefits may be negated if biomechanical efficiency is suboptimal, reinforcing the need for controlled clinical data.17 Therefore, prospective controlled clinical trials are essential to generate data that enhance the predictability of dental movements and improve the effectiveness of IHA, ensuring their reliable application in orthodontic practice.

Despite the widespread evaluation of commercial aligner systems, the biomechanical outcomes of IHA expansion remain largely unexplored, with existing data limited to retrospective reports and laboratory simulations. To our knowledge, no prospective controlled clinical trial has evaluated short-term expansion efficacy, torque expression, and vertical control in IHA systems. Given the clinical reliance on IHA in many regions, rigorous evaluation of their predictability is essential. Therefore, the present exploratory prospective clinical study aimed to assess arch expansion outcomes in canines, premolars, and first molars, and to investigate the influence of different attachment designs on torque and vertical displacement. This study provides preliminary effect size estimates to guide future adequately powered multicenter trials. The primary objective was to assess short-term expansion efficacy, torque expression, and vertical control with IHA, and the secondary objective was to compare the effect of attachment design/position using an exploratory contralateral within-subject comparison.

Material and Methods

Sample

The clinical data were collected between February and October 2024 and followed the CONSORT guidelines.18 This study was approved by the institutional review board of the Pontifical Catholic University of Minas Gerais (#71125723.5.0000.5137) and was also registered in the national clinical trial platform (ReBEC #U1111-1308-6317). This was an exploratory, proof-of-concept contralateral within-subject designed to obtain preliminary effect-size and variance estimates.

A priori sample size calculation was performed using the G*Power software, considering an alpha of 5%, a power of 80%, and a two-tailed calculation for dependent means (paired design), with a clinically acceptable tolerance of 1mm for the pre-specified primary outcome (intercanine-distance change). The assumed SD was 1.1mm based on previously published data on changes in intercanine distance after arch expansion with aligners.12 This corresponds to an effect size of 0.9 and a required sample of 20 patients; one additional participant was enrolled to mitigate potential attrition along the six weeks of treatment.

After examining 40 candidates for orthodontic treatment at the Pontifical Catholic University of Minas Gerais Graduate Program Clinic, 21 patients who met the following inclusion criteria were selected: Class I dentoskeletal and facial patterns, confirmed by clinical and cephalometric exams; need for orthodontic treatment with small negative space discrepancies (< 4 mm); full permanent dentition, including second permanent molars; and potential for compliance with clear aligner therapy, assessed qualitatively during the initial consultation by the treating orthodontist based on general treatment adherence history, patient motivation, and understanding of aligner use. The exclusion criteria were: presence of severe malocclusion; age over 30 years; erupted third molars; teeth presenting morphological anomalies; report of systemic diseases or regular use of medications that could interfere with orthodontic tooth movement.

Nineteen individuals were excluded due to the following criteria: age outside the target range (n = 9), insufficient potential for treatment compliance (n = 6), and negative space discrepancies greater than 4 mm (n = 4).

The research sample consisted of 13 females (61.9%) and eight males (38.1%). Regarding age distribution, eight participants (38.1%) were between 12 and 17 years old, five (23.8%) were between 18 and 24 years old, and another eight participants (38.1%) were in the 25 to 30-year-old age group. This was an exploratory contralateral within-subject comparison; contralateral allocation of attachment configurations (right vs. left) was pre-specified to reduce inter- individual variability and to isolate the effect of attachment shape/position on torque control during expansion.

Data collection and analysis

After the acquisition of initial records (intraoral and extraoral photographs, lateral cephalogram, and panoramic radiograph), digital STL models were obtained using the 3Shape Trios 3 intraoral scanner (3Shape, Copenhagen, Denmark). The treatment planning for IHA was carried out using the ArchForm software (San Mateo, California, USA). Models were printed with a resin printer (Elegoo Saturn 4K, Elegoo, Shenzhen, China) using 3D Cure Basic resin (3D Cure, Betim, Minas Gerais, Brazil). Orthodontic aligners were fabricated using PETG plastic laminates (Bio-Art Equipamentos Odontológicos, São Carlos, São Paulo, Brazil) with a thickness of 0.75 mm and thermoplastification was done using PlastVac P7 vacuum-forming machine (Bio-Art Equipamentos Odontológicos, São Carlos, São Paulo, Brazil). Aligners were manually trimmed using curved scissors (Beck instruments, Schaumburg, Illinois, United States), in a straight line 1 mm above the gingival margins.

All patients were treated by a single team of orthodontists and followed the same protocol regarding the constraints of orthodontic movements, number of aligners (six pair of aligners), daily wear time (22 hours), and replacement intervals (weekly). The three-dimensional position of all teeth was analyzed at three time points: AF (digital planning with ArchForm), T0 (baseline), and T1 (final, after 6 weeks). To achieve arch expansion, attachments (set to scale 1 in the ArchForm platform) were planned to be bonded in the buccal surface of canines and first molars according to a pre-specified right–left allocation scheme (Fig. 1): maxillary right first molar: horizontal rectangular 3 mm; maxillary right canine: slice with incisal base; maxillary left canine: slice with gingival base; maxillary left first molar: beveled; mandibular left first molar: horizontal rectangular 3 mm; mandibular left canine: slice with incisal base; mandibular right canine: slice with gingival base; mandibular right first molar: beveled.

Figure 1. Attachment Designs with varying shapes and positions. Contralateral allocation of attachment configurations (right vs. left) was pre-specified to isolate attachment effects within patients.

After exporting the STL files to the 3D Slicer software (version CMF 3.0), model orientation was performed for AF, T0, and T1 using the Transforms module, followed by model superimposition using the Surface Registration tool. In the maxilla palatal rugae were used as reference structures,[19,20] while in the mandibular arch the border WALA served as reference[21] ensuring a consistent global coordinate system in which X = buccolingual, Y = mesiodistal, and Z = vertical (Fig. 2).

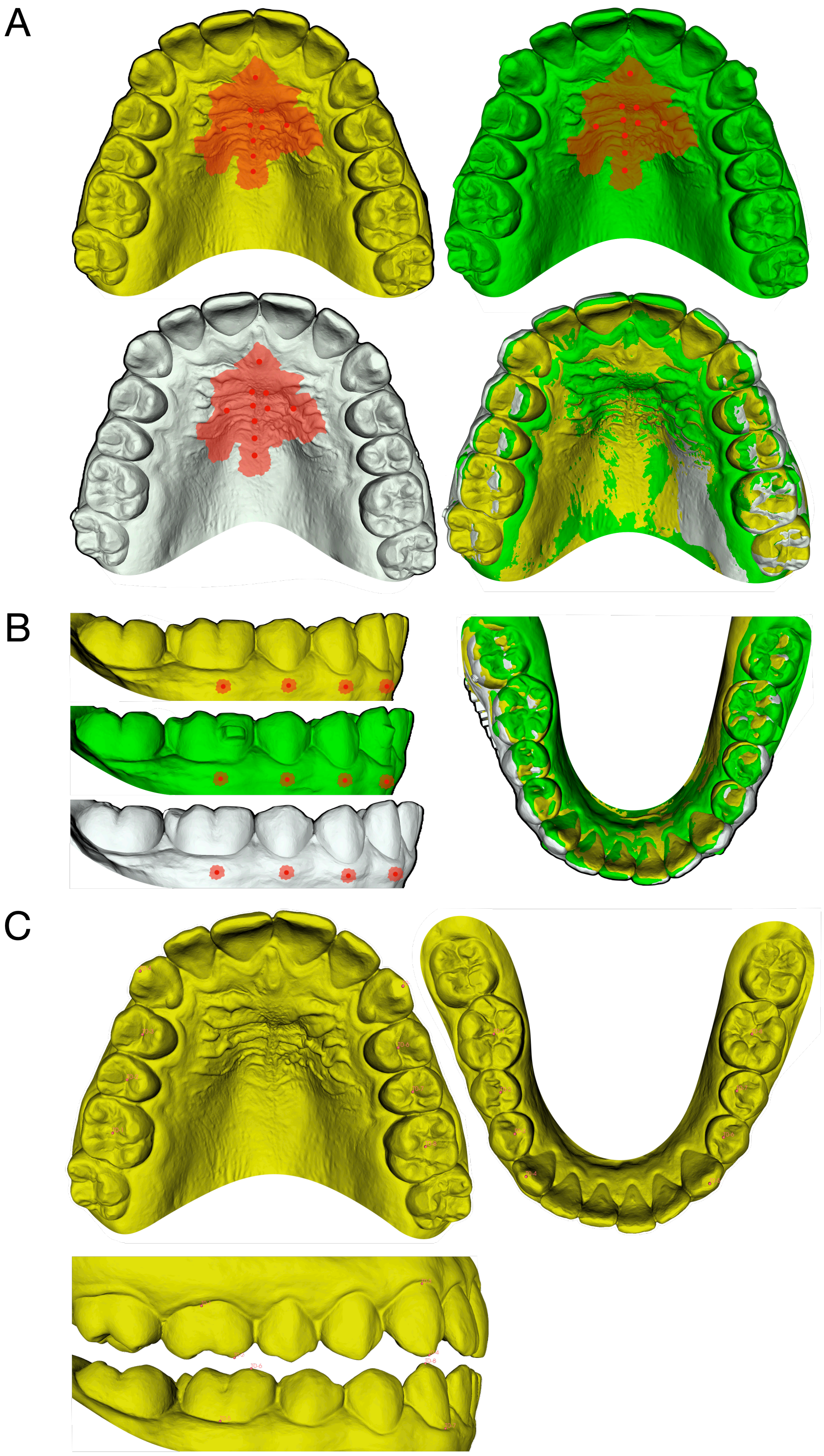

Figure 2. A) Registration surfaces and superimposition of maxillary models; B) Registration surfaces and superimposition of mandibular models; C) Landmarks for the evaluation of buccolingual displacement and the secondary effects of torque and vertical displacement.

Qualitative assessment of the changes was carried out using overlays (AF model, white; T0, yellow; and T1 model, green), and color mapping (Fig. 3). Finally, the Q3DC module was used for the quantitative analysis of point-to-point three-dimensional dental movements. All angular and linear measurements were performed relative to the global XYZ axes of 3D Slicer after model orientation, with buccal and up defined as positive directions for ΔX and ΔZ, respectively. Landmarks were marked on canines and first molars: the gingival zenith, the cusp tip of canines, and the mesiobuccal cusp of first molars, initially on the T0 model using “Create New Markups” in “Connected Landmarks,” and the same procedure was then repeated for the AF and T1.

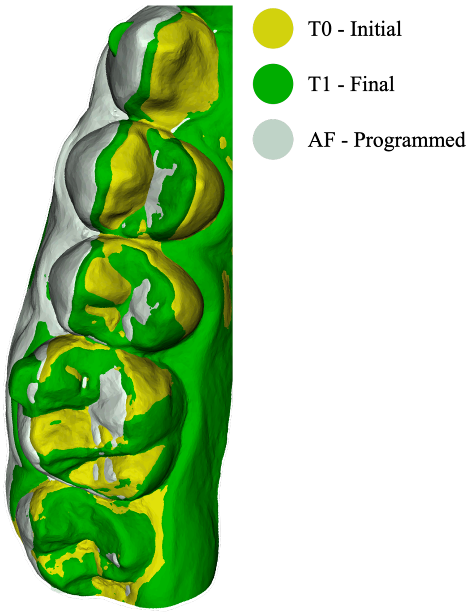

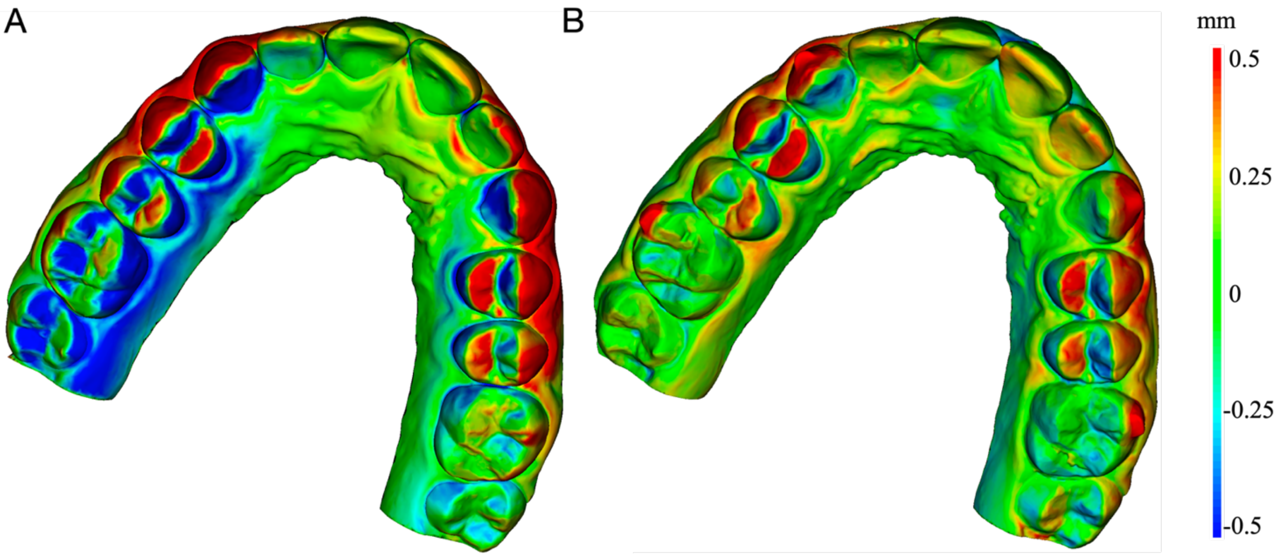

Figure 3. Comparison of T0 – Initial; T1 – Final; and AF - Programmed, after dental expansion movement with IHA. Color mapping. A) Programmed; B) Achieved.

After all landmarks had been placed, tooth movements were calculated as follows: the "Calculate angle between two lines" option was used for angular variables—torque (roll) and rotation (yaw)—and the "Calculate distance between two landmarks" option was used for linear variables—buccolingual and vertical displacements (recording the axis-specific components: ΔX for buccolingual and ΔZ for vertical, rather than the 3D Euclidean distance). For each comparison, "Line 1 Landmark A" and "Line 1 Landmark B" were set to the T0 model and "Line 2 Landmark A" and "Line 2 Landmark B" to the AF model (planned) or T1 model (final). In Q3DC, roll was used to represent torque (the angular change of the line defined by the gingival zenith and cusp tip or mesiobuccal cusp relative to the global horizontal axis), and yaw to represent rotation (angular change around the global vertical axis). All distances were expressed in millimeters (mm) and angles in degrees (°), rounded to two decimals. This workflow provides a reproducible method to derive angular and linear measurements directly from the 3D coordinates of the marked points.

Scanning of the patients' dental arches was performed by the same operator (BQS). Digital model processing in ArchForm, followed by orientation and superimposition, was carried out by a trained operator (RMM), with all models subsequently cross-checked by the senior researcher (BQS). Landmark identification, and measurements were conducted by the same operator (GMA) who was trained by the senior researcher, experienced in this methodology, before the beginning of the trial. The evaluation of reliability of the measurements were assessed using 10 randomly selected models. These models were re-evaluated after a 15-day interval for comparison. The intraclass correlation coefficient (ICC) was used to assess agreement between measurements.

Statistical methods

Data were analyzed in SPSS version 22 (IBM Corp., Armonk, NY, USA). Descriptive statistics (mean, standard deviation) are reported in the tables. The significance level was $\alpha = 0.05$ (two-tailed). Data were screened for outliers and entry consistency. Normality of continuous variables was assessed with the Kolmogorov–Smirnov test, and homoscedasticity with Levene's test when applicable.

For transverse outcomes, maxillary and mandibular arches were analyzed as separate arch-level units (yielding 42 arch-level observations). For each tooth/arch site, one paired difference per patient was analyzed, so observations were independent across patients for that site.

Within-patient comparisons used paired t-tests: (i) planned vs. achieved movements for the same tooth and patient, and (ii) right vs. left sides within the same arch/patient when comparing attachment designs/positions.

The intraclass correlation coefficient (ICC) was calculated from repeated measurements to assess intra-examiner reliability. Systematic error was evaluated with paired t-tests, and random error with Dahlberg's formula.22

Because planned movements were often small, equivalence margins were defined a priori and anchored to measurement error rather than a fixed 1 mm/1° tolerance. To avoid overly permissive thresholds, a relative margin of ±20% of the planned value was also applied; for each outcome, the operative margin was the minimum of the absolute and relative thresholds. Planned–achieved differences were tested for equivalence using a TOST procedure with 90% confidence intervals.23

Results

Agreement between repeated measurements was excellent (ICC 0.998–1.000) with no systematic bias between readings (paired t test, $p > 0.05$). Measurement error was small (Dahlberg: 0.19 mm for linear measures; 0.8° for torque). For TOST, we prespecified row-specific equivalence margins: the smaller of the cap (0.30 mm for linear; 1.0° for angular) and 20% of the planned movement, but never less than the measurement error. The margin used for each row is shown in Table I.

During the short expansion phase (six aligners), no breakages, losses, or tracking issues occurred. The following results were obtained regarding the biomechanical outcomes of orthodontic expansion of canines, premolars, and first molars using IHA, as well as the secondary effects of torque and vertical displacement in canines and first molars associated with different attachment shapes and positions.

Arch expansion with in-house aligners resulted in excessive buccal crown torque of the canines.

Although torque was not intentionally planned in the ArchForm software, it was measured when comparing the T0 and AF models, as well as the T0 and T1 models (Table 1). For canines, the TOST analyses did not demonstrate equivalence of torque (the 90% CIs of the paired difference, Planned − Achieved, extended beyond ±*m*), consistent with small but systematic buccal crown torque during expansion. Paired t-tests were significant for all canines except the mandibular left canine ($p = 0.226$ (Table 1).

Table I. Programmed vs. achieved tooth movements of canines and first molars after IHA-based arch expansion.

	Tooth	Attachment	n	Programmed Mean	Programmed SD	Achieved Mean	Achieved SD	Diff Programmed vs Achieved	Paired P value
Torque	Maxillary right canine	Slice (incisal base)	21	0.20°	1.18°	1.01°	1.60°	0.81°	.023
	Maxillary left canine	Slice (gingival base)	21	0.13°	0.62°	1.26°	1.06°	1.13°	< .001
	Mandibular right canine	Slice (gingival base)	21	0.30°	1.39°	1.31°	1.84°	1.01°	.009
	Mandibular left canine	Slice (incisal base)	21	0.60°	1.15°	1.02°	1.32°	0.42°	.226
	Maxillary right first molar	Horizontal rectangular	21	0.47°	0.82°	-0.36°	1.41°	0.83°	.049
	Maxillary left first molar	Beveled	21	1.20°	1.38°	-0.82°	2.83°	2.02°	.001
	Mandibular right first molar	Beveled	21	0.22°	0.83°	0.22°	1.31°	0.00°	.999
	Mandibular left first molar	Horizontal rectangular	21	0.33°	0.93°	-0.53°	1.33°	0.86°	.013
Buccolingual	Maxillary right canine	Slice (incisal base)	21	0.87 mm	0.38 mm	0.40 mm	0.20 mm	0.47 mm	< .001
	Maxillary left canine	Slice (gingival base)	21	0.98 mm	0.31 mm	0.55 mm	0.29 mm	0.43 mm	< .001
	Mandibular right canine	Slice (gingival base)	21	0.78 mm	0.28 mm	0.24 mm	0.27 mm	0.54 mm	< .001
	Mandibular left canine	Slice (incisal base)	21	1.00 mm	0.27 mm	0.36 mm	0.32 mm	0.64 mm	< .001
	Maxillary right first molar	Horizontal rectangular	21	0.55 mm	0.22 mm	0.19 mm	0.17 mm	0.36 mm	.001
	Maxillary left first molar	Beveled	21	0.83 mm	0.34 mm	0.20 mm	0.19 mm	0.63 mm	< .001
	Mandibular right first molar	Beveled	21	0.62 mm	0.15 mm	0.20 mm	0.17 mm	0.42 mm	< .001
	Mandibular left first molar	Horizontal rectangular	21	0.71 mm	0.23 mm	0.25 mm	0.11 mm	0.46 mm	< .001
Vertical	Maxillary right canine	Slice (incisal base)	21	0.06°	0.24°	-0.04°	0.27°	0.10°	.452
	Maxillary left canine	Slice (gingival base)	21	0.10°	0.31°	-0.02°	0.24°	0.12°	.311
	Mandibular right canine	Slice (gingival base)	21	0.01°	0.15°	0.01°	0.15°	0.00°	.943
	Mandibular left canine	Slice (incisal base)	21	0.05°	0.11°	0.01°	0.19°	0.04°	.329
	Maxillary right first molar	Horizontal rectangular	21	0.03°	0.21°	-0.05°	0.15°	0.08°	.237
	Maxillary left first molar	Beveled	21	-0.02°	0.28°	0.10°	0.26°	0.12°	.131
	Mandibular right first molar	Beveled	21	-0.04°	0.25°	0.05°	0.23°	0.09°	.332
	Mandibular left first molar	Horizontal rectangular	21	0.03°	0.29°	0.01°	0.16°	0.02°	.763

The positioning of the slice attachment plays a pivotal role in determining the control of torque of canines following arch expansion using IHA

After completing arch expansion with IHA, analysis of canine torque using the slice attachment in different positions revealed that an incisally oriented attachment base provided significantly better torque control compared to a gingivally oriented base in both maxillary and mandibular canines ($p < 0.001$) (Table II).

Table II. Torque control and buccolingual displacement of canines and first molars after arch expansion with IHA using different attachment designs.

		Slice (gingival base)			Slice (incisal base)				
		n	Mean	SD	n	Mean	SD	Mean Diff	*P* value
Torque	Maxillary canine	21	1.26°	1.06°	21	1.01°	1.60°	0.25°	< .001
	Mandibular canine	21	1.31°	1.84°	21	1.02°	1.32°	0.29°	< .001
		Beveled			Horizontal rectangular				
		n	Mean	SD	n	Mean	SD	Mean Diff	*P* value
	Maxillary molar	21	-0.82°	2.83°	21	-0.36°	1.41°	0.46°	.091
	Mandibular molar	21	0.22°	1.31°	21	-0.53°	1.33°	0.75°	.330
Buccolingual		Slice (gingival base)			Slice (incisal base)				
		n	Mean	SD	n	Mean	SD	Mean Diff	*P* value
	Maxillary canine	21	0.55 mm	0.29 mm	21	0.40 mm	0.19 mm	0.15 mm	.054
	Mandibular canine	21	0.24 mm	0.26 mm	21	0.36 mm	0.32 mm	0.12 mm	.244
		Beveled			Horizontal rectangular				
		n	Mean	SD	n	Mean	SD	Mean Diff	*P* value
	Maxillary molar	21	0.20 mm	0.19 mm	21	0.19 mm	0.17 mm	0.01 mm	.927
	Mandibular molar	21	0.20 mm	0.17 mm	21	0.25 mm	0.11 mm	0.05 mm	.413

First molar torque was well controlled following dental expansion with IHA

First-molar torque changes were small in magnitude (typically < 1°), yet the TOST criteria were not met for equivalence in the torque rows (Table 1). No significant differences were found between beveled and horizontal rectangular attachments for molars (maxillary $p = 0.091$; mandibular $p = 0.330$; Table II).

Effective vertical dimension management was observed during arch expansion using in-house aligners

As shown in Table I, the arch expansion with IHA facilitated excellent vertical control for both maxillary and mandibular canines and first molars, irrespective of attachment shape or position ($p > 0.05$). The achieved vertical movements closely aligned with the planned movements, indicating the efficacy in maintaining vertical control during expansion. Vertical control was maintained for some teeth, yielding TOST equivalence (Table I).

The effectiveness of IHA orthodontic expansion was greater in the premolar region compared to canines and first molars

The first premolars exhibited the highest expansion effectiveness, achieving nearly 60% of the planned expansion, whereas the first molars had the lowest effectiveness, attaining less than one-third of the planned expansion. However, the buccolingual displacement of posterior teeth following arch expansion with in-house aligners differed significantly between the clinically achieved and digitally planned values, irrespective of whether it was the maxillary or mandibular arch or the attachment type ($p \leq 0.001$) (Table 1; Fig. 3). Expansion effectiveness was greatest in the first and second premolar regions (59% and 46%, respectively), while canines showed an average effectiveness of 42% (51% for maxillary canines and 33% for mandibular canines). Molars demonstrated an overall effectiveness of 31% (29% for maxillary and 33% for mandibular molars) (Table 3). Additionally, variations in attachment shape and position did not significantly influence the buccal-lingual displacement of canines and first molars following in-house aligner expansion ($p > 0.05$) (Table 2).

Table III. Comparison of programmed and achieved buccolingual displacement of canines, premolars, and first molars following arch expansion with IHA.

	Tooth	n	Programmed Mean	Programmed SD	Achieved Mean	Achieved SD	Diff Programmed vs Achieved	Paired P value	Efficacy
Buccolingual	Canine	84	0.91 mm	0.31 mm	0.39 mm	0.27 mm	0.52 mm	< .001	42%
	First premolar	84	1.02 mm	0.18 mm	0.60 mm	0.23 mm	0.42 mm	< .001	59%
	Second premolar	84	0.94 mm	0.30 mm	0.43 mm	0.21 mm	0.51 mm	< .001	46%
	First permanent molar	84	0.68 mm	0.23 mm	0.21 mm	0.16 mm	0.47 mm	< .001	31%

Discussion

This study provides a comprehensive clinical assessment of the biomechanical effects of arch expansion using IHA, specifically aimed at creating interproximal spaces to enhance anchorage for subsequent orthodontic treatment. The analysis focused on expansion outcomes in canines, premolars, and first molars, while also assessing secondary effects such as torque expression and vertical displacement associated with different attachment shapes and positions. To the best of our knowledge, this is the first prospective clinical trial to simultaneously investigate these variables within the context of IHA. Importantly, no instances of aligner breakage, loss, or tracking failure were recorded throughout the treatment period, supporting the reliability of the protocols used.

Previous literature on aligner effectiveness, including expansion movements, has been largely retrospective, with challenges in controlling confounding variables.13,14,24–26 The evaluation of expansion after several months of full orthodontic treatment offers a broad range of advantages but also presents limitations in a research setting where strict control of variables is essential. Controlling variables was the cornerstone of the present investigation. All patients underwent identical orthodontic movements, with no variations in staging, attachment design, wear time, or the one-week interval for aligner changes. The very short interval between T0 and T1, together with a fully standardized protocol (staging, attachment design/placement, wear time, weekly changes) provided sound data to offer a good understanding of what is likely or unlikely to happen during arch expansion with IHA.

Galluccio et al.27 reported a 70% effectiveness in maxillary arch transverse expansion, while Morales-Burruezo et al.14 noted higher effectiveness in the premolar region but lower effectiveness in the canine and second molar areas. In our study, IHA expansion effectiveness was highest in the first and second premolar regions (59% and 46%, respectively), with canines achieving an average effectiveness of 42% (51% for maxillary and 33% for mandibular canines) and first molars reaching 31% (29% for maxillary and 33% for mandibular molars).

Composite resin attachments are pivotal in enhancing aligner retention and ensuring precise tooth movement.10,28 The current findings indicate that the positioning of the slice attachment significantly influences torque control in the region of canines. When the attachment base was oriented incisally, both maxillary and mandibular canines exhibited superior torque control compared to a gingivally oriented base ($p < 0.001$). This improved performance may be attributed to an increased contact surface area between the aligner and the attachment in the direction of movement, which reduces misfit and enhances tracking, a key factor in achieving predictable outcomes. These results suggest that clinicians may benefit from using slice attachments with an incisal base orientation. Although the impact of increasing the attachment scale was not tested in this study (a pre-set scale of 1 was used), it can be inferred that a larger attachment—providing greater anchorage—would likely enhance torque control further. However, it must be considered that the high stiffness of PETG used for IHA make the engagement/disengagement of the aligners combined with large attachments very difficult. To find a balance between the size of the attachment and the patient's perception of quality of the system with an easy insertion and removal of the appliance, must be a goal for the clinicians.

Our findings for the vertical displacement were very close to the planned values, indicating high efficacy across both maxillary and mandibular canines and first molars, irrespective of the attachment configuration. Talens-Cogollos et al.6 reported an unintended molar intrusion of 0.94 mm in 74.2% of patients treated with aligners, after more than 1 year of treatment. In our short-term study (only 6 aligners), no significant vertical changes were detected ($p > 0.05$) after arch expansion, but with less of two months of treatment this is an indication of good vertical control, and no extrusion.

Torque control outcomes varied among teeth, ranging from low efficacy (e.g., maxillary left first molar, mandibular right canine, maxillary left canine) to moderate and high efficacy in other regions. Post-expansion, significant buccal torque was observed in all canines ($p < 0.05$) except for the mandibular left canine ($p = 0.226$). Importantly, first molars demonstrated clinically insignificant torque variations (below 1o), and no significant differences were found between beveled and horizontal rectangular attachments for both maxillary ($p = 0.091$) and mandibular molars.

In terms of outcome measures, while several variables reached statistical significance, the clinical relevance of some findings—for instance, torque changes of less than 1o—remains debatable. The absence of significant differences between attachment types for certain outcomes suggests that, in some cases, the specific design of the attachment may not drastically alter clinical results. The variability in torque control effectiveness among different teeth may be influenced by individual anatomical differences, underscoring the need for further research to elucidate factors contributing to lower efficacy in certain regions. IHA was more effective in the premolar region than in the canine and molar regions, a finding that can inform clinical decision-making regarding treatment planning and expected outcomes, and that has been previously described.3,5,12– 14 Additionally, the study demonstrated excellent vertical control across all teeth, irrespective of the attachment configuration, supporting the reliability of IHA in maintaining vertical dimensions during arch expansion. Finally, the superior torque control achieved with an incisally oriented slice attachment highlights the importance of attachment positioning in optimizing treatment outcomes. This observation is crucial for clinical practice as it provides guidance for refining attachment placement to enhance movement predictability.

Because maxillary expansion forces may produce effects across both hemi-arches, the strict statistical independence assumed in a classical split-mouth design may not apply to this investigation. For this reason, although each patient received different attachment configurations on contralateral sides, the present study should be regarded as an exploratory contralateral comparison within-subject comparison rather than a traditional split-mouth trial. This clarification aligns with the paired statistical analyses performed and with the presentation of mean differences between sides in Table II. Overall, while some statistically significant findings may have limited clinical impact, the higher effectiveness observed in the premolar region and the critical role of attachment positioning underscore the potential of IHA as a reliable treatment modality. Further studies with larger samples are warranted to confirm these results and explore the factors that influence treatment variability.

Conclusion

IHA promoted effective dental arch expansion, with the highest effectiveness observed in the first and second premolars (59% and 46%, respectively). Canine expansion was less predictable and often accompanied by excessive buccal crown torque. Incisally oriented slice attachments enhanced torque control in canines, while first molars demonstrated stable torque behavior regardless of attachment design. Vertical control was consistently maintained across all teeth. These findings support the clinical viability of IHA to achieve dental arch expansion, despite the low effectiveness relative to the digital programmed movements, and underscore the importance of attachment positioning in optimizing biomechanical outcomes

References

1. Cao Y, Wang ZW, Chen D, et al. The effect of space arrangement between anterior teeth on their retraction with clear aligners in first premolar extraction treatment: a finite element study. Prog Orthod. 2023;24(1):39. doi:10.1186/s40510-023-00484-1
2. Li N, Lei X, Cao Y, et al. The effect of increasing the gaps between the front teeth on torque and intrusion control of the incisors for anterior retraction with clear aligners: a prospective study. BMC Oral Health. 2024;24(1):115. doi:10.1186/s12903-024-03867-w
3. Aragon MLS de C, Mendes Ribeiro SM, Fernandes Fagundes NC, Normando D. Effectiveness of dental arch expansion in the orthodontic treatment with clear aligners: a scoping review. Eur J Orthod. 2024;46(6). doi:10.1093/ejo/cjae059
4. Lione R, Cretella Lombardo E, Paoloni V, Meuli S, Pavoni C, Cozza P. Upper arch dimensional changes with clear aligners in the early mixed dentition. Journal of Orofacial Orthopedics / Fortschritte der Kieferorthopädie. 2023;84(1):33-40. doi:10.1007/s00056-021-00332-z
5. Bouchant M, Saade A, El Helou M. Is maxillary arch expansion with Invisalign® efficient and predictable? A systematic review. Int Orthod. 2023;21(2):100750. doi:10.1016/j.ortho.2023.100750
6. Talens-Cogollos L, Vela-Hernández A, Peiró-Guijarro MA, et al. Unplanned molar intrusion after Invisalign treatment. American Journal of Orthodontics and Dentofacial Orthopedics. 2022;162(4):451-458. doi:10.1016/j.ajodo.2021.03.019
7. Aragon MLS de C, Mendes Ribeiro SM, Fernandes Fagundes NC, Normando D. Effectiveness of dental arch expansion in the orthodontic treatment with clear aligners: a scoping review. Eur J Orthod. 2024;46(6). doi:10.1093/ejo/cjae059
8. D'Antò V, Valletta R, Di Mauro L, Riccitiello F, Kirlis R, Rongo R. The Predictability of Transverse Changes in Patients Treated with Clear Aligners. Materials (Basel). 2023;16(5). doi:10.3390/ma16051910
9. Levrini L, Zecca PA, Deppieri A, et al. Predictability of Maxillary Expansion with Invisalign® First: Treatment Planning vs. Outcome. Applied Sciences. 2024;14(21):9871. doi:10.3390/app14219871
10. Rossini G, Parrini S, Castroflorio T, Deregibus A, Debernardi CL. Efficacy of clear aligners in controlling orthodontic tooth movement: A systematic review. Angle Orthod. 2015;85(5):881-889. doi:10.2319/061614-436.1

11. Hahn W, Zapf A, Dathe H, et al. Torquing an upper central incisor with aligners-acting forces and biomechanical principles. The European Journal of Orthodontics. 2010;32(6):607-613. doi:10.1093/ejo/cjq007
12. Rocha AS, Gonçalves M, Oliveira AC, Azevedo RMS, Pinho T. Efficiency and Predictability of Coronal Maxillary Expansion Repercussion with the Aligners System: A Retrospective Study. Dent J (Basel). 2023;11(11):258. doi:10.3390/dj11110258
13. Houle JP, Piedade L, Todescan R, Pinheiro FHSL. The predictability of transverse changes with Invisalign. Angle Orthod. 2017;87(1):19-24. doi:10.2319/122115-875.1
14. Morales-Burruezo I, Gandía-Franco JL, Cobo J, Vela-Hernández A, Bellot-Arcís C. Arch expansion with the Invisalign system: Efficacy and predictability. PLoS One. 2020;15(12):e0242979. doi:10.1371/journal.pone.0242979
15. Karslı N, Ocak I, Akyıldız M, Gögen H, Dalci O. Evaluation of the effect of different attachment configurations on molar teeth in maxillary expansion with clear aligners – a finite element analysis. BMC Oral Health. 2024;24(1):921. doi:10.1186/s12903-024- 04544-8
16. Tozlu M, Özdemir F. In-house Aligners: Why We Should Fabricate Aligners in Our Clinics? Turk J Orthod. 2021;34(3):199-201. doi:10.5152/TurkJOrthod.2021.21157
17. Sachdev S, Tantidhnazet S, Saengfai NN. Accuracy of Tooth Movement with In-House Clear Aligners. J World Fed Orthod. 2021;10(4):177-182. doi:10.1016/j.ejwf.2021.08.003
18. Schulz KF, Altman DG, Moher D. CONSORT 2010 Statement: updated guidelines for reporting parallel group randomised trials. BMJ. 2010;340(mar23 1):c332-c332. doi:10.1136/bmj.c332
19. Stucki S, Gkantidis N. Assessment of techniques used for superimposition of maxillary and mandibular 3D surface models to evaluate tooth movement: a systematic review. Eur J Orthod. 2020;42(5):559-570. doi:10.1093/ejo/cjz075
20. Anacleto MA, Souki BQ. Superimposition of 3D maxillary digital models using open-source software. Dental Press J Orthod. 2019;24(2):81-91. doi:10.1590/2177-6709.24.2.081-091.bbo
21. Ioshida M, Muñoz BA, Rios H, et al. Accuracy and reliability of mandibular digital model registration with use of the mucogingival junction as the reference. Oral Surg Oral Med Oral Pathol Oral Radiol. 2019;127(4):351-360. doi:10.1016/j.oooo.2018.10.003
22. Dahlberg G. Statistical methods for medical and biological studies. Statistical methods for medical and biological students. Published online 1940.

23. Pandis N, Burzykowski T. Comparing prescribed and achieved treatment outcomes in digitally planned orthodontic treatment: statistical approaches. Semin Orthod. Published online June 2025. doi:10.1053/j.sodo.2025.06.002
24. Solano-Mendoza B, Sonnemberg B, Solano-Reina E, Iglesias-Linares A. How effective is the Invisalign® system in expansion movement with Ex30′ aligners? Clin Oral Investig. 2017;21(5):1475-1484. doi:10.1007/s00784-016-1908-y
25. Zhou N, Guo J. Efficiency of Upper Arch Expansion with the Invisalign System. Angle Orthod. 2020;90(1):23-30. doi:10.2319/022719-151.1
26. Vidal-Bernárdez M, Vilches-Arenas Á, Sonnemberg B, Solano-Reina E, Solano-Mendoza B. Efficacy and predictability of maxillary and mandibular expansion with the Invisalign® system. J Clin Exp Dent. Published online 2021:e669-e677. doi:10.4317/jced.58315
27. Galluccio G, De Stefano AA, Horodynski M, et al. Efficacy and Accuracy of Maxillary Arch Expansion with Clear Aligner Treatment. Int J Environ Res Public Health. 2023;20(5):4634. doi:10.3390/ijerph20054634
28. Dasy H, Dasy A, Asatrian G, Rózsa N, Lee HF, Kwak JH. Effects of variable attachment shapes and aligner material on aligner retention. Angle Orthod. 2015;85(6):934-940. doi:10.2319/091014-637.1

4.4 Comparison between Personalized and Standard Facemasks for Early Treatment of Class III Malocclusion: a Crossover Randomized Controlled Trial

Abstract

To compare a personalized facemask and the standard facemask in Class III orthodontic patients, using a randomized crossover design. This is a monocentric, controlled, superiority, randomized, crossover, open study. Twenty-four orthodontic patients between 5 and 12 years of age wore one type of mask for 2 months, followed by the other type for the subsequent 2 months in random order. Participants were recruited from September 2024 to May 2025 and the study was completed in September 2025. Patients were asked which one of the two facemasks they preferred. A questionnaire including Visual Analogue Scale (VAS) for pain and difficulty in sleeping was administered to the patients. Complications with both facemasks were registered. A Theramon sensor was used to monitor the facemask wear time. Seventeen out of 24 patients preferred the personalized facemask (71%, 95% confidence interval [CI]: 49% to 87%; $P = 0.063$). Pain at 2 weeks was significantly lower with the personalized facemask (difference –0.9; 95% CI: –0.1 to –1.8; P = 0.034). No differences in pain at 2 months (difference 0.4; 95% CI from-0.6 to 1.3; P = 0.413), difficulty sleeping at 2 weeks (difference 0.0; 95% CI from-0.7 to 0.7; P = 1.0) or 2 months (difference-0.2; 95% CI from-0.8 to 1.5; P = 0.583), and wearing time (difference 0.2; 95% CI from-0.3 to 0.8; P = 0.394). No differences in skin irritation at 2 weeks (P = 0.0625, McNemar exact test), at 2 months (P = 1.0) and in complications (P = 1.0, McNemar test). The personalized facemask is preferred by of Class III orthodontic patients aged 5–12 years and it is significantly less painful after 2 weeks than standard facemask. The study was registered on ClinicalTrials.gov with registration number NCT06402656 on 06/2024 (https://https://clinicaltrials.gov/study/NCT06402656).

Introduction

Class III malocclusion is typically defined by an anteroposterior discrepancy between the maxilla and the mandible, resulting in either a prognathic mandible, a retrognathic maxilla, or a combination of both [1]. Facemask (FM) therapy is a well-established approach for the early orthopedic correction of skeletal Class III malocclusion, producing forward displacement of the maxilla and a clockwise rotation of the maxillomandibular complex [2]. Ideally, treatment should begin during childhood, before puberty, to optimize occlusal relationships, improve facial esthetics, and reduce the likelihood of future orthognathic surgery [3]. The success of FM therapy depends heavily on patient compliance, which is influenced by comfort, tolerance, and appliance acceptability. Conventional FMs typically consist of standardized frontal and mental acrylic pads, connected by a midline stainless steel rod. Only standard sizes are commercially available, limiting adaptability to individual facial anatomy. Patients frequently report discomfort, instability, bulkiness, and esthetic concerns, as well as feelings of embarrassment or shame. Prolonged wear can cause frontal and chin skin irritations, and hyperkeratosis, ulcers or sores were reported to occur in up to 43% of patients [4]. These factors discourage daytime use. In fact, reported FM wear is generally restricted to approximately 10 hours per day, which does not align with the prescribed usage. Even when monitoring systems are employed, usage is predominantly confined to nighttime [5]. A sample of children rated the FM as the least attractive orthodontic appliance [6]. To overcome these problems clinicians have tried to customize the device on a plaster model of the patient's face obtained by taking an alginate impression. However, the latter procedure is not pleasant for the children [7,8]. More recently, advances in digital design and additive manufacturing have opened new possibilities. Using these technologies, a Petit-type FM with rests and midline bar customized to the patient's facial anatomy was developed and clinically tested in a child requiring early Class III treatment [9], and later evaluated in a larger sample to assess acceptability and adaptability [10]. These case reports demonstrated that patient-specific 3D-printed facemasks could be successfully fabricated, were well accepted, and achieved the desired orthopedic effects. A randomized clinical trial has been recently published and a novel 3D printed customized facemask has been proven to be as effective as the standard facemask in early treatment of Class III malocclusion [11]. To our knowledge, no RCT has previously compared standard and personalized FMs in early Class III treatment with respect to patient preference, wear time, pain, and sleeping difficulty. The objective of the present study was to compare the standard facemask with personalized facemask for early treatment of Class III malocclusion with a randomized crossover design. In particular, the appliance preference, wearing time, pain, and sleeping difficulty were analyzed.

Materials and Methods

The experimental design followed the Consolidated Standards of Reporting Trials (CONSORT 2025) statement and extension checklist for reporting within-person randomized trials [12].

Ethic statement

This study was conducted in accordance with the ethical principles in the Declaration of Helsinki for clinical research involving human subjects. The study was approved by the Paediatric Ethics Committee of the Region of Tuscany, Italy on March 14th, 2024. (approval number 0032309).

Trial registration

The study was registered on ClinicalTrials.gov with registration number NCT06402656 on 06/2024 (https://https://clinicaltrials.gov/study/NCT06402656).

Protocol and statistical analysis

The full trial protocol and the statistical analysis can be accessed in the supplementary material.

Data sharing

Deidentified data collected and presented in this study will be made available upon reasonable request after publication of this Article, following approval by regulatory authorities. Data can be requested by contacting the corresponding author.

Funding and conflicts of interest

No external funding was received for this study, and the authors declare that they have no conflicts of interest.

Trial design

This is a monocentric, controlled, superiority, randomized, crossover, open study. Two facemasks for Class III malocclusion treatment (standard facemask and personalized facemask) were compared.
Each patient was treated with both a personalized facemask and a standard facemask. The first assignment to either facemask type was random. Each patient wore one type of mask for 2 months, followed by the other type for the subsequent 2 months. At 2 weeks and 2 months after delivery of each facial mask, the patient completed a questionnaire assessing pain and difficulty sleeping and were assisted by their parents when necessary. After completing both phases (at the fourth month), the patient indicated a preference for one of the two facemask types, with which the treatment was continued for additional 6 months.

Changes to trial protocol

No changes to trial protocol have been performed.

Trial setting

The subjects were enrolled in the study at the Orthodontic Clinic of the Careggi University Hospital, in Florence, Italy.

Elegibility criteria

To be included in the study, patients had to be aged between 5 and 12 years, diagnosed with Class III malocclusion (Wits appraisal <-3 mm) requiring early orthopedic treatment with a rapid maxillary expander and facemask. Exclusion criteria were cleft lip and/or palate patients and the presence of craniofacial syndromes. Patients' parents signed an informed consent before starting the trial.

Interventions and comparator

All the patients were treated with Hyrax-type RME as intraoral anchorage that was activated only in the presence of transverse discrepancy between the arches. RME was activated at the rate of one quarter turn per day, corresponding to 0.2 mm of expansion, until a slight overcorrection was achieved (palatal cusps of the upper posterior teeth occluding on the buccal cusps of the lower posterior teeth). Patients' face scans were acquired with Face Scanner Maxi 6 (Polishape 3D, Bari, Italy) and Agisoft Photoscan Professional edition software (Agisoft llc, St. Petersburg, Russia). Six Canon reflex cameras 1200D 18Mpx (Canon, Tokyo, Japan) connected with 2 external flashes (Metz BL-400; SB 50-70) simultaneously took a photograph from different angulations. Scanning was conducted in a well-lit room, and a disposable cap was used to hold back the hair, preventing it or its shadow from obscuring facial skin areas. The patients were invited to sit in a resting posture, and to keep the teeth in occlusion and the lips relaxed. The 6 photographs were then digitally processed, and the resulting file was exported in .obj format. The digital design and manufacturing of the FMs were performed by a laboratory technician (Firenze Ortodonzia, Florence, Italy), in accordance with the patented protocol (European Patent N. EP 3752091, USA Patent N. US20200397536). The forehead and chin pads as well as the central bar of the FM were modelled on the 3D image of the patients' face, using the 3D Leone Designer software (Leone S.p.A., Sesto Fiorentino, Firenze, Italy). Then, the pads were printed with SprintRay EU Splint Flex Resin (SprintRay Inc, Los Angeles, CA, USA) using the SprintRay ProS 3D printer (SprintRay Inc, Los Angeles, CA, USA), while the central bar in stainless steel was bent and adapted to the patient's face 3D printed model. Finally, each piece was polished and assembled. Petit-type FM was used in the standard FM group (Leone S.p.A., Sesto Fiorentino, Firenze, Italy) (Fig. 1).

Figure 1. Petit-type standard FM (A) and Personalized FM (B). Theramon sensors were places on the right side of forehead pad.

A pressure and temperature sensor (Theramon, MC Technology, Hargelsberg, Austria) connected to a dedicated cloud was added at the base of the frontal support to monitor the FM wear time. Each customized FM was then delivered to the patients by the orthodontist, who secured the sliding crossbar to the central bar with a setscrew, so that the rubber bands reached a 30° downward inclination relative to the occlusal plane. The orthodontist also selected and delivered extraoral elastics that produced a tensile force of about 400 grams per side (Fig. 2). Patients and their parents or guardians were adequately instructed by the orthodontist on how and for how long (about 14 hours per day) to wear the FM.

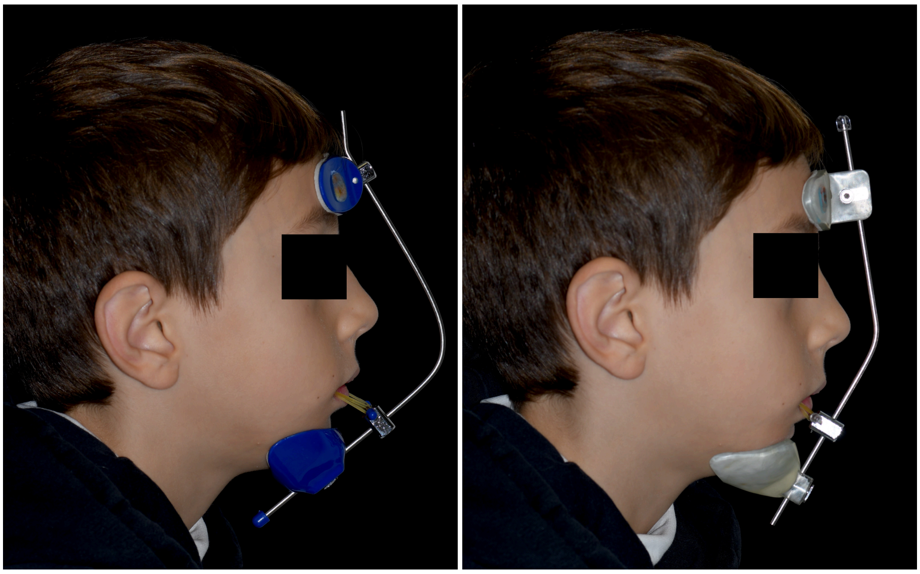

Figure 2. Petit-type standard FM (A) and Personalized FM (B). Elastic forces (400 g per side) were placed at 30° downward from the occlusal plane.

Outcomes

The primary outcome variable of the study was the patient's preference for one of the two facemasks at the end of the second phase of treatment (4 months after delivery of the first facemask). The secondary outcome variables were pain, difficulty sleeping, wearing time, and complications during treatment. For the assessment of pain and difficulty in sleeping a questionnaire including a Visual Analog Scales (VAS) was provided to the patients at 2 weeks and 2 months after delivery of each facial mask. The VAS features scores from 0 to 10 (Fig. 3).

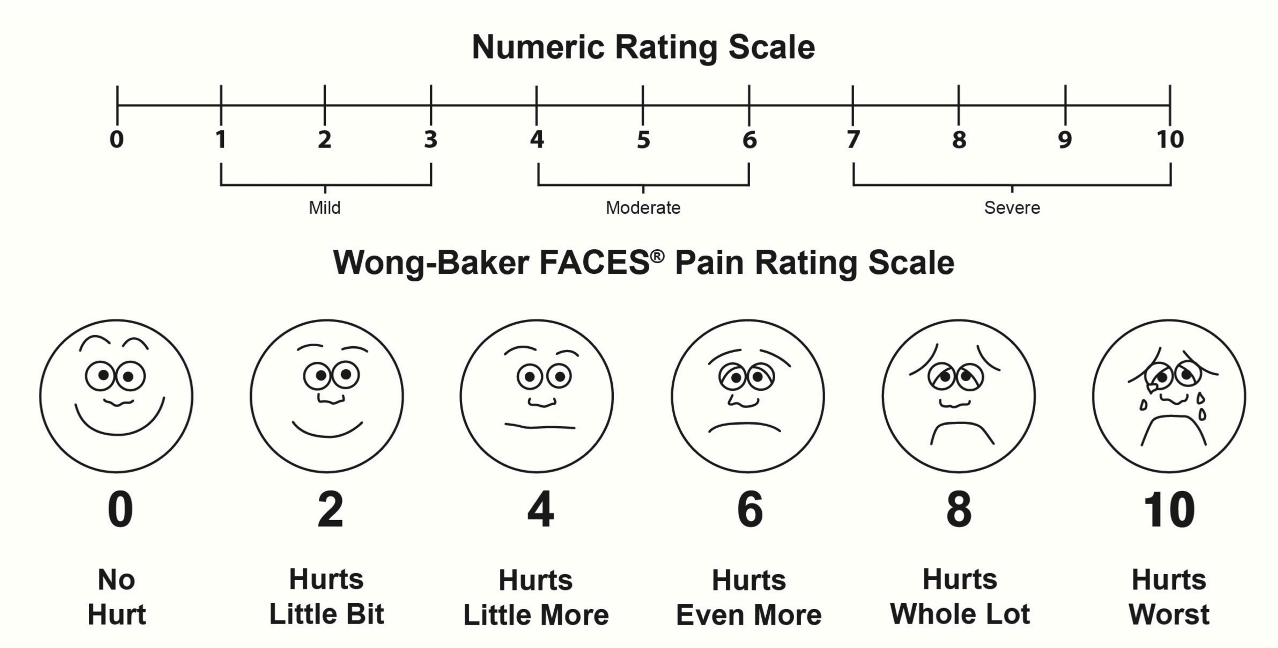

Figure 3. VAS score with numeric rating scale associated to Wong Baker FACES Pain Rating Scale. [13]

In the pain scale 0 corresponded to no pain while 10 to very painful. To facilitate interpretation, the Wong-Baker Scale was also used [13]. In the sleeping difficulty scale 0 corresponded to no sleeping difficulty while 10 to maximum sleeping difficulty.

Information on complications reported by patients or their parents was collected throughout treatment. Total usage time was recorded 2 months after delivery of each facemask.

Harms

Adverse events were assessed clinically and analytically at each monthly follow-up visit.

Sample size

Considering a null hypothesis for a proportion of 50% in the preference between the two facemasks and an alternative hypothesis of 80%, with alpha set at 0.05, a power of 80% and a dropout rate of 15%, 24 patients were required.

Randomization

The order of the two facemasks was block randomized so that 12 patients were allocated to the conventional facemask as the first device and 12 patients were allocated to the personalized facemask as the first device (Fig. 4).

Sequence generation

The randomization list was computer-generated by the statistician (MN) and hidden inside numbered, opaque and sealed envelopes that were opened at the time of facemask delivery. Patients were enrolled by one operator (LF) and they were assigned to each facemask by another operator (CB).

Blinding

Neither the patient nor the operator was blinded. The statistician (MN), however, was blinded to group assignment.

Statistical methods

Descriptive statistics were performed for all variables (frequency and percentage for qualitative variables and mean and standard deviation for quantitative variables). For the primary outcome variable (facemask preference) the test was performed for one proportion and the 95% confidence interval [CI] was calculated using the Clopper-Pearson exact method.

A mixed-effects model was used to evaluate the VAS scores for pain at 2 weeks and 2 months. In the model, the random effect was represented by the patient, and the fixed effects were the type of facemask used and the period (first or second period of use). A similar model was applied for the VAS scores assessing difficulty sleeping at 2 weeks and 2 months, as well as for the total facemask usage time at 2 months. McNemar test was used to evaluate complications.

Statistical analysis was carried out according to the intention-to-treat method. All statistical tests were performed with JMP 13.0 (SAS Institute Inc.) using a level of statistical significance of .05.

Results

Participants were recruited from September 2024 to May 2025 and the study was completed in September 2025.

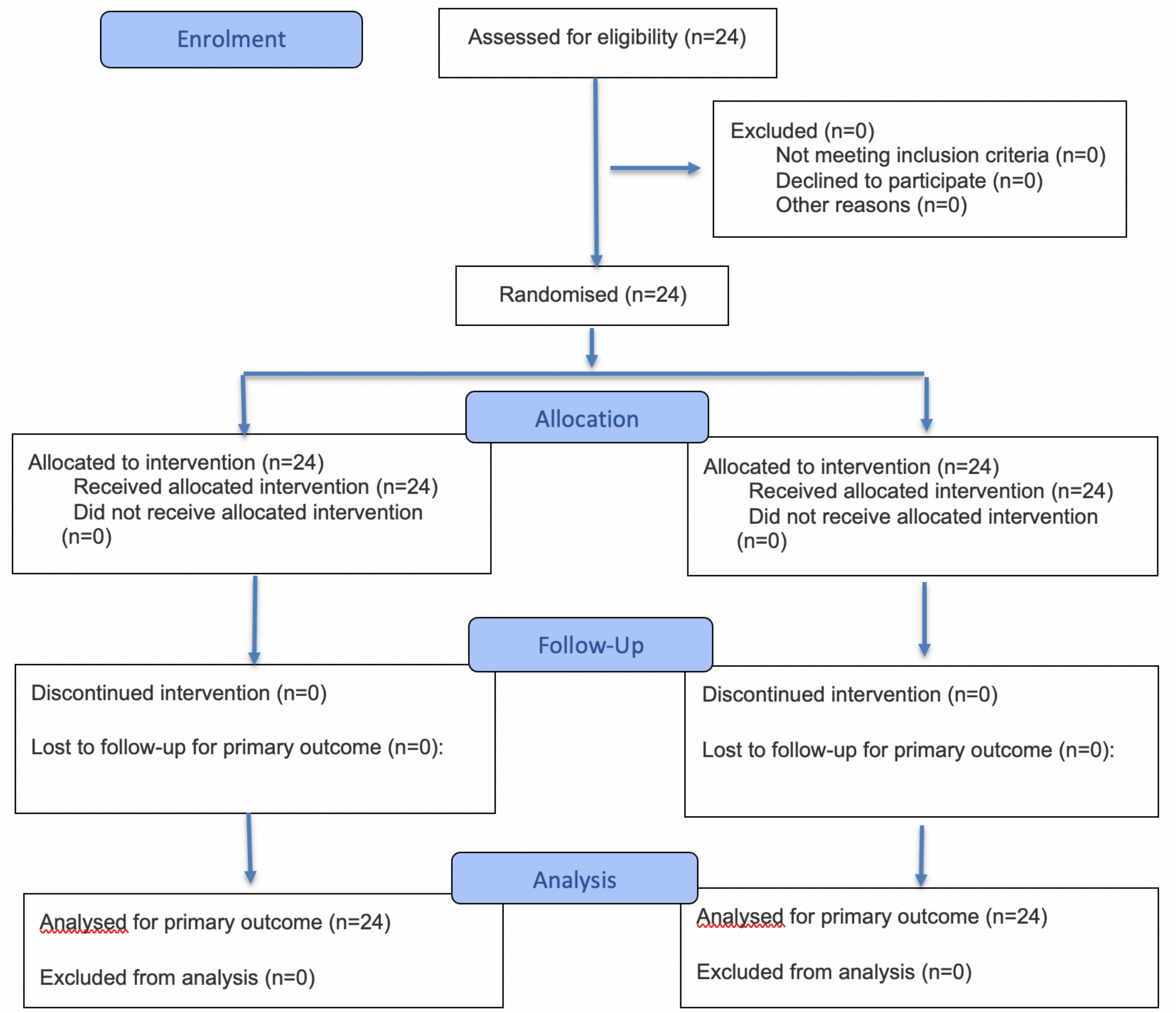

Figure 4. Consort 2025 flow diagram [12]. S, Standard FM Group; P, Personalized FM Group.

There were no dropouts and no deviations from the planned protocol. The mean age of the participants was 8.4 years (standard deviation 1.8, range 5.5-12.5). There were 13 males and 11 females.

Twelve participants were allocated to standard facemask as first facemask (Standard Group) and 12 participants were allocated to personalized facemask as first facemask (Personalized Group).

7 patients preferred standard facemask (29%) while 17 patients preferred personalized facemask (71%, 95% CI: 49% to 87%). This difference in preference was marginally non significant (*P* = 0.064 Exact one sample test on proportions).

The differences between the two facemasks as for usage time, pain, and sleeping difficulty are reported in Table I.

Table I. Pain, sleeping difficulty, and wearing time for the two FMs.

Variable	*Standard N=24 Mean (SD)*	*Personalized N=24 Mean (SD)*	*Difference*	*95%CI*	*P-value*
Pain 2 weeks	2.0 (2.2)	1.0 (2.2)	-0.9	-0.1;-1.8	0.034
Pain 2 months	1.0 (1.4)	1.3 (1.6)	0.4	-0.6; 1.3	0.413
Sleeping difficulty 2 weeks	1.0 (1.8)	1.0 (1.3)	0.0	-0.7; 0.7	1.0
Sleeping difficulty 2 months	0.9 (1.3)	0.7 (1.3)	-0.2	-0.8; 0.5	0.583
Wearing time (hours/day)	8.0 (2.1)	8.2 (1.6)	0.2	-0.3; 0.8	0.394

Pain at 2 weeks was significantly lower with the personalized facemask (difference –0.9; 95% CI: –0.1 to –1.8; P = 0.034). No significant differences were observed in pain at 2 months (difference 0.4; 95% CI from-0.6 to 1.3; P = 0.413), difficulty sleeping at 2 weeks (difference 0.0; 95% CI from-0.7 to 0.7; P = 1.0) or 2 months (difference-0.2; 95% CI from-0.8 to 1.5; P = 0.583), and wearing time (difference 0.2; 95% CI from-0.3 to 0.8; P = 0.394). Skin irritation at 2 weeks occurred in 83% of cases with the standard facemask and 62% with the personalized facemask (P = 0.062, McNemar exact test). At 2 months, irritation occurred in 62% and 58% of cases, respectively (P = 1.0). Complications were reported in 21% of cases with the standard facemask and 17% with the personalized facemask (P = 1.0, McNemar test).

Discussion

The aim of this study was to compare the standard facemask with personalized facemask for early treatment of Class III malocclusion. Literature has demonstrated that among various types of orthodontic devices, the standard facemask has the lowest acceptance rate [6]. This may be due to the main complaints reported by patients to the orthodontist, such as bulkiness, instability on the face, and, overall, uncomfortable use of the device. The discomfort felt by the patient may lead to loss of compliance and, consequently, may contribute to the failure of orthodontic therapy. For this reason, we compared the standard with a new customized digital design to test if it would have been more comfortable in terms of pain, skin irritation and difficulty in sleeping. In our investigation, 71% of patients expressed a preference for the personalized FM. This observed difference in preference was found to be marginally non significant (P = 0.064). This result may be explained by the use of a low-sensitivity exact test for paired data, which may not have adequately captured subtle differences. The Clopper Pearson interval is used to evaluate binomial confidence intervals in small samples and in this study did not indicate a clear preference for the personalized facemask. The observed differences approached statistical significance, and due to this further evaluation in a larger sample is suggested to further clarify these findings. Even though the difference in preference was marginally non significant, it can be attributed to enhanced initial comfort, since there was a statistically significant reduction in patient-reported pain for the personalized facemask after the 2-week assessment. Skin irritation also demonstrated a trend toward significance (P=0.062) during this initial period. However, due to patient adaptability these advantages diminished over time. At the 2-month follow-up, pain, skin irritation, and difficulty in sleeping converged, with no significant differences between the two FMs. Therefore, it may be inferred that these combined short-term effects explain the greater preference for the personalized FM.

For effective results, several authors recommend a facemask wear time ranging from 10 to 24 hours per day [14]. However, literature shows that 92% of patients do not adhere to the prescribed usage times, wearing the device for about 9 hours out of the 13 hours prescribed. This risks to compromise the effectiveness of the orthodontic treatment [15]. To overcome the inherent limitation of assessing appliance wear time based solely on patient-reported adherence, we incorporated a TheraMon sensor (MC Technology GmbH, Hargelsberg, Austria) to precisely quantify patient compliance with both the standard and personalized facemasks. A previous investigation by Stocker et al. [5] utilized TheraMon chip technology to evaluate facemask usage time, reporting an average wear time of approximately 10 hours per day. In contrast, the average wear time observed in our current study was approximately 8 hours per day. This discrepancy in mean wear time may be attributed to differences in the sample size employed. Specifically, the Stocker et al. [5] study evaluated only a single patient, whereas our present study utilized a larger and more representative cohort. Patients in our study were prescribed a recommended wear time of 14 hours per day. The sensor recorded a mean wear time of 8.2 hours for the personalized facemask (PFM) and 8.0 hours for the standard facemask (FM). Independently of the facemask design, this observation confirms data from previous studies showing an average of about 9 hours of actual use of removable devices despite prescriptions of 12 to 15 hours [16–18]. Our study is in accordance with Arreghini et al. [18], who evaluated the influence of various variables on collaboration, including the awareness of being monitored. Their study showed that such awareness does not directly enhance compliance. Similarly, we recorded an average wear time of about 8 hours per day, predominantly during nighttime. Regarding sensor reading reliability, several studies have evaluated the accuracy of TheraMon microsensors in vitro or in vivo only under intraoral conditions [19–22]. The sensor chip is calibrated to record appliance use exclusively when detecting temperature values within the range of 33.5°C to 39°C, a range that encompasses most normal intraoral temperatures. Although the TheraMon system was initially developed to monitor compliance for intraoral appliances [23–28], its application has been evaluated for extraoral devices, including cervical headgear [29] or the facemask [5,30]. Nonetheless, the sensor's recordings have demonstrated certain limitations [31] , as the device appears susceptible to seasonal temperature fluctuations, especially during the summer months [32].

Appliance-related factors that can be controlled to improve patient compliance include appearance, usage instructions, and comfort. Enhancing appliance appearance through customization [9], embellishments and decorations [10] and the integration of gamification [33] have all been proposed and demonstrated promising clinical results. However, this study design avoided including other variables such as changes in the appearance of the appliances. The personalized FMs were as similar as possible to the standard FMs. Despite our efforts, the acrylic pads were not the same color and in the personalized FMs they were transparent which could also have affected patient's preference. Gamification was also intentionally left out of the present investigation since increasing cooperation was not main goal of this study.

In the present study, usage instructions remained consistent across both FM types. Since patients were prescribed the same level of cooperation, the recorded daily wear time for both the standard and personalized FMs was similar, showing no significant differences between the two designs. Regarding comfort and adaptability, the personalized FM was certainly better received, garnering a

70% patient preference. However, this increase in preference was insufficient to significantly increase the actual wearing time, which remained constant at approximately 8 hours per day. The reduced cooperation observed is presumably attributable to the bulkiness of the device, which is predominantly used in a domestic setting. Consequently, greater patient cooperation with the use of intra-oral appliances could be expected [34].

In this context, several authors have proposed reproducing the force system of the facemask intraorally in order to improve adaptability and reduce the bulk associated with extraoral devices, thereby increasing patient acceptance and wear time. Bone-anchored alternative systems have already shown promising results in achieving orthopedic correction of Class III malocclusion [35–39]. However, more importantly than appliance design, the factor that should truly be investigated to improve cooperation is the appliance's psychosocial impact on the child's self-perception, given that our findings demonstrated that cooperation is not necessarily associated with adaptability. A study by Topcuoglu [40] assessed the potential influence of orthodontic extraoral appliances on depression and anxiety levels in both patients and parents. Their findings demonstrated that the 1-year treatment group scored significantly higher on both the depression and trait-anxiety scales when compared to the pre-treatment group. Consequently, thorough consideration of psychological parameters is warranted both before and throughout treatment with extraoral appliances.

Regarding treatment outcome evaluation, a recent study by Abdulkareem et al. [11] assessed differences in the effectiveness of digital versus standard FMs. While both facemask types were found to be effective for Class III correction, better acceptance during sleep was reported in their study, which contrasts with our findings. However, patient comfort and compliance in that study were recorded via self-reported data, which often fail to accurately reflect real wear duration or acceptability. For these reasons, objective compliance monitoring systems are essential, alongside continual reinforcement of the importance of patient cooperation throughout the treatment period. In our current study, appliance use was effectively monitored using the TheraMon sensor, which demonstrated no significant differences in wearing time between the two FM designs.

While the sample size in the current investigation is relatively small, and a larger cohort might be required to increase statistical power and allow for clinically relevant subgroup analyses, the collective data suggest that effectiveness is equivalent, wearing time is equivalent, and preference is statistically similar with marginally non significant results.

Conclusions

In children between 5 and 12 years with Class III malocclusion requiring early orthopedic treatment with facemask:

1. 71% of patients preferred personalized FM, which is marginally non significant.
2. Pain at 2 weeks was significantly lower for the personalized FM compared to the standard one.
3. Skin irritation at 2 weeks was lower for the personalized facemask, which is marginally non significant.
4. No statistically significant differences for wearing time, pain at 2 months, skin irritation at 2 months, difficulty in sleeping and complications between the two FMs were found.

References

1. Guyer EC, Ellis EE, McNamara JA, Behrents RG. Components of class III malocclusion in juveniles and adolescents. Angle Orthod. 1986;56:7–30. https://doi.org/10.1043/0003-3219(1986)056<0007:COCIMI>2.0.CO;2
2. Ngan P, Moon W. Evolution of Class III treatment in orthodontics. American Journal of Orthodontics and Dentofacial Orthopedics. 2015;148:22–36. https://doi.org/10.1016/j.ajodo.2015.04.012
3. Rutili V, Quiroga Souki B, Nieri M, Farnese Morais Carlos AL, Pavoni C, Cozza P, et al. Long-Term Assessment of Treatment Timing for Rapid Maxillary Expansion and Facemask Therapy Followed by Fixed Appliances: A Multicenter Retro-Prospective Study. J Clin Med. 2023;12:6930. https://doi.org/10.3390/jcm12216930
4. Kim H, Kim JS, Kim CS, Becker-Weimann SY, Cha J-Y, Choi S-H. Skin irritation in children undergoing orthodontic facemask therapy. Sci Rep. 2023;13:2200. https://doi.org/10.1038/s41598-023-29253-0
5. Stocker B, Willmann JH, Wilmes B, Vasudavan S, Drescher D. Wear-time recording during early Class III facemask treatment using TheraMon chip technology. Am J Orthod Dentofacial Orthop. 2016;150:533–40. https://doi.org/10.1016/j.ajodo.2016.04.016
6. Abu Alhaija ESJ, Karajeh MA. Acceptability and attractiveness of intra- and extra-oral orthodontic appliances. Int J Orthod Milwaukee. 2013;24:11–7.
7. Turley PK. Orthopedic correction of Class III malocclusion with palatal expansion and custom protraction headgear. J Clin Orthod. 1988;22:314–25.
8. Ierardo G, Luzzi V, Vozza I, Polimeni A, Bossù M. Skin irritation from a facial mask in Class III malocclusion: evaluation of individual silicone chin cups in a group of 100 children. Minerva Stomatol. 2018;67:45–8. https://doi.org/10.23736/S0026-4970.17.04073-0
9. Franchi L, Vichi A, Marti P, Lampus F, Guercio S, Recupero A, et al. 3D Printed Customized Facemask for Maxillary Protraction in the Early Treatment of a Class III Malocclusion: Proof-of-Concept Clinical Case. Materials (Basel). 2022;15:3747. https://doi.org/10.3390/ma15113747
10. Caroccia F, Juloski J, Juloski J, Marti P, Lampus F, Vichi A, et al. 3D printed customized facemask for early treatment of Class III malocclusion: a two-center case series feasibility study. Minerva Dent Oral Sci. 2025;74:42–8. https://doi.org/10.23736/S2724-6329.24.05013-7

11. Abdulkareem GB, Cobourne MT, Abid M. The effectiveness of novel 3D printed customized facemask appliance for treatment of class III malocclusion: a randomized clinical trial. European Journal of Orthodontics. 2025;47:cjaf075. https://doi.org/10.1093/ejo/cjaf075
12. Hopewell S, Chan A-W, Collins GS, Hróbjartsson A, Moher D, Schulz KF, et al. CONSORT 2025 statement: updated guideline for reporting randomized trials. Nat Med. 2025;31:1776–83. https://doi.org/10.1038/s41591-025-03635-5
13. Wong DL, Baker CM. Pain in children: comparison of assessment scales. Pediatr Nurs. 1988;14:9–17.
14. Yepes E, Quintero P, Rueda ZV, Pedroza A. Optimal force for maxillary protraction facemask therapy in the early treatment of class III malocclusion. European Journal of Orthodontics. 2014;36:586–94. https://doi.org/10.1093/ejo/cjt091
15. Schott TC, Ludwig B. Microelectronic wear-time documentation of removable orthodontic devices detects heterogeneous wear behavior and individualizes treatment planning. American Journal of Orthodontics and Dentofacial Orthopedics. 2014;146:155–60. https://doi.org/10.1016/j.ajodo.2014.04.020
16. Schott TC, Schrey S, Walter J, Glasl BA, Ludwig B. Questionnaire study of electronic wear-time tracking as experienced by patients and parents during treatment with removable orthodontic appliances. J Orofac Orthop. 2013;74:217–25. https://doi.org/10.1007/s00056-013-0143-2
17. Tsomos G, Ludwig B, Grossen J, Pazera P, Gkantidis N. Objective assessment of patient compliance with removable orthodontic appliances: A cross-sectional cohort study. The Angle Orthodontist. 2014;84:56–61. https://doi.org/10.2319/042313-315.1
18. Arreghini A, Trigila S, Lombardo L, Siciliani G. Objective assessment of compliance with intra- and extraoral removable appliances. The Angle Orthodontist. 2017;87:88–95. https://doi.org/10.2319/020616-104.1
19. Schott TC, Göz G. Applicative Characteristics of New Microelectronic Sensors Smart Retainer® and TheraMon® for Mea suring Wear Time. J Orofac Orthop. 2010;71:339–47. https://doi.org/10.1007/s00056-010-1019-3
20. Schott TC, Göz G. Wearing times of orthodontic devices as measured by the TheraMon® microsensor. J Orofac Orthop. 2011;72:103–10. https://doi.org/10.1007/s00056-011-0014-7
21. Brierley CA, Benson PE, Sandler J. How accurate are TheraMon® microsensors at measuring intraoral wear-time? Recorded vs. actual wear times in five volunteers. Journal of Orthodontics. 2017;44:241–8. https://doi.org/10.1080/14653125.2017.1365220

22. Kirshenblatt S, Chen H, Dieltjens M, Pliska B, Almeida FR. Accuracy of Thermosensitive Microsensors Intended to Monitor Patient Use of Removable Oral Appliances. J Can Dent Assoc. 2018;84:i2.
23. Sangwattanarat T, Thongudomporn U. Effectiveness of removable anterior bite planes with varied mealtime protocols in correcting deep bites among growing patients: a randomized clinical trial. The Angle Orthodontist. 2024;94:615–22. https://doi.org/10.2319/022124-129.1
24. Atik E, Taner T, Aksu M. Is wear time of Hawley retainers measured with microsensors related to mandibular arch stability? J Orofac Orthop. 2025;86:49–57. https://doi.org/10.1007/s00056-023-00495-x
25. Higgins E, Garvey T, Burns A. The effect of text message reminders on compliance with Twin Block appliances: A randomised controlled trial. J Orthod. 2024;51:202–10. https://doi.org/10.1177/14653125231188378
26. Frilund E, Sonesson M, Magnusson A. Patient compliance with Twin Block appliance during treatment of Class II malocclusion: a randomized controlled trial on two check-up prescriptions. European Journal of Orthodontics. 2023;45:142–9. https://doi.org/10.1093/ejo/cjac046
27. İshakoğlu S, Çokakoğlu S. Evaluation of relapse with thermoplastic retainers equipped with microsensors. The Angle Orthodontist. 2022;92:340–6. https://doi.org/10.2319/072221-578.1
28. Al-Moghrabi D, Pandis N, McLaughlin K, Johal A, Donos N, Fleming PS. Evaluation of the effectiveness of a tailored mobile application in increasing the duration of wear of thermoplastic retainers: a randomized controlled trial. European Journal of Orthodontics. 2020;42:571–9. https://doi.org/10.1093/ejo/cjz088
29. Gratsia S, Cocos A, Vastardis H, Halazonetis D. Cervical headgear effectiveness in distalizing molars in relation to patient compliance. European Journal of Orthodontics. 2024;46:cjad075. https://doi.org/10.1093/ejo/cjad075
30. Alzoubi EE, Camilleri S, Al Muzian M, Attard N. The effect of tooth borne versus skeletally anchored Alt-RAMEC protocol in early treatment of Class III malocclusion: a single-centre randomized clinical trial. European Journal of Orthodontics. 2023;45:517–27. https://doi.org/10.1093/ejo/cjad018
31. Schramm C, Abaza A, Blumenstock G, Bechtold TE, Rickmann A, Bartz-Schmidt K, et al. Limitations of the TheraMon® -microsensor in monitoring occlusion therapy. Acta Ophthalmologica [Internet]. 2016 [cited 2025 Nov 9];94. https://doi.org/10.1111/aos.13134

32. Abaza A, Wahl G, Kortüm C, Januschowski K, Besch D, Schramm C. Objective Monitoring of Spectacle Wearing Times in Adult Subjects Using the Theramon® Thermosensor. OPTH. 2021;Volume 15:1375–89. https://doi.org/10.2147/OPTH.S287508
33. Marti P, Teverini G, Goracci C, Franchi L. Gamification of Orthodontic Treatment with Personalised Facemasks: Enhancing Patient Compliance Through Playful Engagement. Future Internet. 2024;16:446. https://doi.org/10.3390/fi16120446
34. Nahajowski M, Lis J, Sarul M. Orthodontic Compliance Assessment: A Systematic Review. International Dental Journal. 2022;72:597–606. https://doi.org/10.1016/j.identj.2022.07.004
35. Al-Mozany SA, Dalci O, Almuzian M, Gonzalez C, Tarraf NE, Ali Darendeliler M. A novel method for treatment of Class III malocclusion in growing patients. Prog Orthod. 2017;18:40. https://doi.org/10.1186/s40510-017-0192-y
36. Manhães FR, Pereira Da Silva T, André CB, Valdrighi HC, Carmo De Menezes C, Vedovello SAS. Dentoskeletal effects of miniscrew-anchored maxillary protraction: Evaluating the role of mandibular anchorage bar and night facemask. American Journal of Orthodontics and Dentofacial Orthopedics. 2025;167:436–43. https://doi.org/10.1016/j.ajodo.2024.11.004
37. Ngan P, Wilmes B, Drescher D, Martin C, Weaver B, Gunel E. Comparison of two maxillary protraction protocols: tooth-borne versus bone-anchored protraction facemask treatment. Prog Orthod. 2015;16:26. https://doi.org/10.1186/s40510-015-0096-7
38. Lee Y, Park JH, Kim J, Lee N-K, Kim Y, Kook Y-A. Treatment effects of maxillary protraction with palatal plates vs conventional tooth-borne anchorage in growing patients with Class III malocclusion. American Journal of Orthodontics and Dentofacial Orthopedics. 2022;162:520–8. https://doi.org/10.1016/j.ajodo.2021.05.014
39. Miranda F, Cunha Bastos JCD, Magno Dos Santos A, Janson G, Pereira Lauris JR, Garib D. Dentoskeletal comparison of miniscrew-anchored maxillary protraction with hybrid and conventional hyrax expanders: A randomized clinical trial. American Journal of Orthodontics and Dentofacial Orthopedics. 2021;160:774–83. https://doi.org/10.1016/j.ajodo.2021.02.017
40. Topcuoglu T, Yildirim O, Birlik M, Sokucu O, Semiz M. The effect of orthodontic extraoral appliances on depression and the anxiety levels of patients and parents. Niger J Clin Pract. 2014;17:81. https://doi.org/10.4103/1119-3077.122850

Appendix

A) A Diagnostic and Treatment Planning Checklist for Vertical Problems in Orthodontic Patients

Abstract

Vertical discrepancies in orthodontics represent a complex and multifactorial diagnostic challenge. Traditional approaches often lack a consistent correlation between facial patterns, overbite, and occlusal vertical dimension, limiting a comprehensive treatment planning. This article proposes a diagnostic checklist structured around five key factors—lower anterior facial height, incisor display at rest, posterior dental height, overbite, and occlusal wear—to assess vertical problems across macro-, mini-, and microesthetic levels. The amount of incisor display at rest serves as the guiding parameter for planning vertical tooth movements and determining jaw positioning. Each diagnostic factor contributes uniquely to evaluating vertical proportions, esthetic balance, and functional occlusion. The checklist offers clinicians a hierarchical tool to decode clinical and cephalometric findings and translate them into individualized treatment strategies. Possible therapeutic options include anterior or posterior tooth intrusion or extrusion, restoration of worn teeth, and orthodontic or orthognathic repositioning of dental or skeletal structures. Three clinical cases—addressing deep bite, open bite, and occlusal wear—illustrate the application of the checklist. These examples underscore the critical role of incisor display in planning and executing movements that harmonize the face, smile, and occlusion.

Introduction

Throughout human evolution, the capacity for oral communication gradually evolved into graphical representation, beginning with cave paintings and hieroglyphs and eventually leading to the development of our modern alphabet. Humans have the unique ability to create codes that they can decode into meaningful information. Since the classical period of art, we have sought to define standards of beauty using measurements and proportions, thereby codifying our perception of attractiveness [1].

In our field, these principles have been translated into anthropometry and subsequently into cephalometric measurements. Over the history of orthodontics, cephalometric analysis has aimed to establish norms, patterns, and associations within these measurements. Despite the development of these tools to analyze facial proportions, the process of translating a three-dimensional structure into two-dimensional representations often results in the loss of information, especially in the context of diagnosis and treatment planning. For instance, changes in the vertical dimension will affect the sagittal relation of the jaws. A major shortcoming of depending only on a cephalometrically driven treatment plan is that it is focused mainly on the sagittal and vertical planes of space at a single point in time and does not take into account how the face, the jaws, and the teeth can change with treatment and over our lifetime [2].

Vertical problems in craniofacial development can affect three primary aspects: facial proportions, the amount of overbite, and the occlusal vertical dimension (OVD). Interestingly, these factors are not inherently associated with one another. One of the most persistent misconceptions in orthodontics is the supposed association between facial patterns and overbite. In reality, any growth pattern can be linked to an open bite as easily as to a deep bite [3–5]. Similarly, interocclusal distance can vary significantly across different facial patterns [6]. Due to the widespread and often conflicting information surrounding vertical problems, they remain unclear and therefore yet a challenge in orthodontics.

To address these issues effectively, vertical problems must be diagnosed with consideration of their impact on facial proportions, smile aesthetics, and occlusion, as well as the impact of vertical occlusal changes on the sagittal dimension. Therefore, the aim of this article is to provide a comprehensive checklist of diagnostic factors, encompassing the face, the smile, and the occlusion, to guide treatment approaches for managing vertical problems.

Diagnostic factors

The field of contemporary orthodontics has evolved, shifting its focus from merely addressing occlusion to encompassing the smile and overall facial aesthetics. Sarver [2] was the major contributor of looking into these fundamental concepts:

- Macro-esthetics: The profile and vertical facial dimensions, i.e., the face
- Mini-esthetics: The smile esthetic factors, eg, buccal corridors, smile arc, incisor display
- Microesthetics: The teeth and their many parameters, eg, contacts and connectors, embrasures, gingival shape and contour

All of these aspects can be affected in the vertical dimension. To integrate these factors into an effective treatment plan, five key elements should be carefully analyzed. They are:

- Lower anterior facial height (LAFH)

- Maxillary and mandibular incisor exposure at rest
- Posterior alveolar height
- Overbite
- Occlusal wear

These elements guide the therapeutic approach and, ultimately, the treatment plan. Each of these diagnostic factors will be explored in detail.

Lower anterior facial height

Social psychology studies have found certain aspects to be important for beauty: averageness, symmetry, and sexual dimorphism [7]. The search for defining ideal facial proportions has a long history, since the understanding of facial aesthetics has been shaped by prominent figures such as Phidias and the ancient Greek sculptors, as well as Renaissance masters like Leonardo da Vinci and Michelangelo. These artists were among the first to establish the fundamental principles of facial proportions, exploring concepts such as the "facial thirds" [1]. A key aspect in achieving facial balance is the normal vertical dimension of the lower face, with particular emphasis on the measurement of LAFH [8].

The typical facial proportions are defined by dividing the face into thirds: the upper third extends from the hairline to the bridge of the nose, the middle third from the bridge to the ala of the nose, and the lower third from the ala of the nose to the menton (Fig. 1A). The LAFH, measured from anterior nasal spine to menton, should account for approximately 65% of the total facial height, from nasion to menton, typically ranging between 55 and 65 mm in a balanced face (Fig. 1B) [9]. Of the three facial thirds, only the lower one can be modified through orthodontic or surgical treatment. Discrepancies in these proportions result in variations known as long or short faces.

A long face is characterized by an increased LAFH, a high mandibular angle, and lip incompetence (Fig. 1C), while a short face is associated with a decreased LAFH, a low mandibular angle, and overclosure of the lips (Fig. 1D).

With the purpose of defining normal facial proportions and mandibular rotation during growth, Horn [10] described the facial height index as the proportion between the anterior and posterior facial heights. Ranges from 0.55 to 0.85 can be treated with orthodontics only, while cases outside these ranges should be considered for a surgical approach. Legan and Burstone [11] and Proffit et al. [12] have proposed the ratio G-Sn/Sn-Me' (normal = 1:1) to describe soft-tissue proportionality between the upper and lower facial heights. Significant changes to these proportions are largely dependent on surgical interventions, as facial proportions do not typically alter with natural growth [13].

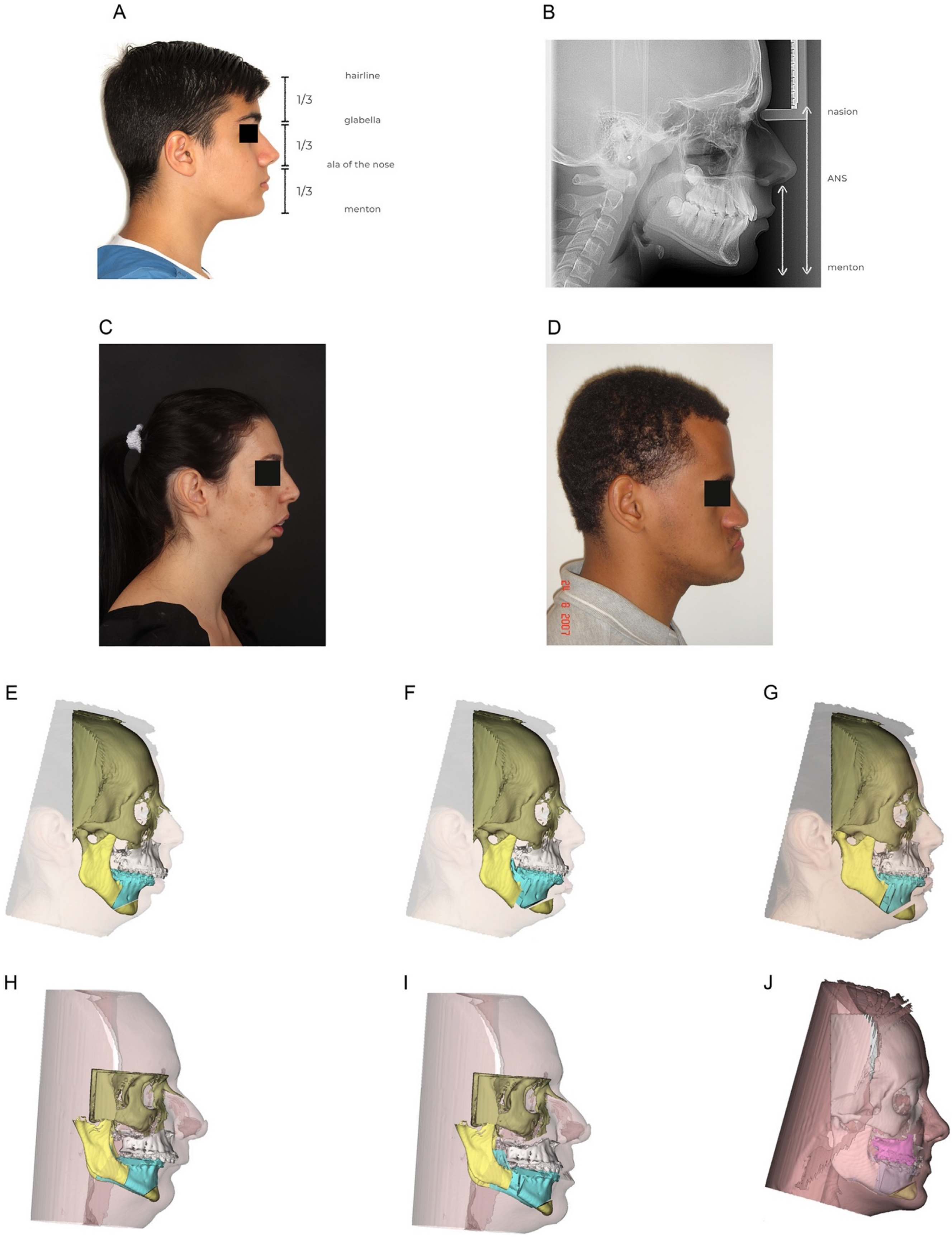

Figure 1. (A) Ideal facial proportions illustrating the division of the face into thirds: hariline to glabella, glabella to subnasale (ala of the nose), and subnasale to menton. (B) Cephalometric assessment of

lower anterior facial height (LAFH), measured from anterior nasal spine (ANS) to menton, representing approximately 65% of the total facial height (nasion to menton). (C) Clinical characteristics of a long face, including increased LAFH, steep mandibular plane angle, and lip incompetence. (D) Clinical features of a short face, characterized by reduced LAFH, a low mandibular plane angle, and lip overclosure. (E) Initial CBCT scan of a patient with a long face for ortho-surgical treatment planning. (F) Treatment planning involving maxillary impaction combined with mandibular advancement. (G) Treatment planning involving maxillo-mandibular counterclockwise rotation. (H) Initial CBCT scan of a patient with a short face for ortho-surgical treatment planning. (I) Treatment planning involving maxillary set-down and mandibular advancement. (J) Treatment planning involving maxillo-mandibular clockwise rotation.

Orthognathic surgery can either increase or decrease the LAFH through different vertical displacement of the jaws, such as maxillary impaction, maxillary set-down, and counterclockwise or clockwise rotations of the maxillomandibular complex (Fig. 1E–J) [14].

These surgical approaches allow for the modification of facial proportions to achieve a more balanced facial aesthetics. Nevertheless, maxillary vertical changes are limited by the amount of incisor exposure at rest. Excessive tooth exposure associated to a vertical maxillary excess permits maxillary impaction, but when tooth exposure is normal, counterclockwise rotation of the maxillomandibular complex is indicated. The same reasoning follows for maxillary set down, which leads to the next pivotal diagnostic factor when analyzing vertical changes in orthodontic patients [14].

Maxillary and mandibular incisor exposure at rest

A critical diagnostic factor in determining vertical movement of the maxilla is the amount of maxillary incisor exposure at rest [15,16], which serves as the foundation for subsequent evaluation and planning. Incisor display at rest is a crucial factor in both smile and speech aesthetics. Ideally, in adults, there should be 2 mm or more of maxillary incisor exposure at rest, with minimal or no visibility of the mandibular incisors (Fig. 2A–C) [15,17].

This parameter can be assessed using cephalometric radiographs (Fig. 2D) or clinical photography, which measures the distance from the maxillary and mandibular incisor borders to the stomion of upper and lower lips, respectively [18,19].

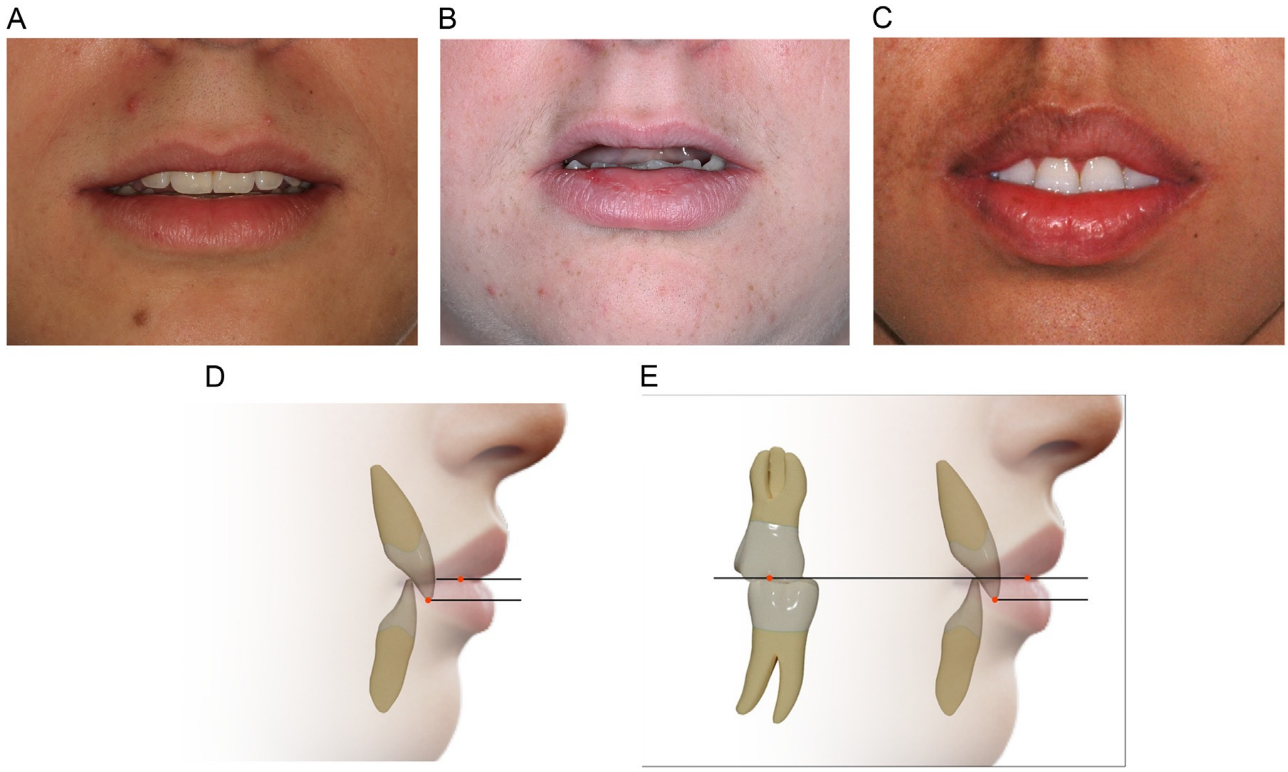

Figure 2. (A) Ideal exposure of the maxillary incisors at rest, 2 to 4 mm from incisal border to upper lip. (B) Decreased maxillary incisor exposure at rest, indicating possible incisor intrusion or vertical maxillary deficiency. (C) Increased maxillary incisor exposure at rest, suggestive of vertical maxillary excess or incisor extrusion. (D) Cephalometric representation of the normal vertical position of the maxillary incisors relative to the upper lip. (E) Illustration of the functional aesthetic occlusal plane (FAOP), as proposed by Câmara [19], used to evaluate the vertical positioning of the maxillary and mandibular incisors in relation to the soft tissue structures.

Videography, particularly when using specific phrases or phonemes such as "ema" or "Mississipi," can also provide valuable insights into incisor display dynamics [20]. Another helpful guideline is the functional aesthetic occlusal plane, defined as a reference line passing through the midcontact point of the maxillary and mandibular first molars and the upper lip stomion (Fig. 2E). Ideally, the edge of the maxillary incisors should be positioned approximately 2 to 4 mm below this line [19].

Inadequate incisor display can arise from a variety of factors, including vertical maxillary deficiency or excess (as explained in the previous section), extruded or nonerupted maxillary incisors, or short clinical crown height. When there is excessive incisor display with no maxillary excess and adequate proportionate crowns, we face dental extrusion; conversely, a lack of vertical anterior exposure will allow dental extrusion. When attrition leads to shorter incisors, cosmetic dentistry is indicated. Additionally, the inclination of the maxillary incisors should be considered, since it can also affect incisor display at rest and on smile. Flared maxillary incisors decrease incisor display, while upright maxillary incisors increase it [21].

While the ideal amount of incisor exposure varies among individuals, achieving proper incisor vertical positioning is fundamental to creating a balanced and aesthetically pleasing smile, particularly in cases involving vertical dimension discrepancies. Regardless of the method used to assess incisor display, any vertical movement of the jaws or teeth must consider this parameter to avoid unintended consequences. Failure to account for incisor display may result in an aged or unbalanced smile, particularly during speech [22].

Posterior alveolar height

Vertical discrepancy malocclusions are influenced by skeletal and dental factors. Measuring posterior alveolar height is essential for diagnosing vertical dimensional issues. This can be done via cephalometric radiographs by measuring the distance from the occlusal surface of the molar to the palatal and mandibular planes. Normal values are 24 mm in the upper arch and 34 mm in the lower arch (Fig. 3A and 3B) [23]. The LAFH plays a key role in the development of molar dentoalveolar heights, with an increase in LAFH positively impacting molar heights. Conversely, jaw divergency negatively affects these dentoalveolar heights. Skeletal abnormalities in the vertical dimension often result from differences in the development of anterior and posterior facial heights, leading to rotational growth or shifts in mandibular position that alter the chin projection and facial proportions. An increase or decrease in the LAFH can have a profound effect on the horizontal relationship of the maxilla and mandible. If LAFH is increased, the mandible will appear to be more retrognathic. If LAFH is decreased, the mandible will appear to be more prognathic [24].

Managing vertical discrepancies requires understanding the relationship between anterior and posterior facial heights and considering the skeletal and dental factors involved. In the maxilla, vertical discrepancies often present as posterior alveolar excess or a posteriorly positioned maxilla. The mandible may show posterior alveolar excess and short mandibular rami, with additional features such as a superiorly positioned condylar fossa, obtuse cranial base angle, and condylar resorption. In the maxilla, posterior alveolar development decreases as the MP-SN angle decreases, while in the mandible, it decreases to a lesser extent [25].

Treatment options for posterior alveolar height issues include surgical intervention for excessively increased maxillary height or skeletal anchorage to intrude posterior teeth and correct vertical discrepancies by counterclockwise mandibular rotation. While extraoral appliances were traditionally used for vertical control, skeletal anchorage has become a more viable treatment option (Fig. 3C) [26].

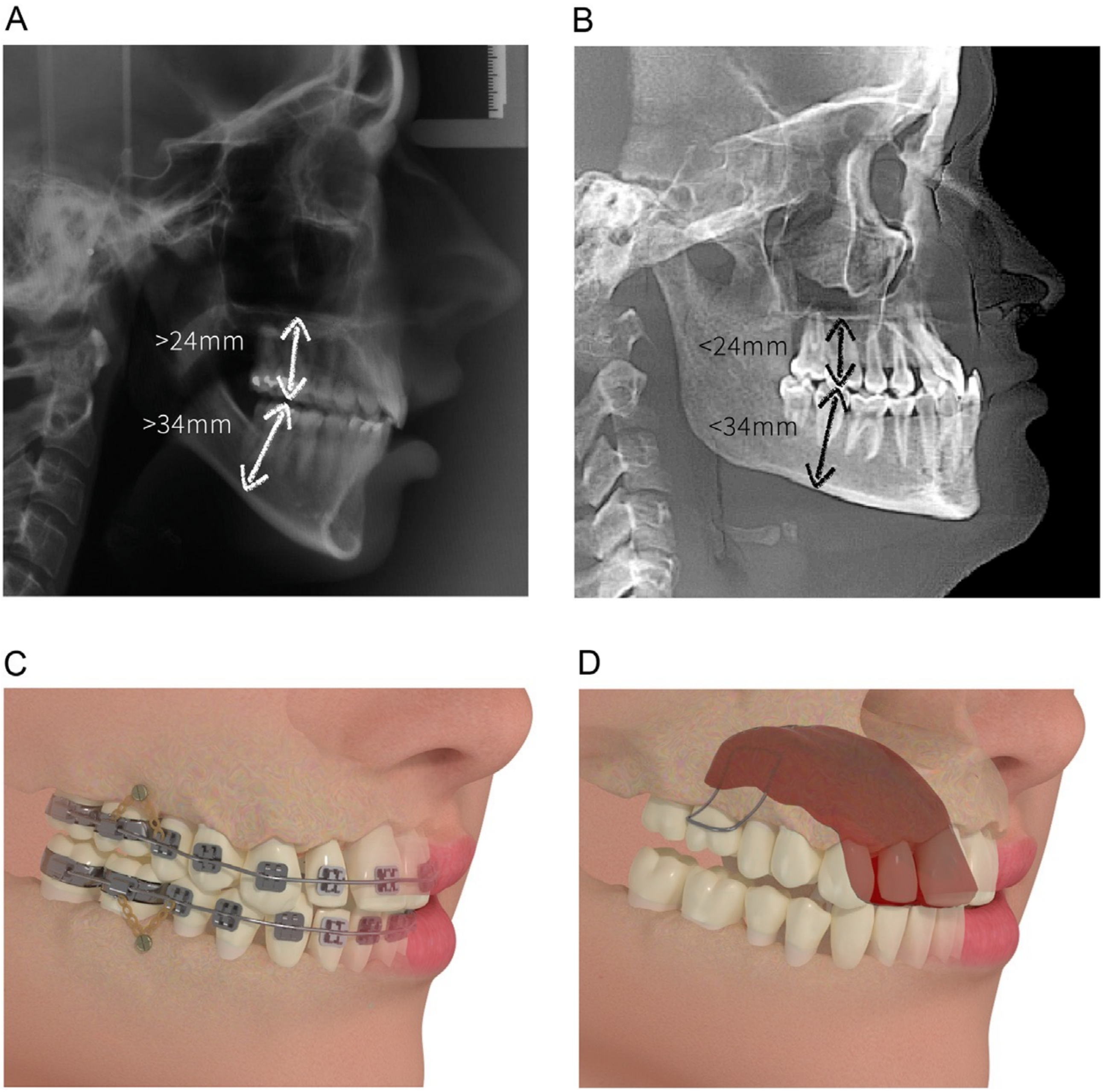

Figure 3. (A) Cephalometric assessment demonstrating increased posterior alveolar height, defined as the vertical distance between the palatal plane and the maxillary first molar exceeding 24 mm, and between the mandibular plane and the mandibular first molar exceeding 34 mm. (B) Cephalometric representation of reduced posterior alveolar height, characterized by a vertical distance less than 24 mm from the palatal plane to the maxillary molar, and greater than 34 mm from the mandibular plane to the mandibular molar. (C) Excessive posterior alveolar height can be corrected by molar intrusion using skeletal anchorage devices (e.g., mini-implants or miniplates). (D) Deficient posterior

alveolar height may be managed by molar extrusion facilitated through the use of an anterior bite plate.

In adult patients undergoing molar intrusion using orthodontic mini-implants, an average maxillary first molar intrusion of 2.67 mm can be achieved, corresponding to 0.86 mm overbite increase per millimeter of molar intrusion, with no significant skeletal changes [27]. Opening or closing 1 mm in the molar area will change the *Y* axis and SNB angle by 2.5° [28]. However, attempts to intrude posterior teeth may result in compensatory extrusion in the mandibular molars, requiring stabilization of the lower arch [29]. For underdevelopment of posterior alveolar height, growth stimulation through anterior bite plates can promote extrusion and counterclockwise rotation of the mandible, improving facial balance (Fig. 3D). In severe cases, when significant changes to LAFH are needed, surgical options like maxillary impaction or mandibular rotation may be considered to restore facial harmony [14].

Overbite

Overbite is also a key diagnostic factor in orthodontic analysis and is defined as the vertical overlap of the incisors. Normally, the lower incisal edges contact the lingual surface of the maxillary incisors at or above the cingulum, resulting in a 1 to 2 mm overbite or about one-third of incisor overlap (Fig. 4A) [30]. When the overlap is absent, it is called an open bite (Fig. 4B), and when it is excessive, it is referred to as a deep bite (Fig. 4C) [30]. However, the goal of managing overbite goes beyond static measurements; it is essential for anterior guidance, which serves to protect the posterior teeth from protrusive and lateral stress, to decrease jaw muscle activity and the force on anterior teeth (Fig. 4D–F). Anterior guidance is the immediate disocclusion of posterior teeth in the protrusive excursion of the mandible, and it depends basically on 3 factors: incisor inclination or interincisal angle, amount of overjet and overbite, and the slope of the articular eminence. Therefore, different combinations of incisor inclination and position will grant incisal guidance (Fig. 4G). Patients with larger overjets will need more proclined incisors, and patients with deeper overbites will accept more upright incisors. The higher the cusps of posterior teeth, more disocclusion will be needed. As such, overbite should not be assessed in isolation, as dynamic occlusion plays a critical role in determining the appropriate correction [31].

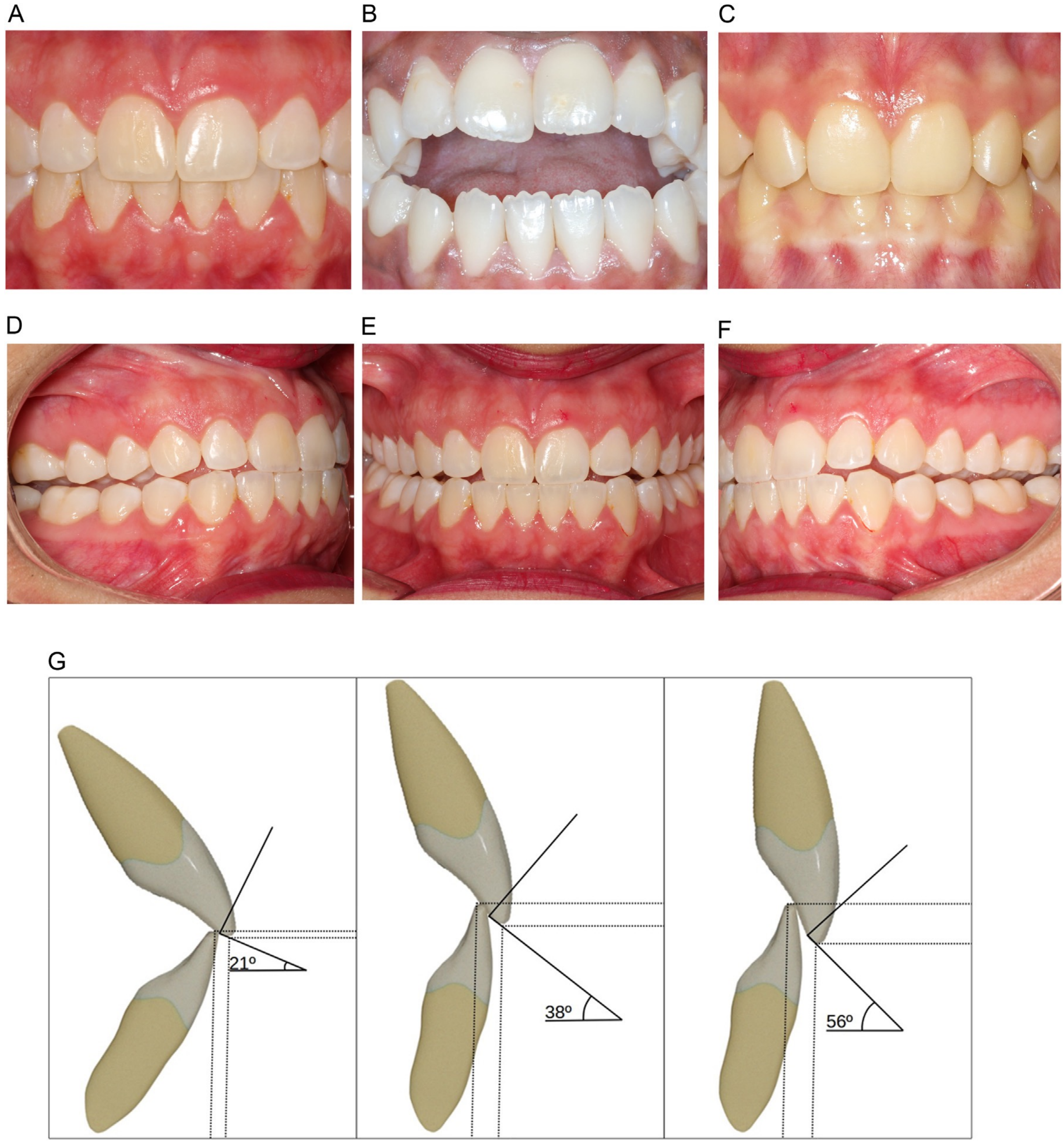

Figure 4. (A) Normal overbite, demonstrating physiologic vertical overlap between maxillary and mandibular incisors. (B) Anterior open bite, defined by the absence of vertical overlap between opposing anterior teeth. C) Deep bite, characterized by excessive vertical overlap of the anterior teeth. (D–F) Functional significance of appropriate overbite in establishing effective canine and protrusive guidance, which facilitates posterior disocclusion during excursive movements, reduces masticatory muscle activity, and minimizes forces on the anterior dentition. (G) The required magnitude of overbite is influenced by the inclination of the incisors, which affects the ability to achieve adequate posterior disocclusion during functional movements.

Deep bites can be corrected through a combination of intrusion of the anterior teeth and extrusion of the posterior teeth. A common orthodontic error in correcting deep bites is the over intrusion of the maxillary incisors, which can reduce maxillary anterior teeth exposure at rest. This misconception can often go unnoticed unless the incisor display is carefully analyzed. As patients age and the upper lip begins to droop, such mistakes can exacerbate the lack of display of anterior teeth [15].

In cases with large overbite, the correction should be individualized for the patient, ensuring that the treatment does not exceed the incisor display limits. If the necessary correction exceeds the space available for maxillary and mandibular incisor adjustment, the additional correction should be allocated to the posterior segment by extrusion of maxillary and mandibular molars.

There are many definitions for anterior open bite (AOB), such as lack of incisor contact, or as mild, moderate, or severe, simple or complex, depending on the number of teeth involved and dental or skeletal, according to the tissues involved. AOB is perhaps one of the sole malocclusions that has a functional impact, negatively affecting quality of life [32], since the lack of incisor contact reduces the capability of biting.

Due to the multifactorial etiology of AOB, many treatment options have been devised, including incisor extrusion, molar intrusion, or a combination of both. In most cases, maxillary incisor extrusion is indicated to improve smile esthetics and enhance incisor display, particularly given the frequent presence of an inverted smile line in AOB patients. Nevertheless, the amount of incisor extrusion required is dictated by the degree of maxillary incisor display at rest, which must be carefully assessed during treatment planning. This diagnostic factor is essential for determining the appropriate biomechanical approach, posterior intrusion, anterior extrusion, or a combination, while ensuring the development of a functional occlusion and the long-term stability of treatment outcomes.

Despite this, overbite stability evaluating different mechanics has been widely studied, but still with very low level of evidence. The best evidence on the relapse rate of different open bite treatment modalities according to which tissue was approached shows that myofunctional therapy tends to yield more stable results than all other treatment modalities [33,34]. Stability of vertical movements are yet not clearly defined. Molar intrusion presents a relapse of approximately 12% to 27% in the upper and lower arch, respectively [35]. The variation in overbite relapse in deep bite cases is very large, ranging from 0% to 82% [36], measured on anterior teeth only, with no information on the posterior region.

Occlusal wear

Dental wear can be defined as hard tissue loss and may partially involve the enamel or extend further to the exposure of dentinal tissue. The wear may affect the occlusal surfaces of posterior teeth (Fig. 5A) or the incisal surfaces of anterior teeth (Fig. 5B) with different clinical implications.

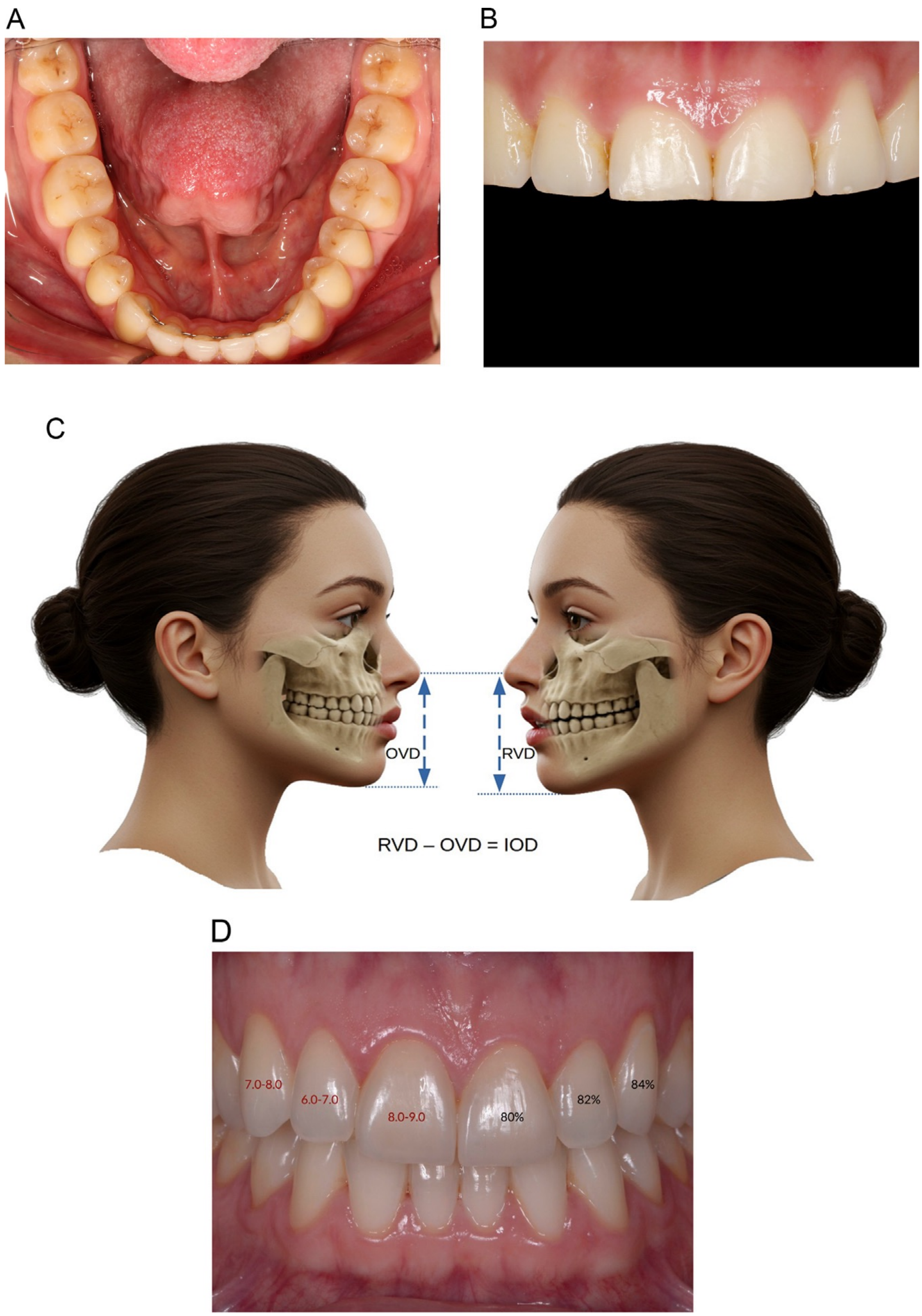

Figure 5. (A) Clinical example of posterior occlusal wear, indicative of loss of vertical dimension or parafunctional activity. (B) Clinical presentation of anterior dental wear, commonly associated with functional or parafunctional loading and loss of anterior guidance. (C) Schematic representation of vertical jaw relationships: Occlusal Vertical Dimension (OVD), defined as the distance between the maxilla and mandible when the teeth are in maximum intercuspation; Rest Vertical Dimension (RVD), the distance between the jaws when the mandibular muscles are at rest; and interocclusal distance (IOD), or freeway space, representing the difference between RVD and OVD. (D) Distribution of combined mean values by gender for each tooth group, illustrating the percentage of teeth within ±0.5 mm of the mean.

Occlusal wear can occur primarily under two conditions: carious and noncarious destruction. Noncarious tooth surface loss includes mechanisms such as attrition, defined as the mechanical wear resulting from tooth-to-tooth contact, and erosion, which involves the chemical dissolution of dental hard tissues without bacterial involvement [37]. Occlusal wear is a vertical problem since it reduces occlsual vertical dimension (OVD). OVD is defined as the distance between the jaws when teeth are in occlusion. Rest vertical dimension is the distance between the jaws when muscles are at rest, and the interocclusal distance is the difference between these two dimensions, also known as freeway space (Fig. 5C) [38].

The OVD should not be considered an immutable reference, but rather a dynamic dimension within a zone of physiological tolerance that can be altered as long as the dentist respects the envelope of function [39]. Among the most commonly accepted techniques for determining the OVD are the morphological or facial proportions, the physiological (based on the physiologic rest position), phonetic, and cephalometric [39]. In cases with posterior bite collapse or in denture wearers, loss of OVD is common [39].

The primary indications for changing the OVD are: harmonizing dentofacial esthetics, providing adequate space for the restorative material, and improving incisal and occlusal relationships [39]. Proper establishment of crown dimensions and OVD prior to orthodontic treatment is essential for effective case management. In cases of posterior tooth wear, OVD should be initially recovered by occlusal restorations (Fig. 6A–F). For anterior wear, teeth must first be positioned appropriately through orthodontic treatment before restorations, according to dental esthetic parameters and accurately planned based on the final occlusal position (Fig. 6G–L). Individual tooth proportion of the maxillary anterior dentition, defined by the anatomic width/length dimensions as a percentage ratio, falls within a range of 72% to 80%, with an average of 76% (Fig. 5D) [40].

Figure 6. (A–C) Initial presentation of a Class II malocclusion with anterior and posterior wear and reduced occlusal vertical dimension. (D–F) Restoration of posterior occlusal vertical dimension with temporary or definitive restorations prior to orthodontic treatment, leading to a temporary bite opening and Class II worsening. (G–I) Tooth positioning precedes esthetic restorations to ensure

proper incisor display, proportion, and alignment according to the planned final occlusion. (J–L) Final correction of the Class II malocclusion.

Checklist application

To integrate these key diagnostic elements, a structured checklist has been established for the assessment of vertical discrepancies in orthodontic patients (Fig. 7).

	LAFH	Incisor Exposure at Rest		Posterior Alveolar Height		Overbite	Crown Height	
		Upper	Lower	Upper	Lower		Anterior	Posterior
Increased								
Normal								
Decreased								
Treatment								

Figure 7. Checklist for vertical problems in orthodontic patients. For each diagnostic parameter in column, a cross (X) or a value is placed in the corresponding row (decreased, normal, or increased) based on clinical and radiographic findings. The final row is used to plan the treatment strategy based on the patient's vertical skeletal and dental characteristics.

This instrument allows for the identification of appropriate therapeutic strategies based on clinical and cephalometric findings. The following section illustrates the application of this checklist through the analysis of three representative clinical cases.

Case 1: Deep bite

The patient exhibited a hypodivergent skeletal pattern, with good lip seal and a flat smile line (Fig. 8A–C). The occlusal relationship was Class I, associated with multiple diastemas in both arches and a deep bite (Fig. 8D–F). Each diagnostic factor included in the checklist for vertical problems was analyzed. The patient presented with a decreased LAFH, with less than 65% of the total facial height (Fig. 8G), which could be increased through molar extrusion. Accordingly, "decreased" was marked in the LAFH column, and "increase with molar extrusion" was written in the treatment row (Fig. 8H).

At rest, the maxillary incisor exposure measured approximately 1 mm (Fig. 8G), indicating a reduced display.

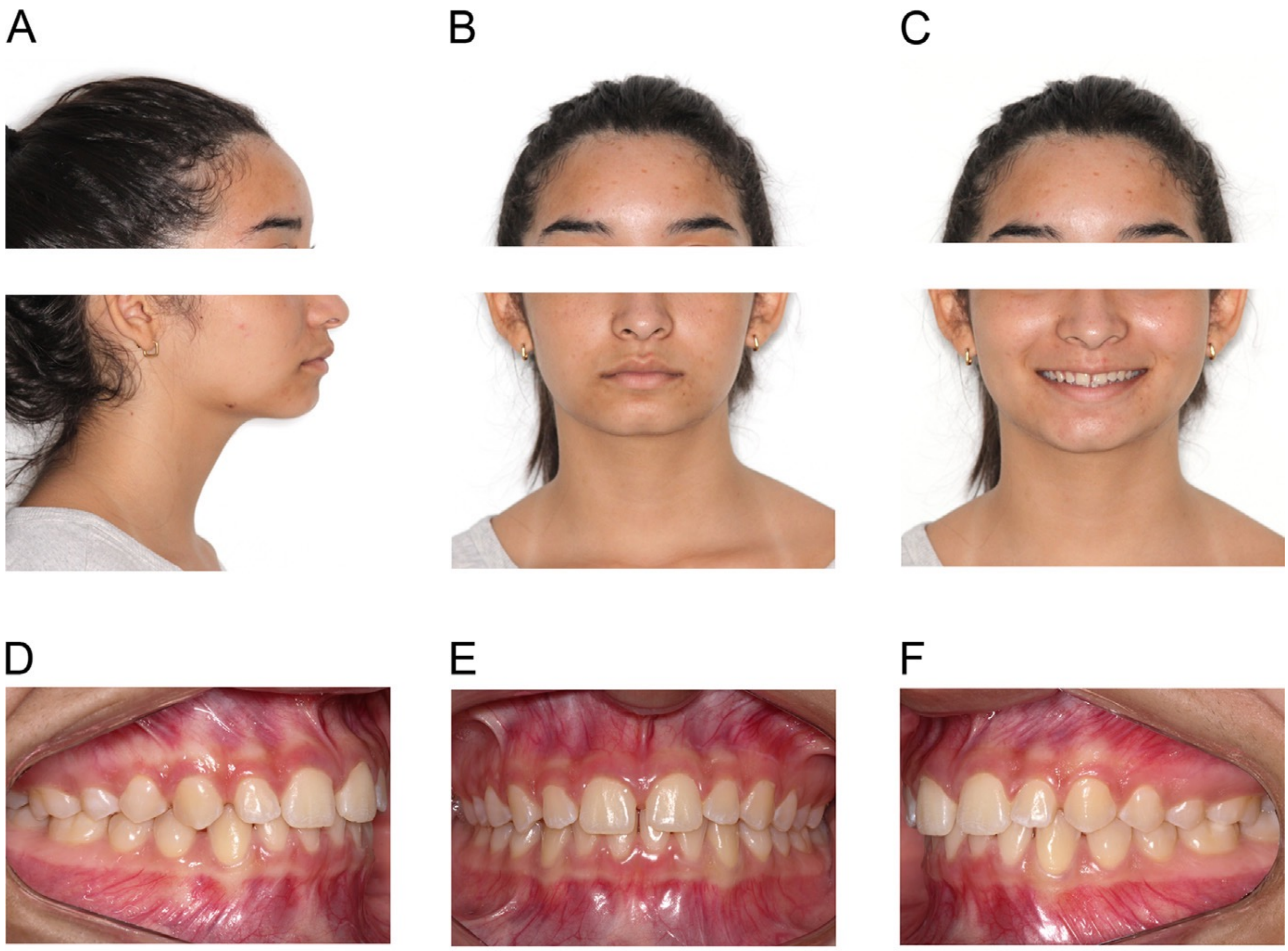

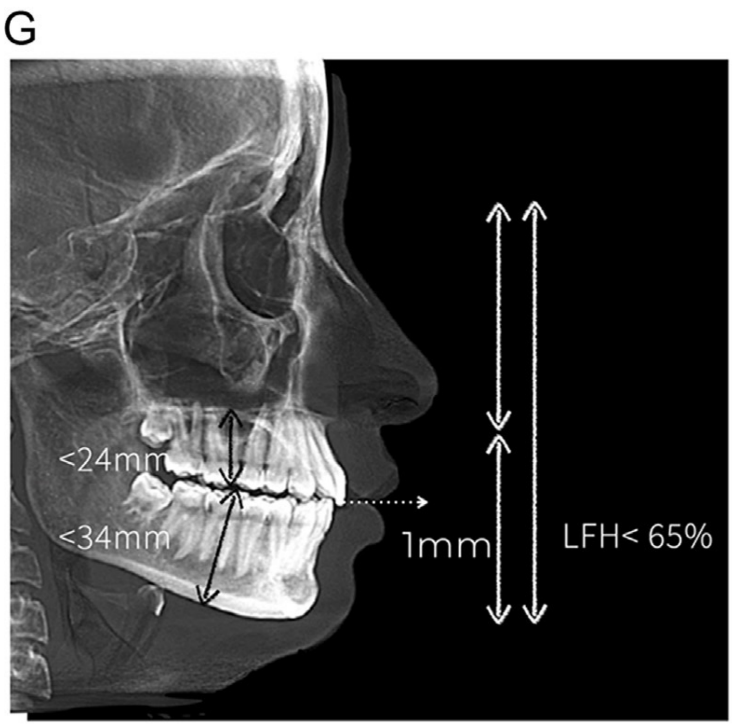

H

	LAFH	Incisor Exposure at Rest		Posterior Alveolar Height		Overbite	Crown Height	
		Upper	Lower	Upper	Lower		Anterior	Posterior
Increased						X		
Normal			X				X	X
Decreased	X	X		X	X			
Treatment	Increase with molar extrusion	Extrude U1	Intrude L1	Extrude U6	Extrude L6	Intrude L1	—	—

Figure 8. (A–C) Initial extraoral photographs showing hypodivergent skeletal pattern, good lip seal, and a flat smile line. (D–F) Initial intraoral photographs showing Class I molar relationship with multiple diastemas and an increased overbite. (G) Initial cephalometric radiograph with diagnostic factors revealing decreased LAFH, reduced maxillary incisor exposure at rest, diminished posterior alveolar height, and increased overbite. (H) Completed checklist for vertical problems, indicating key diagnostic findings and corresponding treatment strategies: molar extrusion, maxillary incisor extrusion, and mandibular incisor intrusion.

Therefore, “decreased” was marked in the corresponding column, with “extrude U1” noted in the treatment row. Posterior alveolar height was also reduced, measuring less than 24 and 34 mm in the upper and lower arches, respectively (Fig. 8G). As this can also be addressed by molar extrusion, “decreased” was marked in the posterior alveolar height column, and “extrude U6 & L6” was added to the treatment row (Fig. 8H). The overbite was increased, while the maxillary incisor exposure at rest remained reduced. Thus, further intrusion of the maxillary incisors to correct the deep bite was contraindicated. Instead, “increased” was marked in the overbite column, and “intrude L1” was indicated in the treatment row (Fig. 8H). No dental wear was observed.

The final treatment plan was determined by summing the individual diagnostic factors, following a hierarchical decision-making process in which the maxillary incisor exposure at rest served as the key determinant. This approach led to the decision to intrude the mandibular incisors, achieved by a reversed curve of Spee, followed by extrusion of the maxillary incisors. This objective was accomplished by inverting the curvature of the occlusal plane. Proclination of the mandibular incisors resulted in their relative intrusion, while simultaneous extrusion of the mandibular premolars and maxillary incisors was performed (Fig. 8P). Consequently, space closure in both arches was accomplished without deepening the bite (Fig. 8L–N). Gingival recontouring and composite restorations were also carried out in the maxillary arch, enhancing the final esthetic result. A consonant smile line was achieved (Fig. 8K), and, most importantly, an appropriate maxillary incisor display was restored (Fig. 8O).

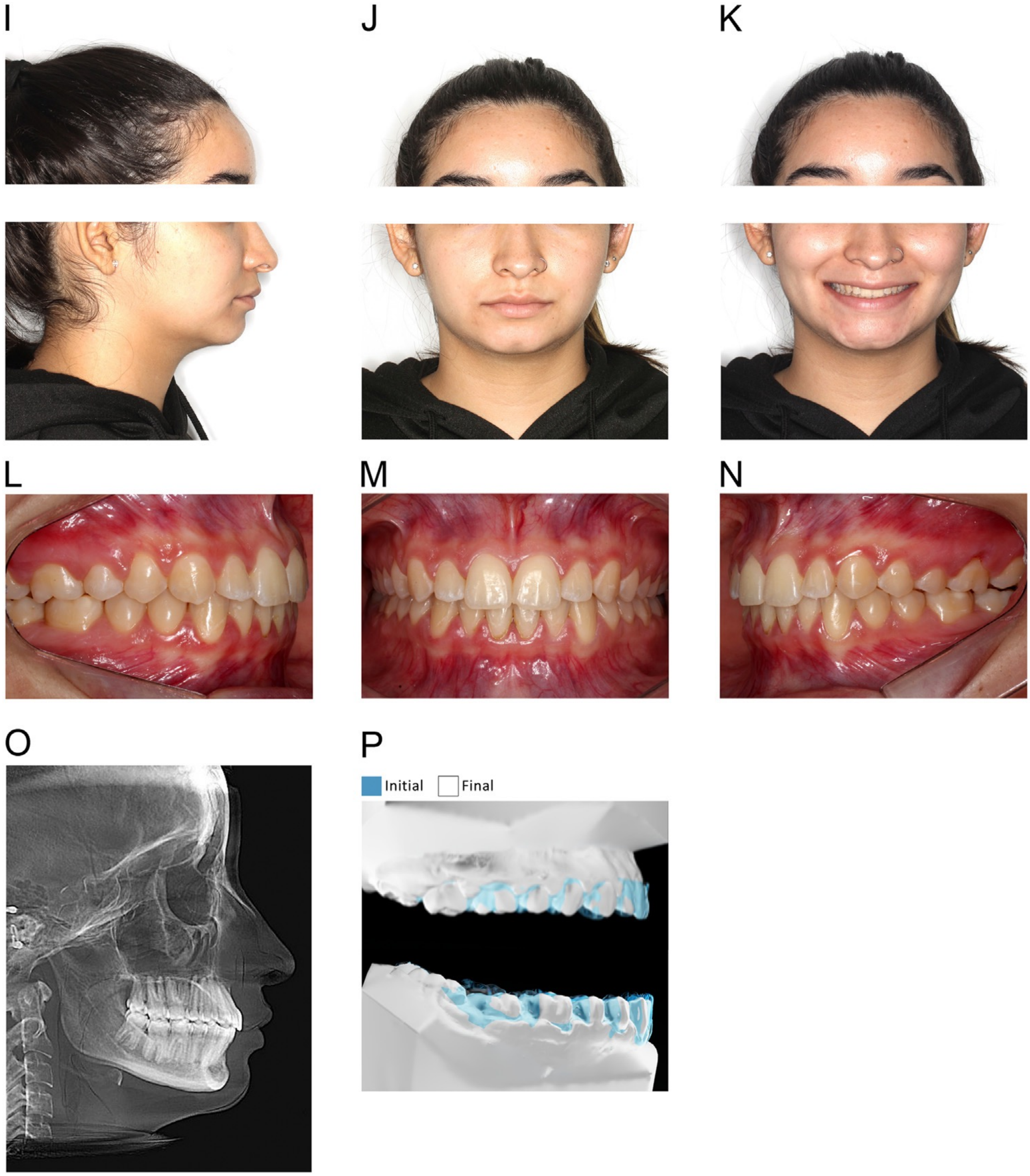

Figure 8. (I–K) Final extraoral photographs showing improved smile line. (L–N) Final intraoral

photographs demonstrating space closure in both arches and corrected bite without deepening. (O) Final cephalometric radiograph displaying improved maxillary incisor exposure. (P) Model superimpositions demonstrating the effects of mandibular incisor proclination and relative intrusion, extrusion of maxillary incisors and mandibular premolars, and occlusal plane inversion.

Case 2: Open bite

The patient exhibited a hyperdivergent skeletal pattern, with good lip seal and an inverted smile line (Fig. 9A–C). Maxillary constriction was observed, with an occlusal relationship of Class I on the right side and Class II with a posterior crossbite on the left side (Fig. 9D–F). Each diagnostic factor included in the checklist for vertical problems was analyzed. The patient presented with an increased LAFH, with the lower facial height measuring more than 65% of the total facial height (Fig. 9G). This could be decreased through molar intrusion. Accordingly, “increased” was marked in the LAFH column, and “decrease with molar intrusion” was written in the treatment row (Fig. 9H).

At rest, the maxillary incisor exposure measured approximately 1 mm (Fig. 9G), indicating a reduced display. Therefore, “decreased” was marked in the corresponding column, with “extrude U1” noted in the treatment row. Posterior alveolar height was also increased, measuring more than 24 and 34 mm in the upper and lower arches, respectively (Fig. 9G). As this can also be addressed by molar intrusion, “increased” was marked in the posterior alveolar height column, and “intrude U6 & L6” was added to the treatment row (Fig. 9H).

The overbite was decreased; thus, “decreased” was marked in the overbite column, and “extrude U1 & L1” was indicated in the treatment row (Fig. 9H). No dental wear was observed.

In the case presented, the final treatment plan began with transverse maxillary expansion using a rapid palatal expander. This was followed by posterior intrusion with inter-radicular mini-implants, with intrusive forces applied on a continuous archwire. This biomechanical setup generated a clockwise moment, promoting molar intrusion and concurrent incisor extrusion. Final vertical adjustments were achieved using vertical elastics.

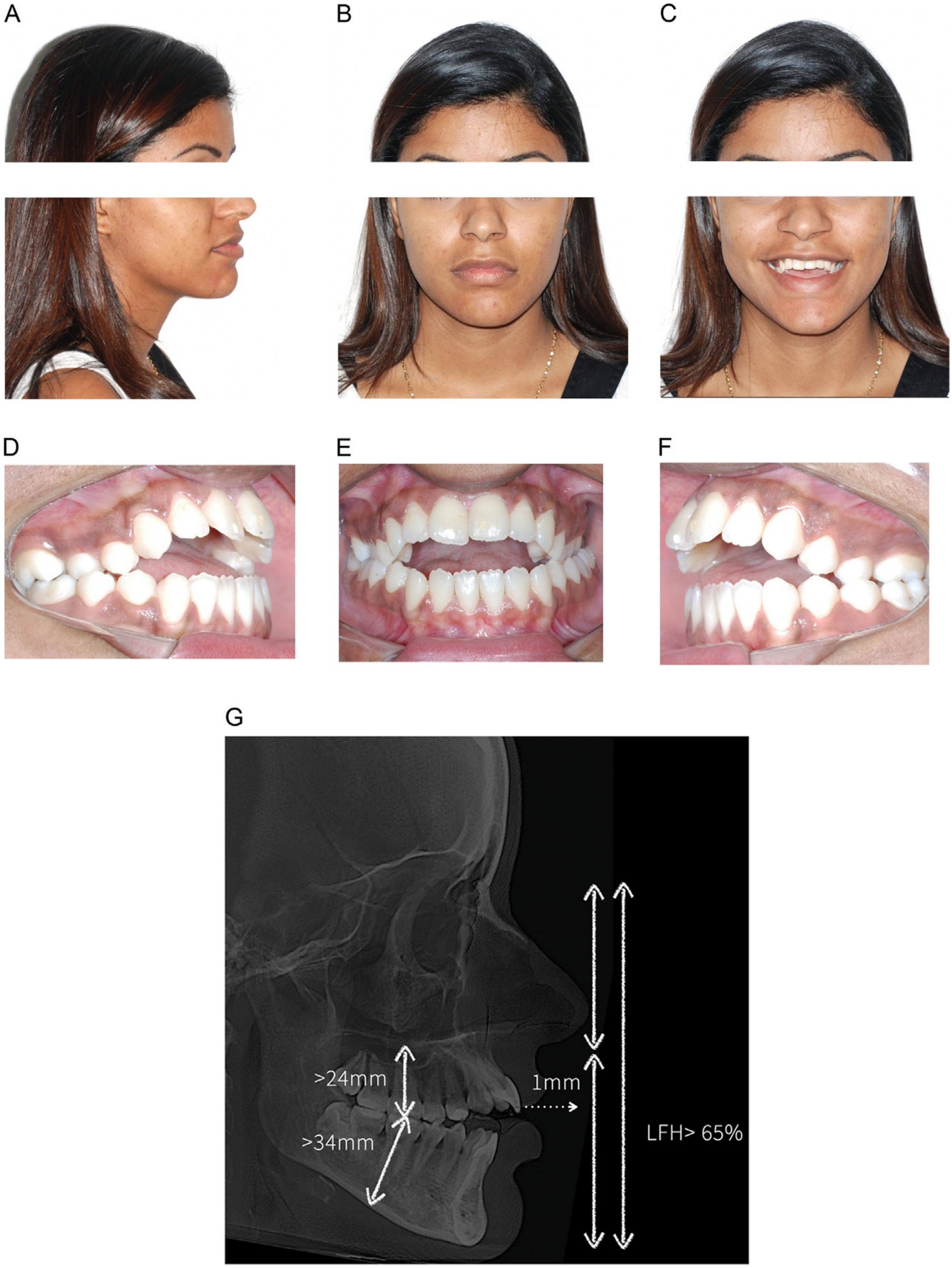
A
B
C
D
E
F
G
>24mm
>34mm
1mm
LFH> 65%

H

	LAFH	Incisor Exposure at Rest		Posterior Alveolar Height		Overbite	Crown Height	
		Upper	Lower	Upper	Lower		Anterior	Posterior
Increased	X			X	X			
Normal			X				X	X
Decreased		X				X		
Treatment	Decrease with molar intrusion	Extrude U1	—	Intrude U6	Intrude L6	Extrude U1&L1	—	—

I

J

K

L

M

N

O

P

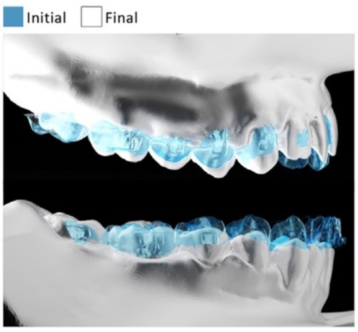

Figure 9. (A–C) Initial extraoral photographs revealing hyperdivergent skeletal pattern, good lip seal, and an inverted smile line. (D–F) Initial intraoral photographs showing right Class I and left Class II occlusion with posterior crossbite and maxillary constriction. (G) Initial cephalometric radiograph with diagnostic factors assessment indicating increased LAFH, reduced maxillary incisor exposure at rest, increased posterior alveolar height, and decreased overbite. (H) Completed checklist for vertical problems, with diagnostic findings and proposed treatments: molar intrusion, maxillary and mandibular incisor extrusion. (I–K) Final extraoral photographs showing improved smile line. (L– N) Final intraoral photographs demonstrating successful open bite closure and corrected occlusal relationships. (O) Final cephalometric radiograph with evidence of maxillary molar and premolar intrusion, with root displacement into the maxillary sinus region. (P) Models superimpositions showing maxillary incisor extrusion, and secondary mandibular incisor extrusion resulting from counterclockwise mandibular rotation.

The outcome demonstrated successful open bite closure (Fig. 9L–N) and the establishment of an adequate smile line (Fig. 9I–K). Intrusion of the maxillary molars and premolars, evidenced by root displacement into the maxillary sinus region, was achieved (Fig. 9O). Additionally, a significant maxillary incisor extrusion was performed. The posterior intrusion induced a counterclockwise mandibular rotation, which further contributed to the extrusion of the mandibular incisors (Fig. 9P). These occlusal modifications, specifically, the combination of posterior dental intrusion and anterior extrusion, resulted in substantial improvement of both functional and esthetic parameters. Incisor extrusion in this case was deemed essential for achieving an esthetically favorable smile line. The patient presented with harmonious facial proportions; therefore, orthognathic surgery was not indicated.

Case 3: Occlusal wear

This young adult, who has already undergone previous orthodontic treatment, exhibited a Class III occlusion with posterior and anterior dental wear (Fig. 10D–F). Compensatory extrusion of the mandibular incisors resulted in excessive display of lower anterior gingiva at smile and exposure of only the mandibular incisors (Fig. 10A–C). Each diagnostic factor included in the checklist for vertical problems was analyzed. The patient presented with an increased LAFH, with the lower facial height measuring more than 65% of the total facial height (Fig. 10G). This could be decreased through molar intrusion. Accordingly, “increased” was marked in the LAFH column, and “decrease with molar intrusion” was written in the treatment row (Fig. 10H).

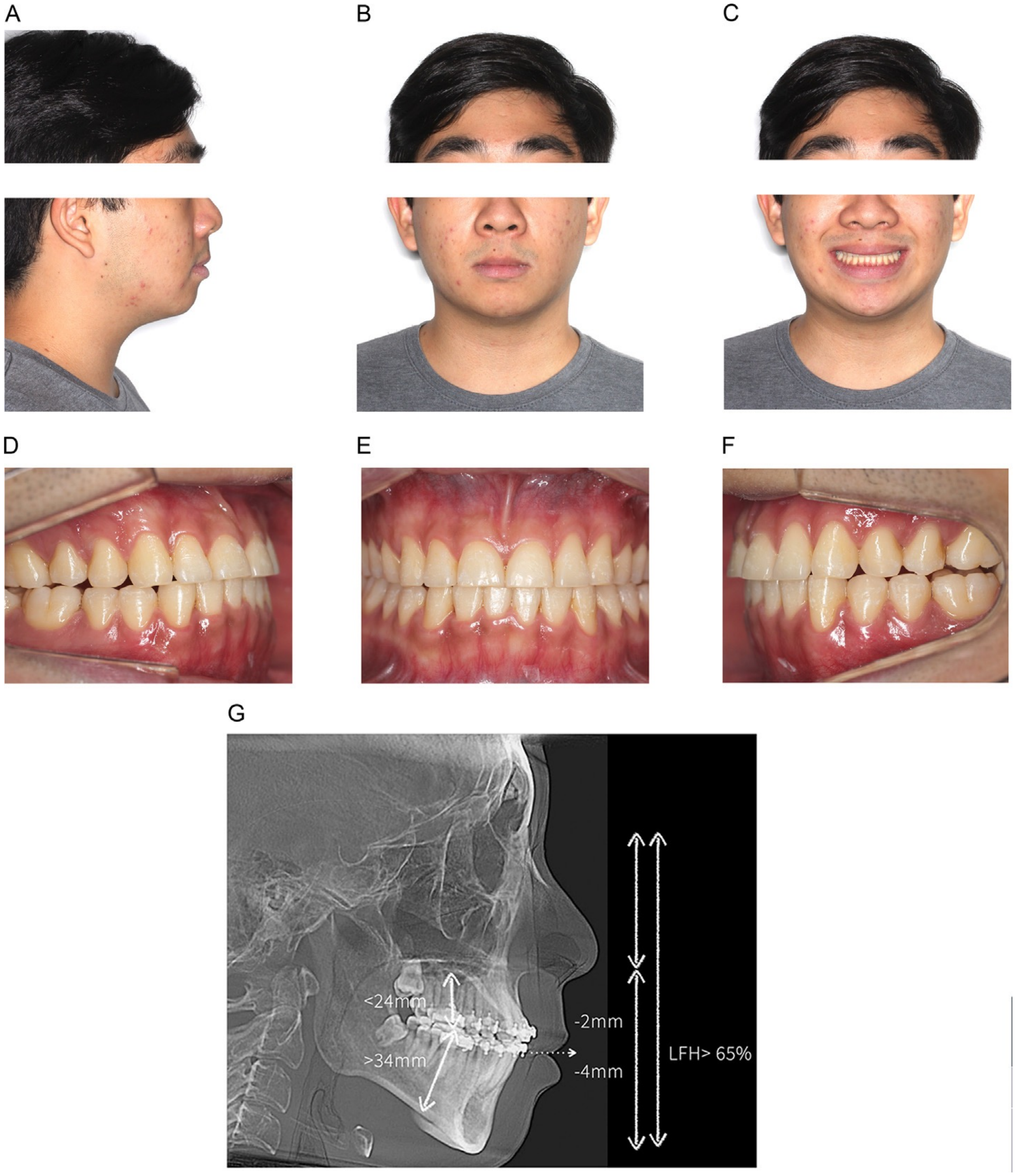

H

	LAFH	Incisor Exposure at Rest		Posterior Alveolar Height		Overbite	Crown Height	
		Upper	Lower	Upper	Lower		Anterior	Posterior
Increased	X		X		X			
Normal								
Decreased		X		X		X	X	X
Treatment	Decrease with molar intrusion	Extrude U1	Intrude L1	Extrude U6	Intrude L6	Extrude U1	Restore U1	Restore L1

Figure 10. (A–C) Initial extraoral photographs showing excessive mandibular incisor display and lack of maxillary incisor exposure due to compensatory mandibular incisor extrusion. (D–F) Initial intraoral photographs revealing a Class III occlusion and anterior and posterior dental wear. (G) Initial cephalometric radiograph with diagnostic factors evaluation indicating increased LAFH, absent maxillary incisor exposure at rest, excessive mandibular incisor display, and an imbalance in posterior alveolar height, with decreased height in the maxilla and with increased height in the mandible. (H) Completed checklist for vertical problems, highlighting diagnostic findings and planned interventions: molar intrusion and extrusion, mandibular incisors intrusion, and restorative treatment.

At rest, the maxillary incisor exposure was absent and lower was excessive (Fig. 10G); therefore, “decreased” was marked in the corresponding column, with “extrude U1” and “intrude L1” noted in the treatment row. Posterior alveolar height was also increased in the lower arch and decreased in the upper arch, measuring less than 24 mm but more than 34 mm, respectively (Fig. 10G). Thus, “increased” was marked in the posterior alveolar height column for the lower arch and “decreased” for the upper arch; “intrude L6” and “extrude U6” were added to the treatment row (Fig. 10H).

The overbite was decreased, thus “decreased” was marked in the overbite column, and “extrude U1” was indicated in the treatment row (Fig. 10H). Upper and lower posterior occlusion and anterior dental wear were observed. Therefore, “decreased” was marked in anterior and posterior crown height column, indicating “restore U1” and “restore L1” in the treatment row (Fig. 10H).

The initial treatment objective was to achieve a positive overjet and establish posterior occlusal contacts with bite opening by mandibular clockwise rotation with bite raisers. Orthodontic brackets were bonded to the mandibular arch and to the posterior segment of the maxillary arch (Fig. 10I–K).

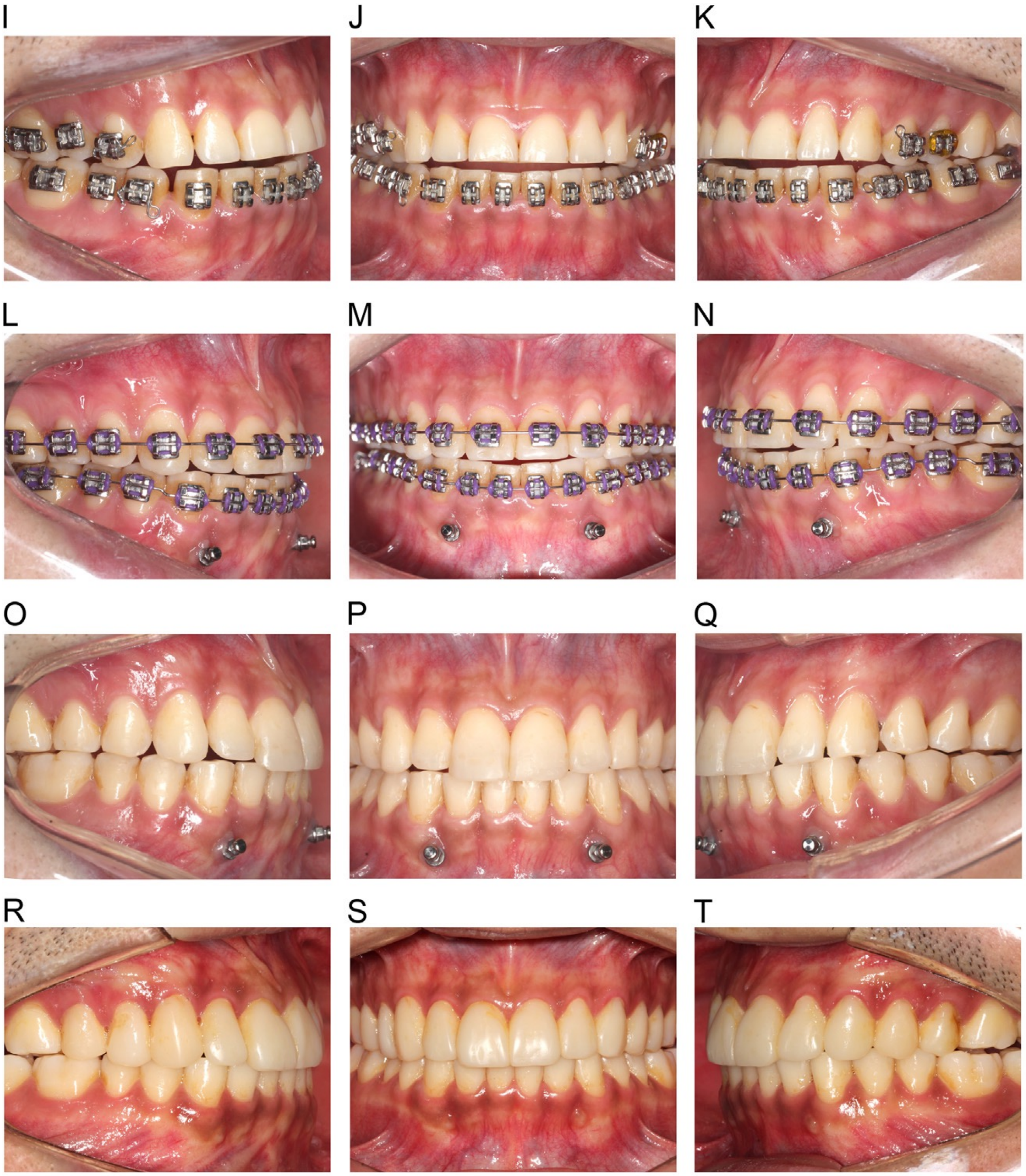

Figure 10. (I–K) Intraoral photographs after bonding of orthodontic brackets to the mandibular and posterior maxillary teeth, with the use of bite raisers and vertical elastics incorporating a Class III vector to achieve bite opening and mandibular incisors intrusion. (L–N) Intraoral photographs after progressive correction with anterior mini-implants enabling intrusion of extruded mandibular incisors, restoration of maxillary incisor length, and bonding of maxillary anterior brackets. (O–Q) Intraoral photographs after provisional composite restorations on maxillary and mandibular incisors

to reestablish crown height and esthetics after vertical repositioning. (R–T) Final intraoral photographs after prosthodontic rehabilitation, resulting in final smile esthetics.

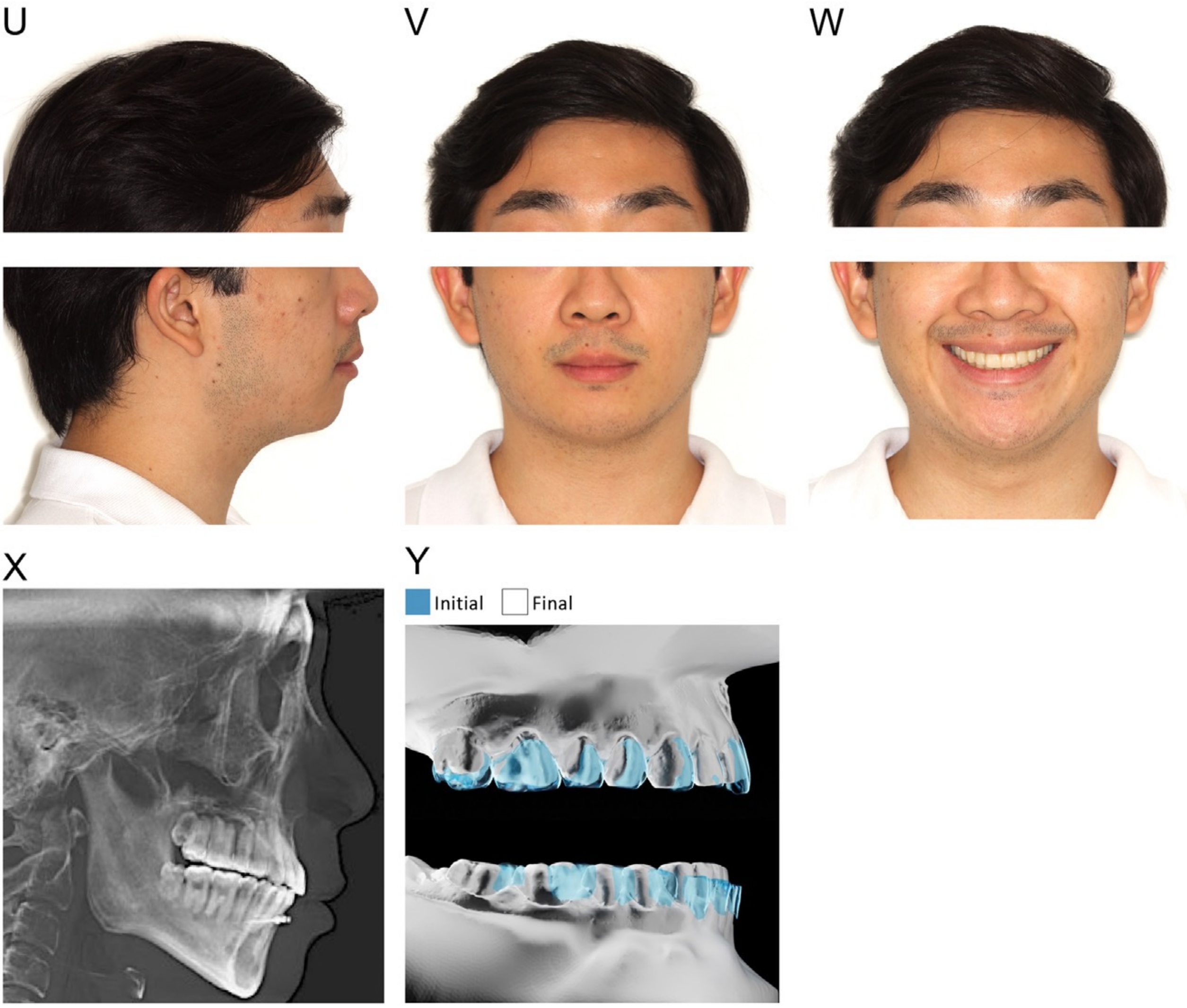

Figure 10. (U–W) Final extraoral photographs showing proper alignment of maxillary incisor margins for restorative enhancement and ideal incisor display. (X) Final cephalometric radiograph showing significant mandibular incisor intrusion via skeletal anchorage. (Y) Models superimpositions demonstrating successful posterior extrusion using bite plate mechanics and mandibular incisor intrusion and proclination.

A bite plate was employed in conjunction with vertical elastics incorporating a Class III vector. This approach enabled sufficient bite opening to permit restoration of the maxillary central incisors, bonding of the upper anterior brackets, and intrusion of the overextruded mandibular incisors using inter-radicular mini-implants in the anterior area (Fig. 10L– N). The vertical repositioning of both maxillary and mandibular incisors enabled provisional composite buildups to restore incisal length and esthetics (Fig. 10O–Q). The patient was subsequently referred to the prosthodontist for final rehabilitation (Fig. 10R–T).

Successful posterior extrusion via bite plate mechanics, significant mandibular incisor intrusion through skeletal anchorage, and proper leveling of the maxillary incisor margins to allow for restorative procedures with optimal tooth proportions and improved incisor display were achieved (Fig. 10U–Y).

Conclusions

The vertical problem can involve three aspects: inadequate facial proportions, overbite, and OVD. These aspects have no common association with each other; therefore, there is a need for an individualised treatment plan. Five diagnostic criteria should be evaluated to establish a treatment plan that includes the face, occlusal condition, and smile. While diagnostic factors alone provide discrete data points, their integration in a structured manner enables the formulation of a coherent treatment strategy. Effective organization in this checklist and interpretation of these diagnostic elements are useful for optimizing clinical outcomes, which include the face, the smile, and the occlusion, with the incisor exposure at rest playing the pivotal role in the decision-making diagnostic process.

References

1. Vaden JL, Pearson LE. Diagnosis of the vertical dimension. Semin Orthod 2002;8:120–9. doi:10.1053/sodo.2002.125431.
2. Sarver DM. Dentofacial esthetics: from macro to micro. Batavia, IL: Quintessence Publishing Co, Inc; 2020.
3. Ludwig M. A cephalometric analysis of the relationship between facial pattern, interincisal angulation and anterior overbite changes. Angle Orthod 1967;37:194–204 <0194:ACAOTR>2.0.CO;2. doi:10.1043/0003-3219(1967)037.
4. Claro CA de A, Abrão J, Reis SAB. Association between overbite and craniofacial growth pattern. Braz Oral Res 2010;24:425–32. doi:10.1590/ s1806-83242010000400009.
5. Ioannidou I, Gianniou E, Koutsikou T, Kolokithas G. Quantitative description of overjet and overbite and their relationship with the craniofacial morphology. Clin Orthod Res 1999;2:154–61. doi:10.1111/ocr.1999.2.3.154.
6. Aradya A, Chowdhary R. Re-evaluation of interarch space determination in fully dentate adults with different facial forms: a clinical study. Indian J Dent Res 2017;28:613. doi:10.4103/ijdr.IJDR_625_15.
7. Rhodes G. The evolutionary psychology of facial beauty. Annu Rev Psychol 2006;57:199–226. doi:10.1146/annurev.psych.57.102904.190208.
8. Milutinovic J, Zelic K, Nedeljkovic N. Evaluation of facial beauty using anthropometric proportions. Sci World J 2014;2014:1–8. doi:10.1155/2014/428250.
9. Munro IR. Anthropometric facial proportions in medicine. Illinois, USA: Thomas: Springfield; 1987.
10. Horn AJ. Facial height index. Am J Orthod Dentofacial Orthop 1992;102:180–6. doi:10.1016/0889- 5406(92)70031- 5.
11. Legan HL, Burstone CJ. Soft tissue cephalometric analysis for orthognathic surgery. J Oral Surg 1980;38:744–51.
12. Bell WH, Proffit WR, White RP. Surgical correction of dentofacial deformities. Philadelphia: Saunders; 1980.
13. Ferring V, Pancherz H. Divine proportions in the growing face. Am J Orthod Dentofacial Orthop 2008;134:472–9. doi:10.1016/j.ajodo.2007.03. 027.
14. Bell WH, Jacobs JD, Legan HL. Treatment of Class II deep bite by orthodontic and surgical means. Am J Orthod 1984;85:1–20. doi:10.1016/0002-9416(84) 90118- 0.

15. Zachrisson BU. Esthetic Factors Involved in Anterior Tooth Display and the Smile: Vertical Dimension. J Clin Orthod. 1998. https://www.jco-online.com/ archive/1998/07/432- esthetic- factors- involved- in- anterior- tooth- display- and- the-smile-vertical-dimension/. Accessed October 27, 2025.
16. Sarver DM. The importance of incisor positioning in the esthetic smile: the smile arc. Am J Orthod Dentofacial Orthop 2001;120:98–111. doi:10.1067/mod. 2001.114301.
17. Kokich VG. Esthetics: the orthodontic-periodontic restorative connection. Semin Orthod 1996;2:21–30. doi:10.1016/S1073-8746(96)80036-3.
18. Arnett GW, Jelic JS, Kim J, et al. Soft tissue cephalometric analysis: diagnosis and treatment planning of dentofacial deformity. Am J Orthod Dentofacial Orthop 1999;116:239–53. doi:10.1016/s0889- 5406(99)70234- 9.
19. Câmara CA, Martins RP. Functional aesthetic occlusal plane (FAOP). Dental Press J Orthod 2016;21:114–25. doi:10.1590/2177- 6709.21.4.114- 125.sar.
20. Sarver DM, Ackerman MB. Dynamic smile visualization and quantification: part 1. Evolution of the concept and dynamic records for smile capture. Am J Orthod Dentofacial Orthop 2003;124:4–12. doi:10.1016/S0889-5406(03)00306-8.
21. Sarver DM, Ackerman MB. Dynamic smile visualization and quantification: part 2. Smile analysis and treatment strategies. Am J Orthod Dentofacial Orthop 2003;124:116–27. doi:10.1016/S0889-5406(03)00307-X.
22. Hamdan AM, Lewis SM, Kelleher KE, Elhady SN, Lindauer SJ. Does overbite reduction affect smile esthetics? Angle Orthod 2019;89:847–54. doi:10.2319/ 030819- 177.1.
23. Turley PK. Orthodontic management of the short face patient. Semin Orthod 1996;2:138–53. doi:10.1016/s1073-8746(96)80049-1.
24. McNamara JA. A method of cephalometric evaluation. Am J Orthod 1984;86:449–69. doi:10.1016/S0002-9416(84)90352-X.
25. Karlsen AT. Association between facial height development and mandibular growth rotation in low and high MP-SN angle faces: a longitudinal study. An- gle Orthod 1997;67:103–10. doi:10.1043/0003-3219(1997)067⟨0103:ABFHDA⟩ 2.3.CO;2.
26. Buschang PH, Carrillo R, Rossouw PE. Orthopedic correction of growing hyperdivergent, retrognathic patients with miniscrew implants. J Oral Maxillofac Surg 2011;69:754–62. doi:10.1016/j.joms.2010.11.013.

27. Peres LR, Rossouw PE, Cousley R, Corsetti MA. Mini-implant assisted posterior intrusion: a quantification of anterior bite closure in nongrowing subjects. Am J Orthod Dentofacial Orthop 2023;163:465–74. doi:10.1016/j.ajodo.2021.12.027.
28. Kim K, Choy K, Park YC, Han SY, Jung H, Choi YJ. Prediction of mandibular movement and its center of rotation for nonsurgical correction of anterior open bite via maxillary molar intrusion. Angle Orthod 2018;88:538–44. doi:10.2319/ 102317- 714.1.
29. Abu Arqub S, Al-Moghrabi D, Iverson MG, Farha P, Alsalman HA, Uribe F. Assessment of the efficacy of various maxillary molar intrusion therapies: a systematic review. Prog Orthod 2023;24:37. doi:10.1186/s40510-023-00490-3.
30. Proffit WR, Fields HW, Larson BE, Sarver DM. Contemporary orthodontics. 6th ed. Philadelphia, PA: Elsevier; 2019.
31. Thornton LJ. Anterior guidance: group function/canine guidance. A literature review. J Prosthet Dent 1990;64:479–82. doi:10.1016/0022-3913(90)90048-H.
32. Curto A, Albaladejo A, Alvarado-Lorenzo A. Oral-health-related quality of life (OHRQoL) and anterior open bite in adult patients: a case-control study. Healthcare 2022;10:129. doi:10.3390/healthcare10010129.
33. Smithpeter J, Covell D. Relapse of anterior open bites treated with orthodontic appliances with and without orofacial myofunctional therapy. Am J Orthod Dentofacial Orthop 2010;137:605–14. doi:10.1016/j.ajodo.2008.07.016.
34. Huang GJ, Justus R, Kennedy DB, Kokich VG. Stability of anterior open-bite treated with crib therapy. Angle Orthod 1990;60:17–24 discussion 25- 26<0017:SOAOTW>2.0.CO;2. doi:10.1043/0003-3219(1990)060.
35. González Espinosa D, de Oliveira Moreira PE, da Sousa AS, Flores-Mir C, Normando D. Stability of anterior open bite treatment with molar intrusion using skeletal anchorage: a systematic review and meta-analysis. Prog Orthod 2020;21:35. doi:10.1186/s40510-020-00328-2.
36. Huang GJ, Bates SB, Ehlert AA, Whiting DP, Chen SSH, Bollen AM. Stability of deep-bite correction: a systematic review. J World Fed Orthod 2012;1:e89 –6. doi:10.1016/j.ejwf.2012.09.001.
37. Rashid H, Hanif A, Nasim M. Tooth surface loss revisited: classification, etiology, and management. J Res Dent 2015;3:37. doi:10.4103/2321- 4619. 156643.
38. Goldstein G, Goodacre C, MacGregor K. Occlusal vertical dimension: best evidence consensus statement. J Prosthodont 2021;30:12–19. doi:10.1111/jopr. 13315.

39. Calamita M, Coachman C, Sesma N, Kois J. Occlusal vertical dimension: treatment planning decisions and management considerations. Int J Esthet Dent 2019;14:166–81.
40. Chu SJ. Range and mean distribution frequency of individual tooth width of the maxillary anterior dentition. Pract Proced Aesthet Dent 2007;19:209–15.

B) Practical guide to in-house aligner fabrication- Part 1: Introduction to the system

Abstract

Clear aligner treatment has gained interest among orthodontists since its introduction in the market two decades ago. The high patients' demand for more aesthetic approaches, with greater comfort, is the primary aspect driving this direction change in the treatment of the malocclusions. However, this drift impacted the management of clinical practices because orthodontists lost absolute control over the flow of assembly and manufacture of conventional appliances. Third-party companies hired for the industrial manufacture of aligners was the concept initially proposed by Align Technology, manufacturer of Invisalign, a pioneer in the commercial system and market leader. Nevertheless, due to the inherent costs of this service and the time limitations imposed by outsourcing, the orthodontists created a digital flow for in-house manufacturing of aligners. This series of three articles brings practical considerations for using in-office aligners. Additionally, the goal is to share experiences related to the manufacture and management of the technique.

Introduction

Orthodontics: a specialty in pursuit of continuous improvement through technological changes

The last decades have witnessed directional changes in the practice of Orthodontics, thanks to the progressive advent of new technologies. Generally, such changes are surrounded by resistance, doubts, and uncertainties, but when they lead to real gains, with the appropriate adaptations and improvements, they can contribute to a better world. In order to place colleagues in training into a historical context, some of the many advances since the creation of the specialty, just over 100 years ago, can be cited.

The presentation of the dental enamel acid-etching technique by Michael Buonocore[1] in the mid-1950s, followed by the introduction of bis-GMA adhesive resin systems in the 1960s by Ray Bowen[2], allowed orthodontic attachments, in the 1980s, to be "bonded" to the enamel instead of being positioned by means of metal bands on all teeth. The development of elastic metal alloys, such as nickel-titanium in the 1960s, enabled progressive improvements over the following two decades for clinical use in Orthodontics, gaining popularity in the 1990s, which allowed orthodontic mechanics to evolve toward more comfortable and efficient therapies. Research on skeletal anchorage in experimental animals, in the 1980s by Eugene Roberts[3], favored the development of commercially available temporary devices in the 1990s. This made it possible for the control of tooth movement to be carried out more predictably than in the past. Harold Kesling's[4] idea in the 1940s of constructing tooth positioners evolved into a technique with greater control of tooth movement, such as the Essix system, originated from the research published by Jack Sheridan[5] in the 1990s. The next step was the conversion of this essentially analog system into a digital one, introduced by Zia Chishti and Kelsey Wirth[6] in the second half of the 1990s, with the founding of Align Technology, owner of the Invisalign brand. The launch of this product on the market took place in the early 2000s and, since then, there has been a global directional change in the search for treatments with aligners. The offer of orthodontic treatments through removable plastic devices has opened the market to contemporary therapeutic solutions for patients who, faced with the traditional fixed multibracket system, would not undergo correction of their malocclusions.

It seems evident that, for each of these technological evolutions, there are positive points and also negative aspects. The disadvantages must be recognized by professionals and, as far as possible, minimized with preventive measures. Directional changes in professional practice do not eliminate the need for a complete and in-depth view of the specialty. New technologies essentially come to add resources.

The Growing Global Demand for Aligners

The rapid popularity gained by aligners in recent years is related to the significant investment made by Align Technology in global market marketing. The Covid-19 pandemic drastically and unprecedentedly impacted the demand for treatment of malocclusions, with growth expectations for the aligner market falling short of projections in the United States in 2020. However, despite the decline in orthodontic treatment demand in 2020 (a 2% decrease in aligner use compared to 2019), with public management of the pandemic, the global market for plastic aligners recovered its upward demand trend. According to a report from Align Technologies[7], the global average utilization rate of aligners increased from 16.8 to 20.1 cases per certified orthodontist in 2021. Financial studies project growth in the orthodontic aligner market from USD 4 billion in 2022 to USD 16 billion in 2029 (Figure 1).

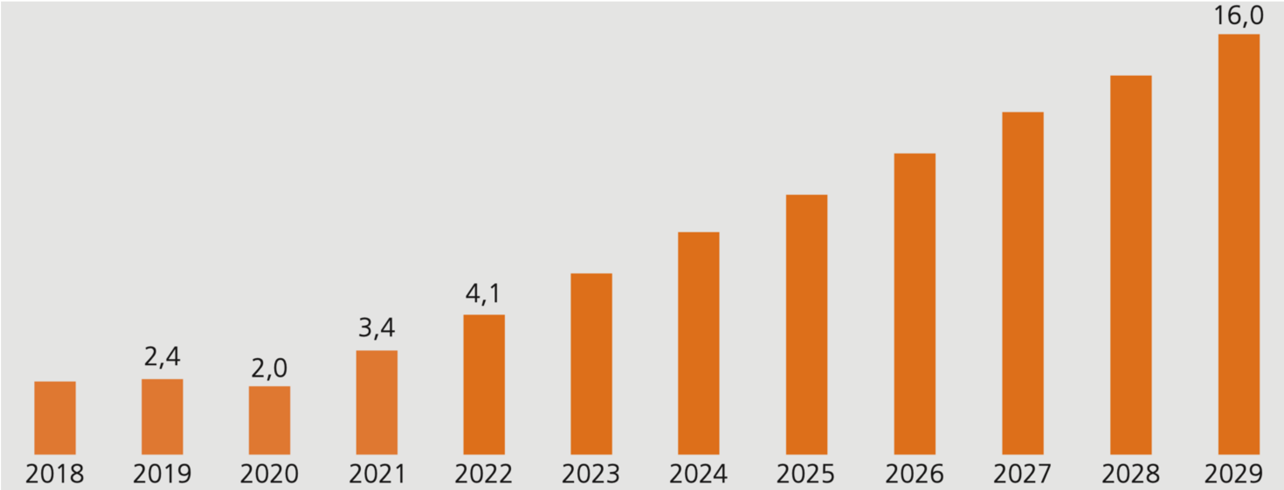

Figure 1. Growth of the orthodontic aligner market, in billions of US dollars, between the years 2018 and 2029.

Factors that may contribute to the ongoing growth in demand for plastic aligners include: 1) technological evolution of computational platforms, facilitating professional management and control; 2) increased predictability of results with gained experience and training in aligner use by orthodontists; 3) increased family investment in health; 4) improvement in global post-pandemic financial indicators; 5) aesthetic and comfort advantages for increasingly demanding patients; and 6) aging of the world population.

Furthermore, the migration of traditional dental companies to the aligner market (e.g., 3M, Straumann, Ormco, Dentsply-Sirona, Henry Schein, Argen) strongly indicates the potential for growth within a short timeframe. Even in developing countries, characterized by younger populations and fewer financial resources, an increase in demand for aligners is observed.

In Brazil, there has been a notable increase in orthodontists' interest in using aligners over the past five years. In private practices, spontaneous demand for "invisible" and removable devices is evident. The offering of aligners by companies that fully outsource appliance fabrication is very convenient for professionals, who receive a quality product without the challenges of managing in-house production. On the other hand, opting for a fully outsourced system imposes financial and production time constraints on the orthodontist, which do not always accommodate the treatment needs and specific demands of some patients. Given the limitations of the outsourced system, the development of technologies and methods that allow aligners to be fabricated directly by clinicians—commonly referred to as in-office, in-house, or DIY (do-it-yourself)—was inevitable (Figure 2).

Figure 2. In-house aligners.

Providing aligners to patients within a matter of hours; offering immediate replacements in cases of loss, breakage, or staining; and balancing production costs according to the specific demands of each market and patient profile are some of the advantages of the in-house system compared to outsourcing.

Given this context, the objective of this series of three articles is to offer novice orthodontists practical considerations for initiating the use of in-house aligner fabrication. Additionally, it aims to share experiences related to the fabrication and management of the technique with professionals who are already users of this system.

In-House Aligner Solutions

Effective, low-cost solutions that meet the current demands of patients can be offered through in-house aligners. Some clinical examples are presented as an introduction to the potential of the technique.

Case 1

A 28-year-old female patient, in the post-retention phase of previous orthodontic treatment, had discontinued the use of fixed lower and removable upper retainers 12 years prior. Her chief complaint was aesthetic discomfort due to crowding of the lower incisors, motivated by her wedding scheduled for 10 weeks (75 days) after the orthodontic consultation. There was a relapse of dental misalignment in the anteroinferior region (Figure 3I). Cephalometric analysis showed proclined lower incisors (L1-GoGn, 109°; 1-NB, 8 mm), limiting the possibility of realignment by tooth projection (Figures 3I and 3K). The panoramic radiograph (Figure 3J) revealed the presence of all teeth except for the lower third molars, which had been previously extracted during the corrective phase due to impaction of the second molars between the first and third lower molars.

Figure 3 (A-K). Case 1 – 28y 11m: A-H) initial extraoral and intraoral photographs, I) initial lateral cephalogram, J) initial panoramic radiograph, and K) initial tracing.

Given the short timeframe to resolve the problem using a commercially outsourced aligner system, and due to the patient's rejection of fixed multibracket appliances, it was decided to treat her with in-house aligners. Intraoral scanning was performed on the same day as the initial consultation (Figure 4A), and within 48 hours, attachments were bonded, interproximal reductions (IPR) were performed, and the first series of aligners (6 sets) was delivered.

Figure 4 (A-B). Case 1: A) Initial intraoral scanning, B) Intermediate scanning after 45 days.

Considering the very short time remaining until the wedding date, the patient was instructed to change the aligners every seven days, with 22 hours of daily wear. Biweekly visits were scheduled to perform additional progressive interproximal reductions (IPRs). After six weeks of use, with four weeks remaining before the wedding, a new scan was performed (Figure 4B), and a complementary series of four aligners was delivered within 24 hours. Basic alignment had already been achieved, and the patient was satisfied with the results obtained within the available timeframe, experiencing minimal social and professional impact during therapy. After the wedding, three additional in-house aligners were fabricated based on a new scan, reaching the outcome shown in Figure 5.

Figure 5. Case 1: Intraoral scan.

Case 2

A 17-year-and-9-month-old male patient in the active finishing phase of fixed multibracket orthodontic treatment, which involved extraction of first premolars to manage severe space discrepancy in both arches (Figures 6A–K).

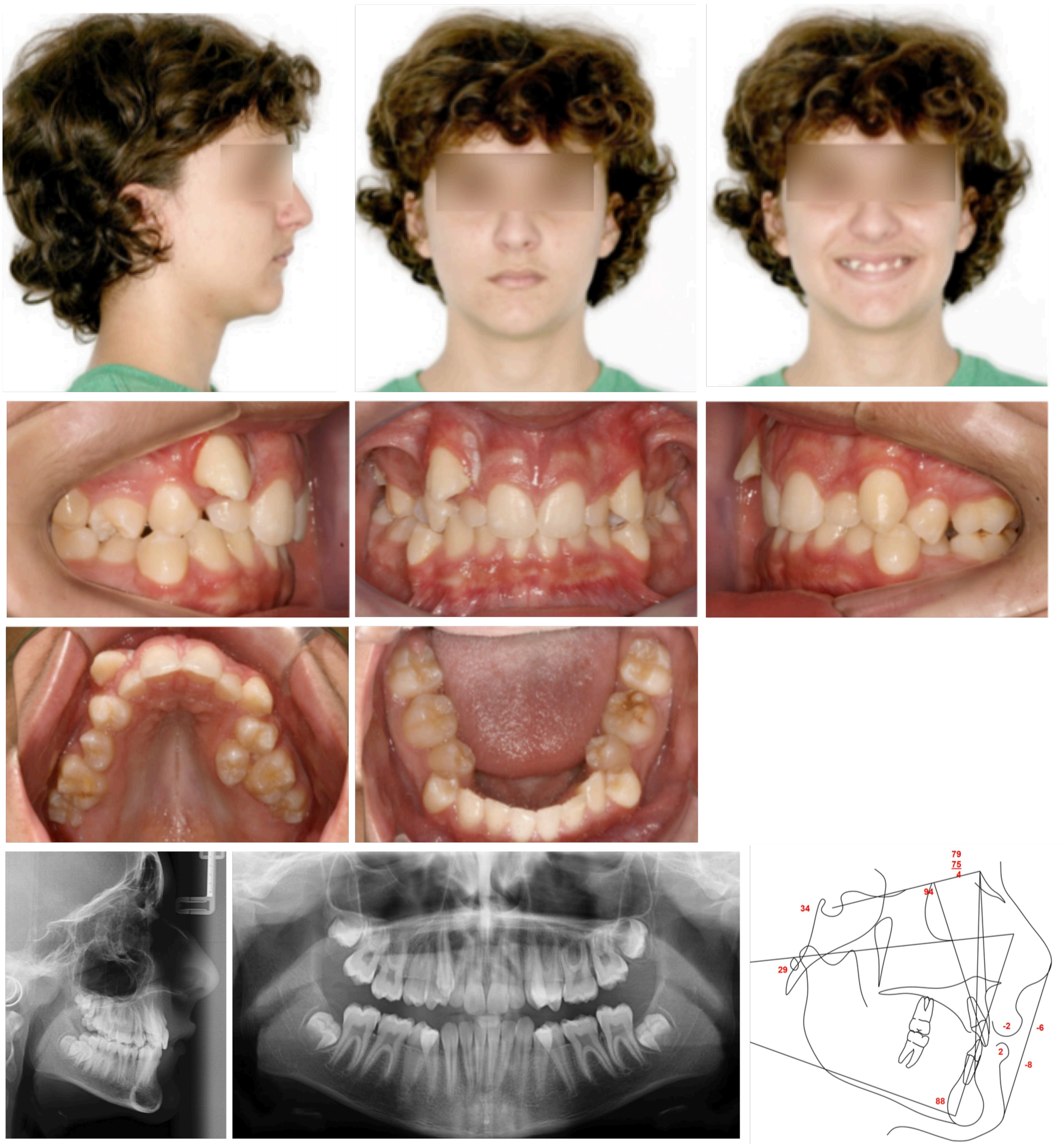

Figure 6 (A-K). Case 2 – 13y 4m: A-H) initial extraoral and intraoral photographs, I) initial lateral cephalogram, J) initial panoramic radiograph, and K) initial tracing.

Already in the advanced stage of therapy with the fixed appliance, the family informed that the patient was relocating abroad for university studies in North America and wished to complete treatment in Brazil to avoid changing providers and incurring additional costs. At that time, the patient presented a significant diastema between the upper right lateral incisor (tooth 12) and the adjacent canine (tooth 13); linear and angular displacement of tooth 13 toward the buccal; deviation of the lower midline to the left; and rotation of the permanent lower right canine (tooth 43) (Figures 7A–H).

Figure 7 (A-H). Caso 2 – 17y 9m: Intermediate initial extraoral and intraoral photographs.

Given that the patient's return to Brazil was expected to be biannual, it was agreed to provide in-house aligners for full-time use (22 hours per day) until the next visit during the upcoming holidays (a five-month interval). Nine pairs of aligners were fabricated, with recommended biweekly changes, and the patient was instructed to continue wearing the last pair until the next appointment. The indicated interproximal reductions (IPRs) were performed during the initial single consultation. All attachments were also bonded at the first visit.

Considering that good function and aesthetics could be achieved with tooth 43 in its current position, correction of its rotation was excluded from the treatment plan, reducing treatment time, the need for additional IPR appointments, and side effects on adjacent teeth.

Good space closure in the maxillary arch, effective control of tooth 13 movement, and midline improvement were achieved, despite the upper space closure occurring contralaterally to the direction of correction (Figures 8A–J).

Figure 8 (A-J). Caso 2 – 18y 3m: A-H) Final extraoral and intraoral photographs, I) Final lateral cephalogram, J) Final panoramic radiograph

Case 3

A 8-year-and-9-month-old female patient in the early mixed dentition phase presented with delayed eruption of the permanent upper right first molar (tooth 16), mild maxillomandibular constriction, and significant misalignment of the permanent lower incisors, with teeth 42 and 32 positioned outside the alveolar ridge contour (Figures 9A–K). Moyers analysis indicated a negative space discrepancy of 2 mm in the lower arch, considering preservation of the future Leeway space (E space).

Given the absence of tooth 16 in the oral cavity (Figure 9G), which would complicate transverse maxillary management by direct expansion at that time (either rapid or slow expansion), dentoalveolar expansion of the mandible using in-house aligners was chosen.

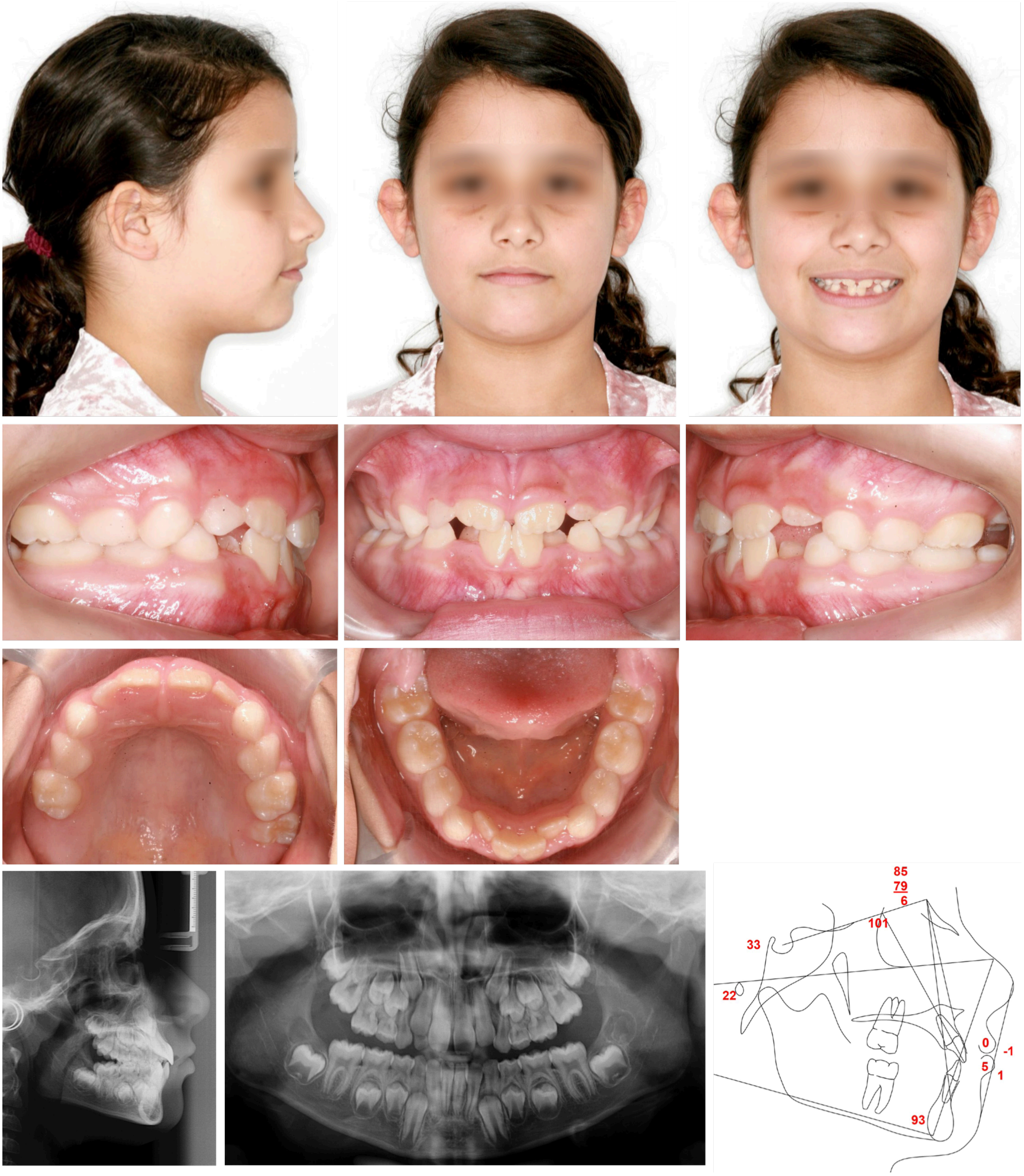

Figure 9 (A-K). Case 3 – 8y 9m: A-H) initial extraoral and intraoral photographs, I) initial lateral cephalogram, J) initial panoramic radiograph, and K) initial tracing.

Five stages of aligners were fabricated exclusively for the lower arch, with changes every three weeks and a recommendation of 20 hours of daily wear. Since in-house aligners typically do not have sufficient durability for full-time use over three weeks, two aligners were fabricated for each stage of the printed subset models. Attachments were bonded to the canines and deciduous second molars of the lower arch. No interproximal reductions (IPRs) were performed.

After four months, a new scan was performed, and an additional five refinement aligners were fabricated (Figure 10), with the same usage characteristics as the initial ones.

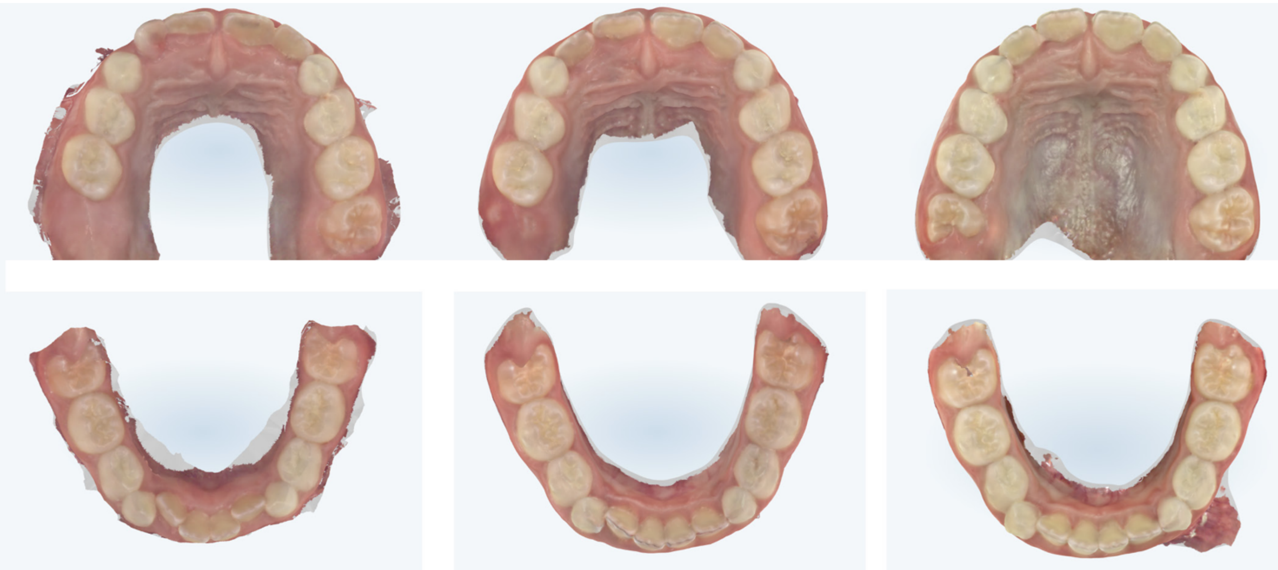

Figure 10. Case 3: sequence of progression.

After eight months of therapy and the use of 10 stages of expansive tooth movements in the lower arch, an improvement in the alignment of the lower incisors was achieved, positioning them over the alveolar ridge (Figure 10), with relatively small transverse gains (0.5 mm at the permanent first molars; 1.5 mm at the deciduous second molars; and 1.9 mm in the deciduous canine region), yet sufficient to manage the negative space discrepancy (Figure 11A).

Concurrently, discrete but clinically significant spontaneous increases in maxillary transverse dimensions were observed, resulting in a desirable maxillary arch form despite the absence of direct expansion appliance intervention (Figure 11B).

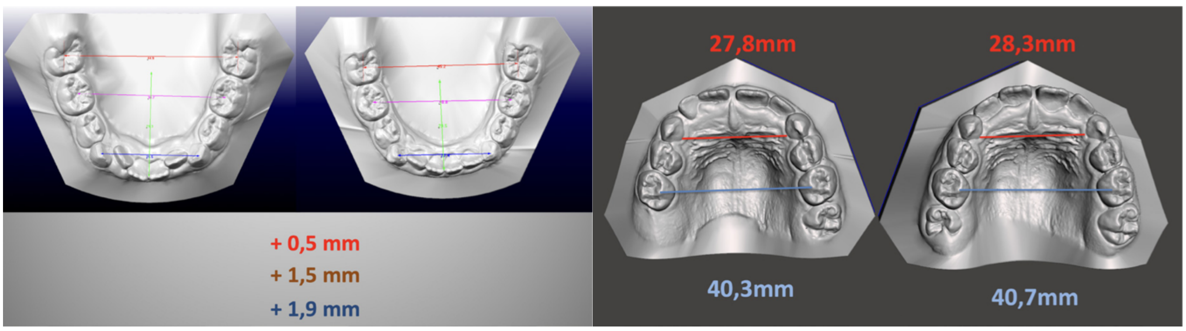

Figure 11 (A-B). Case 3: A) lower space analysis e B) upper space analysis.

Case 4

A 6-year-and-10-month-old female patient in the early mixed dentition phase (Figures 12A–I). She presented with a general Class I pattern and mild maxillomandibular constriction. There was significant misalignment of the permanent left central lower incisor, positioned lingually outside the alveolar ridge.

A negative space discrepancy was suggested in the dental arches, with probable misalignment of the permanent incisors at the time of their future eruption. It was decided to initially intercept the negative space discrepancy with maxillary expansion via palatal disjunction, with the expectation that alveolar compensations in the mandible would favor an increase in arch perimeter and better alignment of the incisors.

Figure 12 (A-I). Case 4 – 6y 10m: A-H) initial extraoral and intraoral photographs, I) initial panoramic radiograph.

After six months of using the palatal expander, an improvement in the position of the upper incisors was observed. On the other hand, in the lower arch, the eruption axis of the incisors and the proximity of their roots to adjacent teeth indicated the need for alveolar expansion, which was performed using a Schwartz acrylic plate.

The decision was made to use the Schwartz plate in the mandible instead of in-house aligners. This choice was based on the complexity of managing the active eruption of permanent incisors simultaneously with the use of aligners. Additionally, the risk of plastic support on the incisor crowns at that time was considered, which could prevent their physiological accommodation and protection against possible pressure from the erupting crowns of adjacent teeth.

After four months of using the Schwartz plate, an improvement in the shape of the lower arch was observed (Figures 13A–J), including space opening between teeth 42 and 83.

Figure 13 (A-K). Case 4 – 8y 1m: **A-H)** intermediate, **I)** lower arch crowding detail e **J)** panoramic radiograph.

As tooth 32 still lacked adequate space for eruption, with a deviation of the lower midline to the left, it was decided to fabricate five aligners exclusively for the lower arch (with biweekly changes), directing movements toward the occupation of the diastema created on the right side, while maintaining positional control of the already erupted incisors and creating space for the eruption of tooth 41 (Figure 14).

Figure 14 (A-E). Case 4 – final intraoral scan.

Digital Workflow: The Framework of the In-House Aligner Fabrication Technique

In the early, fully non-digital techniques for fabricating plastic aligners, plaster models were manually manipulated and/or anatomical deformations were introduced directly into the aligner (such as bubbles) using specialized pliers. This technique was extremely labor-intensive, limiting both the amount of movement possible in a single model and the number of sub-setups. However, the experience gained with this treatment approach enabled a natural evolution with the increased accessibility and improvement of computational systems.

In the current concept, aligners can be fabricated either through direct printing, using special shape-memory resins, or indirectly, by thermoforming polymeric laminates over physical models of sub-setups printed in photosensitive resin, based on the staging of tooth movements in digital virtual models (Figure 15).

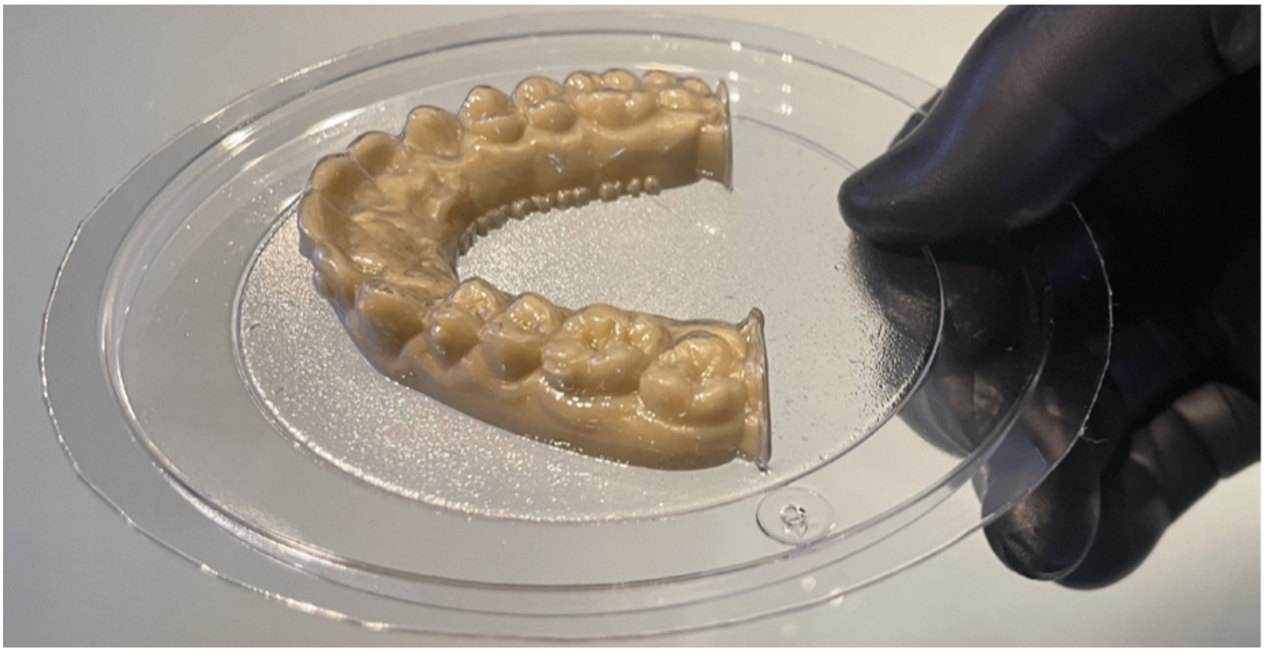

Figure 15. Model printed with photosensitive resin and thermoplastic laminated PETG polymer under pressure.

Thus, the fabrication of in-house aligners necessarily follows a sequence of actions, most of which are digital. In this series of articles, the process of fabricating aligners using the thermoforming technique with polymeric laminates will be presented. The digital workflow will be divided into seven stages, as shown in Figure 16, and detailed in the following tutorial articles.

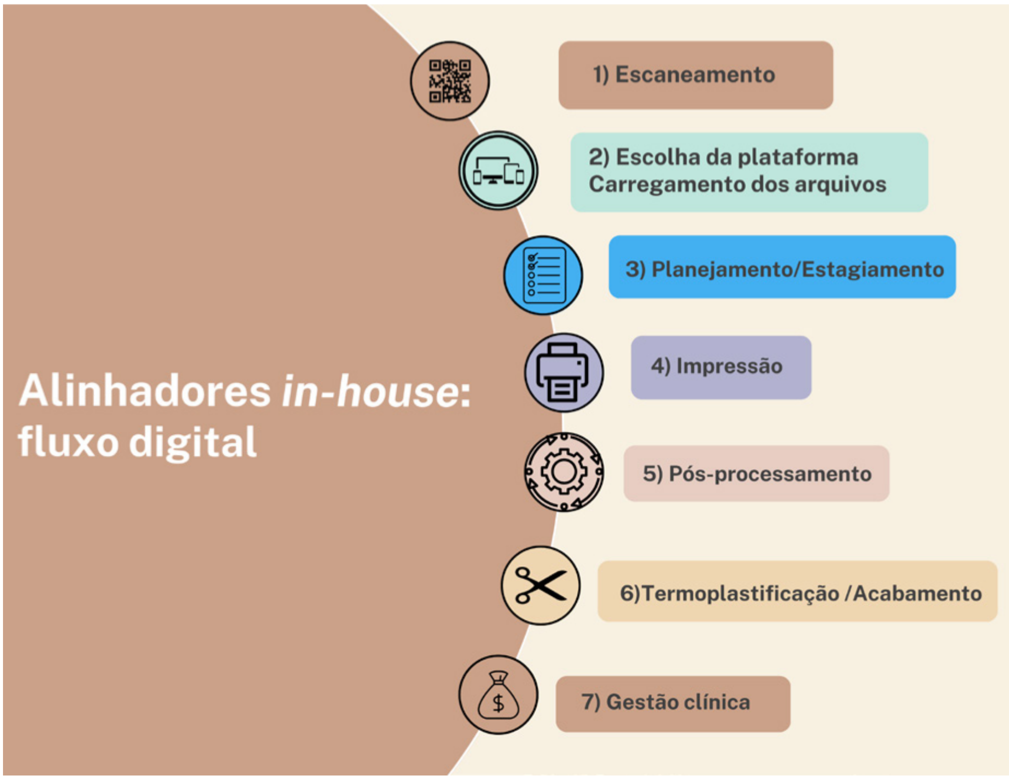

Figure 16. Digital workflow for in-house aligner fabrication.

Stage 1: Intraoral scanning

For the fabrication of modern aligners, which use computer programs to perform orthodontic movements, digital technology is essentially employed through virtual models (usually in ".stl" format) obtained via intraoral scanning. However, until just a few years ago, the technique was more laborious and prone to errors, relying on conventional impressions with high-cost elastomers and a technique-sensitive process. Subsequently, it was necessary to send the impressions by mail to the aligner manufacturer for scanning of the physical impressions with desktop scanners.

With the increased accessibility and ease of acquiring intraoral scanners, as well as the possibility of renting such equipment when needed, the use of intraoral scans has become more frequent in orthodontists' daily practice. Intraoral scanners are devices used for the optical capture of the morphology of the dental arches, collecting information on the shape and size of intraoral structures (Figure 17).

Figure 17. Intraoral scanning.

Currently, orthodontic documentation centers can also provide outsourced scanning services. Intraoral scanning is efficient, less stressful for the patient, and has good acceptance.

By projecting a beam or a grid of light onto the tooth surface, the device captures—through high-resolution cameras—the distortion that the beam or grid undergoes when it hits these structures. The data collected by the cameras are processed by powerful software that reconstructs the three-dimensional model of the identified structures. The most modern devices can even capture the coloration of the teeth and soft tissues.

In simplified terms, the formation of the three-dimensional image occurs through the generation of a *point cloud*. Each of these points has coordinates according to its spatial location. The points are joined in triangular geometry, forming a three-dimensional mesh (Figures 18B-D).

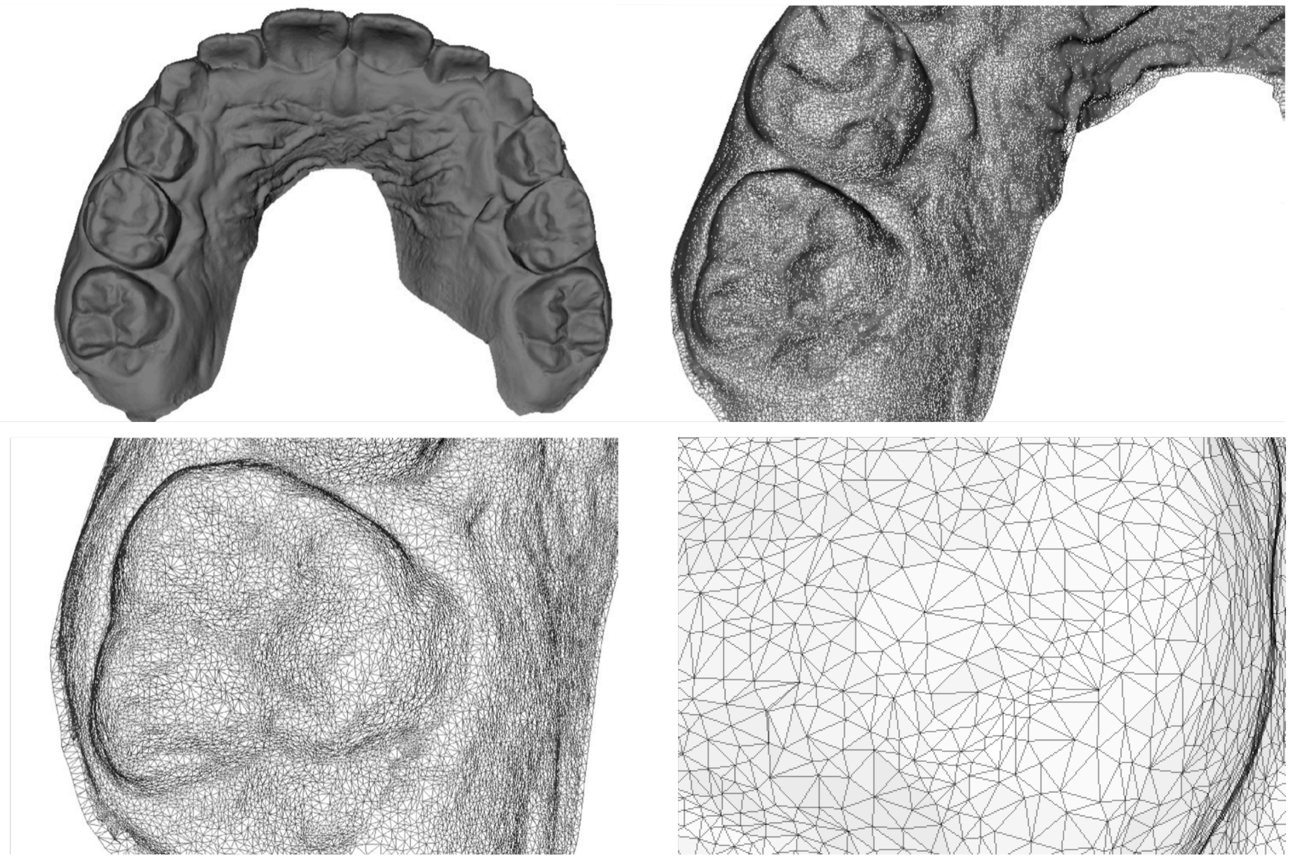

Figure 18 (A-D). 3D virtual model: A) solid model, B) triangle mesh in distant view, C) triangle mesh in intermediate close-up, D) triangle mesh in close-up.

During scanning, numerous images are captured by the system, gathering information about the distance between points. Naturally, images are generated to record the total volume of the object. Finally, the images are transferred to a common coordinate reference system which, using mathematical algorithms, aligns and constructs the object's 3D model.

The intraoral scanning system offers numerous practical advantages, such as the ease of sharing digital models among different work teams and the ability to easily and effectively manipulate the digital positioning of teeth, streamlining the aligner manufacturing process in a short amount of time. In the past decade, several studies have reported the accuracy, reproducibility, and limitations of intraoral scanning. However, with the technical development of equipment in recent years and the emergence of new product generations, improvements in image capture speed, automatic cleaning of unnecessary areas, and precision in the microdimensions of structures have become noticeable. The trend is that, with each new generation of scanners, previous limitations will be corrected and the technique will become easier for users.

The size of the scanner tip has always been a limiting factor for accessing certain areas of the mouth, but manufacturers have been addressing this aspect. The inability to reach posterior regions often makes it impossible to adequately record molars, and in pediatric orthodontics, discomfort in young patients complicates digital handling. For example, the Emerald S model from the Finnish manufacturer Planmeca features a significantly reduced tip size (SlimLine fit).

The possibility of automatic cropping (cleaning) of unnecessary soft tissue areas for orthodontic model fabrication, offered by the scanner's software, makes the clinician's job easier, saving time previously spent preparing models, as seen with the iTero system (Figure 19). Some manufacturers provide scanner-integrated programs for post-processing, with useful tools for model manipulation, such as those offered by 3Shape.

Figure 19 (A-B). A) Clean model e B) Raw model.

Certainly, the main limitation to using intraoral scanning in everyday orthodontics is the high initial investment required to purchase the equipment, as well as the costs of maintenance, upgrades, and insurance against physical damage. Considering the inevitable technological advances over the years—and therefore the depreciation of the device due to technological obsolescence in a short period—it is important to carefully evaluate the best way to access this technology: purchasing the equipment, renting it, or outsourcing the procedure. In any case, not owning an intraoral scanner does not prevent orthodontists from manufacturing their in-house aligners.

Clinical tips to improve the quality of intraoral scanning include:

1. Using dark-colored gloves, which prevents them from being detected by the light beam and helps the software more effectively process the digital cleaning of hard and soft tissue images.
2. Maintaining a uniform and adequate distance between the scanner tip and the tooth surface, generating a valid three-dimensional mesh and allowing faster capture by the system.
3. Using an air jet to completely dry the teeth, occlusal fossae, and interproximal spaces.
4. Checking for the presence of interdental "black spaces" caused by insufficient capture of the region, due to difficulty in light penetration.
5. Exporting scanner models in solid format, allowing raw-shape printing for study or the fabrication of retainers.

Stage 2: Choosing the Platform and Uploading Files

For outsourced aligners, after intraoral scanning, the ".stl" files are automatically or manually uploaded to the proprietary systems of the contracted companies, along with complementary files (photographs and radiographs). Next, orthodontic movements are planned with the assistance of technicians, and approval for aligner fabrication is given, ensuring that the orthodontist receives a complete package with all aligners from the contracted series.

In the in-house aligner fabrication process, the essential and fundamental step is choosing the software platform through which orthodontic movements will be planned. The current market offers orthodontists various options, including systems that work essentially offline, without the need for cloud access, and systems that are entirely dependent on real-time internet access. Evidently, both options have advantages and disadvantages. As a general rule, services with higher costs tend to offer more features and higher quality. The opposite is often a harsh reality. However, the cost–benefit ratio must be evaluated on a case-by-case basis, and combining the use of different platforms seems to be an interesting approach.

Currently, fully free staging platforms for orthodontic movement planning and staging, such as Blue Sky Plan (www.blueskyplan.com), which only charge for the export of printable models, have limitations in movement control and low algorithmic reliability, even for low-complexity treatments. Nevertheless, the possibility of 3D integration with computed tomography is a useful feature unique to this offline platform. Because of its continuous action flow, from a pedagogical perspective, Blue Sky Plan is an adequate tool for beginners to learn basic concepts about the in-office system.

The ArchForm platform (www.archform.com) is very appealing, constantly improving its tools, has no acquisition fee for the software, and charges variable amounts per patient uploaded to the system, depending on usage volume. Being intuitive, it is easy to handle and has a good algorithm for low- and medium-complexity treatments, having gained a large user community. Notable strengths of this platform include: real-time identification of the number of sub-setup stages required within the parameters entered; the ability to prioritize movements; and flexibility in preparing models for printing (hollow or not; with or without a base; vertical or horizontal printing, for example).

Complex platforms with advanced diagnostic (SureSmile Ortho by Dentsply-Sirona) and/or staging features (SureSmile Ortho and Clear Aligner Studio by 3Shape) provide several additional tools and well-tested algorithms. These are outstanding platforms, offering a variety of possibilities for case management and customization. For advanced users, they appear to be the natural path for investment. However, since access to these platforms involves an initial investment in acquiring a usage license and, in some cases, paying per uploaded model (SureSmile Ortho) or even annual system maintenance fees (Clear Aligner Studio), simpler platforms will serve beginners in the technique well at first.

It should be remembered that all software platforms used for this purpose are constantly being improved. Therefore, frequent updates are necessary to address reported shortcomings and meet new market demands. One should not expect a platform to be entirely free or without maintenance costs, as this would likely compromise treatment quality. A thorough market analysis in this constantly changing scenario will always be a wise course of action. The number of cases treated monthly and the quality of the software platform should guide the choice of which program to use. Having technical knowledge and mastery of several platforms is a good strategy. Different cost structures for model generation allow for balancing quality treatment with reasonable expenses.

In in-house aligner manufacturing platforms, virtual model files are uploaded, and in most of them, it is also possible to upload photographs and radiographs (Figure 20).

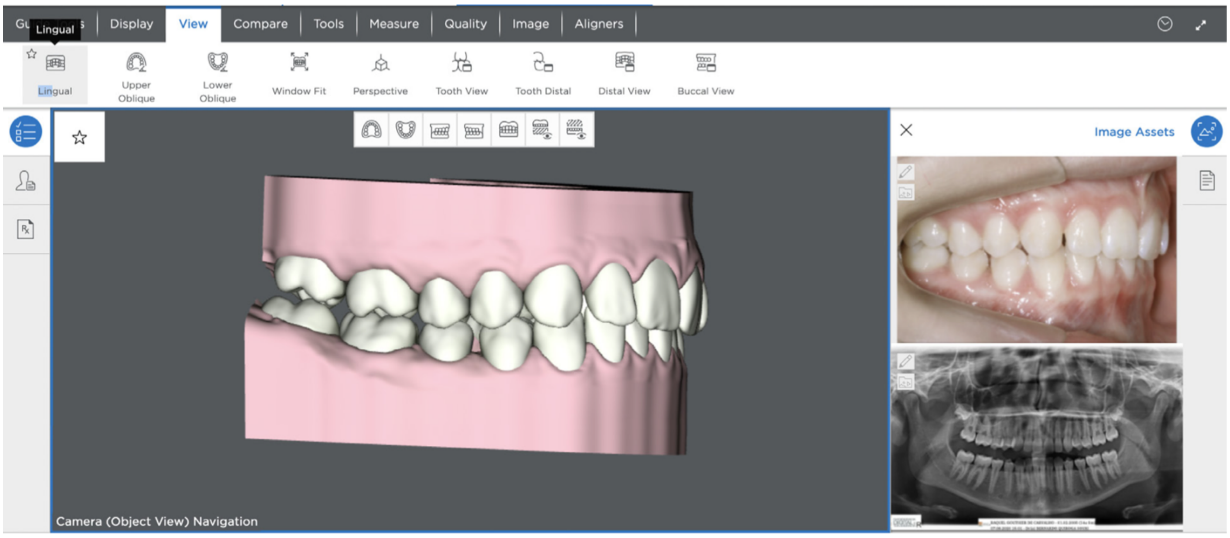

Figure 20. Uploading files in SureSmile..

Ideally, the models should be spatially oriented using the occlusal plane and the patient's face as references. It is recommended that the models be oriented so that the occlusal plane coincides with its inclination on the lateral cephalometric radiograph (pitch control); the vertical position of the incisors is referenced to the exposure of the upper lip; and the palatal raphe is aligned with the midsagittal plane (yaw control) (Figure 21).

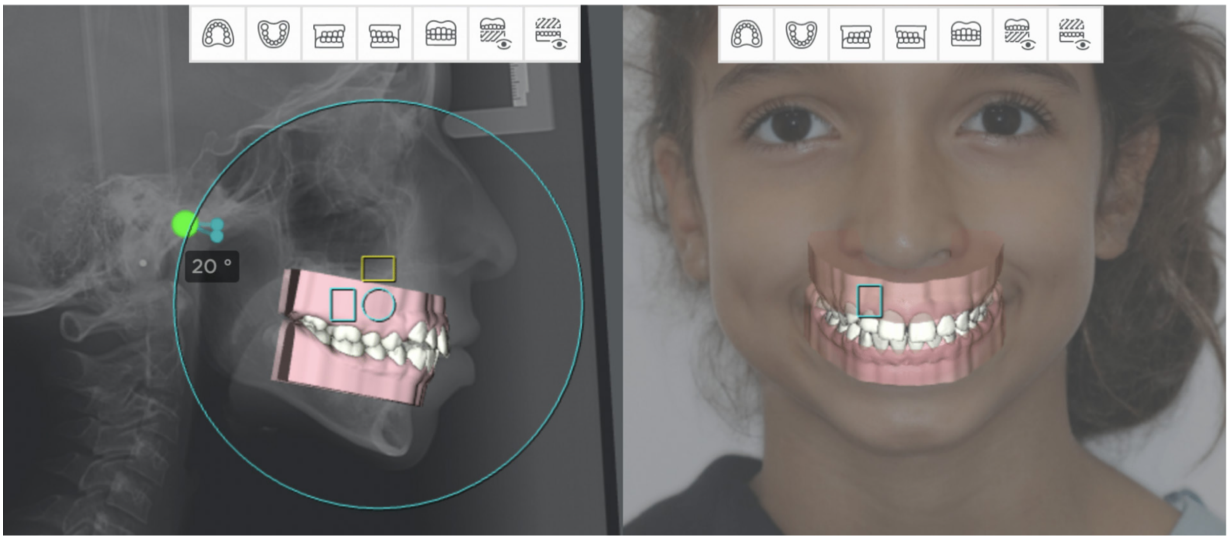

Figure 21. Model orientation in Suresmile.

Thus, the bipupillary line serves as a reference for assessing the rotation of the models around the anteroposterior axis (roll). The SureSmile Ortho platform performs the proper trimming of the models and delivers them ready within approximately 48 hours, which is very convenient, albeit at a cost. For other platforms, it is up to the orthodontist to manipulate the uploaded models within the system, carry out the spatial orientation, and perform the appropriate trimming (Figure 22A–B).

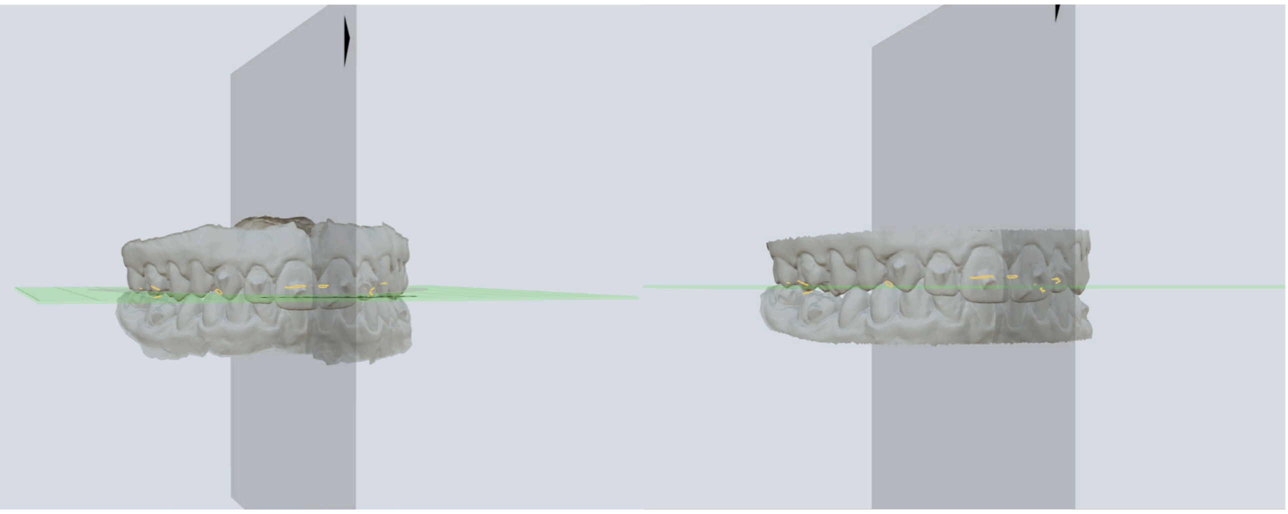

Figure 22 (A-B). Model orientation and trimming on ArchForm platform.

It is strongly recommended that digital trimming of the dental arch models be performed to conserve printing resin. However, care must be taken to preserve a significant extension of gingival tissue, ensuring an adequate area for the plastic to flow during the thermoforming stage (Figure 23).

Figure 23. Model with segmented teeth.

Once properly uploaded onto the platform, the teeth need to be individually segmented (Figure 23), allowing each unit to be manipulated by the orthodontist in the subsequent stage. Generally, the segmentation process in current platforms is reasonably reliable but requires some investment of time to refine the contours suggested by the platform's algorithm. In recent years, there has been a significant improvement in the accurate identification of tooth contours by these systems, saving professional time. Notably, the Dentisply-Sirona platform (SureSmile Ortho) delivers to orthodontists, approximately 48 hours after file upload, oriented, trimmed, and segmented models—saving time for the clinician and ensuring high-quality models. It is anticipated that in the near future, this step of the file-loading stage will be less labor-intensive in other platforms that do not currently provide pre-prepared models.

Upon completion of file upload, virtual orthodontic planning and tooth movement staging can begin. Given the complex combination of: 1) movement types (isolated, synergistic, and antagonistic); 2) various options for plastic laminates (thinner or thicker); 3) different plastic types (single layer versus multilayer, PETG versus polyurethane, for example); and 4) numerous types of attachments, Stage 3 of the in-house aligner digital workflow (Figure 16) will be presented in Part 2 of this tutorial.

References

1. Buonocore MG. A Simple Method of Increasing the Adhesion of Acrylic Filling Materials to Enamel Surfaces. J Dent Res. 1955;34(6):849-853.
2. Bowen RL. Properties of a silica-reinforced polymer for dental restorations. JADA. 1963;66(1):57-64.
3. Roberts WE, Helm FR, Marshall KJ, Gongloff RK. Rigid endosseous implants for orthodontic and orthopedic anchorage. Angle Orthod. 1989;59(4):247-256.
4. Kesling HD. The philosophy of the tooth positioning appliance. Am J Orthod Oral Surg. 1945;31(6):297-304.
5. Sheridan JJ, McMinn R, LeDoux W. Essix thermosealed appliances: various orthodontic uses. J Clin Orthod. 1995;29(2):108-113.
6. Mehta F, Mehta S. Aligners: the rapidly growing trend in orthodontics around the world. Indian J Basic and Applied Medical Research. Published online 2014:402-409.
7. Relatório financeiro anual da Align Technology. Acessado em 27/02/2023 em https://investor.aligntech.com/static-files/c9954d1d-6ee1-4640-b8f2-7f55199898fc
8. Grünheid T, McCarthy SD, Larson BE. Clinical use of a direct chairside oral scanner: An assessment of accuracy, time, and patient acceptance. Am J Orthod Dentofacial Orthop. 2014;146(5):673-682.
9. Imburgia M, Logozzo S, Hauschild U, Veronesi G, Mangano C, Mangano FG. Accuracy of four intraoral scanners in oral implantology: a comparative in vitro study. BMC Oral Health. 2017;17(1):92.
10. Medina-Sotomayor P, Pascual-Moscardó A, Camps I. Correction: Accuracy of four digital scanners according to scanning strategy in complete-arch impressions. PLoS One. 2018;13(12):e0209883.
11. Sfondrini MF, Gandini P, Malfatto M, di Corato F, Trovati F, Scribante A. Computerized Casts for Orthodontic Purpose Using Powder-Free Intraoral Scanners: Accuracy, Execution Time, and Patient Feedback. Biomed Res Int. 2018;2018:18.
12. Aragón MLC, Pontes LF, Bishara LM, Flores-Mir C, Normando D. Validity and reliability of intraoral scanners compared to conventional gypsum models measurements: a systematic review. Eur J Ortho. 2016;38(4):429-434.

B) Practical guide to in-house aligner fabrication- Part 2: Planning and Staging

Abstract

Orthodontic movements with in-house aligners entail specific details and nuances that distinguish them from traditional multi-bracket orthodontic techniques. The orthodontist must acknowledge these details to ensure greater predictability, efficacy, and efficiency in achieving desired outcomes. This second part of the in-house aligners manufacturing tutorial presents insights on tooth-specific movement requirements, anchorage control, movement hierarchy, unique aspects of plastic mechanics, and attachment types.

Introduction

The in-house fabrication of clear aligners requires following a workflow, most of which is digital. As presented in Part 1 of this tutorial series, after intraoral scanning, selection of staging software, and file upload (Stage 1), orthodontic movement planning/staging should be performed (Stage 2), also entirely digital, aiming to achieve the treatment objectives for malocclusion.

Some dental professionals still believe that tooth movements visualized on computer screens and segmented into various stages within the software will occur identically in the clinical setting. However, variables related to the plastic materials, the interactions of dynamic and complex tooth movements, and the distinct ways aligners apply force systems to teeth result in the orthodontic movement simulations not translating on a 1:1 ratio. Thus, the clinician's anticipation of probable clinical outcomes is essential.

Fundamental knowledge from classical orthodontic training—including diagnosis, orthodontic biomechanics, biology of tooth movement, and occlusal biogenesis—remains mandatory in this therapeutic modality. This knowledge also contributes to reducing the discrepancy between the software simulation and the clinical reality.

The aim of this second part of the tutorial is to present basic aspects that must be considered when planning in-house aligner treatments, regardless of the staging software used. Control over tooth movements and the multiple interactions between movement directions on the same tooth and within the dental arch as a whole must rest with the orthodontist. More sophisticated software may facilitate the clinician's work by incorporating advanced algorithms that anticipate potential problems and suggest feasible solutions, but they should not replace the orthodontist's overall responsibility for treatment control.

Recent Evidence on the Effectiveness of In-House Aligners in Orthodontic Movements

There is evidence that teeth respond to various force systems. Forces applied rationally will likely generate the intended orthodontic movements. However, a dramatic paradox persists: after two decades of evolution and refinement of plastic aligner fabrication techniques, including the advent of direct printing of aligners with shape-memory resins, significant doubts and controversies remain about their effectiveness in achieving orthodontic tooth movements. Much of the initial skepticism arose from treatments performed by clinicians lacking expertise in the specific nuances of the technique.

Being an experienced orthodontist with conventional techniques is important for the use of aligners, but it is not sufficient to recognize the system's limitations and know how to overcome them with special maneuvers. This is especially true for in-house aligners, due to the less refined algorithms in most software and the lower technology of plastic laminates used in the thermoplastic fabrication technique. Nevertheless, data already indicate it is possible to plan and execute even complex treatments with thermoplastic in-house aligners.

A recent prospective, controlled, randomized, single-center clinical trial included 36 patients (12 men and 24 women, mean age 21.24 ± 2.33 years), all with severe crowding requiring extraction of four first premolars. Patients were equally and randomly divided into two groups: 1) in-house clear aligners (AT) and 2) fixed appliances (AF). All measurements were performed on pre- and post-treatment plaster models using Little's Irregularity Index and the Peer Assessment Rating (PAR) index. Both groups showed a significant reduction in Little's index, with no differences between groups at treatment completion. The mean PAR score reduction was 28.39 (± 8.51) points for the AT group and 26.39 (± 5.76) points for the AF group, without significant differences. All patients improved dental occlusion; however, a great improvement was achieved in 88.9% of AT patients and 91.7% of AF patients, with no statistically significant differences. The mean treatment duration was 23.27 (± 5.28) months for the AT group and 26.20 (± 5.27) months for the AF group, again with no significant difference. It was concluded that in-house clear aligners are as effective as fixed appliances in achieving good occlusion in complex orthodontic cases when an adequate tooth movement protocol is employed[1].

Currently, the concept is consolidated in the literature that much of the virtual tooth movement programmed in the software will not occur in the complex biological system of dental arches[2],[3]. Regardless of the fabrication process (outsourced or in-house), the average effectiveness of aligners is approximately 50%. Therefore, in any given set of aligners, not all programmed movements will occur clinically, necessitating additional aligner series to approach 100% completion[4,5].

In 2021, a prospective clinical study evaluated 30 patients (259 anterior teeth analyzed: 126 maxillary and 133 mandibular) treated with in-house aligners using the 3Shape OrthoAnalyzer platform. Clinical outcomes were significantly lower than virtual predictions for six tooth movement types (buccal, lingual, mesiodistal, intrusion, extrusion, and rotation). The average efficacy of tooth movement with clear aligners was 56.2%. Mesiodistal movement was the most accurate (72.3%), while intrusion and extrusion were the least predictable, with intrusion being the least precise movement (43.3%)[6].

Studies on in-house aligners emphasize that mechanical control by the treating clinicians and recognition of system capabilities and limitations are essential for treatment success[2,7,8]. What is visualized on the computer screen is only a vector of force direction; the orthodontist's persistent refinement efforts will ultimately lead to excellent final results.

Types of Tooth Movements

For didactic purposes, tooth movements with aligners are classified as isolated, synergistic, and antagonistic. Each type has distinct aspects and often requires different approaches. Synergistic movements are highly predictable, while isolated movements require attachments to occur more effectively. Antagonistic movements not only require attachments but must be hierarchized—i.e., performed sequentially and separately from the antagonistic movement in time.

This classification can also be extended to two levels in relation to adjacent teeth: individual tooth and collective tooth movement. For illustration, an individual movement example is the rotation of the upper left central incisor (Figure 1), which shows higher predictability when it receives only rotational force (isolated movement) compared to when it simultaneously receives an extrusive force (antagonistic to rotation) (Figure 2). The addition of attachments is essential to enable these movements, as will be explained next.

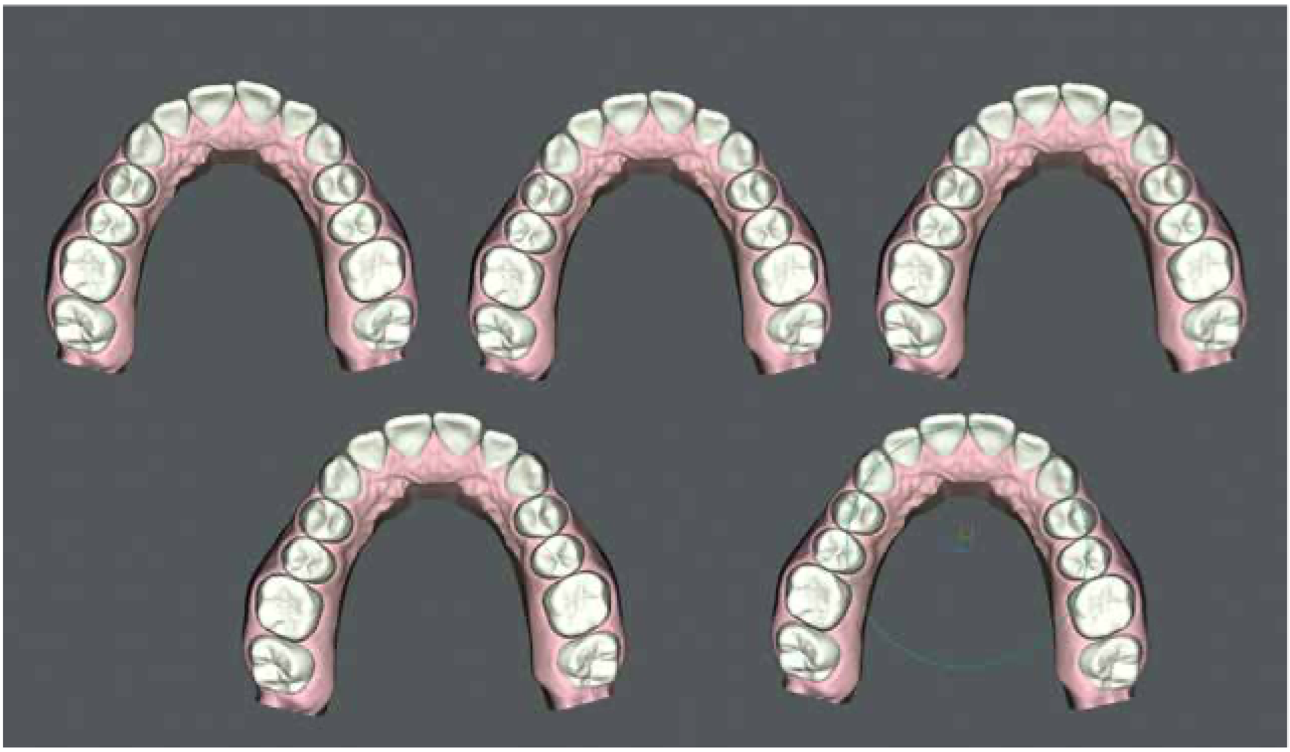

Figure 1. Individual tooth rotational movement planned for the upper left central incisor using SureSmile Ortho software.

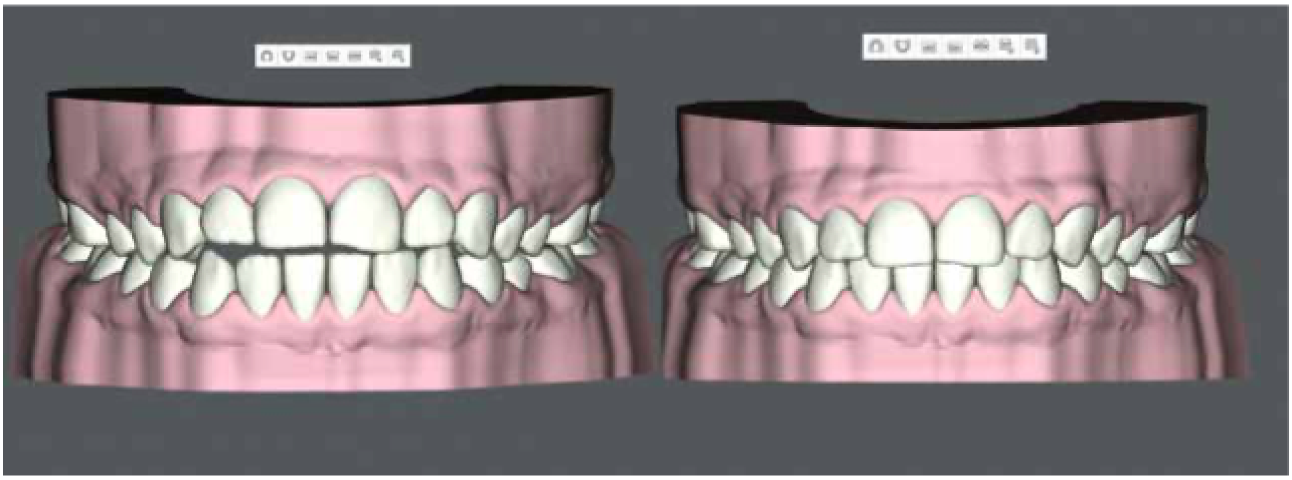

Figure 2. Dental rotational and extrusion movements idealized for didactic purposes in the region of the upper canines and incisors using SureSmile Ortho software. The absence of attachments makes the clinical execution of these movements unfeasible.

On the other hand, rotational movement will likely occur more effectively if the incisor receives a synergistic force (intrusive force) along with the rotational force, as this helps maintain the plastic contact on the longer surfaces of the tooth. However, this is not always possible, as illustrated in Figures 1 and 2, where the patient presented with an anterior open bite. Therefore, for the idealized orthodontic movements to effectively take place, it is necessary to employ hierarchical strategies, including the creation of spaces to increase the surface area and plastic contact, as well as the insertion of attachments (Figures 3 and 4), which will be discussed further in this tutorial.

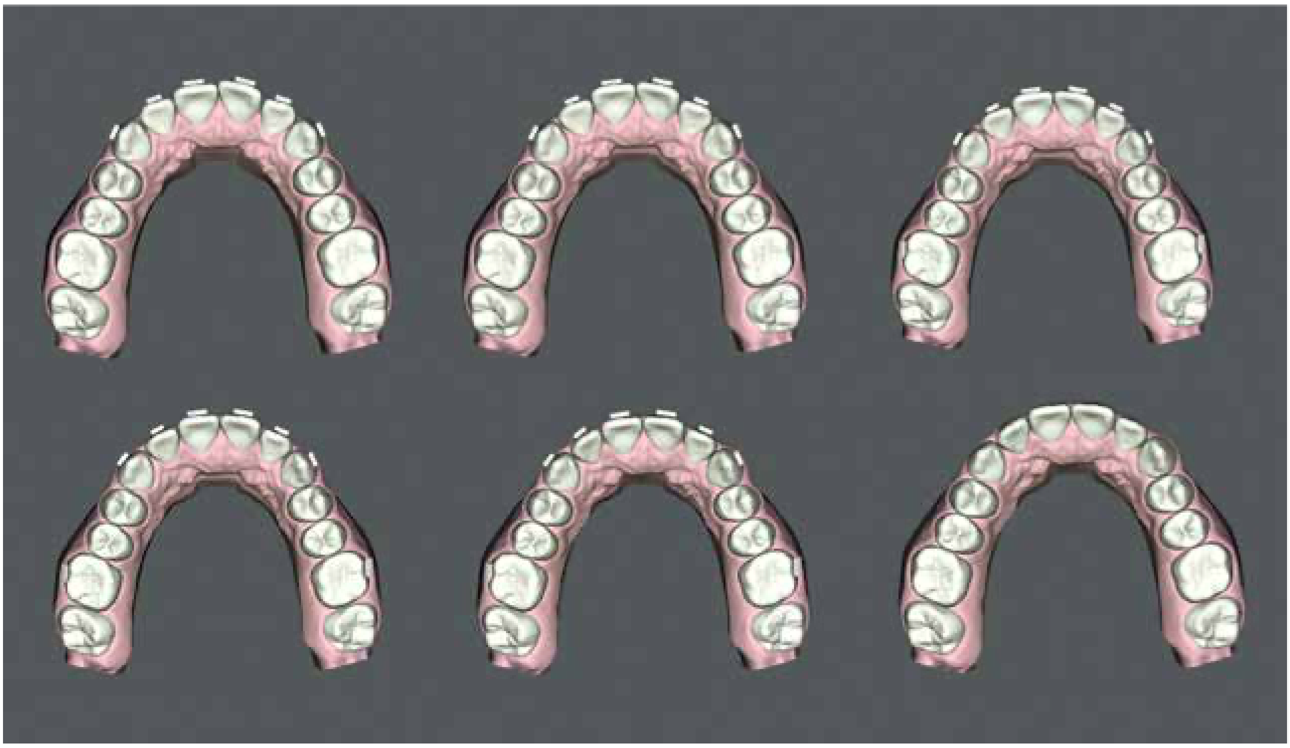

Figure 3. Hierarchization of orthodontic movements. Occlusal view showing the initial creation of spaces and insertion of attachments to enable the desired orthodontic movements to effectively occur. SureSmile Ortho software.

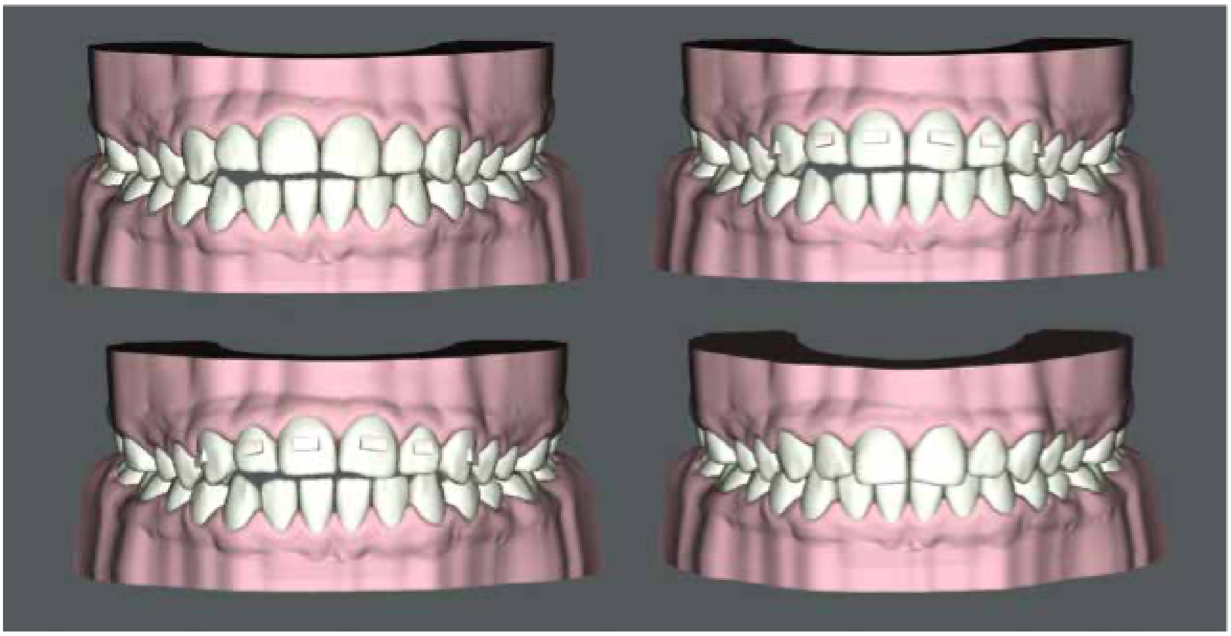

Figure 4. Hierarchization of orthodontic movements. Frontal view of several stages, showing the initial creation of spaces and insertion of attachments to ensure the desired orthodontic movements can effectively take place. SureSmile Ortho software.

At the collective tooth level, a maxillary right central incisor receiving an extrusive force (isolated tooth movement) (Figure 5) will exhibit different movement efficacy depending on whether the adjacent teeth receive no force, antagonistic loads (extrusion), or synergistic loads (intrusion). Intrusive movements of the right lateral incisor and the left central incisor, if indicated, would potentially enhance the extrusion of the right central incisor (synergistic forces applied to the extrusive movement). Conversely, extrusive movements of these two adjacent teeth to the misaligned right central incisor would negatively impact the planned extrusion movement (antagonistic forces).

Figure 5. Extrusive force on the upper right central incisor (isolated movement) using ArchForm software. Note the insertion of attachments on the incisor to be extruded and on the molars for aligner stability and increased patient comfort.

Anchorage unit and prioritization of movements

Considering the previously presented concept about the type of movement each tooth is receiving individually or collectively, avoiding antagonistic forces should be a goal in treatment planning with aligners. Maintaining a significant number of teeth without any movement at a given stage of treatment is an interesting strategy, preventing multidirectional forces that are difficult to control spatially.

Some software platforms allow “freezing” movements of selected teeth, while others do not. The most important thing is that the professional keeps in mind what is intended to be achieved at each stage of the movements, remembering that prioritization of positional changes is necessary to achieve good predictability.

Using prioritization means giving precedence to movements that, if performed chronologically before others, will make the therapy progression more predictable, effective, and efficient. For example: if correction of rotation and extrusion of maxillary incisors is desired, spaces between interproximal surfaces should first be opened, eliminating collisions that would interfere with the desired movements. Next, with the plastic covering the interproximal surfaces, rotation correction is performed without the antagonistic force of extrusion, which would reduce friction and tracking of the plastic over the attachments on the incisors. Finally, at the third hierarchical level, the planned extrusion is performed, complemented by any remaining space closure if necessary (Figures 3 and 4).

Figure 6 illustrates the prioritization of orthodontic movements in a treatment aimed at aligning the maxillary incisors with a slight reduction of dental protrusion. Interproximal reductions of the maxillary and mandibular incisors were planned to allow their retraction. However, to increase the efficiency of the movements and the quality of the interproximal reductions, the system initially created interdental spaces through expansion and projection movements. Retraction and space closure occurred in a second stage.

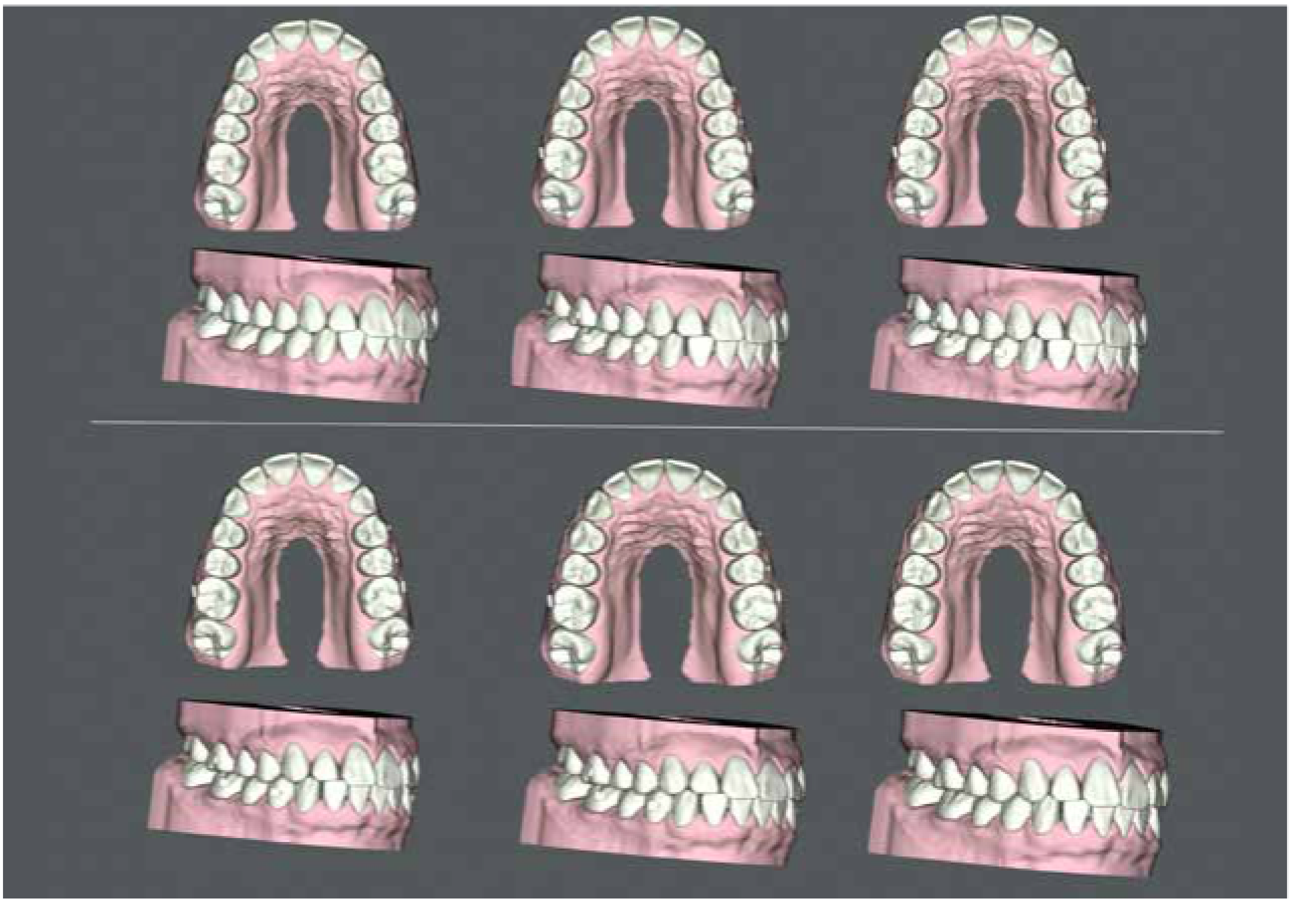

Figure 6. Hierarchization of orthodontic movements using SureSmile Ortho software aiming at dental alignment and some reduction of incisor protrusion. The system initially generated interdental spaces to allow plastic insertion on the interproximal surfaces.

Thus, the orthodontist must keep in mind the sequence and the best timing to perform dental movements, and which movements can be carried out together or separately. Additionally, they should be aware that some movements require overcorrection and that some must be done more slowly due to the difficulty in executing them7,8.

Furthermore, the use of auxiliary anchorage, through intermaxillary elastics or even skeletal anchorage devices, is part of the orthodontist's tools.

Use of intermaxillary elastics

The use of elastics for sagittal control (Class II and Class III elastics), or even vertical force elastics, should be an accessory instrument in the clinical arsenal when planning treatments with in-house aligners. Similarly to the use of this type of force in conventional orthodontics with fixed appliances, elastics provide multidirectional loads that can cause side effects, often compromising treatment efficiency. It is up to the orthodontist to anticipate such adverse effects and employ maneuvers to minimize or avoid negative outcomes.

Elastics combined with the use of aligners can be attached to buttons bonded to the teeth, placed in cutouts made in the aligners, or even buttons bonded directly on the aligners (Figure 7). Using buttons bonded on the aligners favors the predictability of force application without damaging the contour of the aligners, but it is costly and impractical for daily office use. Cutting niches for inserting elastics directly in the aligners is practical but carries the risk of creating sharp edges that can injure the mucosa. Experience will guide the professional to the ideal direction for inserting these cutouts, using specialized pliers to avoid mucosal injuries or shallow grooves in the plastic that could lead to unwanted displacement of the elastics.

Using buttons bonded directly to the teeth presents several problems, such as accidental detachment of the button, esthetic discomfort, plaque accumulation, and, mainly, the application of undesirable forces directly on a tooth, resulting in uncontrolled and improper movements.

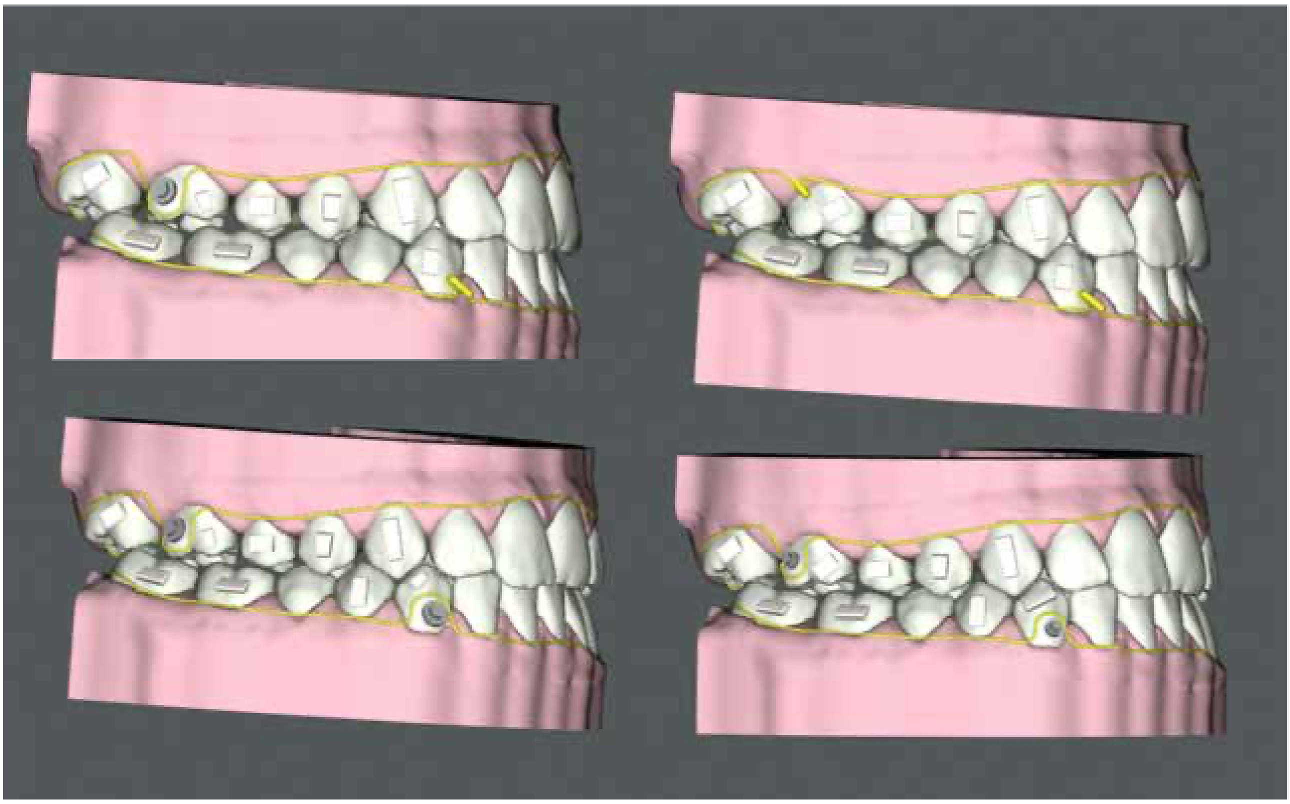

Figure 7 (A-D). Suggested positioning of cutouts for buttons bonded to teeth and elastics directly on aligners, using SureSmile Ortho software for the application of Class III intermaxillary elastics. A) Use of button and cutouts; B) Use of cutouts; C) Use of robust buttons; D) Use of small buttons.

It is recommended to carefully evaluate whether the use of buttons bonded directly to the teeth for Class II and Class III elastics is truly unavoidable, and to consider incorporating preventive biomechanical control measures.

In the case of Class III elastics, if the decision is made to bond buttons directly to the teeth, it is suggested to use small accessories that allow the placement of robust attachments, as illustrated in Figure 7D, in contrast to Figure 7C.

For Class II elastics, ideally, cutouts directly on the aligners should be used (Figure 8A). With buttons bonded on the first permanent lower molars (Figure 8B), the insertion of robust attachments should be planned, for example, on both the first and second permanent molars to help control rotational inclination (crown tip forward).

Additionally, it is recommended to incorporate preventive counter-rotation of the crowns of the first permanent lower molars used as anchorage (crown tip back with 5 degrees) (Figure 8C).

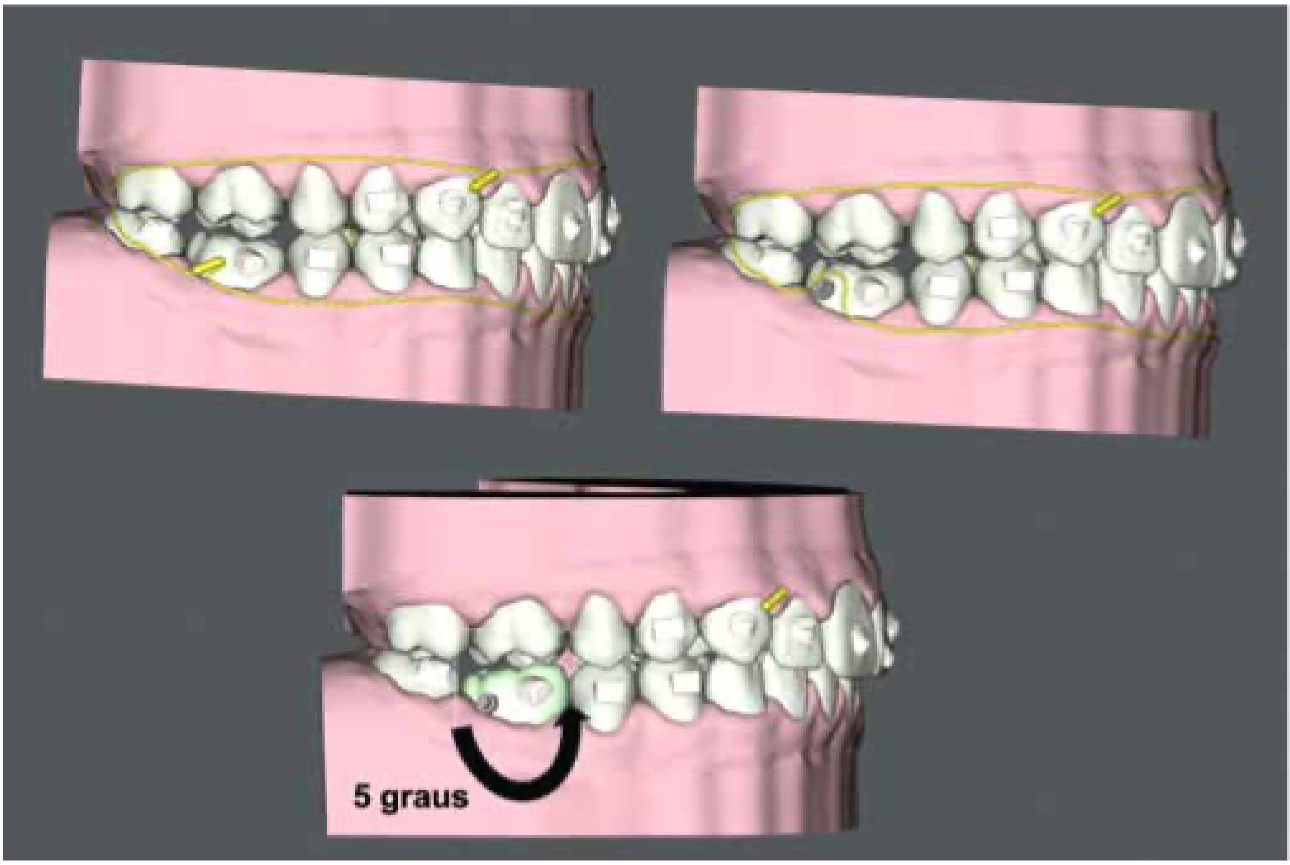

Figure 8 (A-C). Use of buttons and cutouts made directly on the aligners for the application of intermaxillary elastics to correct Class II malocclusion. A) Use of cutouts; B) Use of cutouts and buttons bonded to the first permanent lower molars; C) Use of cutouts and buttons bonded to the first permanent lower molars combined with the incorporation of a preventive counter-rotation of their crowns.

On the other hand, the use of vertical intermaxillary elastics, inserted into buttons bonded directly to the posterior teeth, without the simultaneous use of aligners, in pursuit of rapid vertical interlocking, as a hybrid technique alongside the use of in-house aligners, is a good strategy (Figure 9). This accelerates extrusion movements, which are often difficult to achieve in molars and premolars. Obviously, extreme caution and vigilant control must be exercised when applying free elastic forces.

Figure 9 (A-B). Use of buttons bonded to teeth for the application of intermaxillary elastics, without the support of aligners, aiming at accelerated posterior bite closure. Special caution must be taken with this mechanics due to the limited mechanical control. Frequent short-interval follow-ups are strongly recommended.

Mechanics of the Plastic

While metal wires, attached to brackets, exert their orthodontic effect by traction (pulling the teeth), plastic aligners exert their effect by pressure on the dental surfaces and bonded attachments (pushing the teeth). This concept must be kept in mind by the orthodontist during the planning of the movements. The greater the support for the application of pressure by the plastic, the more predictable and efficient the planned treatment will be.

Thus, the bonding of attachments to the teeth is indispensable within the current aligner treatment system. Extrusions, torque control, and rotational movements demand a combination of anchorage systems with attachments and elastics. Figure 10 illustrates a partial treatment after 39 sets of in-house aligners, combining these principles.

Figure 10. Treatment planning with in-house aligners using the SureSmile Ortho software for a complex malocclusion. Use of intermaxillary elastics and attachments to achieve clinical results as close as possible to the virtual plan.

Another aspect that must be carefully analyzed by the orthodontist is the presence of occlusal and interproximal tooth collisions throughout the course of therapy. Different software programs present this information in distinct ways. It is the operator's responsibility to become familiar with the tools of each system. However, it is clear that these digital analysis and planning tools are valuable advancements of this new era of Orthodontics.

The following figures illustrate the presence and magnitude of occlusal and interproximal collisions using the SureSmile Ortho platform (Figure 11) and ArchForm (Figure 12). The amount of interproximal reduction, when indicated, and the stage at which such reductions should be performed are also indicated by the software.

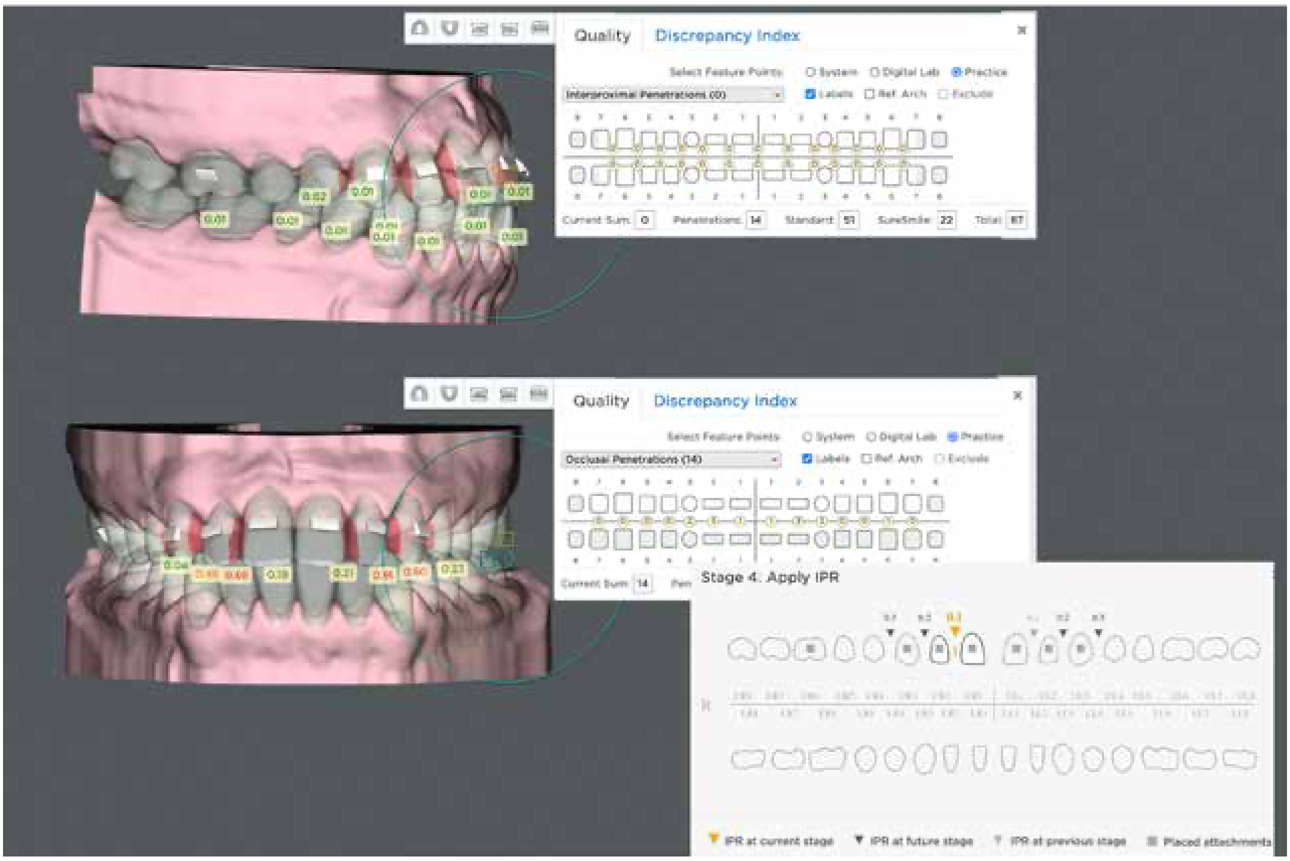

Figure 11. Interproximal contacts and occlusal collisions identified in a digital treatment plan using SureSmile Ortho software.

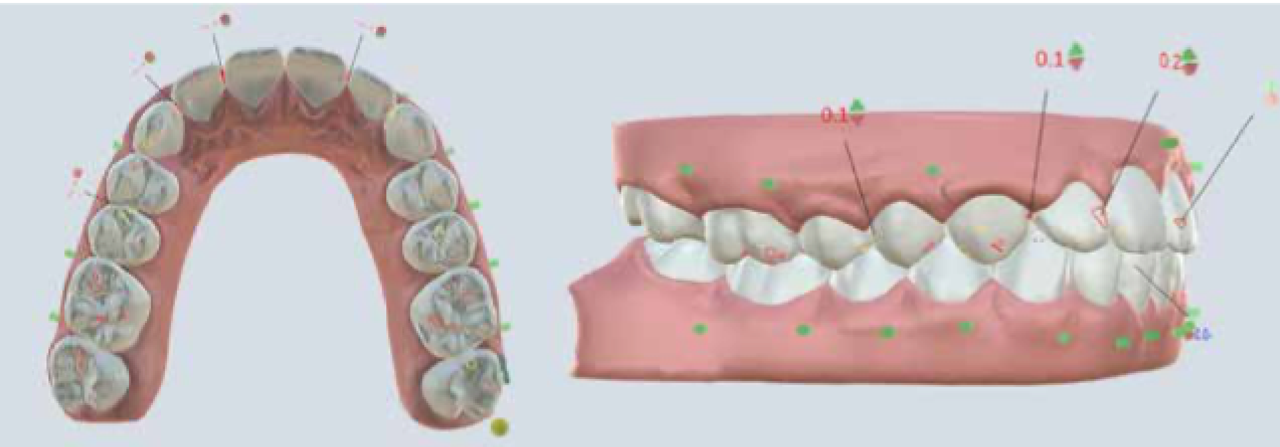

Figure 12. Interproximal contacts and occlusal collisions identified in a digital treatment plan using ArchForm software.

The lower the friction from interproximal collisions, the more predictable and efficient the result will be. Thus, ideally, as previously mentioned, for the clinical realization of certain orthodontic movements, the digital system needs to create interproximal spaces so that the plastic can partially penetrate between the teeth and “embrace” them, exerting the appropriate force. This is particularly common in the control of rotations, extrusions, and distalizations.

The sequential distalization of posterior maxillary teeth, in cases of Class II dental relationships — a movement widely used in treatments with plastic aligners — employs this principle. Through reciprocal accessory anchorage force using Class II elastics, the aligners progressively and individually distalize the posterior teeth up to a certain percentage of the complete movement. This allows the plastic to penetrate the interproximal spaces during much of the distalization mechanics, thus maintaining and reinforcing anchorage while the distalization of all teeth is completed (Figure 13).

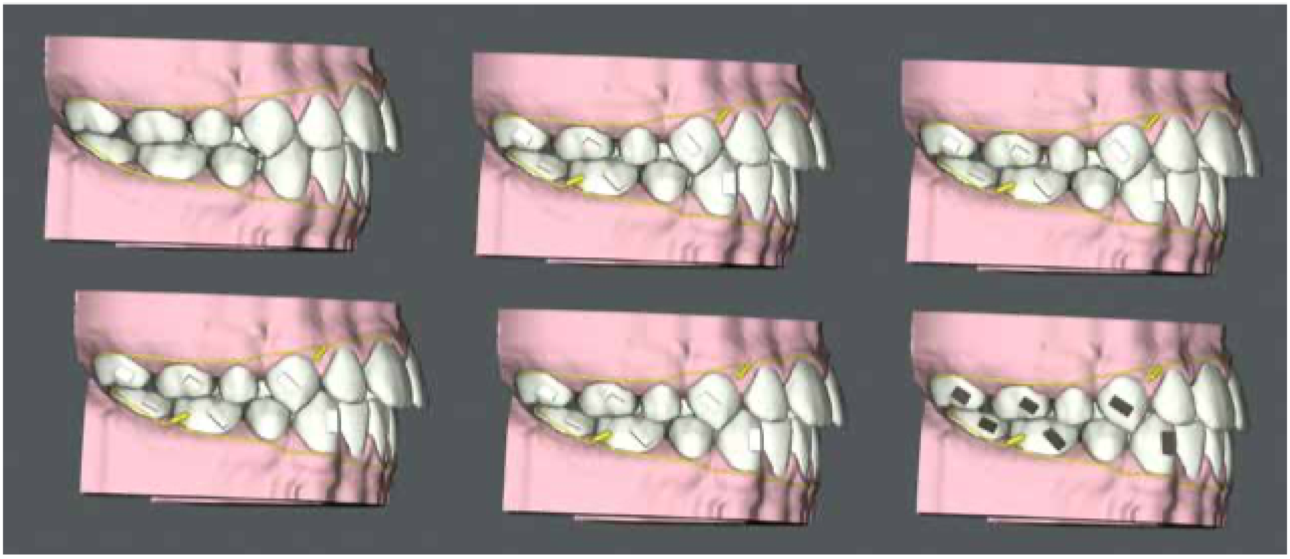

Figure 13. Sequential distalization planned using SureSmile Ortho software. Note the creation of interproximal spaces to reinforce anchorage. Also observe the need for associated Class II elastics.

Figure 13 shows a patient treated with the principle of sequential distalization for the correction of a Class II dental relationship. Initially treated with fixed appliances, after the extraction of the first premolars, the patient had his brackets removed during the period he studied abroad, before the completion of his treatment. Upon returning, it was decided to use in-house aligners combined with Class II elastics for the distalization of molars, premolars, and canines, as well as retraction of the incisors. Figure 13 presents only six stages of the treatment, which had a total of 28 stages. Note the sequential distalization, with opening of spaces to allow plastic penetration on the interproximal surfaces, generating anchorage for the distalization of canines and subsequent retraction of the incisors.

Insertion of attachments

Attachments are photoactivated composite resin devices, tooth-colored to match the patient's dentition, made on the dental enamel and bonded to the tooth surface through a combination of composite resin and adhesive system. Usually, the vestibular surface of the teeth is used, due to easier bonding and because the insertion/removal axis of the aligner is easier for the patient (Figures 7, 8, and 10).

During aligner therapy, some tooth movements simply will not occur if attachments are not inserted or if they have been planned with inadequate size and shape. Initially, it was believed that only the aligner would be able to generate the necessary movement for tooth correction without the use of an auxiliary accessory. However, clinical experience and scientific studies have shown that the incorporation of attachments into plastic aligners favors the idealized movement for tooth correction, optimizing, assisting, and directing the applied force.

As an example of an orthodontic movement that will not occur without the addition of attachments, dental extrusion is cited. It depends entirely on sufficient support (Figures 5 and 10). For other movements, such as correction of mesiodistal angulation, two attachments may be necessary (as illustrated on tooth 21 in Figure 14) to favor correction.

Figure 15 presents four types of isolated movements that are included in the planning of in-house aligner treatments, with a suggested attachment format for each. The decision to insert or not, and the choice of attachment shape and size, is exclusively the responsibility of the professional conducting the therapy, and this tutorial does not aim to define a specific protocol.

Once the attachments are inserted and the STL files with various sub-setup stages are generated, the orthodontist can print the models to be used for thermoforming the aligners or send them to a third-party company for printing. Such details will be presented in part 3 of this tutorial.

Figure 14. "Slice"-shaped attachments positioned on a maxillary central incisor to correct mesiodistal angulation, using ArchForm software. Note the use of attachments on the first permanent molars to enhance aligner stability and patient comfort.

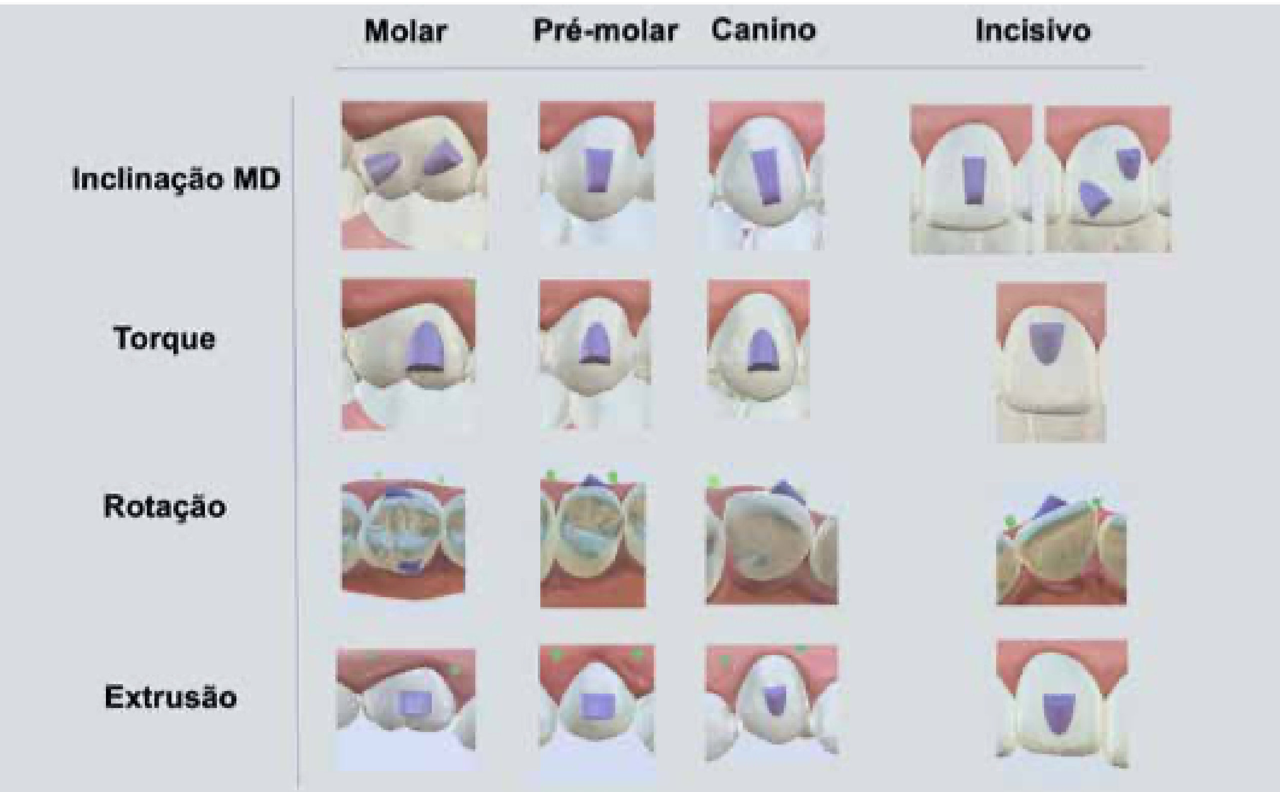

Fig 15. Suggested positioning and shapes of attachments for achieving mesiodistal inclination, torque, rotation, and dental extrusion, using ArchForm software.

References

1. Jaber ST, Hajeer MY, Burhan AS. The Effectiveness of In-house Clear Aligners and Traditional Fixed Appliances in Achieving Good Occlusion in Complex Orthodontic Cases: A Randomized Control Clinical Trial. Cureus. 2022;14(10):e30147.
2. Castroflorio T, Sedran A, Parrini S, et al. Predictability of orthodontic tooth movement with aligners: effect of treatment design. Prog Orthod. 2023;24(1):2.
3. Palone M, Pignotti A, Morin E, et al. Analysis of overcorrection to be included for planning clear aligner therapy: a retrospective study. Angle Orthod. 2023;93(1):11-18.
4. Haouili N, Kravitz ND, Vaid NR, Ferguson DJ, Makki L. Has Invisalign improved? A prospective follow-up study on the efficacy of tooth movement with Invisalign. American Journal of Orthodontics and Dentofacial Orthopedics. 2020;158(3):420-425.
5. Lombardo L, Arreghini A, Ramina F, Huanca Ghislanzoni LT, Siciliani G. Predictability of orthodontic movement with orthodontic aligners: a retrospective study. Prog Orthod. 2017;18(1):35.
6. Sachdev S, Tantidhnazet S, Saengfai NN. Accuracy of Tooth Movement with In-House Clear Aligners. J World Fed Orthod. 2021;10(4):177-182.
7. Mehta S, Patel D, Yadav S. Staging Orthodontic Aligners for Complex Orthodontic Tooth Movement. Turk J Orthod. 2021;34(3):202-206.
8. Bilello G, Fazio M, Amato E, Crivello L, Galvano A, Currò G. Accuracy evaluation of orthodontic movements with aligners: a prospective observational study. Prog Orthod. 2022;23(1):12.
9. 9. Hennessy J, Al-Awadhi EA. Clear Aligners Generations and Orthodontic Tooth Movement. J Orthod. 2016;43(1):68-76. 10. Kravitz ND, Kusnoto B, Agran B, Viana G. Influence of attachments and interproximal reduction on the accuracy of canine rotation with Invisalign. A prospective clinical study.
10. Angle Orthod. 2008;78(4):682-687.
11. Rossini G, Parrini S, Castroflorio T, Deregibus A, Debernardi CL. Efficacy of clear aligners in controlling orthodontic tooth movement: A systematic review. Angle Orthod. 2015;85(5):881-889.
12. Cortona A, Rossini G, Parrini S, Deregibus A, Castroflorio T. Clear aligner orthodontic therapy of rotated mandibular round-shaped teeth: A finite element study. Angle Orthod. 2020;90(2):247-254.

D) Practical guide to in-house aligner fabrication - Part 3: model printing, post-processing, thermoplasticisation, finishing and clinical management

Abstract

Once the orthodontic movements have been virtually planned using appropriate digital platforms and several sub-setup models have been exported, the laboratory phase can fabricate the aligners. Beginning with models being printed with photosensitive resin using 3D printing technology, they are next subject to washing and post-curing steps. Plastic aligners are then prepared using a range of thermoplastic polymer laminate choices. After this, aligners are meticulously trimmed, refined, sterilized, and packed into the branded recipients. Part 3 of the tutorial will focus on the practical concepts involved in the in-house production of aligners.

Introduction

For the fabrication of in-house aligners, following the digital procedures described in the two previous articles referring to Stage 1 (intraoral scanning), Stage 2 (selection of the staging software and file uploading)[1], and Stage 3 (planning/staging of orthodontic movements)[2], we now proceed to the laboratory and clinical stages, which will be presented in Part 3 of this tutorial series. The aim of the present article is to describe Stage 4, in which the models are printed; Stage 5, which involves the post-processing of the models; Stage 6, related to the thermoforming of polymeric laminates and the finishing of the aligners; and Stage 7, when the aligners are finally ready to be delivered to patients.

Stage 4: Model printing

In recent years, orthodontics has undergone a significant transformation with the incorporation of 3D printing technology for the production of orthodontic models, whether for diagnostic purposes or for the fabrication of in-house aligners. This innovation has offered numerous advantages to orthodontists, including the possibility of eliminating impression materials and dental plaster in clinical settings, better use of office space, integration with diagnostic and treatment planning software, and, most importantly, greater accuracy in producing sequential dental arch models that allow the fabrication of orthodontic aligners. However, not all 3D printers used in orthodontics are alike. Understanding the differences between various types of equipment—especially those specifically developed for orthodontic applications and those not originally intended for orthodontics but still suitable—is crucial for guiding orthodontists' investment decisions and ensuring maximum benefit from this technology. Part 3 of this tutorial will highlight the main differences, in terms of technology and cost, between the types of 3D printers that are useful to orthodontists.

3D printing technologies used in orthodontics

Currently, two main types of 3D printing technologies are employed in orthodontics for model fabrication: FDM (Fused Deposition Modeling) and photopolymer resin technology. FDM technology is recognized for its cost-effective approach, as it uses plastic filaments (e.g., PLA, PETG, ABS, polycarbonate) melted by the printer's heated extrusion system to create objects through successive layer deposition. Advantages include relatively low initial and operational costs, as well as the absence of demanding or labor-intensive post-printing processes. However, disadvantages of FDM include long printing times, limitations on the number of models that can be produced simultaneously, and generally lower resolution compared with resin-based printers, which may affect model accuracy for in-house aligner production. Nevertheless, FDM printers are highly useful for the fabrication of diagnostic and planning models (Figure 1).

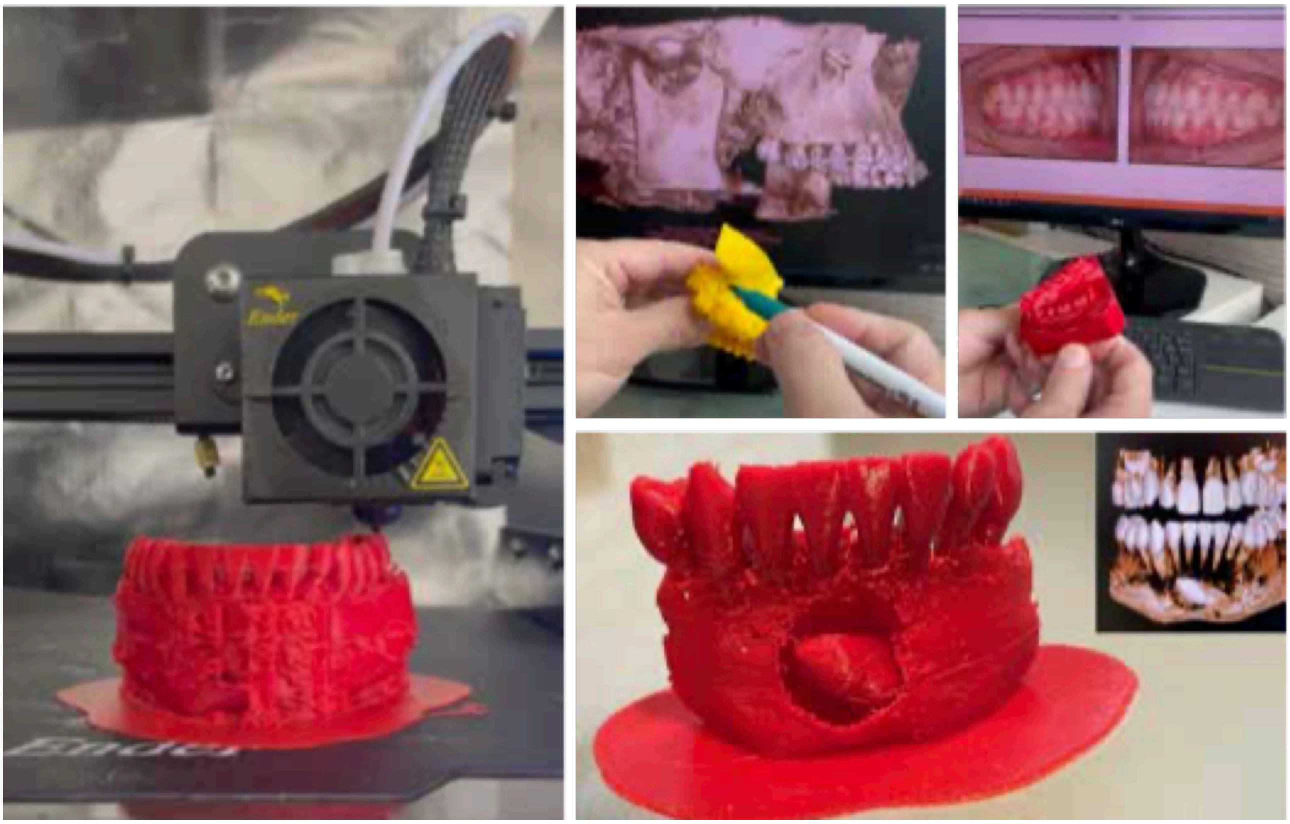

Figure 1 (A–D). Filament printer: A) Printing in progress. B) Site localization for skeletal anchorage insertion. C) Study model. D) Identification of dental ectopias.

Conversely, photopolymer resin–based technology is highly recommended for the fabrication of aligners due to its ability to produce models with high resolution (Figure 2) and high printing speed. This technology employs liquid, photosensitive resins that are cured layer by layer through exposure to various light sources, thereby generating the 3D-printed object (Figure 3).

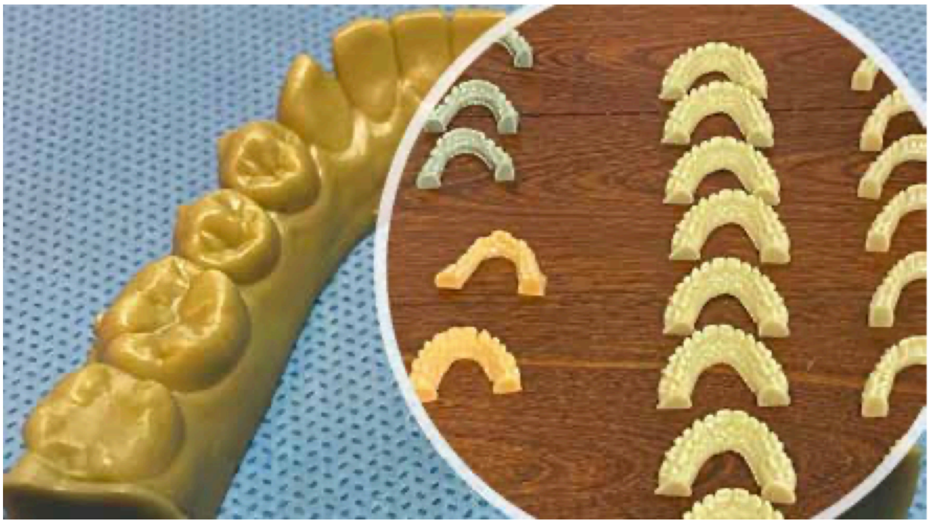

Figure 2. Models printed with 405 nm photosensitive resin at high resolution.

Figure 3. MSLA/LCD Elegoo Saturn printer with a tank filled with 405 nm photosensitive resin and a printing platform with models already printed.

Its main advantages include the ability to produce highly detailed models and a rapid manufacturing process. However, photopolymer resin–based technology presents notable drawbacks, including higher costs for both printer acquisition and the resin itself. In addition, the requirement for a complex post-processing phase—comprising removal of unpolymerized resin and final curing of the printed objects—limits its adoption by many orthodontists due to the time investment required and the biological risks associated with handling such materials (Figure 4).

Figure 4. Finger injury caused by direct contact with 3D printing resin without the proper use of rubber gloves.

Orthodontic Resin 3D Printers

Resin-based 3D printers specifically designed for orthodontic applications offer numerous advantages, including partial automation of processes and dedicated technical support (Figure 5). Equipped with features optimized for the production of aligners and other laboratory-fabricated dental appliances, these systems aim to provide maximum precision and operational convenience. They employ either stereolithography apparatus (SLA), in which a focused laser beam cures the resin layer by layer (e.g., Formlabs, Somerville, MA, USA), or digital light processing (DLP), which projects a visible light image onto a vat of photosensitive resin (e.g., SprintRay Pro, Los Angeles, CA, USA, using high-power LEDs).

Key features include:

- Precision: High-resolution output with ultra-thin print layers ensures a professional finish and accurate fit of aligners to the patient's dentition.
- Biocompatible resins: Most systems operate with proprietary resins, often FDA-approved for intraoral use. Their photosensitivity is calibrated to the printer's optics, and they are typically supplied in sealed cartridges, minimizing manual handling, reducing occupational exposure, and ensuring patient safety.
- Advanced software: Integrated software platforms streamline the workflow and, in some models, enable customization of aligner fabrication. Certain units automate specific steps, saving time, reducing resin contact, and lowering the risk of error.
- Speed and efficiency: Professional-grade units are optimized for rapid production, making them suitable for high-volume orthodontic practices.

Figure 5 (A-B). Orthodontic 3D printer *Formlabs 4P*: A) Sealed resin cartridge. B) Automation of the printing process and unloading of already printed models.

Non-Orthodontic Resin 3D Printers (MSLA/LCD)

Non-orthodontic 3D resin printers are general-purpose devices originally designed for a wide range of applications, including jewelry manufacturing, hobbyist use, and general prototyping. In orthodontics, they can be effectively repurposed for aligner production. These systems typically employ masked stereolithography apparatus (MSLA) or liquid crystal display (LCD) technology, in which ultraviolet light is selectively filtered to cure each two-dimensional layer of the print (Figure 6). Although generally more affordable to purchase and operate, they present certain limitations compared with specialized orthodontic printers.

- Precision: While their accuracy is slightly lower than that of dedicated orthodontic printers, advances in non-orthodontic technology have substantially narrowed the resolution gap with each new generation. Current models can achieve sufficient precision for the fabrication of high-quality in-house aligners.
- Resin biocompatibility: These printers may not support FDA-approved dental resins, which could pose risks to operators and patients if proper handling protocols are not strictly followed.

- Software limitations: Bundled software is designed primarily for basic machine operation and does not enable direct creation of dental models. As outlined in Part 2 of this tutorial, external software platforms must be employed for orthodontic applications.
- Speed and efficiency: With appropriate configuration, non-professional printers can achieve print speeds comparable to specialized orthodontic models. Later in this tutorial, we discuss resolution adjustments—within clinically insignificant limits—that can further optimize production efficiency.

Figure 6. MSLA/LCD Saturn "S" printer in its original factory condition.

Acquisition and Maintenance Costs of 3D Printers

Investing in a resin-based 3D printer specifically designed for orthodontics involves a substantial initial financial outlay, as well as ongoing operational expenses related to maintenance and the consumption of materials. These printers are manufactured with advanced technical specifications and specialized materials, which make them more costly than their generic, non-orthodontic equivalents. However, when high precision, maximum efficiency (with minimal print failure rates), reliable technical support, and operational safety are essential, such an investment becomes justifiable.

Conversely, non-orthodontic resin 3D printers are considerably more affordable from the outset, making them an attractive alternative for professionals working with limited budgets. Their operational and maintenance costs are generally low, but certain hidden costs must be taken into account. Components such as LCD screens and the plastic film forming the base of the resin tank have a relatively short service life, requiring frequent replacement (Figure 7). For example, while the lighting system of a DLP printer is typically designed for approximately 20,000 hours of operation, a non-orthodontic MSLA/LCD printer (commonly referred to simply as MSLA) may not exceed 2,000 hours of optimal performance.

Additionally, the absence of direct technical support from MSLA printer manufacturers should be carefully considered by orthodontists intending to implement in-house aligner production. Furthermore, potential risks associated with handling generic resins should be clearly communicated to professionals and minimized through strict adherence to safety protocols and preventive measures.

Figure 7 (A-B). M MSLA/LCD printer maintenance: A) Motherboard replacement. B) LCD replacement.

Technology of Non-Orthodontic 3D Printers

Although DLP-based non-orthodontic printers have recently appeared on the market, the most commonly employed 3D printing method in this category remains MSLA technology, using 405 nm photosensitive resin. This system has attracted considerable attention in the orthodontic field for in-house aligner fabrication due to its simplified, low-cost approach, offering several advantages over traditional SLA and DLP methods. In this tutorial, MSLA technology will be emphasized, highlighting its benefits and limitations. MSLA 3D printing shares similarities with SLA and DLP, but differs in several important operational aspects.

Light Source: In MSLA, a UV light source is projected through an LCD screen containing millions of tiny pixels. Each pixel can be individually activated or deactivated, allowing precise control over the curing process of the hundreds of 2D layers that form a volumetric model of a dental arch.

Photosensitive Resin: Similar to other resin-based 3D printing methods, MSLA uses a 405 nm photosensitive resin. This resin hardens when exposed to UV light, although its photosensitivity varies across different brands. It is therefore recommended to test each resin before initiating production to avoid material waste and, importantly, prevent errors or frustrations. The lifespan of the LCD screen also affects resin curing. The combination of printer quality, LCD lifespan, and resin photosensitivity determines the optimal printing parameters, which will be described below.

Layer-by-Layer Construction: The model is built incrementally, layer by layer, with each layer exposed to UV light through the LCD screen. The LCD acts as a mask, selectively allowing UV light to cure the resin in designated areas, progressively constructing a volumetric 3D model.

Advantages of MSLA Technology Compared to DLP and SLA

Speed: Depending on the printer and print configuration selected by the operator, MSLA is generally faster than SLA and DLP. Because an entire layer—including all models—is exposed to UV light simultaneously, there is no need for a moving laser or projector, reducing overall printing time. Some modern DLP printers now feature static components, matching the speed of MSLA printers.

Resolution: MSLA can achieve levels of detail and accuracy comparable to SLA and DLP. The use of 4K, 6K, 8K, and, more recently, 12K LCD screens ensures excellent resolution, precise control of millions of pixels, and high print quality.

Cost-efficiency: MSLA printers are more affordable than SLA or DLP machines. The use of an LCD screen, which is less expensive than a DLP projector or laser, contributes significantly to cost savings.

Durability: LCD screens have a shorter lifespan compared to DLP and SLA projectors, making MSLA printers more prone to maintenance over time due to component wear.

Ease of Use: MSLA printers are user-friendly for daily operations. Maintenance of LCD screens and FEP films in the resin tanks can be performed directly by the clinician or a technical assistant without major complications. MSLA printers are suitable for both novice and experienced users.

Disadvantages of MSLA Technology

Despite its advantages, it is important to recognize the limitations of MSLA technology:

Layer Lines: MSLA printing may produce visible layer lines on the printed object. This aspect does not significantly affect in-house aligner fabrication and can be minimized, if necessary, by adjusting the print layer thickness settings (Figure 8).

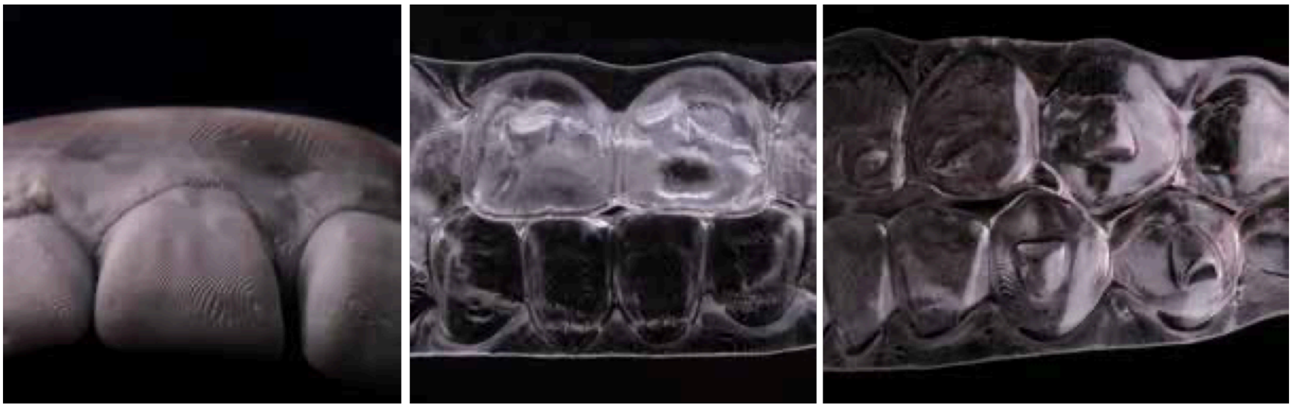

Figura 8 (A-C). Incremental printing lines: A) Marks on the printed model from the incremental layers left by the 0.05 mm resolution. B-C) Marks left on the aligner after thermoforming the laminates over models with incremental printing lines.

Material Compatibility: MSLA printers are generally limited to using specific types of resins formulated for UV light curing via LCD screens. This may restrict material options compared to professional orthodontic printers.

Resin Exposure: Handling photosensitive resin can be hazardous and requires strict precautions by both the clinician and the supporting team. Users must wear appropriate personal protective equipment (PPE).

Resin Odor: 3D printing with petrochemical-based resins emits unpleasant odors during the curing process, necessitating well-ventilated areas for operation. The use of suitable masks is recommended. Newly developed vegetable-oil-based resins present fewer issues related to odor (Figure 9).

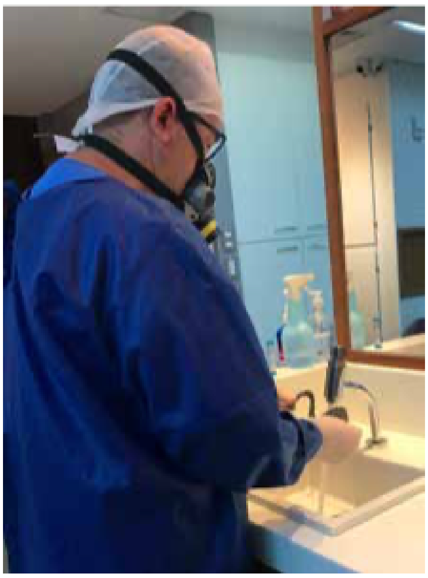
Figure 9. Use of PPE for the proper handling of 3D resins.

Steps to Achieve High-Quality Printing

Efficiency in 3D resin printing is crucial to obtain high-quality results while minimizing the waste of time and materials. To maximize efficiency, 3D models should be carefully digitally trimmed to remove unnecessary regions. Hollowing the models reduces material consumption while maintaining structural integrity. Balancing wall thickness with internal infill ensures faster printing and cost savings (Figure 10).

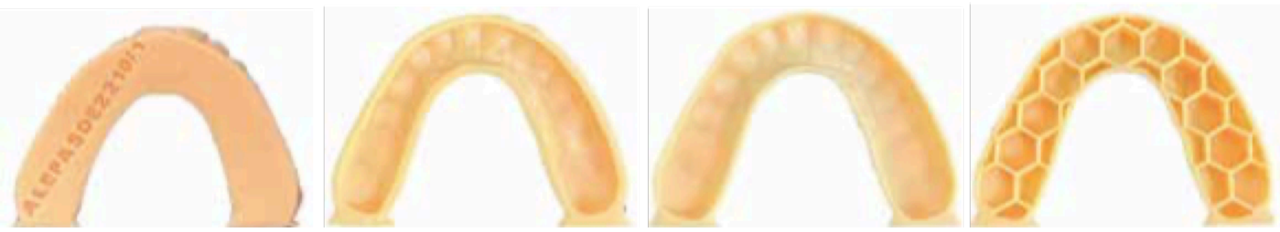
Figure 10 (A-D). Resin models: A) Solid model. B) Hollow model with 2 mm wall. C) Hollow model with 1 mm wall. D) Hollow model with 1 mm wall and hexagonal infill.

Additionally, it is recommended to apply a rational orientation of the models when arranging them on the printing platform (Figure 11). Position multiple models strategically on the platform, ensuring they do not interfere with each other during printing, while maximizing the efficiency of the process and preserving the printer's lifespan. Implementing these technical strategies in 3D resin printing optimizes workflow, saving both time and material resources.

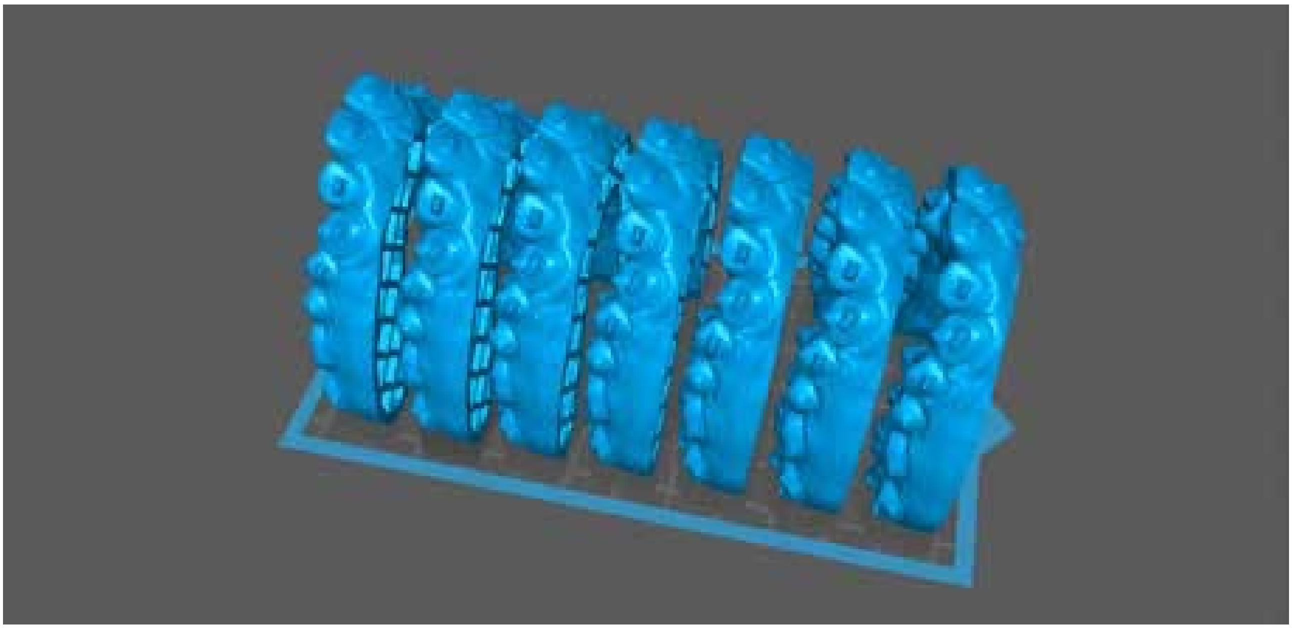

Figure 11. Model arrangement on the virtual printing platform using the Chitubox software.

Resins for 3D Printing

The 3D photosensitive resins with a 405 nm wavelength available in the Brazilian market, commonly used in MSLA printers, exhibit variations in composition and material properties. The exact formulation varies between manufacturers and resin types and is considered proprietary; however, the main components generally include:

Monomers: Photosensitive resins contain liquid monomers that are UV-sensitive. Upon exposure to light, these monomers polymerize, forming long chains that create a solid matrix.

Photoinitiators: Photoinitiators are chemical compounds that trigger the polymerization of monomers when exposed to light. They absorb the light energy and transfer it to the monomers, initiating the curing reaction.

Oxygen inhibitors: Photosensitive resins often contain oxygen inhibitors to prevent undesired polymerization during storage. Oxygen can act as a polymerization inhibitor, and these compounds help ensure the resin remains stable before printing.

Additives: Depending on the specific application, additives may be included to impart desired properties to the resin, such as hardness, flexibility, chemical resistance, transparency, or color.

Pigments or dyes: Pigments or dyes are added to provide color to the resin, facilitating better visualization of dental details in printed models.

Stabilizers and modifiers: Additional additives may be included to stabilize the resin, improve adhesion to the print platform, and adjust mechanical or chemical properties.

While conventional, petrochemical-based resins are still widely used, plant-based resins are emerging as a noteworthy alternative. Derived from renewable sources such as soybean oil, these resins offer several advantages. First, they tend to be more environmentally friendly, reducing the carbon footprint associated with production. Second, they often emit fewer volatile organic compounds, creating a safer and more comfortable working environment for orthodontic professionals. Additionally, these resins may exhibit biocompatible properties, minimizing the risk of allergic reactions or irritation when used in dental applications. As environmental awareness increases, the demand for plant-based and eco-friendly resins is expected to grow, driving further innovation and development in the field. This evolution is likely to result in safer, more efficient, and sustainable 3D printing processes for orthodontics, benefiting both professionals and patients.

Digital Preparation of Models for MSLA 3D Resin Printing

As previously discussed, the workflow for obtaining a printed model involves several digital steps, including slicing the virtual model, exporting files, and configuring the printer. The following five steps describe the process for producing printed models from the digital export of the subsetups containing the orthodontic movements, as detailed in Part 2 of this tutorial (Stage 3).

Step 1: Slicing the Virtual Model

Software selection: Begin by choosing a slicing software compatible with the MSLA printer, such as Chitubox or proprietary software provided with the printer (Figure 12).

Model importation: Open the slicing software and import the 3D model files to be printed. Ensure that the models are correctly positioned within the virtual build area of the printing platform.

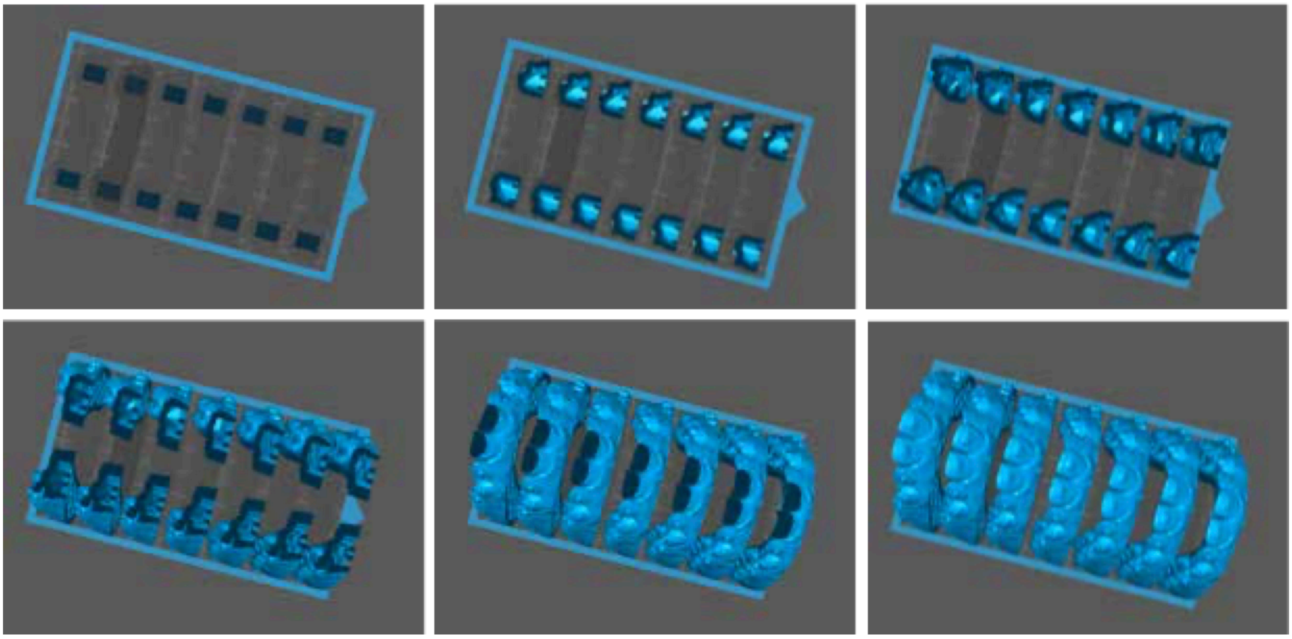

Figura 12 (A-F). Digital slicing of 3D models using the Chitubox software.

Initial Settings: Configure the printer dimensions and model within the slicing software, ensuring that the software generates a print-ready file compatible with the specific 3D printer (Figure 13).

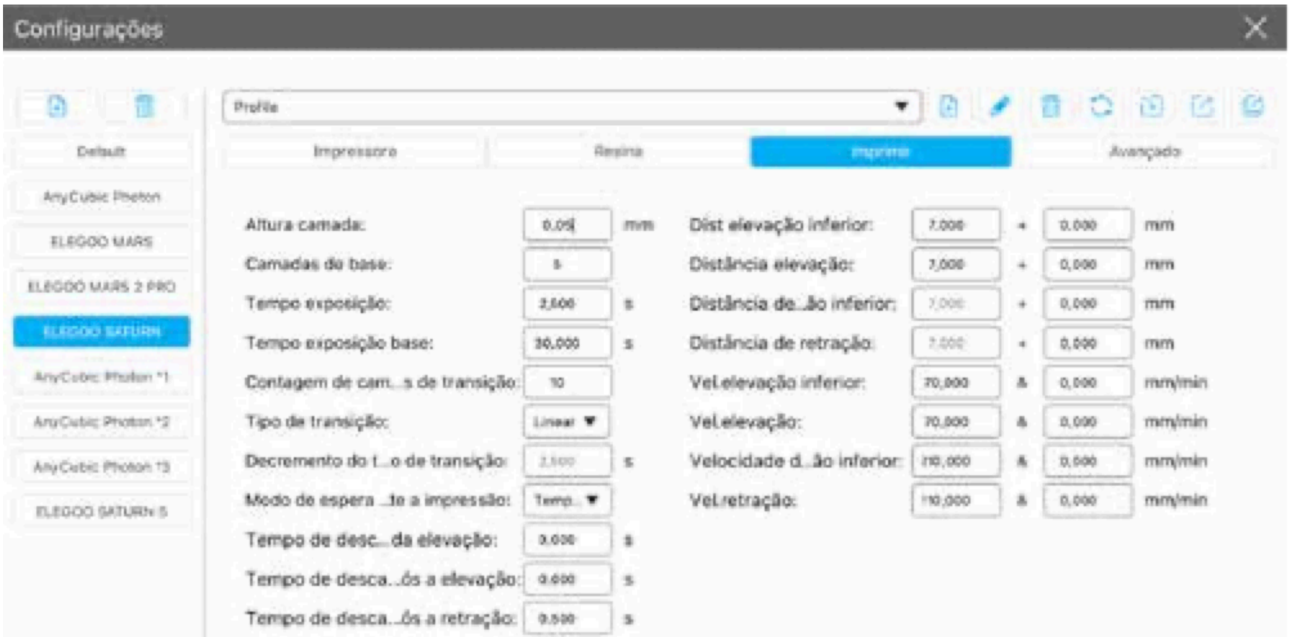

Figure 13. Printing configuration in the Chitubox software. Note the parameters that the practitioner must choose to adjust the equipment to the type of resin in use.

Step 2: Slicing Settings

Quality versus speed: Adjust the slicing settings according to your priorities. The print can be optimized for high quality or faster production. High-quality settings increase printing time, whereas faster settings may compromise some fine details.

Layer thickness: Select the desired layer height. Thinner layers generally yield higher resolution but increase the total printing time.

Exposure per layer: Set the exposure time for each layer, determining how long the UV light is applied. Proper adjustment ensures adequate curing of the resin. These settings directly influence layer adhesion, final model hardness, and overall print quality.

Number of base layers: Depending on the model morphology, the lifespan of the printer's LCD screen, and the photopolymer resin used, a higher or lower number of initial base layers may be required. Follow the resin manufacturer's recommendations and perform initial tests with your printer to determine the minimum number of base layers necessary. Base layers require longer UV exposure and significantly affect both total print duration and printer lifespan. Reducing the number of base layers increases process efficiency.

Step 3: Export and Preview

Generate the print file: Once all slicing options are configured, generate the print file (typically in the proprietary format required by each printer) and save it in an accessible location. Preview: Prior to printing, use the preview function to examine all virtual layers of the model and ensure that everything appears correct. Proper adhesion of the initial layers to the build platform is critical for a successful print. This step helps identify potential issues before initiating the print (Figure 14).

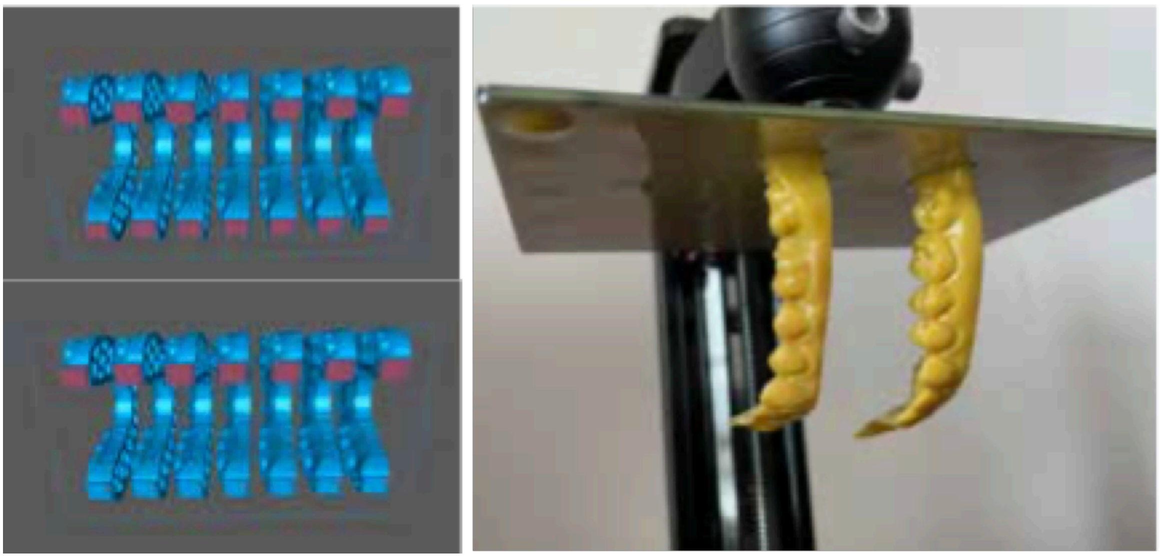

Figure 14 (A-B). Base layers: A) Digital models arranged on the virtual platform using Chitubox software. Note that the base layer is symmetrically supported in the upper part of the image, favoring model retention at the beginning of the printing process. In the lower part, the model is asymmetrically supported, leading to printing failure. B) Printing failure due to improper positioning of the models on the base layers.

Step 4: Printer Adjustments

Printer setup: Ensure that your MSLA printer is properly configured, connected to a reliable power source (preferably through an uninterruptible power supply), filled with the appropriate resin level, and placed in an environment with ambient temperature between 20°C and 30°C. Verify that the Z-axis of the build platform is correctly leveled and that the workspace is clean, ventilated, and free of dust.

Loading the file: Transfer the print file generated by the slicing software to the printer using a compatible method, such as USB, wired network, Wi-Fi, or another supported connection.

Step 5: Starting the Print

Initiating the print: Once all configurations have been verified and the printer is ready, start the print. The MSLA printer will construct the model layer by layer, accurately curing the resin to produce a precise 3D object.

Stage 5: Post-Processing

Post-processing of 3D resin models using MSLA technology

Freshly printed models require a careful post-processing workflow to achieve strong, durable structures that are safe for handling by both the professional team and patients. Because the materials used are potentially toxic, always use appropriate personal protective equipment (PPE) before beginning the cleaning process, including rubber gloves, a vapor filtration mask or equivalent, and safety goggles. Begin by allowing excess resin to drain back into the resin tank. Although often overlooked, this step is essential to avoid material waste and prevent contamination of cleaning tanks with excess resin. Carefully remove the build platform and place it on a dedicated oblique support to allow proper drainage (Figure 15).

Figure 15. Draining excess resin after printing.

Care must be taken to avoid damaging the delicate LCD screen or other printer components. During this process, any drips of excess resin should be carefully removed, ensuring that the build platform does not come into contact with the bottom of the resin tank or the LCD. Using a plastic scraper, gently remove any remaining uncured resin without scratching or damaging the surface.

After visible excess resin has drained, immerse the build platform, still with the models attached, in a high-concentration alcohol bath, typically 90% or higher. Gently agitate the platform to remove resin adhered to the model surfaces, using a soft brush to assist with cleaning the retentive areas. Leave the platform in the bath for a few minutes—typically two to three minutes are sufficient for gross removal of excess resin. Repeat this step in a second fresh high-concentration alcohol bath for an additional two to three minutes.

Finally, place the metal build platform, with the resin models still attached, into a mechanical agitation cleaning device (e.g., Anycubic Wash & Cure, Elegoo Mercury Plus, Creality UW-01, Prusa CW1) containing isopropyl alcohol, and agitate for 15 minutes (Figure 16). This procedure ensures that the models are completely free of excess resin on all external surfaces.

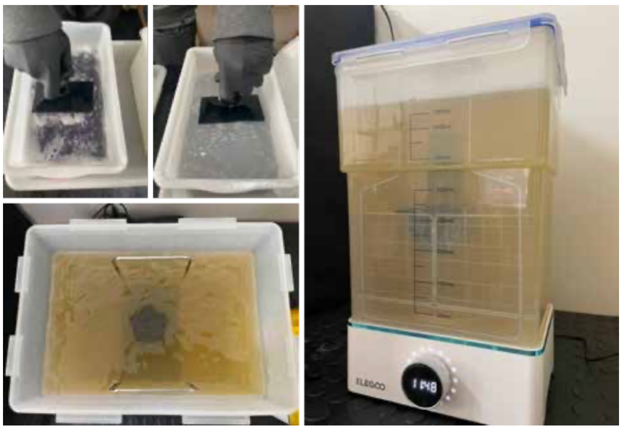

Figure 16 (A-D). Sequential washing of models: A) Initial manual bath in ethyl alcohol for coarse removal of excess resin. B) Second manual bath in ethyl alcohol to continue resin removal. C-D) Bath under mechanical agitation in isopropyl alcohol.

After removing the platform from the isopropyl alcohol bath, rinse it under running water and dry it using a lint-free cloth or allow it to air dry, ensuring that no water spots or residues remain. With the build platform clean, it is time to detach the 3D-printed orthodontic models from the platform.
To facilitate removal of models that are strongly adhered, gently heat the top side of the platform (the side opposite the models) using a hairdryer set to warm air. This approach aids in detaching the models without causing deformation or compromising the leveling of the build platform (Figure 17).

Figure 17. Use of a hair dryer in heated mode to facilitate the removal of resin models from the printing platform.

Carefully remove the models from the build platform using a plastic scraper or an appropriate sharp metal spatula. Take care to avoid damaging the models or the platform itself. Allow the models to air dry or use a UV light chamber to fully solidify them.
UV curing of the models, preferably using a rotary system, is critical. This approach ensures consistent and uniform exposure to the light source, preventing any areas from being insufficiently cured. A complete post-processing workflow results in models that are not only durable but also less prone to degradation or the release of uncured resin components when used in clinical applications.
UV light chambers designed specifically for this purpose are widely available in the market and enable effective post-processing of orthodontic models. Manufacturers such as Anycubic, Elegoo, Prusa, Creality, and Peopoly offer professional-grade options at relatively low cost. For beginners, low-volume production, or limited workspace, hobbyist UV chambers are also available and suitable for post-curing purposes (Figure 18).

Figure 18 (A-C). UV light post-processing: A) Professional rotary light chamber. B) Professional mirrored light chamber. C) Low-cost amateur UV light chamber.

Following these steps, the orthodontist will be well-prepared to obtain high-quality models using an MSLA printer, adjusting the slicing software settings and generating printer-compatible files to meet requirements for quality, speed, and efficiency without distortions. It is important to emphasize that following the printer and resin manufacturers' guidelines is essential to achieve reproducible and superior-quality results.

Stage 6: Thermoforming and Finishing

Thermoforming of plastic sheets for in-house aligner fabrication

Understanding the properties of different polymers and the mechanics of thermoforming plastic sheets allows orthodontists to produce aligners that meet the highest standards of quality and patient satisfaction.

Various polymers can be used in the fabrication of sheets for orthodontic aligners. Thermoplastic polymers are a class of materials capable of softening and melting when heated. When subjected to vacuum or pressure over printed models, a transparent plastic aligner is obtained (Figure 19). Commonly used polymers include polyester, polyurethane or copolyester, polypropylene, polycarbonate, ethylene-vinyl acetate (EVA), and polyvinyl chloride (PVC), either individually or in combination, for the production of orthodontic aligners[3,4].

With technological evolution in aligner fabrication, materials have progressed from single-layer plastics to the latest generation of commercially available multi-layer materials, which combine soft and hard layers. The soft layer of the aligner contributes to elastic deformation properties, while the hard layer ensures durability and structural robustness. For dental movement, stress distribution through the periodontal ligament and the application of mechanical load to the alveolar bone is more favorable with multi-layer transparent aligners than with single-layer aligners. This is particularly true in cases where the ratio of soft to hard layer exceeds 50%. Additionally, multi-layer transparent aligners exhibit fewer side effects compared to single-layer aligners[5].

Polyethylene terephthalate glycol (PETG), an amorphous non-crystalline copolymer derived from PET, is widely used for transparent aligners. PETG is preferred mainly for its excellent mechanical and optical properties. It exhibits exceptional clarity, favorable thermoforming characteristics, and can be punched and cut—routine actions in aligner fabrication. Moreover, PETG is minimally hydrophilic, allowing less demanding storage requirements and reduced cost[6].

Thermoplastic polyurethane (TPU) is a polymer with a broad range of desirable properties, including exceptional mechanical and elastomeric characteristics, as well as high resistance to occlusal wear. When subjected to load, thermoplastic polyurethane deforms but is capable of returning to its original shape after load removal, thanks to its inherent flexibility that allows stretching and subsequent recovery[7].

It is desirable that transparent thermoplastic orthodontic aligners provide consistent and controlled forces to achieve expected tooth movements[3]. Therefore, commercial sheets made of copolymers—combinations of two or more polymers—are often used to improve mechanical properties. Mechanical enhancement can be achieved by incorporating mixtures of polymers such as polyester, polyurethane, and polypropylene. Commercial production of transparent aligners frequently employs polymer blends consisting of these three polymers[8].

The selection of polymer blend ratios has a significant impact on the characteristics of the resulting plastic sheet. For example, a 70/10/20 blend of PETG, polycarbonate (PC), and TPU exhibited superior mechanical properties compared to other ratios. This particular mixture demonstrated the ability to generate adequate and durable orthodontic forces, outperforming other commercially available products[3]. In another study, a 70/30 PETG/PC blend showed the most favorable combination of tensile strength, impact resistance, and elongation at break[9].

Figure 19 (A-C). Fabricating the aligner: A) Laminate immediately after thermoforming. B) After initial trimming. C) After final trimming and finishing.

Thermoforming technique for plastic sheets in in-house aligner fabrication

Two primary methods are employed for thermoforming plastic sheets over orthodontic models: pressure forming and vacuum forming[10]. The first method uses heat combined with positive pressure to mold the plastic onto the model. A pneumatic press applies controlled pressure, typically measured in bars, to ensure precise and consistent adaptation. The typical pressure range for pressure-forming machines varies between 2 and 6 bars, depending on the material being used and the specific machine.

Pressure thermoforming is ideal for reproducing fine anatomical details, ensuring accurate fit and contour of the aligner. An additional advantage of pressure-forming machines is the ability to standardize production through automated control of heating time, applied pressure, and plastic cooling. Examples of pressure thermoforming machines include the German Ministar by Scheu and the Drufomat by Dreve (Figure 20).

Figure 20 (A-B). Ministar Scheu pressure thermoforming machine: A) Infrared heat source activated. B) Pressure, temperature, and time settings.

Vacuum thermoforming, in contrast, employs negative pressure (vacuum) to pull the heated plastic sheet over the model. Vacuum machines typically operate at lower pressures, ranging from 0.2 to 0.8 bar. Despite the lower applied force, this method remains efficient and suitable for the production of retainers and in-house aligners[10].

The main disadvantages of vacuum thermoforming are the difficulty in standardizing the process through automation and the greater dependence on operator skill. An example of a vacuum thermoforming machine is the P7 by the Brazilian company Bio-Art Equipamentos Odontológicos (São Carlos/SP) (Figure 21).

Figure 21. Plastivac vacuum thermoforming machine.

Overall, the thermoforming of plastic sheets over resin-printed models, whether by pressure or vacuum, provides adequate precision, ensuring that orthodontic aligners fit comfortably on the teeth and deliver satisfactory clinical outcomes in orthodontic tooth movement. This represents a cost-effective method for in-house aligner production compared to outsourcing the process.

Since thermoforming machines are directly accessible to the orthodontist and their team, aligners can be produced rapidly, offering a more advantageous turnaround time to meet patient demands. Depending on the characteristics of the case, the orthodontist can choose from different types of polymers, providing flexibility in aligner design.

Embossed numbering on the aligner, corresponding to the treatment stage, is important for monitoring by both the orthodontist and the patient. The placement of this numbering should be carefully selected to avoid interference with attachments (Figure 22).

Figure 22 (A-B). Finished in-house aligners: A) Detail of the stage numbering imprint. B) Detail of tooth anatomy and attachment reproduction.

Negative aspects of in-house aligner thermoforming include the existence of a learning curve in the process and the need for a thorough understanding of the characteristics of various plastic sheets. Some of these materials are extremely hygroscopic, and exposure to the environment for just a few minutes can be enough to compromise their properties. Achieving the desired results requires operator skill and experience. Additionally, one aspect that needs to be evaluated by the professional is the investment cost in thermoforming equipment, especially if it is a professional-grade pressure machine. Finally, special attention must be given to the proper disposal of excess plastic sheets, an essential measure for environmental responsibility.

Finishing in-house aligners: the final touch of quality

The fabrication of in-house aligners allows orthodontists to create customized solutions for their patients with clinically adequate precision. However, the workflow from a 3D printed model to a perfect aligner does not end with printing and thermoforming. The meticulous finishing of aligners, using manual techniques with sharp/curved scissors and handpieces equipped with abrasive discs, is the simplest way to achieve excellent finishing within the clinic. It is important to note that automated cutters (milling machines) are also available on the market, operating in CNC (Computer Numerical Control) systems, with rotary bits or lasers that provide a high standard of finishing through uniform cutting lines. Nevertheless, the initial investment cost, as well as maintenance, often exceed the benefits within the reality of private practices, being currently intended for companies that commercialize aligner production services.

During the finishing stage, cleaning, sanitization, and packaging of the aligners ensure they are professionally ready for use.

Step 1: precision cutting with scissors. Precise cutting is essential to obtain a comfortable, aesthetically pleasing, and functional fit of the aligners. Use a sharp, fine-tipped scissor to carefully trim the excess material along the aligner edges. The orthodontist can choose to make either a straight or fenestrated cut. In general, the straight cut is more appropriate in most cases, leaving the fenestrated design for situations in which periodontal conditions require the absence of plastic contacting the gingival mucosa. Care should be taken not to cut too close to the teeth, leaving part of the crown exposed without plastic coverage, which could irritate the patient's labial mucosa. Mechanically, a "higher" cut, leaving approximately 2 mm of plastic above the gingival contour of the crowns, provides better biomechanical control. However, the likelihood of excess plastic causing patient discomfort and requiring chairside adjustments is higher than if the cut is limited to a 1 mm distance.

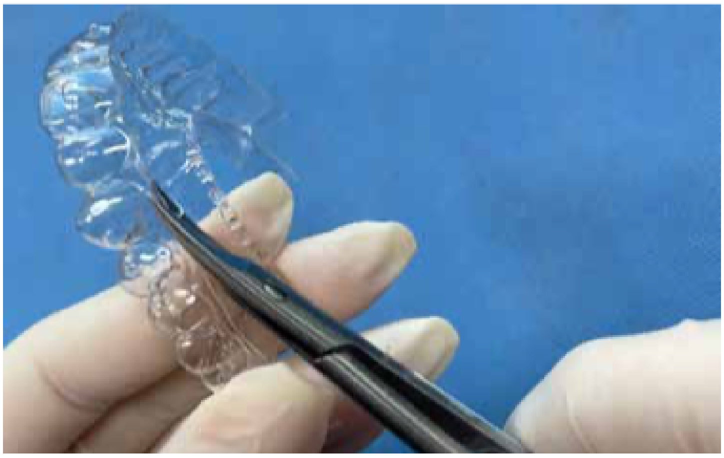

Figure 23. Trimming of the in-house aligner with sharp curved scissors.

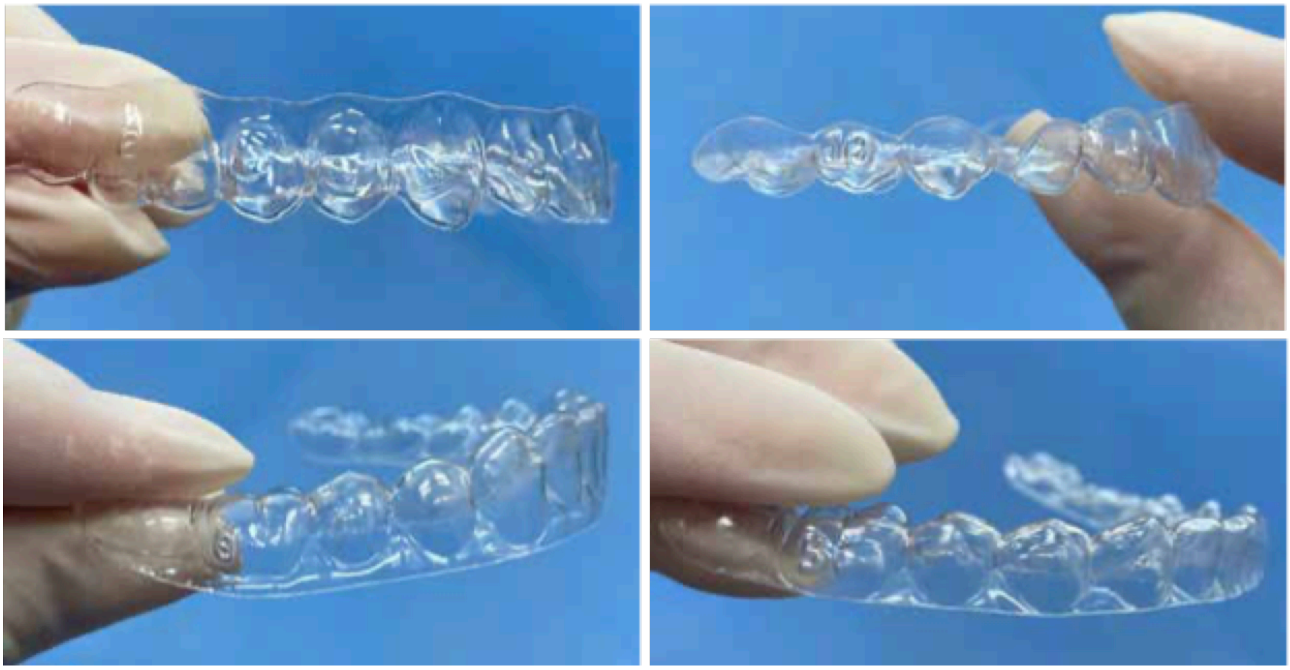

Figure 24 (A-D). Types of trimming: A) High scalloped. B) Low scalloped. C) High straight. D) Low straight.

Step 2: to achieve a perfect finish, a handpiece equipped with 3M abrasive discs (Saint Paul, MN, USA) is very useful. This tool allows controlled and precise smoothing of any edges and removal of sharp corners. Gently contour the surface of the aligner to ensure a comfortable and polished fit. Care should be taken not to overdo it; gradual refinement ensures the maintenance of the aligner's structural integrity.

Figure 25. Finishing with abrasive discs.

Step 3: proper cleaning of the aligners is crucial for patient hygiene and comfort. A comprehensive approach involves water and detergent to remove residual oils left by the model's release agent. Begin by rinsing the aligners in warm water to remove loose debris. Place the aligners in an ultrasonic cleaning bath dedicated exclusively to aligners, using neutral detergent and water for 10 minutes.

Check for any remaining oil residues, and if present, gently brush with a soft toothbrush and neutral detergent. Rinse thoroughly to ensure no soap residue remains.

Step 4: allow the aligners to dry in a closed, clean environment. This space can include mechanical ventilation to facilitate faster drying. Once dry, place the aligners in a UVC chamber designed for disinfection and leave them for the recommended duration. This step enhances cleanliness and ensures a higher-quality final product.

Figure 26. Models drying.

Step 5: The final touch of personalization for in-house aligners is the careful packaging of the aligners, ensuring they arrive to the patient in perfect condition. Place each pair of aligners in an individual airtight bag to avoid contamination and preserve hygiene. Print identification labels on a thermal printer, indicating not only the patient's name but also the treatment stage number to which those devices included there refer. Inform the total number of aligners in that series. Provide clear instructions to the patient on how to use and care for the aligners. Encourage them to maintain regular oral hygiene routines and to store the aligners safely when not in use. Provide a storage case to keep the aligners protected when they are removed during meals and cleaning routines (Figure 27).

Figure 27. Patient delivery kit.

Stage 7: clinical management

Managing the routine use of in-house aligners in the orthodontist's daily practice represents a significant shift from traditional approaches to orthodontic treatment. Adopting this system requires the professional to be open to adjustments in their workflow. This includes incorporating new habits, such as using digital platforms for production tracking among team members (for example, ClickUp, Asana, ProofHub, Trello). This digital integration becomes essential to ensure process efficiency and proper coordination with the production and delivery of in-house aligners.

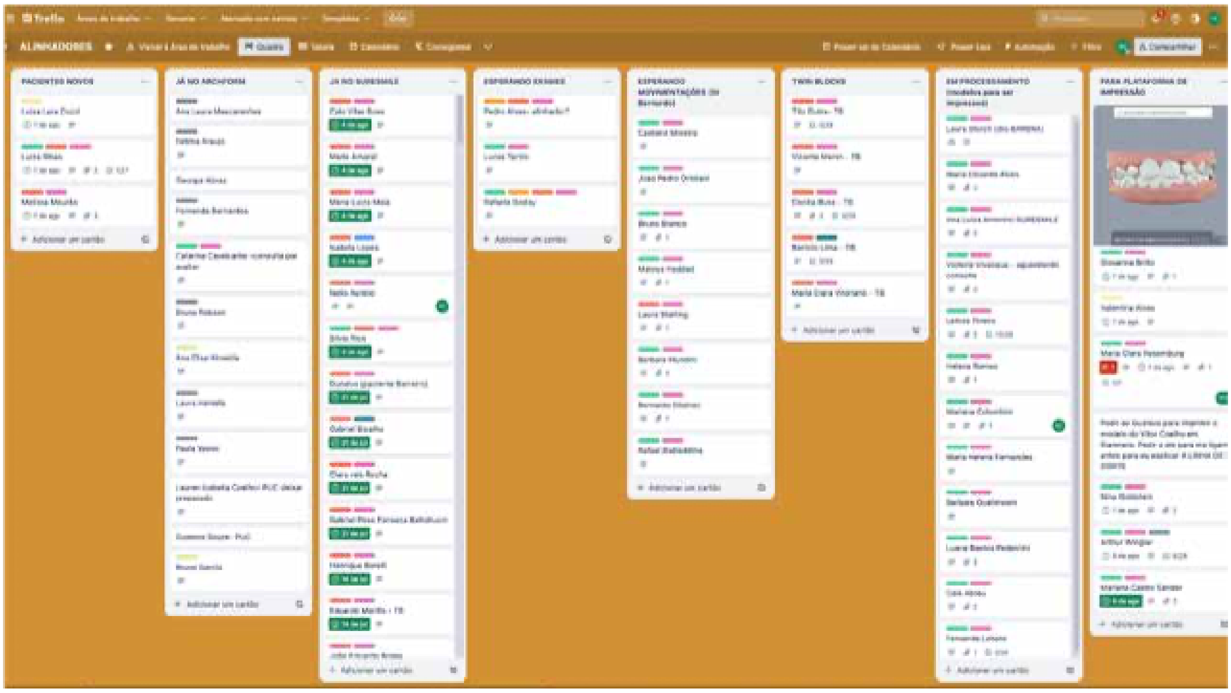

Figure 28. Management of in-house aligner production using online tools. Enhancing efficiency of internal processes for manufacturing and patient delivery.

In addition, it is necessary to allocate a specific space within the dental office for the 3D printer and other post-processing equipment, thereby ensuring an appropriate environment for the fabrication of the aligners. This logistical adjustment is crucial to maintain process quality, environmental and device hygiene, and the precision of the in-house manufactured appliances (Figure 29).

Figure 29. In-house aligner laboratory with MSLA/LCD printers of different generations.

Another important adaptation involves a shift in the mechanical paradigm. Traditional orthodontic training with brackets and wires provides experienced professionals with a system where the challenges are already well known and can therefore be addressed with familiar strategies. With aligners, however—especially those fabricated in-house—much less is known to date about many aspects of their performance. Orthodontists must learn to recognize the limitations of in-house aligners, while also maximizing their strengths. This requires a deep understanding of how the system works and the ability to adapt the treatment plan according to the specific characteristics of these appliances. The flexibility and customization offered by this technology can be a considerable advantage when used properly.

The adoption of in-house aligners also has a significant financial impact for the orthodontist. Although the initial investment in equipment and training may be substantial, in-house production can reduce costs in the long run. However, it is crucial to balance financial savings with treatment efficiency, as proper resource management is fundamental.

Another consideration is the scheduling of follow-up visits, which must be carefully planned. With in-house aligners, appointments can be spaced further apart, as multiple sets of aligners can be delivered to the patient at once, saving valuable clinical time. Moreover, internal fabrication accelerates production, eliminating the long waiting periods associated with industrial aligner delivery. This allows for greater efficiency in the orthodontist's schedule and an overall optimization of clinical time.

In summary, the decision to adopt an in-house aligner system is complex and requires a strong commitment to adapting to new practices and technologies. Nevertheless, given the many clinical applications and the long-term financial advantages, this approach becomes an attractive option for orthodontists willing to invest time and resources in its implementation. It is important to acknowledge the inevitable learning curve, but with dedication, professionals can reap the benefits of this innovative method.

Conclusions

At the end of this tutorial, presented in three parts, the key message is that in-house aligners are a viable technical alternative for orthodontists who wish to overcome the current limitations of outsourced aligners, particularly in terms of cost and delivery times. The fabrication of in-house aligners involves a complex series of steps, which may limit widespread adoption. However, for professionals who commit to training themselves and their teams, significant opportunities will arise. The vast range of orthodontic solutions that can be offered to patients through mastery of this technique justifies the effort of overcoming the learning curve and the initial investment. The ongoing development of direct aligner printing technology promises, in the near future, to simplify many of the steps outlined in this tutorial. It is worth waiting—and taking advantage of what is to come.

References

1. Souki BQ, Azevedo GM, Maia RM, Tavares LDF, Bosoni C. Guia prático de fabricação de alinhadores in-house – Parte 1: Introdução ao sistema. Orthodontic Science and Practice. 2023; 16(61):91-108.
2. Souki BQ, Azevedo GM, Maia RM, Tavares LDF, Bosoni C. Guia prático da fabricação de alinhadores in-house – Parte 2: Planejamento e estagiamento. Orthodontic Science and Practice. 2023; 16(62):119-130.
3. Zhang N, Bai Y, Ding X, Zhang Y. Preparation and characterization of thermoplastic materials for invisible orthodontics. Dent Mater J. 2011; 30(6):954-959.
4. Alexandropoulos A, Al Jabbari YS, Zinelis S, Eliades T. Chemical and mechanical characteristics of contemporary thermoplastic orthodontic materials. Aust Orthod J. 2015; 31(2):165-170.
5. Jia L, Wang C, Wang C, Song J, Fan Y. Efficacy of various multi-layers of orthodontic clear aligners: a simulated study. Comput Methods Biomech Biomed Engin. 2022; 25(15):1710-1721.
6. Ihssen BA, Willmann JH, Nimer A, Drescher D. Effect of in vitro aging by water immersion and thermocycling on the mechanical properties of PETG aligner material. Journal of Orofacial Orthopedics/Fortschritte der Kieferorthopadie. 2019; 80(6):292-303.
7. Frick A, Rochman A. Characterization of TPU-elastomers by thermal analysis (DSC). Polym Test. 2004; 23(4):413-417.
8. Golkhani B, Weber A, Keilig L, Reimann S, Bourauel C. Variation of the modulus of elasticity of aligner foil sheet materials due to thermoforming. J Orofac Orthop. 2022; 83(4):233-243.
9. Ma YS, Fang DY, Zhang N, Ding XJ, Zhang KY, Bai YX. Mechanical properties of orthodontic thermoplastics PETG/ PC2858 after blending. The Chinese Journal of Dental Research. 2016; 19(1):43-48.
10. Dogramaci E, Chubb D, Rossi FG. Orthodontic thermoformed retainers: a two-arm laboratory study into post-fabrication outcomes. Aust Dent J. 2018; 63(3):347-355.
11. Elshazly TM, Keilig L, Salvatori D, Chavanne P, Aldesoki M, Bourauel C. Effect of trimming line design and edge extension of orthodontic aligners on force transmission: an in vitro study. J Dent. 2022; 125:104276.

Summary

The aim of this PhD thesis was to evaluate, through both in vitro and in vivo studies, the impact of digital orthodontics on 3D imaging and the additive manufacturing of appliances. A total of ten papers were included: six of an experimental nature and four illustrating the application of the topics discussed herein.

With regard to 3D imaging, two experimental studies were conducted. The first assessed the preference between intra-oral scanning and alginate impressions in children, revealing that intraoral scanning is faster, more comfortable and it is preferred by young patients. The emergence of intra-oral scanning has enabled the acquisition of 3D models, which serve as a valuable tool for evaluating various treatment outcomes without exposing patients to radiation.

The accuracy of 3D model superimposition was examined in a sample of adult patients, demonstrating that it is a reliable and reproducible method. However, further research is necessary to establish a reliable reference area for these superimpositions, particularly in growing patients or those presenting significant changes in the occlusal plane. When combined with cephalometric radiographs, this approach serves as an effective means of illustrating 3D tooth movement without the superimposition of other anatomical structures, as demonstrated in the paper entitled "A diagnostic and treatment planning checklist for vertical problems in orthodontic patients" included in the appendix.

Stereolithography has enabled the conversion of intra-oral scans into dental models or appliances that are constructed directly from these .stl files. The 3D printing process is performed by the sequential deposition of resin layers, utilizing a variety of printers and resins available on the market, with new materials continually being introduced. As a result, extensive evaluation is required to determine the properties of these materials and the methods by which they are handled. Accordingly, the in vitro studies assessed the physical characteristics of different resins, considering variables such as printing orientation, exposure to water ageing, and the resultant surface roughness and gloss. The findings indicated that the printing orientation and water ageing affect flexural strength and modulus of 3D printing resins for occlusal splints, as well as surface roughness and gloss of 3D printed aligners.

However, perhaps the most significant transformation in orthodontics brought about by the digital workflow has been the development and improvement of aligners. This represents a complete shift, both aesthetically and mechanically, from conventional fixed appliances. Aligner treatment now offers numerous possibilities, ranging from outsourced to in-house fabrication, each utilizing different printers and materials. The production of in-house aligners remains somewhat cumbersome, as illustrated by the three practical guidelines included in the appendix of this thesis. Nevertheless, there exists a clinical niche for their use, particularly in low complexity cases. The expansion of the

upper arch using in-house aligners was evaluated in a prospective clinical study, with results demonstrating that it is more effective in the premolar area than in the canine area, with canine torque control that is affected by attachment positioning. Despite these advancements, much remains to be explored in aligner therapy, especially as treatment outcomes now rely heavily on patient cooperation.

Patient cooperation has long posed challenges for orthodontists, a situation further complicated when extra-oral appliances are required. The advent of 3D printing offers the potential to customize these devices, aiming to enhance patient comfort. This hypothesis was explored by comparing standard facemasks with those personalized via additive manufacturing in a crossover randomized clinical trial. While there was a slight preference for the personalized facemasks, the findings ultimately revealed no significant differences in terms of wear time, pain, or sleep-related discomfort. Larger-scale studies are necessary to determine whether the customization of facemasks is truly beneficial.

Conclusions and future directions

Digital orthodontics has undoubtedly been adopted by the professional community, as the digital workflow generally offers increased comfort, greater predictability and, most importantly, enhanced diagnostic capability thanks to 3D imaging. Digital records require no physical storage space, can be accessed remotely, and facilitate improved assessment of treatment outcomes through radiation-free methods. Nonetheless, current literature reveals considerable limitations in the clinical performance of new appliance mechanisms. Consequently, practitioners must carefully weigh the predictability of outcomes before embracing new technologies or resources, particularly when managing complex cases. The progression of digital orthodontics is unavoidable, and it is understandable that it remains somewhat behind, given that conventional treatment methods benefit from over a century of research. However, it is essential to consider not only the clinical implications but also the significant shift in material usage within orthodontics, with the environmental and health impacts of resin handling warranting further investigation. Just as many analogue processes have faded or disappeared with technological advancement, it can be concluded that digital orthodontics is still in its early stages yet and it will certainly become a pivotal advance leading to more precise and efficient orthodontic care.